



# **Asphalt Research Consortium**

## **Quarterly Technical Progress Report October 1-December 31, 2011**

February 2012

Prepared for  
Federal Highway Administration  
Contract No. DTFH61-07-H-00009

By  
Western Research Institute  
Texas A&M University  
University of Wisconsin-Madison  
University of Nevada-Reno  
Advanced Asphalt Technologies

[www.westernresearch.org](http://www.westernresearch.org)  
[www.ARC.unr.edu](http://www.ARC.unr.edu)

# TABLE OF CONTENTS

|  |     |
|--|-----|
| INTRODUCTION .....   | 1   |
| GENERAL CONSORTIUM ACTIVITIES .....  | 3   |
| PROGRAM AREA: MOISTURE DAMAGE.....   | 5   |
| Category M1: Adhesion.....   | 5   |
| Category M2: Cohesion.....   | 9   |
| Category M3: Aggregate Surface .....   | 15  |
| Category M4: Modeling.....   | 15  |
| Category M5: Moisture Damage Prediction System .....                             | 16  |
| Table of Decision Points and Deliverables for Moisture Damage .....              | 17  |
| Gantt Charts for Moisture Damage.....  | 20  |
| PROGRAM AREA: FATIGUE.....   | 23  |
| Category F1: Material and Mixture Properties .....                               | 23  |
| Category F2: Test Method Development.....  | 36  |
| Category F3: Modeling.....   | 55  |
| Table of Decision Points and Deliverables for Fatigue .....                      | 78  |
| Gantt Charts for Fatigue.....  | 82  |
| PROGRAM AREA: ENGINEERED MATERIALS.....  | 85  |
| Category E1: Modeling.....   | 85  |
| Category E2: Design Guidance.....  | 108 |
| Table of Decision Points and Deliverables for Engineered Materials .....         | 125 |
| Gantt Charts for Engineered Materials .....                                      | 131 |
| PROGRAM AREA: VEHICLE-PAVEMENT INTERACTION.....                                  | 133 |
| Category VP1: Workshop.....  | 133 |
| Category VP2: Design Guidance.....   | 133 |
| Category VP3: Modeling.....  | 137 |
| Table of Decision Points and Deliverables for Vehicle-Pavement Interaction ..... | 140 |
| Gantt Charts for Vehicle-Pavement Interaction.....                               | 141 |
| PROGRAM AREA: VALIDATION.....  | 143 |
| Category V1: Field Validation.....   | 143 |
| Category V2: Accelerated Pavement Testing.....                                   | 144 |
| Category V3: R&D Validation .....  | 145 |
| Table of Decision Points and Deliverables for Validation .....                   | 152 |
| Gantt Charts for Validation.....   | 154 |

## **TABLE OF CONTENTS (continued)**

|  |     |
|--|-----|
| PROGRAM AREA: TECHNOLOGY DEVELOPMENT .....                             | 157 |
| PROGRAM AREA: TECHNOLOGY TRANSFER .....                                | 163 |
| Category TT1: Outreach and Databases .....                             | 163 |
| Table of Decision Points and Deliverables for Technology Transfer..... | 176 |
| Gantt Charts for Technology Transfer .....                             | 177 |

## **INTRODUCTION**

This document is the Quarterly Report for the period of October 1 to December 31, 2011 for the Federal Highway Administration (FHWA) Contract DTFH61-07-H-00009, the Asphalt Research Consortium (ARC). The Consortium is coordinated by Western Research Institute with partners Texas A&M University, the University of Wisconsin-Madison, the University of Nevada Reno, and Advanced Asphalt Technologies.

The Quarterly Report is grouped into seven areas, Moisture Damage, Fatigue, Engineered Paving Materials, Vehicle-Pavement Interaction, Validation, Technology Development, and Technology Transfer. The format of the report is based upon the Research Work Plan that is grouped by Work Element and Subtask. At this point in the project, much of the planned work is completed or near completion, therefore, many of the Subtasks and some Work Elements have coalesced into a larger product (as planned) and current activity is reported there.

This Quarterly Report summarizes the work accomplishments, data, and analysis for the various Work Elements and Subtasks. This report is being presented in a summary form. The Quarter of October 1 to December 31, 2011 is third quarter of the Year 5 contract year. Reviewers may want to reference the previous Annual Work Plans and many other documents that are posted on the ARC website, [www.ARC.unr.edu](http://www.ARC.unr.edu). The more detailed information about the research such as approaches to test method development, data collection, and analyses will be reported in research publications as part of the deliverables. This quarterly report contains updates to the Table of Deliverables that was presented in the Year 5 Work Plan.

## **SUPPORT OF FHWA AND DOT STRATEGIC GOALS**

The Asphalt Research Consortium research is responsive to the needs of asphalt engineers and technologists, state DOT's, and supports the FHWA Strategic Goals and the Asphalt Pavement Road Map. More specifically, the research reported here supports the Strategic Goals of safety, mobility, and environmental stewardship. By addressing the causes of pavement failure and thus determining methods to improve asphalt pavement durability and longevity, this research will provide the motoring public with increased safety and mobility. The research directed at improved use of recycled asphalt pavement (RAP), warm mix asphalt, and cold mix asphalt supports the Strategic Goal of environmental stewardship.



## **GENERAL CONSORTIUM ACTIVITIES**

### **PROGRESS THIS QUARTER**

Several ARC members attended and made presentations at the 2<sup>nd</sup> Warm-Mix Asphalt Conference in St. Louis, Missouri during the week of October 10, 2011.

ARC members met with FHWA personnel on November 9 and 10, 2011, made presentations, and discussed the ARC 21-Month Extension Work Plan.

### **WORK PLANNED FOR NEXT QUARTER**

Several ARC members are planning to attend and make presentations at the 91<sup>st</sup> Annual TRB Meeting in Washington DC during the week of January 22, 2012. ARC members also participate on TRB committees.

Dr. Jean-Pascal Planche from WRI is planning on attending the Annual Association of Modified Asphalt Producers (AMAP) meeting in Albuquerque, New Mexico on February 7 – 8, 2012.

Several ARC members will attend and make presentations at the Binder, Mix & Construction, and Fundamental Properties & Advanced Models ETG meetings in Baton Rouge, Louisiana during the week of March 19 – 23, 2012.

ARC members are planning to attend and participate in the Annual Association of Asphalt Paving Technologists (AAPT) meeting in Austin, Texas on April 1 – 4, 2012.



## PROGRAM AREA: MOISTURE DAMAGE

### CATEGORY M1: ADHESION

#### Work Element M1a: Affinity of Asphalt to Aggregate (UWM)

##### Work Done This Quarter

In this quarter, the research group focused its efforts on comparing the results from the Bitumen Bond Strength (BBS) test and mixture moisture sensitivity testing results using the Tensile Strength Ratio (TSR). The TSR is an indication of the loss of indirect tensile strength at 25°C due to moisture conditioning for 24 hours at 60°C. Results show that the BBS test can rank many materials similarly to the TSR test conducted on compacted mixtures for evaluating stripping potential.

The selected asphalt binders used for the comparison are shown in Table M1a.1. Note that Elastomer3 refers to Styrene-Butadiene-Styrene (SBS) polymer. Plastomer1 and Plastomer2 refer to oxidized polyethylene polymers. A granite fine-graded mixture designed to meet WisDOT (2011) requirements was used.

Table M1a.1. Asphalt binder used to compare BBS and TSR.

| Asphalt Binder  | Polymer Modified Base Stock | Polymer Modifier      | Anti-Stripping (%) |
|-----------------|-----------------------------|-----------------------|--------------------|
| 65% of PG 64-22 | 35% SBS                     | Elastomer3            | 0                  |
|                 |                             |                       | 0.5                |
| 85% of PG 64-22 | 15% SBS                     | SBS + 2.5% Plastomer1 | 0                  |
|                 |                             |                       | 0.5                |
| 85% of PG 64-22 | 15% SBS                     | SBS + 3.5% Plastomer2 | 0                  |
|                 |                             |                       | 0.5                |
| PG 64-22        | None                        | 6% Plastomer2         | 0                  |
|                 |                             |                       | 0.5                |
| PG 64-22        | None                        | 3.5% Plastomer1       | 0                  |
|                 |                             |                       | 0.5                |

##### Significant Results

Table M1a.2 shows the ratio of the wet to dry indirect tensile strength (ITS) of the asphalt mixtures tested. It can be seen that the mixtures containing anti-stripping (AS) had higher TSR than the control mixture (i.e., 76-22+Elastomer3), indicating that the anti-stripping improved the moisture resistance of HMA mixtures. It should be mentioned that obtaining TSR values higher than 1.0 is not uncommon. It is hypothesized that storing mixtures at 60°C for an extended



period could improve bonding between asphalt binder and aggregate due to absorption in surface pores.

Table M1a.3 shows the BBS results after dry and wet conditioning (i.e., 24 hours) of the selected asphalt binders with granite aggregate. It can be seen that Binder 64-22+Plastomer2 has high moisture sensitivity as measured in the indirect tensile strength test. Also, it can be seen that AS additive improved the bond strength after moisture conditioning for all asphalt binders.

Table M1a.2. TSR mixture results.

| Sample              | Dry Conditioning | Wet Conditioning | TSR  | Rank |
|---------------------|------------------|------------------|------|------|
|                     | ITS (psi)        | ITS (psi)        |      |      |
| 76-22+Elastomer3    | 151.4            | 76.0             | 0.50 | C    |
| 76-22+Elastomer3+AS | 161.9            | 128.3            | 0.79 | B    |
| 64-22+Plastomer1    | 112.4            | 111.4            | 0.99 | A    |
| 64-22+Plastomer1+AS | 109.2            | 122.9            | 1.13 | A    |
| 85-15+Plastomer1    | 119.4            | 117.1            | 0.98 | A    |
| 85-15+Plastomer1+AS | 132.9            | 132.2            | 0.99 | A    |
| 64-22+Plastomer2    | 137.8            | 94.0             | 0.68 | C    |
| 64-22+Plastomer2+AS | 137.9            | 125.8            | 0.91 | B    |
| 85-15+Plastomer2    | 134.8            | 70.3             | 0.52 | C    |
| 85-15+Plastomer2+AS | 138.1            | 122.5            | 0.89 | B    |

Table M1a.3. BBS results for asphalt binders on granite aggregate.

| Sample              | Dry conditioning        |        |                   | Wet conditioning        |        |                   | Loss of dry Pull-out Strength (%) | Rank |
|---------------------|-------------------------|--------|-------------------|-------------------------|--------|-------------------|-----------------------------------|------|
|                     | Pull-out Strength (MPa) | CV (%) | Main Failure Type | Pull-out Strength (MPa) | CV (%) | Main Failure Type |                                   |      |
| 76-22+Elastomer3    | 2.445                   | 2.4    | Cohesive          | 1.869                   | 1.80   | Adhesive          | 23.56                             | A    |
| 76-22+Elastomer3+AS | 2.724                   | 1.2    | Cohesive          | 2.085                   | 5.30   | Adhesive          | 23.46                             | A    |
| 64-22+Plastomer1    | 2.683                   | 1.2    | Cohesive          | 1.274                   | 2.90   | Adhesive          | 52.52                             | C    |
| 64-22+Plastomer1+AS | 2.739                   | 0.5    | Cohesive          | 1.997                   | 0.60   | Cohesive          | 27.09                             | A    |
| 85-15+Plastomer1    | 2.672                   | 0.5    | Cohesive          | 1.655                   | 2.00   | Adhesive          | 38.06                             | C    |
| 85-15+Plastomer1+AS | 2.726                   | 0.8    | Cohesive          | 2.327                   | 5.30   | Cohesive          | 14.64                             | A    |
| 64-22+Plastomer2    | 2.698                   | 0.6    | Cohesive          | 1.534                   | 2.60   | Adhesive          | 43.14                             | C    |
| 64-22+Plastomer2+AS | 2.737                   | 0.2    | Cohesive          | 1.808                   | 3.20   | Cohesive          | 33.94                             | B    |
| 85-15+Plastomer2    | 2.636                   | 0.8    | Cohesive          | 1.765                   | 6.10   | Adhesive          | 33.04                             | B    |
| 85-15+Plastomer2+AS | 2.611                   | 0.4    | Cohesive          | 1.587                   | 1.80   | Adhesive          | 39.22                             | C    |

Table M1a.4 shows the ranking according to loss of dry strength in the BBS test and the TSR results of mixtures. It can be seen that the two tests do not rank asphalt binders similarly with respect to moisture susceptibility (i.e., range of lower, medium, and higher moisture resistance).

However in five cases the ranking is matched and it appears that both tests can identify the effect of the anti-stripping additive.

A better relation between the BBS and TSR results could be achieved if a failure type is considered in analysis. Further evaluation of the differences and what is causing them will be investigated in the next quarter. If better results are found, the final report will be amended to include the new findings.

Table M1a.4. BBS and TSR ranking after wet conditioning.

| <b>Sample</b>       | <b>BBS Rank</b> | <b>TSR Rank</b> |
|---------------------|-----------------|-----------------|
| 76-22+Elastomer3    | A               | C               |
| 76-22+Elastomer3+AS | A               | B               |
| 64-22+Plastomer1    | C               | A               |
| 64-22+Plastomer1+AS | A               | A               |
| 85-15+Plastomer1    | C               | A               |
| 85-15+Plastomer1+AS | A               | A               |
| 64-22+Plastomer2    | C               | C               |
| 64-22+Plastomer2+AS | B               | B               |
| 85-15+Plastomer2    | B               | C               |
| 85-15+Plastomer2+AS | C               | B               |

#### Work Planned Next Quarter

The research team will continue the effort to understand the differences between BBS and TSR rankings. Also, the team will work on the development of a standardized procedure to measure contact angle of asphalt binders using the Sessile Drop Method.

It should also be mentioned that the draft report “L” for this task has been submitted in the 508 format. Additionally, a “Tech Brief” has been drafted and submitted for review.

#### References

Wisconsin Department of Transportation, 2011, “*Standard Specifications, Section 460 - Hot Mix Asphalt Pavement*”, pp. 193-205.

## **Work Element M1b: Work of Adhesion Based on Surface Energy**

### ***Subtask M1b-1: Surface Free Energy and Micro-Calorimeter Based Measurements for Work of Adhesion (TAMU)***

#### Work Done This Quarter

The main goal of this subtask is to provide material property inputs required in other work elements as required. Any data obtained from this subtask will be included in the material properties database. In the last quarter surface free energy of some aggregates and asphalt binders that are being used to develop test methods were measured.

#### Significant Results

None.

#### Significant Problems, Issues and Potential Impact on Progress

None.

#### Work Planned Next Quarter

Work on this subtask will be conducted in conjunction with and as required by other work elements.

### ***Subtask M1b-2: Work of Adhesion at Nano-Scale using AFM (WRI)***

#### Work Done This Quarter

Work reported under subtask M2a-2 (Work of Cohesion) is also directly relevant to this subtask.

#### Significant Results

See subtask M2a-2.

### ***Subtask M1b-3: Identify Mechanisms of Competition Between Water and Organic Molecules for Aggregate Surface (TAMU)***

#### Work Done This Quarter

This work element was completed and findings were reported in previous quarterly reports. There was no activity this quarter.

#### Work Planned Next Quarter

None.

## **Work Element M1c: Quantifying Moisture Damage Using DMA (TAMU)**

### Work Done This Quarter

This work element was completed and findings were reported in previous quarterly reports. There was no activity this quarter.

### Work Planned Next Quarter

None.

## **CATEGORY M2: COHESION**

### **Work Element M2a: Work of Cohesion Based on Surface Energy**

#### ***Subtask M2a-1: Methods to Determine Surface Free Energy of Saturated Asphalt Binders (TAMU)***

Note about Work Element M2a: Per the Year 5 work plan, the objectives of this work element will be accomplished in other tasks.

#### ***Subtask M2a-2: Work of Cohesion Measured at Nano-Scale using AFM (WRI)***

### Work Done This Quarter

Experiments conducted in the previous quarter indicate rate dependence when work of adhesion (essentially fracture energy) was determined for an asphalt/glass contact using AFM force displacement measurements. The rate dependence of the measured work of adhesion is attributed to energy dissipation mainly as visco-plastic flow in an area around the ‘fracture zone’ when the AFM probe tip is pulled away from the surface. For the asphalt glass system, as used in our testing, the work of adhesion indicated by AFM pull-off force measurements can be considerably larger than the (reversible) work predicted by the JKR (Perutz 1998) model. This additional work is a measure of the dissipated or non-reversible work that is involved in the fracture of an asphalt/glass adhesive bond. These preliminary experiments indicate that variable rate AFM force displacement measurements can provide a method to quantitatively evaluate this dissipative component of the work of adhesion for an asphalt substrate. Quantifying fracture energy in terms of reversible and dissipative components will help to advance ongoing efforts to model in-service fracture (and healing potential) of asphalt pavements.

The experimentally determined work of adhesion for an asphalt/glass contact, as measured by AFM force displacement testing, depends upon both the temperature and the rate used for the loading and unloading of the tip/sample contact. The time-dependence of the measured work of adhesion is commonly observed in force displacement type testing of adhesive joints. For polymeric adhesives this time dependence can be ascribed to viscoelastic dissipation and/or

interfacial structural rearrangements (e.g. Barthel 2009). While not a true polymer, asphalt shares a number of characteristics (e.g., viscoelastic flow) with these materials. We believe that concepts devised for the analysis of fracture in polymers can be adapted to help understand the fracture of asphalt materials.

Barthel (2009) notes the close functional relationship between elastomeric adhesion and the cracking of viscoelastic materials. In viscoelastic fracture the concept of a cohesive zone at the crack tip is introduced to accommodate the velocity dependence of the fracture energy. The cohesive zone concept is commonly applied by the asphalt research community in models designed to predict fracturing in asphalt pavements. A similar cohesive zone concept can be applied in the analysis of the AFM force displacement curve (FDC) data collected as an asphalt/glass bond is fractured.

Work conducted this quarter focused mainly on the problem of separating and beginning to quantify the reversible and dissipative components that contribute to the overall work of adhesion as measured during ‘fracture’ of an asphalt adhesive contact. Our work this quarter demonstrates an AFM technique that can provide quantitative, or at least semi-quantitative, evaluation of the dissipative component of the overall work of adhesion related to the fracture of an asphalt/substrate bond. We also report the results of preliminary testing of an adhesive microprobe on the rough surface created when a miniature aggregate core is fractured diametrically.

In experiments conducted this quarter an asphalt film was probed with a glass micro-bead tip and force curves were collected at multiple rates and temperatures. Work of adhesion was then calculated as the area bounded by the unloading curve and the zero-force axis and plotted against rate for each temperature. The FDC data used to generate the work of adhesion versus rate plots shown below was collected using a sample film of SHRP core asphalt AAA-1 on glass. The film thickness was calculated to be  $\sim 5\text{-}\mu\text{m}$ . A cantilever with a  $10\text{-}\mu\text{m}$  diameter borosilicate glass bead tip and  $\sim 14\text{-N/m}$  spring constant was used to collect the force curve data that was used to generate the figures shown below.

### Significant Results

Figure M2a-2.1 shows the change in work of adhesion with increasing separation velocity for one experiment as the glass bead tip is pulled away from the asphalt surface at 12, 25, and 40°C. At  $\sim 25^\circ$  the apparent work expended to fracture the asphalt glass contact is seen to increase with increasing separation velocity. When cooled slightly ( $\sim 12^\circ\text{C}$ ) work of adhesion, for this asphalt/glass contact, becomes independent of separation velocity over the range used in these experiments. At  $\sim 40^\circ$  the fracture energy (work of adhesion) increases sharply with increasing separation velocity. Figure M2a-2.2 shows these same data plotted as work of adhesion versus temperature.

For quantitative comparison across this temperature range the reported work of adhesion values need to be normalized with respect to contact area. With the spherical probe tip and assuming a viscoelastic system there is a relationship between penetration depth and effective contact area due to non-recovered surface deformation. It is therefore reasonable, given the same loading

condition, to expect a larger contact area for the warmer (i.e., softer) asphalt. The large work of adhesion at low velocity shown for the asphalt glass contact at 40°C could be due, at least partially, to an increase in the contact area related to the increased temperature. We are currently working to develop an appropriate normalization technique.

Figure M2a-2.3 shows the data with the 11°C data and the 40°C offset to show the trend when all three curves start at the same value. In this figure, the initial work of adhesion is set at an equal value for all three temperatures at the lowest separation rate. The adjusted figure still clearly indicates a large increase in work of adhesion (i.e. fracture energy) for the 40°C asphalt as the separation rate is increased. This excess work of adhesion is a measure of the dissipative component of the overall fracture energy as represented by work of adhesion. The offset applied to generate figure M2a-2.3 is only for the purpose of illustration and cannot be justified as a method of quantitatively comparing contact areas for the various temperatures represented in the figure. Work to develop a series of appropriate contact models that will work across the desired temperature range is ongoing.

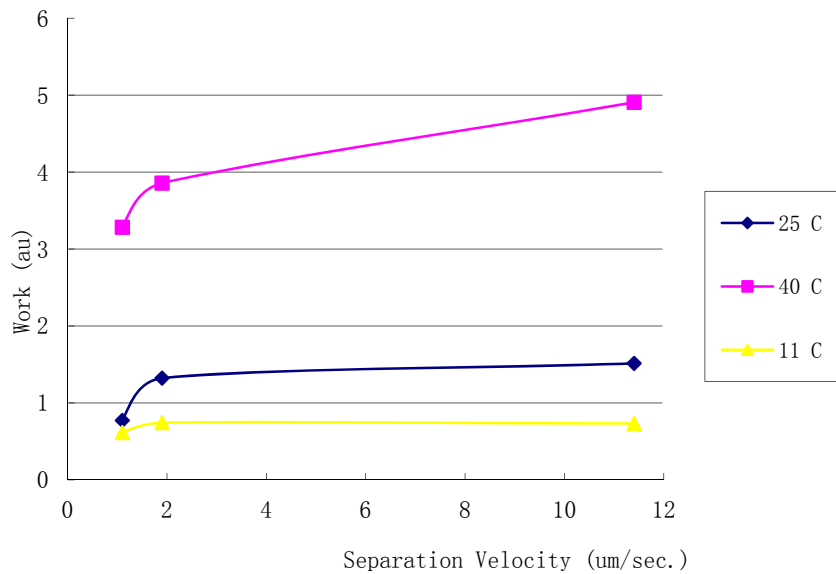


Figure M2a-2.1. Work of adhesion vs. pull-off speed for AAA-1 asphalt on glass at three temperatures.

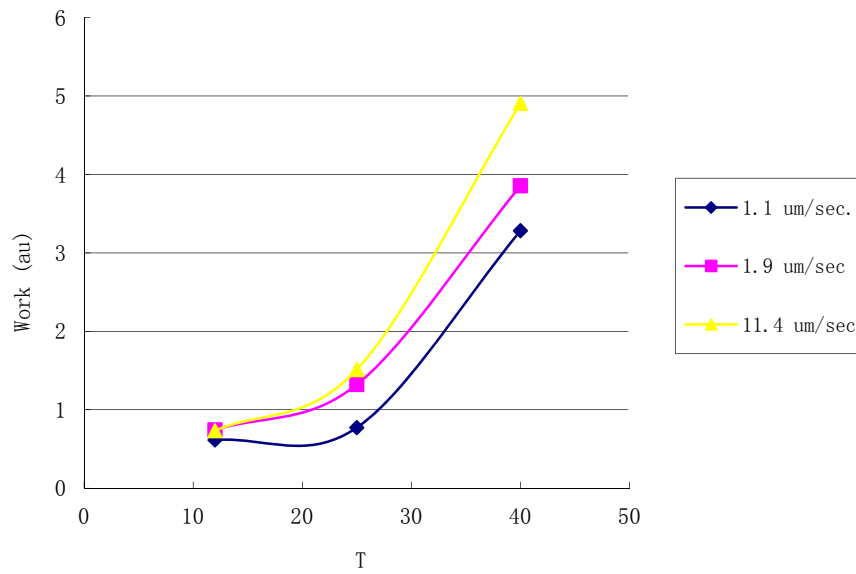


Figure M2a-2.2. Work of adhesion vs. temperature for three pull-off rates.

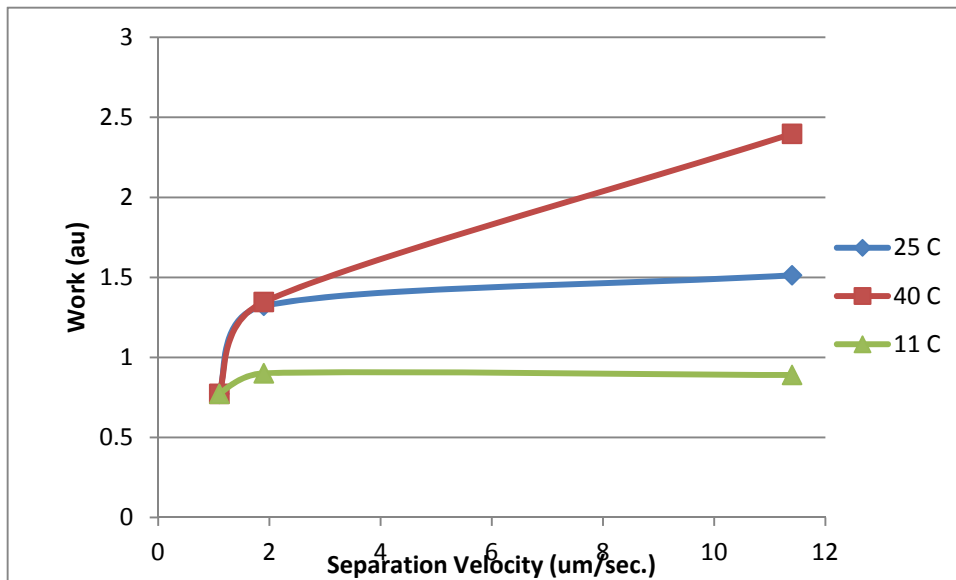


Figure M2a-2.3. Work of adhesion vs. temperature for three pull-off rates.

Adhesive microprobe testing, as described in last quarter's report, was attempted on a fractured aggregate surface. The aggregate sample was prepared by drilling a small (~5-mm diameter) core from a sawed slab of granite (SHRP MRL RB aggregate). The small core was then split diametrically by simultaneously applying pressure to four sharp points around the circumference of the cylinder. The sample was then mounted, fractured side up, for pull-off-force measurement

using the AFM. When viewed under a low-power microscope, the fractured surface exhibited significant roughness.

We had hoped that the 10- $\mu\text{m}$  probe tip diameter would be large enough to span across peaks and valleys to establish an essentially rigid contact with the fractured surface. As shown in figure M2a-2.4, this did not prove to be the case. When the asphalt coated tip was pressed onto the surface with an applied force of  $\sim 2.8\text{-}\mu\text{N}$ , the tip appeared to sink steadily into the surface of the granite. Instead of spanning peaks and valleys, the tip appears to slide down the peaks and into valleys. Little or no adhesion (in terms of a measureable pull-off force) was detected between the adhesive microprobe and the fractured aggregate surface. The possible importance of this observation with respect to how individual mastic particles may interact with an aggregate surface is being considered while we begin to conduct this type of testing on more polished aggregate surfaces.

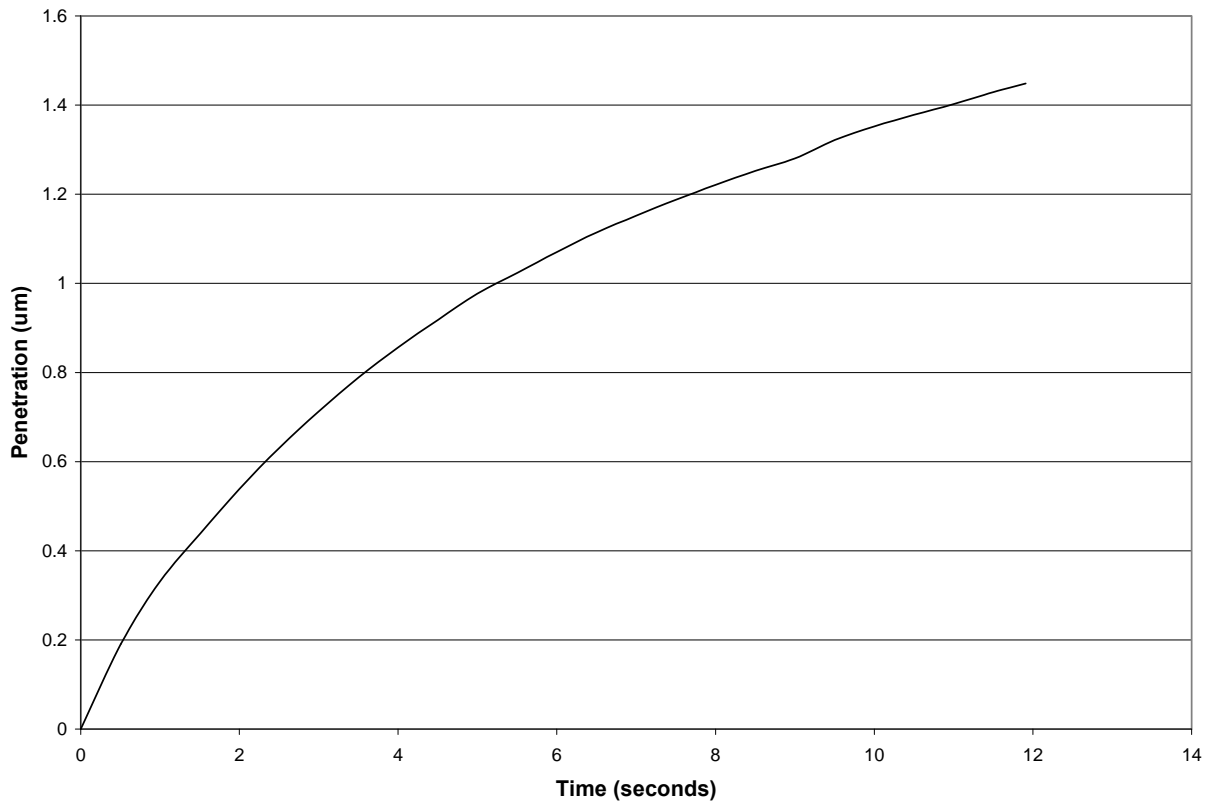


Figure M2a-2.4. Apparent penetration of 10- $\mu\text{m}$  glass bead tip into fractured aggregate surface.

### Significant Problems, Issues and Potential Impact on Progress

We are currently training two new people to conduct these experiments. The training effort has temporarily slowed data collection.



### Work Planned Next Quarter

For the next quarter work will continue toward quantifying the reversible and the dissipative components of asphalt binder fracture energy. Tests will be conducted to optimize experimental conditions and to determine appropriate ranges for the temperature and separation rate variables. Work toward modeling of the contact area over the desired temperature range will continue. Adhesive microprobe testing will continue, but much smoother aggregate surfaces with differing degrees of polish will be employed.

### Cited References

Barthel, E., and C. Fretigny, 2009, Adhesive contact of elastomers: effective adhesion energy and creep function. *Journal of Physics D: Applied Physics*, 42, 195302 (9 pp).

Perutz, S., E.J. Kramer, J. Baney, C.-Y. Hui, and C. Cohen, 1998, Investigation of Adhesion Hysteresis in Poly (dimethylsiloxane) Networks Using the JKR Technique. *Journal of Polymer Science: Part B: Polymer Physics*, 36, 2129-2139.

### **Work Element M2b: Impact of Moisture Diffusion in Asphalt Mixtures**

***Subtask M2b-1: Measurements of Diffusion in Asphalt Binders and Mixtures (TAMU)***

***Subtask M2b-2: Kinetics of Debonding at the Binder-Aggregate Interface (TAMU)***

### Work Done This Quarter

There was no activity this quarter.

### Work Planned Next Quarter

We have accomplished significant portions of this work element including measurement of diffusion through binders and fine aggregate matrix. Further work will be conducted if prioritized based on the requirements from other work elements.

### **Work Element M2c: Measuring Thin Film Cohesion and Adhesion Using the PATTI Test and the DSR (UWM)**

The remaining activity is reported under Work Element M1a.

## **CATEGORY M3: AGGREGATE SURFACE**

### **Work Element M3a: Aggregate Surface Characterization (TAMU)**

This work element was completed and findings were reported in previous quarterly reports. There was no activity this quarter.

## **CATEGORY M4: MODELING**

### **Work Element M4a: Micromechanics Model (TAMU, UNL)**

#### ***Subtask M4a-1: Model Development***

##### Work Done This Quarter

In the last quarter, we have worked on the final report. A draft final report completed was submitted to the Texas A&M University for review.

##### Significant Problems, Issues and Potential Impact on Progress

None.

##### Work Planned Next Quarter

In the next quarter we will update the final report based on feedback/comments from the Texas A&M University.

### **Work Element M4b: Analytical Fatigue Model for Mixture Design (TAMU)**

This work element is addressed under Work Element F1b-1 and E1a.

### **Work Element M4c: Unified Continuum Model (TAMU)**

##### Work Done This Quarter

The work done this quarter concentrated on completing the development of a thermodynamic-based moisture-induced damage model that takes into consideration the effects of the presence and the flow of the moisture. Emphasis is placed on the consideration of the pore-water pressure that accelerates crack evolution and propagation due to presence of moisture. In addition, the flow of moisture washes away the mastic material causing erosion. It is also emphasized to take into account the effect of this erosion damage caused by moisture flow through the asphalt mixtures. Both energetic and dissipative processes are clearly distinguished through this thermodynamic framework. This model is going to be calibrated and validated with the results of

ARC 2x2 experimental data which its moisture conditioning protocol and tests types are assigned to be done.

Moreover, three-dimensional (3D) micromechanical moisture-damage simulations have been done. Several simulations on the 3D micromechanical model have been done in order to investigate the effect of moisture conditioning time, moisture content, material properties parameters, strain rate, and temperature at both tension and compression. The results completely show the crack propagation and damage concentration after moisture conditioning the specimens. These simulations can be used to conduct virtual moisture-damage simulation experiments.

#### Significant Results

None

#### Significant Problems, Issues and Potential Impact on Progress

The ARC 2x2 experimental data for validating the moisture-induced damage modeling is not available yet.

#### Work Planned Next Quarter

The next quarter work will be focused on completing the thermodynamic framework that is taking into consideration the different degradation mechanisms due to presence of moisture. This thermodynamic framework is necessary in order to correctly consider the different moisture-induced damage mechanisms and the coupling between them. Moreover, work will continue on conducting three-dimensional micromechanical moisture-damage simulations. Virtual specimens based on the ARC mixtures will be generated using X-ray CT and the finite element method.

### **CATEGORY M5: MOISTURE DAMAGE PREDICTION SYSTEM (All, TAMU lead)**

Work on individual components such as test methods and micromechanics models required in the system is complete. The components will be put together in the form of a methodology towards the end of this project.

**TABLE OF DECISION POINTS AND DELIVERABLES FOR MOISTURE DAMAGE**

| <b>Name of Deliverable</b>   | <b>Type of Deliverable</b> | <b>Description of Deliverable</b>   | <b>Original Delivery Date</b> | <b>Revised Delivery Date</b> | <b>Reason for changes in delivery date</b>  |
|--|----------------------------|---|-------------------------------|------------------------------|---|
| M1a-5: Propose a novel testing protocol (UWM)  | Draft Report               | Development and Implementation of the Bitumen Bond Strength test for Moisture Damage Characterization       | 1/10                          | 8/11 Complete                | Additional analysis/verification on the BBS test is included: operator sensitivity data, validation with TSR mixture testing and comparison with contact angle measurements. Report has been consolidated as one chapter and suggested to be included in TAMU report for moisture damage. |
|  | Final Report               | Report in 508 format on the use of the Bitumen Bond Strength test for Moisture Damage Characterization      | 1/11                          | 4/12                         | First round of revisions by FHWA being implemented. (Report "L").<br>Second draft submitted to FHWA after implementing first round of revisions.  |
| M1b-2: Work of Adhesion at Nano-Scale using AFM (WRI)  | Test Method                | A method to determine surface roughness of aggregate and fines based on AFM                                 | 12/30/11                      |                              | N/A   |
| M1b-3: Identify mechanisms of competition between water and organic molecules for aggregate surface (TAMU) | Draft Report               | Final report documenting the testing protocol and findings of experiments on asphalt-aggregate interactions | 10/31/10                      | Complete                     | To be included in the comprehensive report on moisture damage from Texas A&M University.  |
|  | Final Report               |   | 4/30/12                       |                              |   |
| M1c: Quantifying Moisture Damage Using DMA (TAMU)  | AASHTO procedure           | AASHTO procedure for preparing Fine Aggregate Matrix (FAM) specimens for the DMA testing                    | 9/30/10                       | Complete                     | N/A   |
|  | Draft Report               | Use of the method to characterize various mixtures with comparison to field performance                     | 12/31/10                      | Complete                     |   |
|  | Final Report               |   | 3/31/11                       | 6/30/11                      | Report to be made 508 compliant   |
| M2a-2: Work of Cohesion at Nano-Scale using AFM (WRI)  | Test Method                | A method to determine ductile-brittle properties via AFM measurements                                       | 12/30/11                      |                              | N/A   |

| <b>Name of Deliverable</b>  | <b>Type of Deliverable</b> | <b>Description of Deliverable</b>  | <b>Original Delivery Date</b> | <b>Revised Delivery Date</b> | <b>Reason for changes in delivery date</b>   |
|---|----------------------------|--|-------------------------------|------------------------------|--|
| M2b-1: Measurement of diffusion of water through thin films of asphalt binders and FAM (TAMU) | Draft Report               | Mechanism and model for the diffusion of moisture through films of asphalt binder, methods to measure diffusivity in binders and mortars, and the influence of wet-dry cycles on the cumulative moisture induced damage.                         | 6/30/10                       | Complete                     | The dissertation was completed at TAMU and needs editing for 508 format                  |
|   | Final Report               |  | 9/30/11                       | 12/31/11                     |  |
| M3a: Aggregate Surface Characteristics (TAMU)   | Research report            | Report on methods and experimental findings and utility of methodology and findings  | 6/30/10                       | Complete                     | To be included in the comprehensive report on moisture damage from Texas A&M University. |
|   | Research report            | Describes implementation of findings into PANDA and expands experiments to characterization for four aggregates used for validation experiments  | 6/30/11                       |                              |  |
| M4a: Micro-mechanics Model (TAMU)   | Draft Report               | Numerical micromechanical model of moisture-induced damage in asphalt mixtures. This report will include the algorithm and modeling method.  | Sep-11                        | Complete                     |  |
|   | Final Report               |  | Sep-11                        | Mar-12                       |  |
| M4a: Micromechanics Model Development (Moisture Damage) (UNL)                                 | Models and Algorithm       | Cohesive zone modeling with moisture damage of asphalt mixtures considering mixture microstructure: modeling methodology, constitutive theory, testing protocols, test data, model simulation/calibration/validation, and user-friendly manuals. | 3/31/11                       | Complete                     | Models will be included in final report.   |
|   | Draft report               |  | 06/30/11                      | 12/11                        | More time needed to finish extra simulations and documenting final report                |
|   | Final report               |  | 12/31/11                      | 8/14/12                      |  |
| M4a: Lattice Micromechanics Model (NCSU)  | Draft Report               | Documenting development of lattice micromechanical model   | 2/14/12                       |                              | N/A  |
|   | Final Report               | Documenting development of lattice micromechanical model   | 8/14/12                       |                              |  |
| M4a: Model to Bridge Continuum Damage and Fracture (NCSU)                                     | Draft Report               | Documenting development of continuum damage-to-fracture model  | N/A                           | 2/14/12                      | N/A  |
|   | Final Report               | Documenting development of continuum damage-to-fracture model  | 2/14/12                       | 8/14/12                      |  |

| <b>Name of Deliverable</b>                  | <b>Type of Deliverable</b>                              | <b>Description of Deliverable</b>  | <b>Original Delivery Date</b> | <b>Revised Delivery Date</b> | <b>Reason for changes in delivery date</b>   |
|---|---|--|-------------------------------|------------------------------|--|
| M4c: Unified Continuum Model (TAMU)         | Models and Algorithm                                    | Algorithm for including moisture damage in the model   | 6/30/11                       | 12/31/12                     | Model needs to be updated based on calibration with experimental measurements            |
|   | Draft Report  | Draft Report on the moisture-damage modeling   | 9/30/11                       | 12/31/12                     |  |
|   | Final Report (M5, M4c, F1b-1, F1c, F1d-8, F3c, and V3c) | Report in 508 format that describes a comprehensive and integrated approach to assessing moisture damage on three scales; binder and aggregate components, fine aggregate matrix with DMA and in the full mix – Alternative to more sophisticated PANDA approach | 03/31/12                      | 3/31/13                      | Work is progressing in the validation based on ARC experiments.                          |
| M5: Moisture Damage Prediction System (All) | Protocol  | Protocol for implementation of component selection   | 6/30/11                       | Complete                     | To be included in the comprehensive report on moisture damage from Texas A&M University. |
|   | Experimental method                                     | Experimental method for measuring moisture damage resistance of full mixture   | 9/30/11                       | Complete                     |  |
|   | Draft Report (M5, M4c, F1b-1, F1c, F1d-8, F3c, and V3c) | Report in 508 format that describes a comprehensive and integrated approach to assessing moisture damage on three scales; binder and aggregate components, fine aggregate matrix with DMA and in the full mix – Alternative to more sophisticated PANDA approach | 12/31/11                      |                              |  |
|   | Final Report (M5, M4c, F1b-1, F1c, F1d-8, F3c, and V3c) |  | 3/31/12                       | 3/31/13                      | Preparation of a comprehensive report.   |


| Moisture Damage Year 5   |  | Year 5 (4/11-3/12) |   |   |   |   |   |    |    |    |        |   |    | Team              |
|--------------------------|--|--------------------|---|---|---|---|---|----|----|----|--------|---|----|-------------------|
|                          |  | 4                  | 5 | 6 | 7 | 8 | 9 | 10 | 11 | 12 | 1      | 2 | 3  |                   |
| <b>Adhesion</b>          |  |                    |   |   |   |   |   |    |    |    |        |   |    |                   |
| <b>M1a</b>               | <b>Affinity of Asphalt to Aggregate - Mechanical Tests</b>                   |                    |   |   |   |   |   |    |    |    |        |   |    |                   |
| M1a-1                    | Select Materials   |                    |   |   |   |   |   |    |    |    |        |   |    | UWM               |
| M1a-2                    | Conduct PATTI and modified DSR tests   |                    |   |   |   |   |   |    |    |    |        |   |    |                   |
| M1a-3                    | Evaluate the moisture damage of asphalt mixtures                             |                    |   |   |   |   |   |    |    |    |        |   |    |                   |
| M1a-4                    | Correlate moisture damage between DSR, PATTI, and mix tests                  |                    |   |   |   |   |   |    |    |    |        |   |    |                   |
| M1a-5                    | Propose a Novel Testing Protocol   |                    |   |   |   |   |   |    |    |    |        |   |    |                   |
| M1a-6                    | Standard Testing Procedure and Recommendation for Specifications             |                    |   |   |   |   |   |    |    |    |        |   |    |                   |
| <b>M1b</b>               | <b>Work of Adhesion</b>  |                    |   |   |   |   |   |    |    |    |        |   |    |                   |
| M1b-1                    | Adhesion using Micro calorimeter and SFE                                     |                    |   |   |   |   |   |    |    |    |        |   |    | TAMU              |
| M1b-2                    | Evaluating adhesion at nano scale using AFM                                  |                    |   |   |   |   |   |    |    |    |        |   |    | WRI               |
| M1b-3                    | Mechanisms of water-organic molecule competition                             |                    |   |   |   |   |   |    |    |    |        |   |    | TAMU              |
| <b>M1c</b>               | <b>Quantifying Moisture Damage Using DMA</b>                                 |                    |   |   |   |   |   |    |    |    |        |   |    | TAMU              |
| <b>Cohesion</b>          |  |                    |   |   |   |   |   |    |    |    |        |   |    |                   |
| <b>M2a</b>               | <b>Work of Cohesion Based on Surface Energy</b>                              |                    |   |   |   |   |   |    |    |    |        |   |    |                   |
| M2a-1                    | Methods to determine SFE of saturated binders                                |                    |   |   |   |   |   | JP |    |    |        |   |    | TAMU              |
| M2a-2                    | Evaluating cohesion at nano scale using AFM                                  |                    |   |   |   |   |   |    |    |    |        |   |    | WRI               |
| <b>M2b</b>               | <b>Impact of Moisture Diffusion in Asphalt</b>                               |                    |   |   |   |   |   |    |    |    |        |   |    |                   |
| M2b-1                    | Diffusion of moisture through asphalt/mastic films                           |                    |   |   |   |   |   | F  |    |    |        |   |    | TAMU              |
| M2b-2                    | Kinetics of debonding at binder-aggregate interface                          |                    |   |   |   |   |   |    |    |    |        |   |    |                   |
| <b>M2c</b>               | <b>Thin Film Rheology and Cohesion</b>                                       |                    |   |   |   |   |   |    |    |    |        |   |    |                   |
| M2c-1                    | Evaluate load and deflection measurements using the modified PATTI test      |                    |   |   |   |   |   |    |    |    |        |   |    | UWM               |
| M2c-2                    | Evaluate effectiveness of the modified PATTI test for Detecting Modification |                    |   |   |   |   |   |    |    |    |        |   |    |                   |
| M2c-3                    | Conduct Testing  |                    |   |   |   |   |   |    |    |    |        |   |    |                   |
| M2c-4                    | Analysis & Interpretation  |                    |   |   |   |   |   |    |    |    |        |   |    |                   |
| M2c-5                    | Standard Testing Procedure and Recommendation for Specifications             |                    |   |   |   |   |   |    |    |    |        |   |    | see Subtask M1a-6 |
| <b>Aggregate Surface</b> |  |                    |   |   |   |   |   |    |    |    |        |   |    |                   |
| <b>M3a</b>               | <b>Impact of Surface Structure of Aggregate</b>                              |                    |   |   |   |   |   |    |    |    |        |   |    |                   |
| M3a-1                    | Aggregate surface characterization   |                    |   |   |   |   |   |    |    |    |        |   |    | TAMU              |
| <b>Modeling</b>          |  |                    |   |   |   |   |   |    |    |    |        |   |    |                   |
| <b>M4a</b>               | <b>Micromechanics model development</b>                                      |                    |   |   | D |   |   | DP |    |    | F,SW   |   | JP | TAMU              |
| <b>M4b</b>               | <b>Analytical fatigue model for use during mixture design</b>                |                    |   |   |   |   |   |    |    |    | M&A, D |   | F  | TAMU              |
| <b>M4c</b>               | <b>Unified continuum model</b>   |                    |   |   | D |   |   | DP |    |    | F,SW   |   |    | TAMU              |
| <b>M5</b>                | <b>Moisture Damage Prediction System</b>                                     |                    |   |   |   |   |   |    |    |    |        |   |    | ALL               |

**LEGEND**

**Deliverable codes**

- D: Draft Report
- F: Final Report
- M&A: Model and algorithm
- SW: Software
- JP: Journal paper
- P: Presentation
- DP: Decision Point

[x]

-  Work planned
-  Work completed
-  Parallel topic

**Deliverable Description**

- Report delivered to FHWA for 3 week review period.
- Final report delivered in compliance with FHWA publication standards
- Mathematical model and sample code
- Executable software, code and user manual
- Paper submitted to conference or journal
- Presentation for symposium, conference or other
- Time to make a decision on two parallel paths as to which is most promising to follow through
- Indicates completion of deliverable x


| Moisture Damage Year 2 - 5 |  | Year 2 (4/08-3/09) |    |    |      | Year 3 (4/09-3/10) |    |    |    | Year 4 (04/10-03/11) |    |    |     | Year 5 (04/11-03/12) |    |       |                   | Team |
|----------------------------|--|--------------------|----|----|------|--------------------|----|----|----|----------------------|----|----|-----|----------------------|----|-------|-------------------|------|
|                            |  | Q1                 | Q2 | Q3 | Q4   | Q1                 | Q2 | Q3 | Q4 | Q1                   | Q2 | Q3 | Q4  | Q1                   | Q2 | Q3    | Q4                |      |
| <b>Adhesion</b>            |  |                    |    |    |      |                    |    |    |    |                      |    |    |     |                      |    |       |                   |      |
| <b>M1a</b>                 | <b>Affinity of Asphalt to Aggregate - Mechanical Tests</b>                   |                    |    |    |      |                    |    |    |    |                      |    |    |     |                      |    |       |                   |      |
| M1a-1                      | Select Materials   |                    | DP |    |      |                    |    |    |    |                      |    |    |     |                      |    |       | UWM               |      |
| M1a-2                      | Conduct PATTI and modified DSR tests   |                    | P  |    | P    |                    |    |    |    |                      |    |    |     |                      |    |       |                   |      |
| M1a-3                      | Evaluate the moisture damage of asphalt mixtures                             |                    |    |    | DP   |                    | P  |    |    | P                    | JP |    | P   |                      |    |       |                   |      |
| M1a-4                      | Correlate moisture damage between DSR, PATTI, and mix tests                  |                    |    |    |      |                    | P  |    | P  |                      |    |    |     |                      |    |       |                   |      |
| M1a-5                      | Propose a Novel Testing Protocol   |                    |    |    | P    |                    |    |    | P  |                      |    |    | JP  |                      |    |       |                   |      |
| M1a-6                      | Standard Testing Procedure and Recommendation for Specifications             |                    |    |    |      |                    |    |    |    | P                    |    |    |     |                      | D  | F     |                   |      |
| <b>M1b</b>                 | <b>Work of Adhesion</b>  |                    |    |    |      |                    |    |    |    |                      |    |    |     |                      |    |       |                   |      |
| M1b-1                      | Adhesion using Micro calorimeter and SFE                                     |                    |    |    |      |                    | JP |    |    |                      |    |    |     |                      |    |       | TAMU              |      |
| M1b-2                      | Evaluating adhesion at nano scale using AFM                                  |                    |    |    |      |                    |    | JP |    |                      |    |    |     |                      |    | JP, F | WRI               |      |
| M1b-3                      | Mechanisms of water-organic molecule competition                             |                    |    |    | JP   |                    |    |    |    |                      |    |    |     |                      |    |       | TAMU              |      |
| <b>M1c</b>                 | <b>Quantifying Moisture Damage Using DMA</b>                                 |                    |    |    |      |                    |    |    |    |                      | JP | D  | F   |                      |    |       | TAMU              |      |
| <b>Cohesion</b>            |  |                    |    |    |      |                    |    |    |    |                      |    |    |     |                      |    |       |                   |      |
| <b>M2a</b>                 | <b>Work of Cohesion Based on Surface Energy</b>                              |                    |    |    |      |                    |    |    |    |                      |    |    |     |                      |    |       |                   |      |
| M2a-1                      | Methods to determine SFE of saturated binders                                |                    |    |    |      |                    |    |    |    |                      |    |    |     | JP                   |    |       | TAMU              |      |
| M2a-2                      | Evaluating cohesion at nano scale using AFM                                  |                    |    |    |      |                    |    | JP |    |                      |    |    |     |                      |    | JP, F | WRI               |      |
| <b>M2b</b>                 | <b>Impact of Moisture Diffusion in Asphalt</b>                               |                    |    |    |      |                    |    |    |    |                      |    |    |     |                      |    |       |                   |      |
| M2b-1                      | Diffusion of moisture through asphalt/mastic films                           |                    |    |    |      |                    | JP | D  | F  | D                    | F  |    |     |                      | F  |       | TAMU              |      |
| M2b-2                      | Kinetics of debonding at binder-aggregate interface                          |                    |    |    |      |                    |    |    |    |                      |    |    |     |                      |    |       |                   |      |
| <b>M2c</b>                 | <b>Thin Film Rheology and Cohesion</b>                                       |                    |    |    |      |                    |    |    |    |                      |    |    |     |                      |    |       |                   |      |
| M2c-1                      | Evaluate load and deflection measurements using the modified PATTI test      | DP                 | JP | D  | F    |                    |    |    |    |                      |    |    |     |                      |    |       | UWM               |      |
| M2c-2                      | Evaluate effectiveness of the modified PATTI test for Detecting Modification |                    |    | D  | DP,F |                    |    |    |    |                      |    |    |     |                      |    |       |                   |      |
| M2c-3                      | Conduct Testing  |                    |    |    |      |                    | JP |    |    |                      |    |    |     |                      |    |       |                   |      |
| M2c-4                      | Analysis & Interpretation  |                    |    |    | P    |                    |    | D  |    |                      |    |    |     |                      |    |       |                   |      |
| M2c-5                      | Standard Testing Procedure and Recommendation for Specifications             |                    |    |    |      | D                  |    |    |    |                      |    |    |     |                      |    |       | see Subtask M1a-6 |      |
| <b>Aggregate Surface</b>   |  |                    |    |    |      |                    |    |    |    |                      |    |    |     |                      |    |       |                   |      |
| <b>M3a</b>                 | <b>Impact of Surface Structure of Aggregate</b>                              |                    |    |    |      |                    |    |    |    |                      |    |    |     |                      |    |       |                   |      |
| M3a-1                      | Aggregate surface characterization   |                    |    |    |      |                    |    |    |    | JP                   |    |    |     |                      |    |       | TAMU              |      |
| <b>Models</b>              |  |                    |    |    |      |                    |    |    |    |                      |    |    |     |                      |    |       |                   |      |
| <b>M4a</b>                 | <b>Micromechanics model development</b>                                      |                    |    |    | JP   |                    |    |    | JP |                      |    |    | M&A | D                    | DP | F, SW | JP                | TAMU |
| <b>M4b</b>                 | <b>Analytical fatigue model for use during mixture design</b>                |                    |    |    |      |                    |    |    |    |                      |    |    |     |                      |    | M&A,D | F                 | TAMU |
| <b>M4c</b>                 | <b>Unified continuum model</b>   |                    |    |    |      |                    |    | JP |    |                      |    |    | M&A | D                    | DP | F, SW | TAMU              |      |
| <b>M5</b>                  | <b>Moisture Damage Prediction System</b>                                     |                    |    |    |      |                    |    |    |    |                      |    |    |     |                      |    |       |                   | ALL  |

**LEGEND**

**Deliverable codes**

- D: Draft Report
- F: Final Report
- M&A: Model and algorithm
- SW: Software
- JP: Journal paper
- P: Presentation
- DP: Decision Point

[x]

-  Work planned
-  Work completed
-  Parallel topic

**Deliverable Description**

- Report delivered to FHWA for 3 week review period.
- Final report delivered in compliance with FHWA publication standards
- Mathematical model and sample code
- Executable software, code and user manual
- Paper submitted to conference or journal
- Presentation for symposium, conference or other
- Time to make a decision on two parallel paths as to which is most promising to follow through
- Indicates completion of deliverable x





## **PROGRAM AREA: FATIGUE**

### **CATEGORY F1: MATERIAL AND MIXTURE PROPERTIES**

#### **Work Element F1a: Cohesive and Adhesive Properties (TAMU)**

##### Work Done This Quarter

This task was completed.

##### Significant Results

The results demonstrated that a multiplicative relationship exists between the ideal and practical work of fracture. The relationship between these two quantities depends on binder compliance, loading rate, and temperature. This work has validated that the ideal work of fracture, which is calculated from surface energy, is a fundamental property than can be used to rank asphalt-aggregate systems based on their resistance to fracture under dry and wet conditions.

#### **Work Element F1b: Viscoelastic Properties (Year 1 start)**

##### ***Subtask F1b-1: Viscoelastic Properties under Cyclic Loading (UT and TAMU)***

##### Work Done This Quarter

The accuracy of computational models being used at different length scales is contingent on the accuracy of the material properties that are used to drive such models. Most computational models assume a linear viscoelastic model without any interaction (effect of shear and normal forces acting together) and a constant Poisson's ratio. To this end, during the previous quarters we had developed a method to measure the interaction nonlinearity in asphalt binders using the DSR. The nonlinear response was modeled by modifying a thermodynamic-based constitutive model developed by Schapery (1969). The model was also verified by conducting tests with loading histories other than those used to obtain the model parameters. This will be extended to sand-asphalt mixtures (FAM) in future work. During the last quarter we developed and executed an experiment design to determine the time dependency of Poisson's ratio and bulk modulus of asphalt binders.

The bulk modulus of an asphalt binder was obtained by measuring the change in axial stress,  $\sigma_z(t)$ , in the poker-chip geometry specimen under step strain load in compression,  $\epsilon_0$ . Solving the boundary value problem, it can be shown that the stress in the poker-chip test changes as a function of bulk modulus and shear modulus:

$$\sigma_z(t) = \left[ \frac{4}{3} \mu(t) + K(t) \right] \varepsilon_0 \quad (\text{F1b-1.1})$$

where  $K(t)$  is the bulk modulus and  $\mu(t)$  is the shear relaxation modulus. Therefore, in order to obtain the bulk modulus from the poker-chip test, the shear modulus of the asphalt binder was also measured at the same temperature. This was done using a Dynamic Shear Rheometer (DSR) with a cone and plate geometry. A cone and plate geometry was used in order to achieve a uniform stress and strain distribution within the specimen. Having a uniform stress and strain distribution ensures measuring the true shear properties of asphalt binders. The poker chip tests were carried out using Instron ElectroPuls E1000 test instrument. This instrument has a linear motor that is capable of applying step loads with a very small raising time. Figure F1b-1.1 shows the test geometries used in this study. The tests were conducted on two ARC asphalt binders (B001 and B002) at 20°C. These binders were RTFO-aged to simulate the short-term.

### Significant Results

The test results show that the bulk modulus of the asphalt binder changes with time and is not constant. It was also observed that the rate of change in bulk modulus does not follow the rate of change in shear relaxation modulus. Considering the relation between shear and bulk modulus, this implies that the Poisson's ratio is not constant and changes with time.

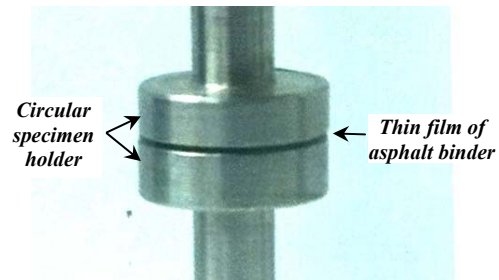
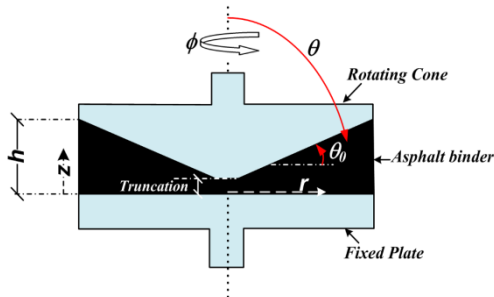
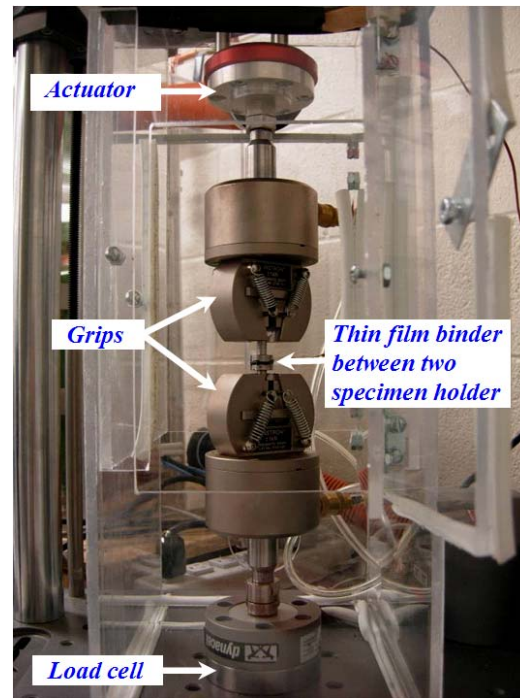
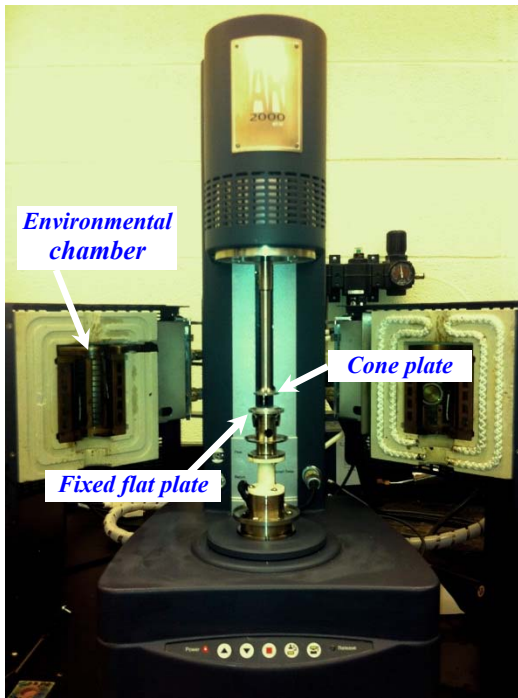
The understanding of the bulk response combined with the nonlinear viscoelastic model will significantly improve both the accuracy of computational micromechanics models and the understanding of asphaltic materials behavior. In addition the extension of these measurements to FAM and full asphalt mixtures in future will also significantly improve the accuracy of characterizing mixture performance.

### Significant Problems, Issues and Potential Impact on Progress

None.

### Work Planned Next Quarter

In the next quarter we plan to finish the analysis related to the measurement of bulk modulus and document the findings in a technical paper. This paper will not only present a method to measure the bulk modulus of asphalt binder, but also addresses the issues such as linearity and edge effects.



Cone and plate geometry in DSR

Poker-chip geometry in Instron

Figure F1b-1.1. Test geometries used to measure the shear and bulk properties of asphalt binders.

***Subtask F1b-2: Separation of Nonlinear Viscoelastic Deformation from Fracture Energy under Repeated and Monotonic Loading (TAMU)***

Work Done This Quarter

The reader is referred to Work Elements F2c and E1a.

Work Planned Next Quarter

The reader is referred to Work Elements F2c and E1a.

## **Work Element F1c: Aging**

### ***Subtask F1c-1: Critical Review of Binder Oxidative Aging and Its Impact on Mixtures (TAMU)***

#### Work Done This Quarter

Several oxidation mechanisms of asphalt binder were reviewed in previous quarterly report. Specifically, they are Petersen's dual-reaction free radical chain reaction (FRCR) mechanism, King's oxycyclic electron transfer initiated oxidation (ETIO) mechanism, and Herrington's inhibited free radical autoxidation (IFRA) mechanism. All mechanisms have difficulty explaining the “fast-rate plus constant-rate” scheme of binder oxidation. One possible reason is that reactions during the fast-rate period and the constant-rate period might go through different reaction pathways so that no simple mechanism is able to explain the kinetics. One way to probe this possibility is by using antioxidants. By comparing the aging kinetics of antioxidant-treated binders with control, we might see the stage when the antioxidants take effect and differentiate the oxidation mechanism for the fast-rate period. For this purpose, a literature review of antioxidants was conducted.

The search for effective antioxidants to retard binder oxidation started as early as 1960, and the study of effective and economic antioxidants is ongoing. For example, Williams et al. (2008) were investigating lignin-containing ethanol co-products as an economic performance enhancer for asphalt. Through the years, many antioxidants were examined. Mainly, they were aromatic amines, metal (lead or zinc) compounds, phenolic antioxidants, carbon black, and hydrated lime. A detailed review of antioxidants for asphalt binder is available from Apeageyi (2006).

During the evaluation of the effectiveness of antioxidants, very few people (Martin 1968) studied the effect of antioxidants on binder oxidation chemistry. Most address the effectiveness of antioxidants based on comparison of rheological properties, typically viscosity. However, antioxidants might have changed the binder hardening in two ways, 1) by slowing down oxidation rates and 2) by making the binder softer or harder by changing the binder composition and compatibility. Therefore, for the purpose of a study of mechanism, those two effects should be studied separately.

Furthermore, while the oxidation of asphalt goes through an early fast-rate period followed by a constant-rate period, most antioxidant studies evaluated binders after RTFO and PAV aging without considering these two different reaction paths. It is possible that antioxidants only work during one of these two periods while the other is not affected. Therefore, binders should be aged and sampled during both the fast-rate and constant-rate period. This approach will provide a more detailed view of the function of antioxidants and of the nature of the two oxidation mechanisms.

#### Significant Results

N/A

### Significant Problems, Issues and Potential Impact on Progress

There are no problems or issues.

### Work Planned Next Quarter

Based on this review, an experimental design will be developed for the study of oxidation mechanisms using selected antioxidants and the experimental work will begin.

Review of the literature and work on other research projects is ongoing.

### Cited References

Apegyei, A.K., 2006, Laboratory Evaluation of Antioxidants for Asphalt Binders. Ph.D. dissertation at University of Illinois at Urbana- Champaign.

Williams, R. C., and N. S. McCready, The Utilization of Agriculturally Derived Lignin as an Antioxidant in Asphalt Binder. Center for Transportation Research and Education Final Report No. 06-260, Iowa.

Martin, K. G., 1968, Laboratory Evaluation of Antioxidants for Bitumen. *Proc.*, Australian Road Research Board, Vol. 4, Part 2.

### ***Subtask F1c-2: Develop Experimental Design (TAMU)***

#### Work Done This Quarter

No work this quarter.

#### Significant Results

None.

### Significant Problems, Issues and Potential Impact on Progress

The planned experiments using ARC core binders is underway, as well as measurements on mixtures fabricated using other binders.

### Work Planned Next Quarter

Measurements of mixture rheology and fatigue continue. Also, rheological measurements of binders extracted and recovered from these mixtures will be made as part of the effort to link binder oxidation to changes in mixture properties.

### ***Subtask F1c-3: Develop a Transport Model of Binder Oxidation in Pavements (TAMU)***

#### Work Done This Quarter

##### *Measurements of Recovered Binder Properties*

Measurements of the WRI test section sites await delivery of the field cores.

##### *Model Validation with Preliminary Field Measurement*

The previous quarter, work was reported on recent work towards an improved fundamentals-based oxygen transport and reaction model for predicting asphalt binder oxidation rates in pavements. Model elements include pavement temperature, pavement air voids characteristics (total air voids, pore sizes and distribution), asphalt binder oxidation kinetics, and oxygen diffusivity in asphalts. In this quarter, and in lieu of having WRI field cores for analysis, field oxidation rates for a number of pavements in Texas and Minnesota, determined for TxDOT project 0-6009, were compared to calculations made using the more detailed transport model developed in this ARC work. In addition, the effects of model elements including pavement temperature, air void properties, and binder oxidation kinetics on field oxidation rates were evaluated by comparing field oxidation rates at these different pavement sites.

Table F1c-3.1 summarizes six pavement sites from Texas and Minnesota. The Texas sites range from Amarillo in the North to Laredo in the South, and to the Lufkin in the East. Most of the field cores are taken from top surface layers of pavements, but also from layers far below the surface. For example, IH35 #5 at Waco is a 4 inch rich bottom layer (high asphalt binder content), placed on a 6 inch flex base, at a depth of 16 inches below the pavement surface. (Here the number after the name of the highway indicates the pavement layer studied. If not specified in table F1c-3.1, the payment layer is the surface layer.) The thicknesses of the various pavement layers ranged up to 4 inches but down to as little as 2 inches. The Bryan district pavement (US290) contained unmodified binders, while other pavements are SBS polymer modified. Oxidation and hardening kinetics for all the binders were measured separately for either the recovered binders from the field cores or for the same binders obtained from the manufacturer. Additionally, IH35 #5 at Waco has lowest accessible air void of 5.9 percent, while US290 at Bryan has accessible air void as high as 12.4 percent; and most of pavement layers have intermediate values from 7.3 to 7.9 percent. The ages of the pavements range from new construction (US277) to 6 years old (Amarillo US54) at the time of the first coring date. Coring at two times provided field oxidation rates.

Also included in the study is Cell 1 from the MnRoad test site in Minnesota. The thickness of the core layer is 4.5 inches, taken from pavement surface. Oxidation reaction kinetics parameters were measured with binder recovered from the field cores. The accessible air void content for this pavement layer was 4.8 percent. Cell 1 was constructed in 1993 and cores were obtained from this MnRoad site in November 2004 and November 2008.

This collection of pavement cores covers a large variety of key elements that affect pavement oxidation, and provided data that could be used to assess the effects of pavement temperature (Texas versus Minnesota; surface layer versus bottom layer), air void properties (from a low accessible air void of 5.9 percent to a high accessible air void of 12.4 percent), and asphalt

oxidation and hardening kinetics (a variety of asphalt binders) on measured or modeled oxidation rates.

Table F1c-3.1. List of field sites studied.

| District (State) | Highway | Thickness (inch) | PG (modifier) | Binder Supplier | AAV (%) | Cons. | 1 <sup>st</sup> Coring | 2 <sup>nd</sup> Coring |
|------------------|---------|------------------|---------------|-----------------|---------|-------|------------------------|------------------------|
| Laredo (TX)      | US277   | 2.5              | 70-22 (SBS)   | Valero-C        | 7.3     | 2008  | 07/2008                | 09/2009                |
| Lufkin (TX)      | US69    | 2                | 70-22 (SBS)   | Marlin          | 7.9     | 2003  | 02/2005                | 06/2008                |
| Bryan (TX)       | US290   | 2.5              | 64-22 (Un)    | Eagle           | 12.4    | 2002  | 10/2005                | 08/2008                |
| Waco (TX)        | IH35 #5 | 3                | 70-22 (SBS)   | Alon            | 5.9     | 2003  | 10/2005                | 08/2008                |
| Amarillo (TX)    | US54    | 2.5              | 70-28 (SBS)   | Alon            | 7.3     | 1998  | 12/2004                | 07/2008                |
| Laredo (TX)      | IH35 #4 | 2                | 70-22 (SBS)   | Valero-C        | 2.0     | 2007  | --                     | 06/2008                |
| Metro Area (MN)  | I-94    | 4.5              | AC-120(Un)    | --              | 4.8     | 1993  | 11/2004                | 11/2008                |

Cores taken from fields were analyzed for interconnected air voids (by X-ray CT) and total and accessible air voids (by CoreLok or SSD) first, and then sliced into 0.5 inch layers, each for separate binder extraction and recovery. The recovered binders were analyzed for oxidation by infrared spectroscopy (FT-IR) and for physical properties by dynamic shear rheometry (DSR) to provide data on asphalt binder oxidation and hardening rates in pavements.

In addition, pavement temperature, air void properties, and asphalt oxidation kinetics were characterized for these pavement cores. Then, layer-by-layer, oxidation rates were modeled as a function of time and depth in the pavement cores based on the improved oxygen transport and reaction model. One should note that model calculation provided a range, instead of a single value, of oxidation rates, depending on the upper or lower limit of  $P_{av}$  (the oxygen partial pressure in the pore) used. The higher values of  $P_{av}$  and thus the higher oxidation rates are obtained by assuming that convective flow through the pavement pores is sufficient to maintain the oxygen partial pressure at 0.2 atm. The lower values of  $P_{av}$  and thus the lower oxidation rates are obtained by assuming that replenishment of oxygen in the pores is achieved only by diffusion of oxygen from the pavement surface.

Because of the limited number of cores that can be obtained, the relatively short time between corings (due to the project length relative to the slow field oxidation rate), and the inherent variability that tends to exist between cores, the ability to make layer-by-layer comparisons of these field oxidation measurements, especially considering the fairly modest layer-by-layer differences indicated by the model calculations, is necessarily limited. Consequently, the overall binder oxidation rates for each pavement core (rather than slice by slice comparisons) were compared using the field measurements and model calculations.



Table F1c-3.2 summarizes yearly oxidation rates (in terms of carbonyl growth) measured for these six validation cores. Maximum and minimum oxidation rates calculated from the model are also reported. The visual comparison is shown in figure F1c-3.1. The ranking of predicted oxidation rates from high to low is the same as the ranking established by field measurement except for US277 and the oxidation rates measured in the field can be quite close to the range of predicted oxidation rates that were established by the maximum and minimum oxidation rates. For example, the measured oxidation rate is only 3 percent higher than the maximum oxidation rate calculated for US290, and for US54 the measured oxidation rate is 6 percent lower than the minimum oxidation rate predicted.

Table F1c-3.2. Comparison of measured and modeled field oxidation rates.

| STATES | Site        | Oxidation rate modeled (CA/year) |         | Bulk oxidation rate measured (CA/year) |
|--------|-------------|----------------------------------|---------|--|
|        |             | Maximum                          | Minimum |  |
| MN     | Cell 1      | 0.0200                           | 0.0195  | 0.0256                                 |
|        | US277-LRD   | 0.0465                           | 0.0451  | 0.0705                                 |
| TX     | US69-LFK    | 0.0258                           | 0.0255  | 0.0370                                 |
|        | US290-BRY   | 0.0651                           | 0.0620  | 0.0671                                 |
|        | IH35-WAC #4 | 0.0264                           | 0.0243  | 0.0340                                 |
|        | US54-AMR    | 0.1117                           | 0.0994  | 0.0935                                 |

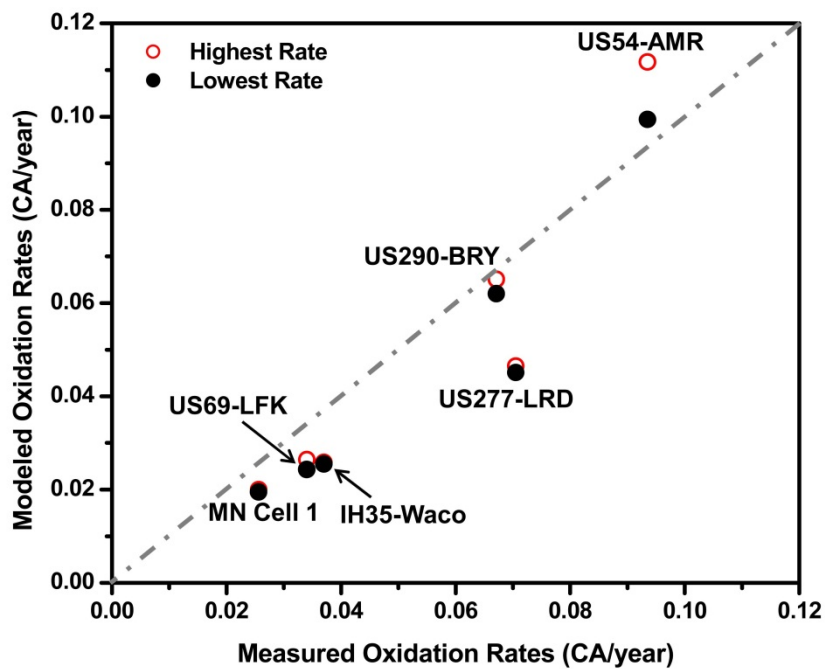


Figure F1c-3.1. Comparison of measured and modeled field oxidation rates.

On the other hand, there are exceptions. For example, for pavements from US277, US69, IH35-Waco, and MN Cell 1, the respective measured oxidation rates are 34, 30, 22, and 21 percent higher than the maximum oxidation rates predicted.

A possible explanation of these higher rates is that these pavements were all newly constructed pavements, at least relative to their oxidation rates; at the time of their first core, the Texas pavement's respective service lives were 0, 1.5, and 2 years. For MN Cell 1, the first core was taken after 11 years in the road. Oxidation of a neat asphalt binder is characterized by an initial rapid rate period that declines over time until a constant-rate period is reached. It has been estimated that the fast oxidation rate period can last as long as 2~3 years for Texas pavements, and 12 years or longer for Minnesota pavements. Thus, the asphalt binder oxidation for these pavement cores was most likely dominated by the initial rapid oxidation period, rather than the slower constant-rate reaction regime. However, in the model calculations, only the slower constant-rate reaction kinetics parameters were used to calculate the field oxidation rates, thereby likely providing a significant underestimation of the oxidation rates. The reaction rate for the constant rate period can generally be described using an Arrhenius expression for temperature variation and pressure dependence, while the reaction mechanisms are still not fully understood for initial rapid rate period. An extensive understanding of oxidation mechanisms and oxidation kinetics in this rapid oxidation period is essential to incorporating the fast reaction period into this model and to providing a more accurate prediction of oxidation rates during the first several years of service for newly constructed pavements.

In spite of this disagreement of model predictions for pavements that are largely in the fast rate oxidation period, in general this fundamentals-based model provides a very good match with field measurements, suggesting that it captures the critical elements that affect asphalt binder oxidation in pavements.

### Significant Results

Recent developments on pavement temperature modeling, oxygen diffusivity measurement, and pavement air voids characterization, coupled with a thermal and oxygen transport model in pavements, provide a good foundation for model calculations. This is a very important result that is the culmination of many years of work towards such a model.

### Significant Problems, Issues and Potential Impact on Progress

The effort to obtain cores from pavement sites in different climate zones continues. Cores from such sites will provide 1) data on binder oxidation as a function of time and depth in pavements and 2) data on changes to mixture rheology and fatigue resistance that occur in response to binder oxidation.

### Work Planned Next Quarter

Field cores from studied pavement sites will be continue to be collected and measured to provide more accurate data on binder oxidation as a function of time and depth in these pavements.

Field cores from sites as available from WRI will be tested to provide data on binder oxidation as a function of time and depth in pavements in different climate zones.

Oxidation mechanism and kinetics in this fast reaction period will be studied to incorporate into the improved oxygen transport and reaction model.

Model verification and validation with above mentioned pavement sites is an ongoing effort throughout the entire project.

***Subtask F1c-4: The Effects of Binder Aging on Mixture Viscoelastic, Fracture, and Permanent Deformation Properties (TAMU)***

The reader is referred to Work Elements F2c and E1a.

***Subtask F1c-5: Polymer Modified Asphalt Materials (TAMU)***

Work Done This Quarter

A number of base asphalts and their corresponding polymer modified asphalts (PMB) were oxidized at different temperatures and at 1 atm air pressure. Samples collected at different oxidation levels were measured for oxidation level (carbonyl content) and rheological properties including low shear limiting viscosity and DSR function.

The ratios of the limiting viscosity (or DSR function) for the polymer modified binder to the limiting viscosity (or DSR function) for the base binder, are being used to analyze oxidation susceptibility and oxidation kinetics for different polymer modifiers in terms of polymer functional type.

Work Planned Next Quarter

This experiment will be continuing throughout the next quarter with additional asphalt binders and their corresponding PMB.

Decreases in this rheological ratio with oxidation at different temperatures will be analyzed for polymer oxidation susceptibility and polymer oxidation kinetics.

## **Work Element F1d: Healing (TAMU)**

*Subtask F1d-1: Critical review of the literature*

*Subtask F1d-2: Material selection*

*Subtask F1d-3: Experiment design*

*Subtask F1d-4: Test methods to measure properties related to healing*

*Subtask F1d-5a: Testing of materials and validating healing model*

*Subtask F1d-5b: Thermodynamic model for healing in asphalt binders*

### Work Done This Quarter

In the previous quarters, we reported a test and analytical procedure to measure the overall healing in asphalt composites (fine aggregate matrix) using a dynamic shear rheometer (DSR). The characteristic overall healing curve for the material was shown to be independent of the mode of loading used to obtain the curve. This approach is largely based on the Viscoelastic Continuum Damage theory (VECD) that is currently used for the analysis of fatigue cracking resistance of asphalt mixtures using the asphalt materials performance tester (AMPT). The advantage of this approach is that it can easily be adapted and integrated with the AMPT to characterize the healing characteristics of full asphalt mixtures. However, in its current form the test requires the use of several specimens to get the full damage-healing-time characteristic at one temperature. As a part of this task we are currently modifying the test procedure so that similar results could be obtained by using fewer test specimens. At this time all tests are being conducted on FAM specimens subjected to cyclic shear.

### Significant Results

None to report at this time.

### Significant Problems, Issues and Potential Impact on Progress

None.

### Work Planned Next Quarter

We plan to complete the development of the modified test procedure to determine the healing characteristic curve for FAM specimens subjected to cyclic shear. In addition we will also start testing of FAM specimens subjected to cyclic tension-compression loading. This will result not only in the properties of the FAM being characterized in both shear and tension-compression but also provide valuable inputs for computational modeling at the mixture length scale.

***Subtask F1d-6: Evaluate Relationship Between Healing and Endurance Limit of Asphalt Binders (UWM)***

Work Done This Quarter

The consolidated draft report “M” has been submitted in 508 format. Report “M” includes findings from work elements F2e, F1d-6, and F2a. Additionally, a tech brief has been drafted and submitted. The research team is working on preparing a document containing captions for figures to allow for interpretation by the visually impaired.

Significant Results

The consolidated draft report “M” has been submitted.

Significant Problems, Issues and Potential Impact on Progress

None.

Work Planned Next Quarter

Address comments from technical reviewers on the draft report.

Presentations and Publications

The paper submitted to TRB was accepted for publication. It was revised to include reviewers comments and submitted for the annual conference.

***Subtask F1d-7: Coordinate with Atomic Force Microscopic (AFM) Analysis (WRI)***

Work Done This Quarter

The emphasis of this subtask is to integrate the results from Subtasks M1b-2 and M2a-2, and other pertinent past experimental work where physico-chemical properties including chemical potentials and phase separation phenomena can be used in the asphalt microstructure model discussed in Work Element F3a. The data generated from these analyses is discussed and incorporated into the chemo-mechanical models of asphalt and asphalt mastic structures in Work Element F3a.

Significant Results

See Work Element F3a.

Significant Problems, Issues and Potential Impact on Progress

None

### Work Planned Next Quarter

Activity in Subtask is included in the discussion in Work Element F3a.

### ***Subtask F1d-8: Coordinate Form of Healing Parameter with Micromechanics and Continuum Damage Models (TAMU)***

### Work Done This Quarter

In this quarter, for the first time, a general continuum damage-healing mechanics framework has been developed, which has appeared in Darabi et al. (2012). This framework extends the well-known effective (undamaged) configuration in continuum damage mechanics to an effective-healed natural configuration. This framework, which is also presented within a systematic thermodynamic formulation, can be used to properly couple healing and damage mechanics. In this quarter, special emphasis is placed on validating the derived healing evolution law based on the ALF data.

### Significant Results

The significant results from the developed continuum damage-healing frameworks have been detailed in Darabi et al. (2012).

### Significant Problems, Issues and Potential Impact on Progress

None

### Work Planned Next Quarter

The main focus of the coming quarter is on further validation of the micro-damage healing model against available experimental data. Moreover, special emphasis will be placed on the development of a simplified approach for calibrating the micro-damage healing model based on simple experimental procedure. As soon the data from the ARC testing plan is ready, calibration and validation based on this data will be started.

### Cited References

Darabi, M.K., R. K. Abu Al-Rub, and D. N. Little, 2012, A continuum damage mechanics framework for modeling micro-damage healing. *International Journal of Solids and Structures*, 49 (3-4), 492-513. <http://dx.doi.org/10.1016/j.ijsolstr.2011.10.017>

## **CATEGORY F2: TEST METHOD DEVELOPMENT**

### **Work Element F2a: Binder Tests and Effect of Composition (UWM)**

#### Work Done This Quarter

The consolidated draft report “M” has been submitted in 508 format for review. This report also includes findings from work elements F1d-6 and F2e.

#### Significant Results

The consolidated draft report “M” has been submitted for review.

#### Significant Problems, Issues and Potential Impact on Progress

None.

#### Work Planned Next Quarter

Revise draft report “M” according to reviewers’ comments.

### **Work Element F2b: Mastic Testing Protocol (TAMU)**

This work element is completed and the reader is referred to work element M1c.

### **Work Element F2c: Mixture Testing Protocol (TAMU)**

#### Work Done This Quarter

One technical paper entitled “Mechanistic Modeling of Fracture for Asphalt Mixtures in Compression” was drafted in this quarter and will be submitted for publication in a scientific journal.

Two major achievements were made in this quarter: 1) a radial strain decomposition method was proposed to decompose the radial strain that was measured using the modified radial deformation measuring system in the destructive dynamic modulus tests; and 2) based on the radial viscofracture strain decomposed from the total radial strain, the anisotropic viscofracture for the asphalt mixtures in compression was characterized by calculating the axial and radial damage densities. The evolution of the anisotropic damage density was determined using the pseudo J-integral Paris’ law. Details of the achievements made in this quarter are summarized as follows.

#### **1) Radial Strain Decomposition Methodology**

The axial strain decomposition method was proposed in previous quarters. The extended elastic-viscoelastic correspondence principle that was initiated by Schapery (Schapery 1984) was employed to conduct the axial strain decomposition. Motivated by Schapery’s theory, a modified

elastic-viscoelastic correspondence principle was proposed in this quarter and the radial strain decomposition was performed on different asphalt mixtures that vary in the binder type, air void content and aging condition.

### 1.1) Modified Elastic-Viscoelastic Correspondence Principle

In the extended elastic-viscoelastic correspondence principle, Schapery formulated a linear constitutive law for the viscoelastic material as shown in equation F2c.1.

$$\sigma(t) = E_R \varepsilon_1^R(t) \quad (\text{F2c.1})$$

where  $E_R$  is reference modulus and  $\varepsilon_1^R(t)$  is the axial pseudo strain that is expressed as:

$$\varepsilon_1^R(t) = \frac{1}{E_R} \int_0^t E(t-\xi) \frac{d\varepsilon_1(\xi)}{d\xi} d\xi \quad (\text{F2c.2})$$

where  $\varepsilon_1(\xi)$  is the axial strain measured in the test and  $E(t)$  is the relaxation modulus of the undamaged material. We found that, if the reference modulus is assigned as the Young's modulus, the viscous portion in the total strain can be eliminated by using  $\varepsilon_1^R(t)$ , which mathematically equals  $\varepsilon_1^R(t) = \varepsilon_1(t) - \varepsilon_1^{ve}(t)$ , where  $\varepsilon_1^{ve}(t)$  is the viscoelastic strain component.

Inspired by equations F2c.1 and F2c.2, another linear constitutive law is formulated for the viscoelastic material to relate the axial and radial strains as follows:

$$\varepsilon_1(t) = -\frac{1}{\nu_{12}^R} \varepsilon_2^R(t) \quad (\text{F2c.3})$$

where  $\nu_{12}^R$  is the reference Poisson's ratio that is assigned as the elastic Poisson's ratio.  $\varepsilon_2^R(t)$  is the radial pseudo strain that can be calculated by:

$$\varepsilon_2^R(t) = -\nu_{12}^R \left[ -\int_0^t \pi_{12}(t-\xi) \frac{d\varepsilon_2(\xi)}{d\xi} d\xi \right] \quad (\text{F2c.4})$$

where  $\varepsilon_2(\xi)$  is the total radial strain measured in the test and  $\pi_{12}(t)$  is named as the inverse viscoelastic Poisson's ratio for the undamaged viscoelastic material.  $\pi_{12}(t)$  is a newly proposed viscoelastic variable that is used to determine the axial strain when the radial strain is given and can be defined through equation F2c.5.

$$\varepsilon_1(t) = -\int_0^t \pi_{12}(t-s) d\varepsilon_2(s) \quad (\text{F2c.5})$$



If the axial strain ( $\varepsilon_1(t)$ ) and radial strain ( $\varepsilon_2(t)$ ) are measured in a nondestructive creep test,  $\pi_{12}(t)$  can be determined by taking the Laplace transform of equation F2c.5 and yields:

$$\pi_{12}(t) = \mathcal{L}^{-1} \left\{ -\frac{\bar{\varepsilon}_1(s)}{s\bar{\varepsilon}_2(s)} \right\} \quad (\text{F2c.6})$$

It is known that the viscoelastic Poisson's ratio can be defined through equation F2c.7 and determined by equation F2c.8 based on the measured axial and radial strains.

$$\varepsilon_2(t) = -\int_0^t \nu_{12}(t-s) d\varepsilon_1(s) \quad (\text{F2c.7})$$

$$\nu_{12}(t) = \mathcal{L}^{-1} \left\{ -\frac{\bar{\varepsilon}_2(s)}{s\bar{\varepsilon}_1(s)} \right\} \quad (\text{F2c.8})$$

Equation F2c.6 and F2c.8 indicate that, in the Laplace domain, we have:

$$s\bar{\pi}_{12}(s) = \frac{1}{s\bar{\nu}_{12}(s)} \quad (\text{F2c.9})$$

Figure F2c.1 shows an example for  $\pi_{12}(t)$  and  $\nu_{12}(t)$  that are determined by conducting a nondestructive compressive creep test to an asphalt mixture. It is found that the viscoelastic Poisson's ratio is an increasing power curve and can be greater than 0.5 for an anisotropic viscoelastic material. The inverse viscoelastic Poisson's ratio is a decreasing curve and always greater than 1. The measured  $\pi_{12}(t)$  and  $\nu_{12}(t)$  are well fitted by the Prony series models that are shown in equations F2c.10 and F2c.11, respectively.

$$\nu_{12}(t) = \nu_0 + \sum_{i=1}^M \nu_i \left[ 1 - \exp\left(-\frac{t}{r_i}\right) \right] \quad (\text{F2c.10})$$

$$\pi_{12}(t) = \pi_\infty + \sum_{j=1}^M \pi_j \exp\left(-\frac{t}{z_j}\right) \quad (\text{F2c.11})$$

where  $M$  = total number of Kelvin elements in the Prony series model;  $\nu_0$ ,  $\nu_i$ ,  $r_i$ ,  $\pi_\infty$ ,  $\pi_j$  and  $z_j$  are fitting parameters.

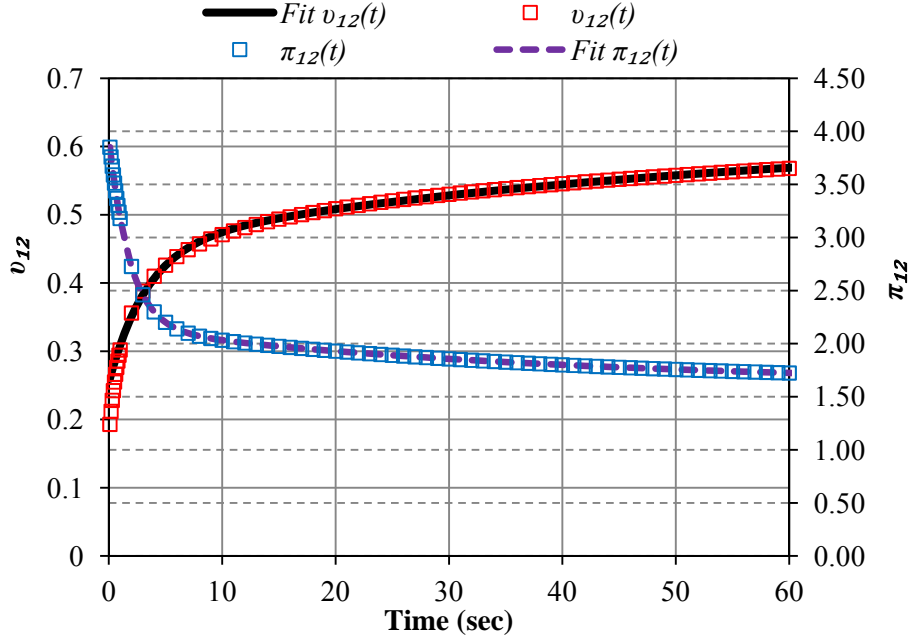


Figure F2c.1. Viscoelastic Poisson's ratio and inverse viscoelastic Poisson's ratio for an asphalt mixture (AAD, 4%, aged).

### 1.2) Radial Strain Decomposition

Similar to the axial strain decomposition, the total radial strain is decomposed into five components as follows:

$$\varepsilon_2^T = \varepsilon_2^e + \varepsilon_2^p + \varepsilon_2^{ve} + \varepsilon_2^{vp} + \varepsilon_2^{vf} \quad (\text{F2c.12})$$

where  $\varepsilon_2^T$  = radial total strain;  $\varepsilon_2^e$  = radial elastic strain;  $\varepsilon_2^{ve}$  = radial viscoelastic strain;  $\varepsilon_2^p$  = radial plastic strain;  $\varepsilon_2^{vp}$  = radial viscoplastic strain;  $\varepsilon_2^{vf}$  = radial viscofracture strain. By inputting the measured total radial strain into equation F2c.4, the radial pseudo strain is calculated and the effect of viscosity on the measured radial strain is removed. Thus:

$$\varepsilon_2^R = \varepsilon_2^T - \varepsilon_2^{ve} = \varepsilon_2^e + \varepsilon_2^p + \varepsilon_2^{vp} + \varepsilon_2^{vf} \quad (\text{F2c.13})$$

The radial strain decomposition is performed as follows:

- 1) The radial elastic strain is calculated using the axial elastic strain multiplied by the reference Poisson's ratio that is the elastic Poisson's ratio, which is shown in equation F2c.14a.
- 2) The radial viscoelastic strain is obtained by subtracting the calculated radial pseudo strain from the radial total strain based on equation F2c.13 and is shown in equation F2c.14b.

- 3) Since  $\varepsilon_2^{vp}(t=0) = \varepsilon_2^{vf}(t=0) = 0$ , the radial plastic strain is determined using equation F2c.14c.
- 4) Since the viscofracture strain due to the growth of cracks does not occur until the tertiary stage (Part III), the radial pseudo strain in the primary and secondary stages ( $\varepsilon_2^R(I, II)$ ) only include the radial elastic strain, radial plastic strain and radial viscoplastic strain. As a result, the radial viscoplastic strain in the primary and secondary stage ( $\varepsilon_2^{vp}(I, II)$ ) can be calculated using equation F2c.14d. Equation F2c.14e is the Tseng-Lytton model which is employed to fit  $\varepsilon_2^{vp}(I, II)$  and then to predict the radial viscoplastic strain during the entire deformation process including the primary, secondary and tertiary stages.
- 5) The radial viscofracture strain can be computed using equation F2c.14f by rearranging equation F2c.12.

Thus the radial strain decomposition is accomplished by a complete separation of each strain component in the total radial strain.

$$\varepsilon_2^e = -\nu_{12}^R \varepsilon_1^e \quad (\text{F2c.14a})$$

$$\varepsilon_2^{ve} = \varepsilon_2^T - \varepsilon_2^R \quad (\text{F2c.14b})$$

$$\varepsilon_2^p = \varepsilon_2^R(t=0) - \varepsilon_2^e \quad (\text{F2c.14c})$$

$$\varepsilon_2^{vp}(I, II) = \varepsilon_2^R(I, II) - (\varepsilon_2^e + \varepsilon_2^p) \quad (\text{F2c.14d})$$

$$\varepsilon_2^{vp} = \varepsilon_{\infty 2}^{vp} \exp\left[-(\rho_2/N)^{\lambda_2}\right] \quad (\text{F2c.14e})$$

$$\varepsilon_2^{vf} = \varepsilon_2^R - (\varepsilon_2^e + \varepsilon_2^p) - \varepsilon_2^{vp} \quad (\text{F2c.14f})$$

An example is given in figure F2c.2 to show the radial strain decomposition for an asphalt mixture in a compressive dynamic modulus test. It is found that the radial elastic and plastic strains are time-independent and the radial viscoelastic strain shows three stages and has a large proportion of the radial total strain. The radial viscoplastic strain shows a power curve and the viscofracture strain increases with load cycles at an increasing strain rate in the tertiary stage. All of the findings on the radial strain components are similar to the characteristics of the corresponding axial strain components.

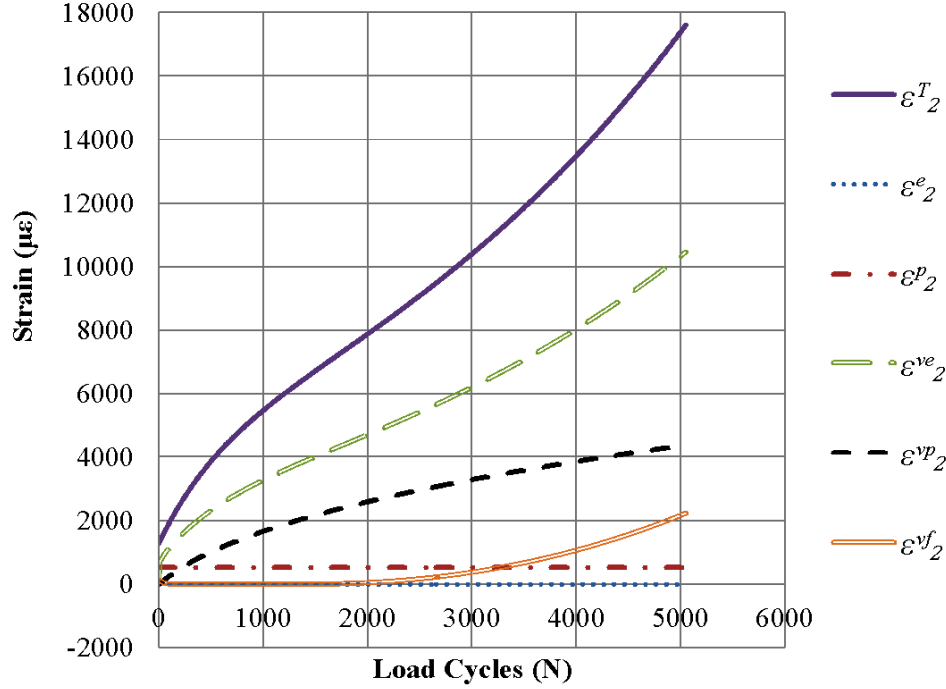


Figure F2c.2. Radial strain decomposition for an asphalt mixture (AAD, 4%, aged).

## 2) Anisotropic Damage Density and Pseudo J-integral Paris' law

### 2.1) Anisotropic Damage Density

Damage density is employed in this study to characterize the fracture of the asphalt mixture in compression and it is defined as a ratio of the lost area due to cracks to the total area of a cross section in a specific direction. Since the projections of the cracks are different in different directions, the damage density is anisotropic. The axial damage density ( $\xi_1$ ) was determined in previous quarterly reports by employing the incremental dissipated pseudo fracture strain energy equilibrium principle. To determine the radial damage density ( $\xi_2$ ), a geometrical method is proposed in this study as follows.

First, the axial and radial viscofracture strains are obtained by strain decomposition and both characterize the effect of the cracks on the deformation of the asphalt mixture. For a cylindrical asphalt mixture specimen with a height of  $H$  and a radius of  $R$ , the decrease of height and increase of radius that are purely caused by the growth of cracks under a uniaxial compressive load are assumed to be  $\Delta H$  and  $\Delta R$ , respectively. Then we have:

$$\begin{cases} \varepsilon_1^{vf} = \frac{\Delta H}{H} \\ \varepsilon_2^{vf} = \frac{\Delta R}{R} \end{cases} \quad (\text{F2c.15})$$

Second, the cracks disperse randomly in the asphalt mixture. If assuming that all cracks are collected in a cylinder whose height and radius are  $r$  and  $h$ , respectively; then the damage densities can be calculated based on their definitions as follows:

$$\begin{cases} \xi_1 = \frac{\pi r^2}{\pi R^2} \\ \xi_2 = \frac{2\pi r \cdot h}{2\pi R \cdot H} \end{cases} \quad (\text{F2c.16})$$

Third, since  $\Delta H$  and  $\Delta R$  are purely caused by the cracks, the increased volume of the cylindrical asphalt mixture specimen should equal to the volume of cracks, that is:

$$\pi (R + \Delta R)^2 (H - \Delta H) - \pi R^2 H = \pi r^2 h \quad (\text{F2c.17})$$

Finally, equations F2c.15, F2c.16 and F2c.17 yield an expression to determine the radial damage density based on the axial and radial viscofracture strains as well as the axial damage density, which is shown as follows:

$$\xi_2 = \frac{(1 + \varepsilon_2^{vf})^2 (1 - \varepsilon_1^{vf}) - 1}{\sqrt{\xi_1}} \quad (\text{F2c.18})$$

Figure F2c.3 shows the axial and radial damage densities for an asphalt mixture with 4% air voids and figure F2c.4 shows the axial and radial damage densities for an asphalt mixture with 7% air voids. It can be concluded that the asphalt mixture with 4% air voids has a higher radial damage density and a lower axial damage density while the asphalt mixture with 7% air voids has a lower radial damage density and a higher axial damage density. The same conclusion is found for all of the 16 asphalt mixtures that vary by two binders (AAD, AAM), two air void contents (4%, 7%) and two aging conditions (Unaged, 6-month 60°C aged). In fact, the asphalt mixture with 4% air voids is stiffer than the asphalt mixture with 7% air voids and has more vertical cracks during rupture, which is called a brittle-like fracture. The vertical cracks have a larger projection area on the circumferential surface, which yields a higher radial damage density. In contrast, the asphalt mixture with 7% air voids is relatively soft and tends to have a ductile-like fracture. The cracks grow along the plane of the maximum shear stress, which yields a larger projection area on the horizontal plane and eventually causes a higher axial damage density.

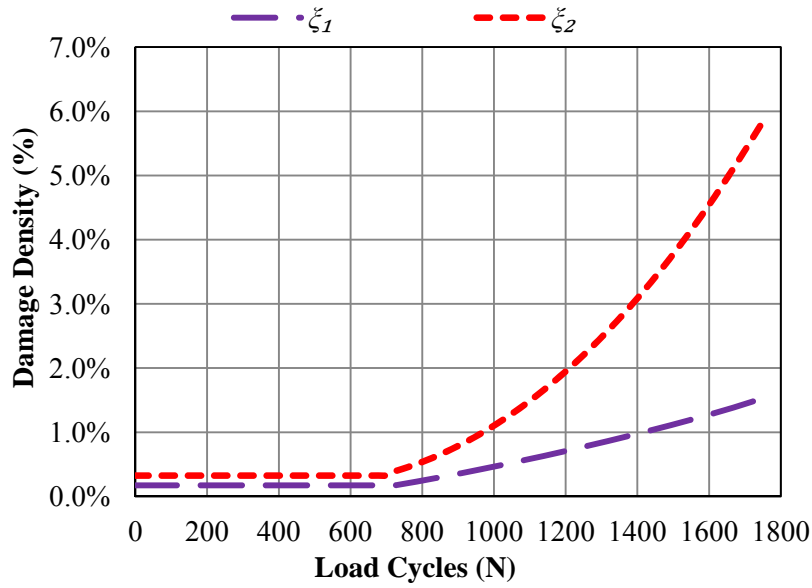


Figure F2c.3. Damage densities for an asphalt mixture with 4% air voids (AAM, 4%, unaged).

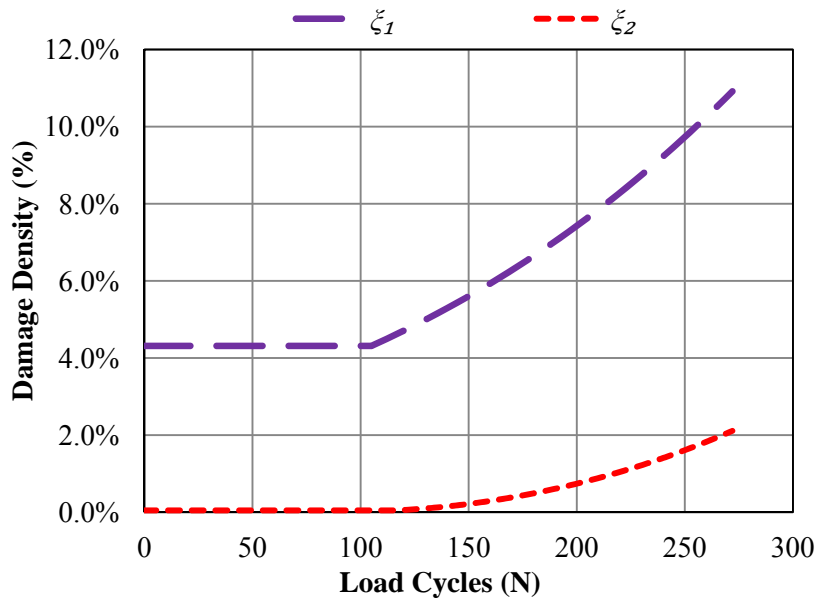


Figure F2c.4. Damage densities for an asphalt mixture with 7% air voids (AAM, 7%, unaged).

### 2.2) Pseudo J-integral Paris' Law

The pseudo J-integral based Paris' law was employed to characterize the evolution of the axial damage density in the previous quarterly report. The same model can be used for the characterization of the radial damage density. To generalize the evolution equation for the anisotropic damage density, the anisotropic Paris' law is expressed as:

$$\frac{d\xi_i}{dN} = A_i (J_{Ri})^{n_i} \quad i = 1, 2 \quad (\text{F2c.19})$$

where  $A_i$  and  $n_i$  are coefficients of Paris' law that are material constants and  $J_{Ri}$  is pseudo J-integral that can be written as:

$$J_{Ri} = \frac{\partial DPFSE^A}{\partial (c.s.a.)_i} = \frac{\partial DPFSE^A / \partial N}{\partial (c.s.a.)_i / \partial N} = \frac{\partial [\sigma_1 \varepsilon_1^{vf} (N)] / \partial N}{\partial [2A_{0i} \xi_i (N)] / \partial N} \quad (\text{F2c.20})$$

where  $A_{0i}$  is the original area of a cross section in a specific direction.  $(c.s.a.)_i$  is crack surface area that is two times of the projected area of the cracks in the specific direction. It is noteworthy that the energy that caused cracks is  $DPFSE^A$ , which is the apparent dissipated pseudo fracture strain energy. Since energy is a scalar and direction independent,  $DPFSE^A$  remains the same for the calculation of  $J_{R1}$  and  $J_{R2}$  and equals to  $\sigma_1 \varepsilon_1^{vf} (N)$  based on conclusions in the previous quarterly report. Equations F2c.19 and F2c.20 yield:

$$\xi_i (N) = \xi_{0i} + C_i \left[ e^{D_i(N-N_f)} - 1 \right] \quad (\text{F2c.21})$$

where  $\xi_{0i}$  is the initial damage density and  $C_i$ ,  $D_i$  are model parameters that can be expressed as:

$$\begin{cases} C_i = A_i^{\frac{1}{1+n_i}} \left( \frac{\theta \sigma_1 \varepsilon_0^{vf}}{2A_{0i}} \right)^{\frac{n_i}{1+n_i}} \left( \frac{1+n_i}{\theta n_i} \right) \\ D_i = \frac{\theta n_i}{1+n_i} \end{cases} \quad (\text{F2c.22})$$

Once the model fitting parameters ( $C_i$  and  $D_i$ ) are determined by fitting equation F2c.21 to the damage density curves, the material constants in Paris' law can be determined as follows:

$$\begin{cases} A_i = \left( \frac{2A_{0i}}{\theta \sigma_1 \varepsilon_0^{vf}} \right)^{n_i} (C_i D_i)^{1+n_i} \\ n_i = \frac{D_i}{\theta - D_i} \end{cases} \quad (\text{F2c.23})$$

By applying the above strain decomposition and fracture theories to the testing data of asphalt mixtures with different binder types, air void contents and aging periods, the axial and radial damage density curves are obtained and the material constants in Paris' law are determined. Table F2c.1 summarizes the material constants in Paris' law for the axial and radial damage densities. It is found that  $n_2$  is positive for the asphalt mixture with 4% air void while  $n_2$  is

negative for the asphalt mixture with 7% air void. Thus  $n_2$  is an indicator to differentiate the brittle-like fracture and the ductile-like fracture when the asphalt mixture is loaded in compression.

Significant Results

By proposing a modified elastic viscoelastic correspondence principle, the radial strain measured for the asphalt mixture in compression is decomposed into radial elastic, plastic, viscoelastic, viscoplastic and viscofracture components. The radial viscofracture strain is found to increase with load cycles at an increasing strain rate in the tertiary stage, which characterizes the anisotropic effect of the cracks on the deformation in the asphalt mixture. The radial damage density is determined by employing a geometric method and the evolution of the radial damage densities is characterized by the pseudo J-integral Paris’ law. The material constants in the Paris’ law are determined for both axial and radial damage density. It is found that, in compression, the asphalt mixture with 4% air voids has a brittle-like fracture while the asphalt mixture with 7% air voids has a ductile-like fracture. The exponent in Paris’ law for the radial damage density ( $n_2$ ) can be an indicator for differentiating brittle and ductile fracture.

Table F2c.1. Material constants in Paris’ law for different asphalt mixtures.

| Binder | Aging Period | Air Void (%) | $A_1$ (%/cycle) | $n_1$ | $A_2$ (%/cycle) | $n_2$  | Fracture |
|--------|--------------|--------------|-----------------|-------|-----------------|--------|----------|
| AAD    | 0-month      | 4            | 2.50E-10        | 0.08  | 5.89E-74        | 16.65  | Brittle  |
|        |              | 7            | 1.05E-04        | 0.06  | 1.72E+11        | -2.73  | Ductile  |
|        | 6-month      | 4            | 2.65E-20        | 3.36  | 3.44E-46        | 9.00   | Brittle  |
|        |              | 7            | 1.01E-12        | 1.32  | 6.93E+78        | -17.01 | Ductile  |
| AAM    | 0-month      | 4            | 2.88E-09        | 0.71  | 6.75E-42        | 8.18   | Brittle  |
|        |              | 7            | 1.07E-05        | 0.54  | 8.50E+07        | -2.21  | Ductile  |
|        | 6-month      | 4            | 3.56E-23        | 3.41  | 3.83E-12        | 1.29   | Brittle  |
|        |              | 7            | 3.20E-24        | 4.02  | 3.62E+12        | -2.94  | Ductile  |

Significant Problems, Issues and Potential Impact on Progress

None.

Work Planned in Next Quarter

The mechanistic theories and testing protocols proposed in previous and current quarterly reports will be performed on new asphalt mixtures to characterize a variety of properties in compression including anisotropy, viscoelasticity, viscoplasticity and viscofracture. The new asphalt mixtures



will be fabricated using two new binders (NuStar and Valero) and two new aggregates (Hanson limestone and Wyoming siliceous).

#### Cited Reference

Schapery, R. A., 1984, Correspondence principles and a generalized J-integral for large deformation and fracture analysis of viscoelastic media. *International Journal of Fracture*, 25(3), 195-223.

### **Work Element F2d: Structural Characterization of Micromechanical Properties in Bitumen using Atomic Force Microscopy (TAMU)**

#### Work Done This Quarter

There have been two significant findings related to the micro-characterization of asphalt binders based on mapping of physical properties of asphalt phases using Atomic Force Microscopy (AFM) during the past year. The first finding (presented in the latest quarterly report) included results of statistical analysis of the AFM phases and creep measurements for binders AAB, AAD, and ABD, which revealed statistically significant differences amongst phase detection microscopy (PDM)-separated asphalt phases. Furthermore, the results verified statistically significant changes in the properties of these phases due to aging. The second finding (presented in this report) includes the extraction of viscoelastic properties of each asphalt phase and composite viscoelastic properties before and after aging, which are compared to macro-scale elastic and viscoelastic properties. For conciseness, **select results** from asphalt binder AAD are presented with some detail, followed by a summary of significant findings related to **all binders** (original and aged binders AAB, AAD, and ABD).

Figure F2d.1 shows formerly presented phase images of asphalt AAD before and after aging to serve as reference for the following results. The terms Phase 1, Phase 2, and Phase 3 are used interchangeably with Continuous Phase, Dispersed Phase, and “Bee Structure” Phase, respectively as depicted in figure F2d.1. Furthermore, the “Bee Structure” Phase is considered to be a sub-phase of the dispersed phase, and therefore, the two phases are often referred to as the dispersed phase(s).

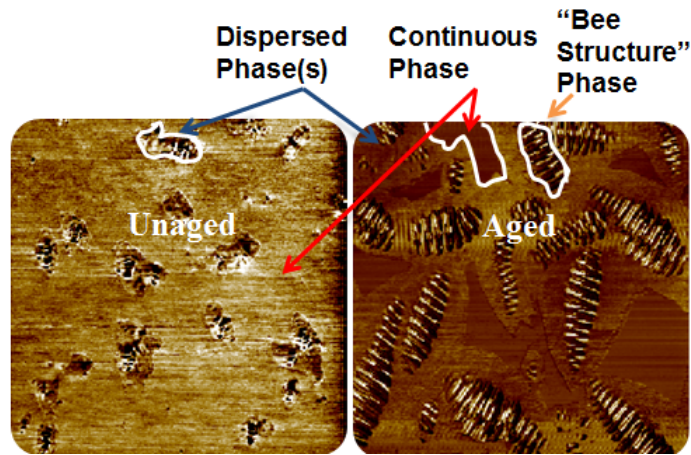


Figure F2d.1. Asphalt AAD phase images before and after aging.

### *Viscoelastic Properties of Asphalt Phases*

#### **Theory**

A typical AFM nanoindentation creep experiment performed in this study consists of contact between a an asphalt thin film and an AFM tip with known properties and geometry while a load,  $P$ , is applied and the corresponding penetration depth,  $h$ , is recorded with respect to time,  $t$ . A depiction of the AFM indentation test geometry into an asphalt thin-film is shown in figure F2d.2. The elastic-viscoelastic correspondence principle, which is commonly employed to convert elastic analytical solutions to viscoelastic solutions based on the relationship between elastic and Laplace transformed viscoelastic field equations, was used to extract viscoelastic properties from the AFM creep measurements.

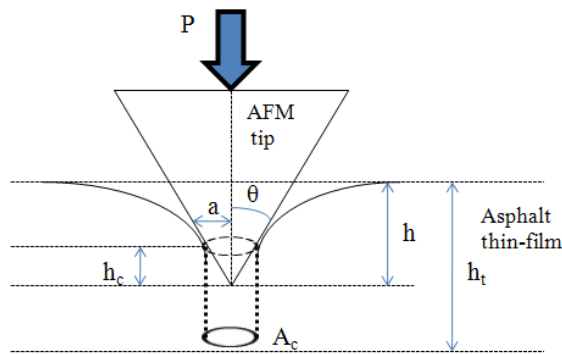


Figure F2d. 2. Geometry of AFM indentation test.  $P$  is the indentation load,  $h_t$  is the asphalt film thickness,  $h$  is the indentation depth,  $h_c$  is the contact depth,  $A_c$  is the projected contact area, and  $a$  is the contact radius (Adapted from Vandamme [1]).

The general solution for a rigid axisymmetric indenter into an isotropic solid is given by the Galin-Sneddon solution and reduced to the following equation [2-3].

$$h^2(t) = \left( \frac{\pi}{2 \tan \theta} \right) \left[ \frac{P(t)(1-\nu^2)}{E} \right] \quad (\text{F2d.1})$$

Where  $\theta$  is the half-angle of the indenter,  $E$  is the elastic Young's modulus, and  $\nu$  is the Poisson's ratio.

The viscoelastic Young's modulus under constant creep loading was fitted using the prony series model relationship given in (F2d.2).

$$E(t) = E_0 + \sum_{j=1}^M E_j \exp\left(-\frac{t}{k_j}\right) \quad (\text{F2d.2})$$

A range of composite elastic Young's modulus values were derived from each of the individual asphalt phases using the series/parallel bounds method, given in equation F2d.3. The composite bounds provide modulus ranges for two-phase media such as the system of continuous and dispersed asphalt phases and also provides the simplest solution for placing bounds on the composite elastic Young's modulus [4].

$$\frac{1}{\frac{\nu_1 + \nu_2}{E_1 + E_2}} \leq E^* \leq E_1 \nu_1 + E_2 \nu_2 \quad (\text{F2d.3})$$

Where  $E$  and  $\nu$  are the respective Young's modulus and volume fraction of Phase 1 and Phase 2 as denoted.

### Composite Viscoelastic Young's Modulus

Figure F2d.3 emphasizes two significant results regarding the viscoelastic Young's modulus. The first result, shown on the left side of each figure (Graph I), is the bounds for the composite viscoelastic Young's modulus  $[E(t)]$  of the unaged and aged Asphalt AAD. Graph I also highlights the viscoelastic Young's modulus value ( $E_i$ ) from the unaged and aged asphalts at a specific point in time (approximately four seconds) under constant load, which corresponds to the same highlighted areas in the graph on the right side of the figure (Graph II). Graph II illustrates the relationship between individual phase modulus values, phase volume concentration, and the resulting composite  $E(t)$  values given in Graph I. Furthermore, the volume concentration of each phase before and after aging gives a unique depiction of the microstructural shift that occurs during the aging process. Graph II essentially provides information which distinguishes this AFM nanoindentation experiment from an experiment using a non-imaging, larger radius nanoindenter tip, such as a Berkovich tip or a spherical tip. Although the small-radius conical AFM tip is not as robust for collecting force measurements as the large-radius tips, the tips offer the ability to collect semi-quantitative viscoelastic properties that can be associated with different phases depicted in high resolution phase images; furthermore, viscoelastic properties extracted from age-altered phases of the same respective asphalt provides important information regarding the link between microstructural change and changes in composite viscoelastic properties.

The  $E(t)$  values at approximately four seconds ( $E_1$  values) and composite  $E_1$  bounds are given in table F2d.1. The range of bounds are a function of the magnitude of difference between the moduli values of the multi-phase media for each asphalt; the bounds of the composite moduli range from less than one percent for aged Asphalt ABD to roughly 30 percent for Asphalt ABD. Furthermore, the coefficient of variance (COV) of the  $E_1$  values (based on ten different measurements taken from each phase) ranged from 10 to 30 percent for the different asphalts. The elastic Young's modulus ( $E(t)$  values at  $t=0$  or the  $E_2$  values given in table F2d. 1) obtained from this study ranged from 0.73 MPa to 2.95 MPa and 5.48 MPa to 28.17 MPa for the unaged and aged asphalt composites, respectively. It was noted that aging of Asphalt ABD resulted in a substantial increase in composite elastic Young's modulus (approximately 16 times greater than the elastic Young's modulus prior to aging). In comparison, the increase in elastic Young's modulus due to aging of Asphalts AAB and AAD were approximately two and eight times greater than the respective values prior to aging. The elastic Young's modulus values from this study were compared to bulk values reported by Lu and Isacsson [5] to establish a relationship between nano-scale and bulk Young's modulus values for asphalt. Furthermore, Young's modulus values determined from this study were also compared to nanoindentation Young's modulus values reported by Terefter et al. and Jäger and Lackner [6-7].

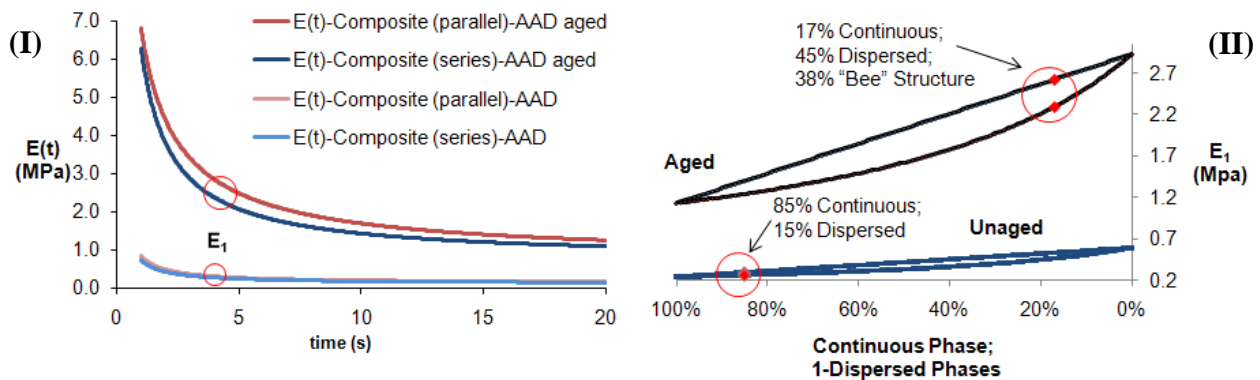


Figure F2d. 3. (I) Bounds for the composite relaxation modulus [ $E(t)$ ] of unaged and aged Asphalt AAD and (II) the relationship between individual phase modulus, phase distribution, and composite  $E(t)$  values.

Table F2d.1.  $E(t)$  values at approximately four seconds ( $E_1$  values) and composite  $E_1$  bounds.

| Asphalt Binder  | $E_1$ (MPa) |         |         |                |                  | Composite $E_1$ (MPa) |                      |      |      |
|-----------------|-------------|---------|---------|----------------|------------------|-----------------------|----------------------|------|------|
|                 | Phase 1     | Phase 2 | Phase 3 | Series (lower) | Parallel (upper) | St. Dev.              | Coeff. of var. (COV) |      |      |
| <b>AAB</b>      | 52%         | 0.65    | 48%     | 1.25           | -                | 0.85                  | 0.94                 | 0.22 | 0.25 |
| <b>AAB-aged</b> | 20%         | 1.33    | 70%     | 2.04           | 10%              | 1.83                  | 1.88                 | 0.56 | 0.30 |
| <b>AAD</b>      | 85%         | 0.19    | 15%     | 0.54           | -                | 0.21                  | 0.24                 | 0.03 | 0.13 |
| <b>AAD-aged</b> | 17%         | 1.08    | 45%     | 3.88           | 38%              | 2.17                  | 2.70                 | 0.68 | 0.28 |
| <b>ABD</b>      | 48%         | 0.23    | 52%     | 0.79           | -                | 0.36                  | 0.52                 | 0.08 | 0.19 |
| <b>ABD-aged</b> | 41%         | 8.76    | 59%     | 10.02          | -                | 9.46                  | 9.50                 | 0.99 | 0.10 |

Lu and Isacson reported bulk complex modulus values for various asphalts (B1-B7) at 25°C ranging from 0.044 MPa to 0.839 MPa and 0.090 MPa to 1.37 MPa for unaged asphalts and RTFO-aged asphalts, respectively. Terefter et al. tested virgin asphalt binder and polymer modified binders but was unable to obtain meaningful results for a virgin asphalt binder using the Oliver and Pharr method. The reported Young's modulus values for polymer modified performance grade PG 70-22 and PG 76-28 binders were 0.76 MPa and 5.22 MPa, respectively. Jäger and Lackner reported Young's modulus values for B50/70 binder at 10°C ranging from 1.5 GPa to 2.5 GPa (1,500 Mpa to 2,500 Mpa). Young's modulus values for aged asphalt binders were not included in either study [6-7]. For the purpose of comparing Young's modulus values to other values obtained via nanoindentation, differences in the methods and equipment used to obtain the values are highlighted. For instance, the nanoindentation Young's modulus values reported by Terefter et al. and Jäger and Lackner were collected using a nanoindenter fitted with a spherical tip and Berkovich tip, respectively, which place the obtained Young's modulus values at larger length scales than the values obtained in this study. AFM imaging tips have a tip radius of approximately 8 nm, whereas a Berkovich tip has a radius of approximately 150 nm. Terefter et al. used a spherical tip with a nominal tip radius of 10 $\mu$ m (10,000 nm), so values reported in [7] were actually collected on the micrometer length scale rather than the nanometer length scale. As previously reported, several of the PDM-identified asphalt phases were as small as 1  $\mu$ m to 5  $\mu$ m in diameter, so it is clear that a tip radius larger than one of these phases would fail to capture the Young's modulus value for the isolated phase but rather a composite value of the phase, the surrounding phase, and the interfacial bond between the two phases. It should also be distinguished that the bulk values reported by Lu and Isacson were short-term aged using the thin-film oven test (TFOT); whereas, aged asphalt specimens that were tested in this study were long-term aged using the rolling thin-film oven test (RTFOT) and the pressure aging vessel (PAV).

## **Summary and Conclusions**

The overall importance of these findings is that the application of AFM imaging and nanoindentation to collect creep measurements in this study resulted in validation of the statistical significance of the asphalt micro-phases and original AFM creep data; furthermore, semi-quantitative viscoelastic properties have been obtained and associated with AFM phase images. The viscoelastic Young's modulus values extracted from age-altered phases of the same respective asphalts have provided important relationships between microstructural changes depicted in the images and changes in composite viscoelastic properties obtained from the measurements. Based on comparison of the composite viscoelastic Young's modulus values obtained from this study to values obtained at larger length scales, it was concluded that modulus values appear to decrease in magnitude as the length scale increases, which agrees with similar results reported by Jones [8] in the nanoindentation study of cement paste. Possible causes for higher modulus values could be due to tighter molecular clustering at the nano-scale or due to weaknesses between phase interfaces as theoretically depicted by Kringos et al. [9].

## Current Status/Next Steps

Modified samples of PG 64-22 with 2.5% SBS (elastomer) and PG 64-22 with 2.5% 7686 (plastomer) have recently been prepared for testing. These samples will be tested with the AFM

beginning in late January/early February 2012; the study will be identified as a nano-modification study and is part of the Task 1 deliverables for Year Six.

### Issues Identified During the Previous Year and Their Implications on Deliverables

Renovation of the McNew Materials lab and the Advanced Characterization of Infrastructure Materials (ACIM) lab have limited material preparation and testing during the previous quarter. The lab renovations should not cause a major delay in the deliverables scheduled for Year Six. The AFM camera was not functioning properly; therefore, a remote session was performed with an Agilent Technologies scientist in an effort to resolve the problem. The session was unsuccessful, and the camera was shipped to Agilent Technologies for diagnostics and repair. Testing will resume once the camera is received; expected receipt date is late January. This interruption in testing should not cause a major delay in the deliverables scheduled for Year Six. Asphalt samples were shipped to Saskatoon, Saskatchewan for soft x-ray beamline testing with the synchrotron. The samples were mostly damaged during transport, and the salvaged samples generated inconclusive results. This interruption in testing will likely cause a slight delay in the deliverables scheduled for Year Six.

### Work Plan Year Six

#### **Task 1**

The chemistry and micro-rheology of the microstructures within the asphalt binder influence its macroscopic properties such as stiffness, viscoelasticity and plasticity, adhesion, fracture and healing. By developing a clearer understanding of the micromechanical behavior or micro-rheology of the asphalt binder and linking that behavior to its chemical makeup and macroscopic properties, one can engineer asphalt binders and modifiers for asphalt binders that will result in improved mechanical properties and eventually longer-lasting and better performing pavements. The focus of this task will be to link previously obtained physical properties of AFM phases to chemical properties and determine how the relationship is influenced by aging. Associations will be made between asphalt chemistry and asphalt micromechanical properties through asphalt chemical mapping using methods such as soft x-ray beamline testing and AFM testing with functionalized AFM tips. These methods will result in the diffusion of atoms and molecular species and carbonyl grouping of the same asphalts in which physical properties have been extracted. The fabrication and testing of synthetic asphalt binders and individually extracted asphalt components will also significantly aid in validating the relationship between micromechanical properties and chemical composition. Special focus will be placed on viscoelastic properties and associated patterns of particular asphalt phases, which give a strong indication that weak zones somehow form during the molecular bonding and re-organization of phases as the binder ages. This suggests that while asphalt becomes stronger and more stable during this process, the formation of inevitable weak zones hinders composite performance properties and, thus, induces pavement distress. The application of AFM imaging, nanoindentation, and chemical mapping of asphalt binder will be presented as a potential method to understand and modify weaknesses amongst phase interfaces while improving the fatigue and fatigue healing characteristics of asphalt binders.

## **Task 2**

Closed form solutions for nanoindentation that exist in the literature do not provide accurate values for large deformation, and non-uniform tip geometry. This is due to the assumption that uniform tip geometry exists, and during indentation only small strains occur. However, through the finite element method (FEM) large strains along with changes in geometry can be accounted for, and a more accurate solution can be obtained. FEM can also be used to study sharp conical indenters for which analytical solutions may prove to be inaccurate. In this work, a finite element model is being developed to compare with the closed form solution for different geometry, loading, material behavior, and indentation depth. Correction factors will be given for large deformation indentation where the closed form expressions provide an inaccurate solution. The finite element model will then be extended to include viscoelastic material properties such as that of asphalt.

Some of the various assumptions that are made during an AFM indentation test include conical or spherical tip geometry, small deformations, and homogeneous and isotropic material response. During the next year various finite element models will be developed to study the effects of AFM tip geometry, and complex constitutive behavior of asphalt with application to AFM indentation. These constitutive models will include plasticity, viscoelasticity, and viscoplasticity. The results of the finite element simulations of different material models mentioned will be compared to AFM indentation test data. The purpose of these comparisons is to more accurately understand the recorded data during an AFM test and provide calibration factors to obtain data that is numerically more precise than the data that can be calculated with analytical expressions available in the literature [10-11].

## **Task 3**

Asphalt is currently assumed to be a homogenous material. However, composite behavior of asphalt binder has already been observed through AFM imaging and indentation testing [12]. The images obtained have shown the presence of different phases, and creep measurements have shown that micromechanical properties corresponding to each phase are also different. A finite element model consisting of multiple viscoelastic phases in agreement with experimental images and data will be analyzed and the indentation response will be compared to that of a uniformly distributed homogeneous material. This will show the difference in response of a composite asphalt binder as opposed to one containing a single phase. This in turn will help characterize asphalt more accurately and describe its mechanical response (e.g., composite elastic modulus, composite viscoelastic creep compliance) under any stimuli.

## **Task 4**

Fatigue damage is directly related to number of load cycles and plastic strain. Therefore, understanding the plastic behavior of the asphalt binder is of high interest. Further AFM tests will be performed to study the effect of aging on the plasticity of asphalt binder. AFM images have shown the existence of beehive structures in aged asphalt samples [12]. These structures may exhibit different plastic response under loading compared to an unaged sample. The beehive regions will be indented and the residual deflection will be measured. This will be compared to

the residual deflection of an unaged sample for the same type of test. The comparison will show whether the beehive regions are a physical representation of increased plastic response. This will help characterize aging along with the effects of aging on fatigue damage of asphalt binder.

### **Task 5**

During an AFM indentation test, the measurements taken are affected by the surface van der Waals force interactions between the AFM tip and the asphalt sample. These forces are both of attractive and repulsive in nature at various times during the test. This van der Waals attraction and repulsion as a function of the distance between the tip and the sample is referred to as the Lennard-Jones Potential [13]. At the nanoscale these forces can be significant enough to affect the measured data. The next phase of this work will involve the inclusion of the Lennard-Jones Potential into a finite element model.

All finite element modeling will be done using an open source finite element code or a commercial software such as ABAQUS. The development of an open source finite element model will provide with a tool to accurately carry out AFM indentation tests without having to run the experiments. This will prove to be cost effective in terms of time, resources, and expenditures. Also, the commercialization of such code will prove to be an effective tool for analyzing indentation for research and design purposes. A complete package will include complex constitutive behavior, will account for non-uniform tip geometry, and also include surface interactive forces. The end product will determine the material response under loading. For example, it will be able to quantify the plastic response and predict fatigue damage. This will result in the proper selection of binder, which will lead to an effective pavement design with long service life. This in turn will save millions of dollars that otherwise would be spent for maintenance and rehabilitation each year.

### **Cited References**

- [1] Vandamme, M., 2008, “The nanogranular origin of concrete creep: a nanoindentation investigation of microstructure and fundamental properties of calcium–silicate–hydrates.” Massachusetts Institute of Technology.
- [2] Galin, L., I. Sneddon, and H. Moss, 1961, “Contact problems in the theory of elasticity.” Raleigh (NC): Dept. of Mathematics, School of Physical Sciences and Applied Mathematics, North Carolina State College.
- [3] Sneddon, I.N., 1965, Relation between load and penetration in axisymmetric Boussinesq problem for punch of arbitrary profile. *Int J Eng Sci*, 3, 47–57.
- [4] Hashin, Z., 1983, Analysis of Composite Materials. *Journal of Applied Mechanics*, 50, 481-505
- [5] Lu, X., and U. Isacsson, 2002, Effect of aging on bitumen chemistry and rheology. *Construction and Building Materials*, 16, 15-22.



- [6] Jäger, A., R. Lackner, and J. Eberhardsteiner, 2007, Identification of viscoelastic properties by means of nanoindentation taking the real tip geometry into account. *Meccanica*, 42, 293-306.
- [7] Tarefder, R.A., A.M. Zaman, and W. Uddin, 2010, Determining Hardness and Elastic Modulus of Asphalt by Nanoindentation. *International Journal of Geomechanics*, 106-116.
- [8] Jones, C.A., 2011, “Contact Mechanics Based on Mechanical Characterization of Portland Cement Paste.” Ph.D. Dissertation. Texas A&M University, College Station, TX.
- [9] Kringos, N., A. Schmets, T. Pauli, and T. Scarpas, 2009, A Finite Element Based Chemo-Mechanical Model to Simulate Healing of Bitumen.” *Proc.*, International Workshop on Chemo-mechanics of Bituminous Materials, Delft, Netherlands.
- [10] Fischercripps, A., 2004, A simple phenomenological approach to nanoindentation creep. *Materials Science and Engineering A*, 385 (1-2), 74-82.
- [11] Vandamme, M., and F. Ulm, 2006, Viscoelastic solutions for conical indentation. *International Journal of Solids and Structures*, 43 (10), 3142-3165.
- [12] Allen, R.G., 2010, Structural Characterization of Micromechanical Properties in asphalt using atomic force microscopy. Master’s Thesis, Texas A&M University.
- [13] Johnson, K., 1998, Mechanics of adhesion. *Tribology International*, 31(8), 413-418.

## **Work Element F2e: Verification of the Relationship between DSR Binder Fatigue Tests and Mixture Fatigue Performance (UWM)**

### Work Done This Quarter

The consolidated draft report “M” has been submitted in 508 format for review. This report includes findings from work elements F1d-6 and F2a. Additionally, a “Tech Brief” has been drafted and submitted for this report.

### Significant Results

The consolidated draft report “M” has been submitted for review. Also, comments from reviewers of paper accepted in TRB were reviewed and addressed.

### Significant Problems, Issues and Potential Impact on Progress

None.

### Work Planned Next Quarter

Revise draft report “M” according to reviewers’ comments.

## CATEGORY F3: MODELING

### Work Element F3a: Asphalt Microstructural Model

#### Work Done This Quarter

#### ***Subtask F3a-1. ab initio Theories, Molecular Mechanics/Dynamics and Density Functional Theory Simulations of Asphalt Molecular Structure Interactions (URI)***

Progress in the quarter focused on implementing methods to convert more output results from the molecular simulations into forms that can be compared with experimental data. This was pursued in part to help a new graduate student with coming up to speed on the project.

The instantaneous stresses during a simulation can be combined and averaged into a stress correlation function,  $\langle \sigma(0)\sigma(t) \rangle$ , which quantifies how the stress tensor  $\sigma$  fluctuates as a function of time. In past work (Zhang 2007, Zhang 2010), this correlation function has been integrated to provide an estimate of the zero-shear viscosity of a model asphalt. Work this quarter aimed to use numerical Fourier transforms to convert the stress fluctuation results into the complex modulus  $G^*(\omega)$ . This is possible through the relationships

$$G(t) = \sigma / \gamma = \frac{V}{10k_B T} \sum_{u,v} \langle \sigma_{uv}^{st}(0) \sigma_{uv}^{st}(t) \rangle$$
$$G^*(\omega) = i\omega \int_0^{\infty} e^{-i\omega t} G(t) dt$$

in which  $(u,v)$  refer to coordinate directions (i.e.  $x,y,z$ ), st indicates a stress tensor matrix that has been made symmetric and traceless,  $k_B$  is the Boltzmann constant, and  $V$  and  $T$  are system volume and temperature. The first equation comes from the molecular simulation literature (Daivis and Evans 1994) and the second from the classic text on viscoelasticity (Ferry 1980).

The software code implementing the Fourier transformation (second equation) and accompanying unit conversions was still being debugged and tested at the end of the quarter. Results are expected during the next quarter for all model asphalts simulated to date.

Progress was made on manuscripts that describe molecular dynamics simulations of a next-generation model asphalt that is representative of SHRP AAA-1. Additional analyses of diffusion coefficient results were conducted during the quarter.

#### ***Subtask F3a-2. Develop algorithms and methods for directly linking molecular simulation outputs and phase field inputs (URI, VT)***

Asphalt binder, known as the most important pavement material, has been analyzed by the traditional empirical analysis and other methods such as Finite Element Method (FEM), Discrete Element Method (DEM) and etc during the past years. Having considered the advantages of these methods, there still exist many shortcomings of the traditional analysis.

Recently, the Phase Field Method (PFM) has emerged as a powerful computational way to simulate and forecast the microstructure evolution of asphalt binder. Not like the traditional analysis method using mechanics approach, it analyzes the problems from the energy aspect and can provide a view of the whole microstructure evolution process.

During the past quarter, we mainly make progress in three aspects by using PFM in analyzing the asphalt performance:

First, we've established a theoretical multi-phase model coupling with N-S equation for the asphalt binder analysis. In our case, the components of asphalt are simplified to three: asphaltene, resin and oil. The reason why we do not consider wax as a component is that although wax plays a negative effect, it is dissolved in oil. The distribution of oil represents the distribution of wax. Besides, in order to reflect the rheological property of asphalt, it is considered as a viscoelastic fluid in the mathematical treatment. Based on these assumptions, a Multi-Phase Model is developed. Further research shows that phase separation will happen in a given thermodynamic condition and result in uneven distributions of these components. Second, the theoretical PFM analysis in crack propagation is given. The traditional theory of crack propagation is Fracture Mechanics introduced by Griffith. The theoretical and calculation process are very complex. Here, by using PFM, we can simplify the problem to two categories: the broken part is considered as 0 while the intact part is considered as 1. The imbalances of the surface free energy and bulk energy as well as elastic energy lead to the development of crack. Not like considering asphalt as a fluid in the first part, we consider it as a viscoelastic material. Based on the field displacement and material properties such as viscosity, elastic modulus and etc, we use Allen-Cahn equation to establish a theoretical analysis of crack propagation with the introduction of artificial initial crack.

Last but not least, the ideal self-healing model of asphalt binder is given. By using PFM, we suggest that the way of Minimum Path Free Energy is the development direction if an initial crack is given. The form of free energy in self-healing is totally different from that in crack propagation. Although they both have a double well potential form, the former has two uneven wells while the latter has two even wells. The system has a lower free energy at the stable state  $\phi = 1$  while it has a higher free energy at the metastable state  $\phi = 0$ . And thus the system favors the intact state ( $\phi = 1$ ) and tends to heal itself.

Generally, our current researches are mainly focused on the theoretical part of the application of phase field method in the asphalt binder analysis. And this task has been finished by the end of January 2012. Our next target is to carry out the numerical simulation by using the software COMSOL as well as the experiment. The numerical part is expected to obtain the initial results by the end of February 2012 and the initial comprehensive analysis by the end of March. The experimental part is also expected to carry out during the same time.

## **Current progress**

### **1.1 Analysis of asphalt performances based on asphalt chemistry by Multi-Phase field modeling**

Asphalt, known as the petroleum product, consists of asphaltene, wax, aromatics, resin and many other chemical components. Each component will affect the overall physical properties of asphalt and even mechanical behaviors. Especially, the contents of asphaltene and wax are the two most important factors, in which the wax will be a negative factor. And thus the determination of the relationship between wax content as well as other components and physical properties needs for research. During this quarter, a mathematical multi-phase model is established to determine the relationship.

Generally, asphalt is solid at normal temperature. Further study shows that it actually has the viscoelastic property. In the SHRP report, asphalt binder, from a rheological standpoint, is classified as a viscoelastic fluid rather than a viscoelastic solid. And thus here we consider the asphalt as a viscoelastic fluid and employ the classic fluid mechanical equation Navier-Stokes equation coupled with the Phase field model for analysis. With the development of phase separation, the physical property of asphalt binder such as critical temperature and viscosity can be determined. And furthermore, the asphalt performance such as yield, limiting strength, grading criterion and so on can be obtained.

#### **1.1.1 Phase separation kinetics**

Consider an adiabatic isolated system, based on the classic thermodynamic theory, it is well known that the microstructure evolution development is determined by the free energy. Especially, the Allen-Cahn equation and Cahn-Hilliard equation explain the driven force by the chemical potential (non-conserved case) or gradient of chemical potential (conserved case), respectively. A normal expression of the free energy model is the double –well potential, which is shown in figure 1.

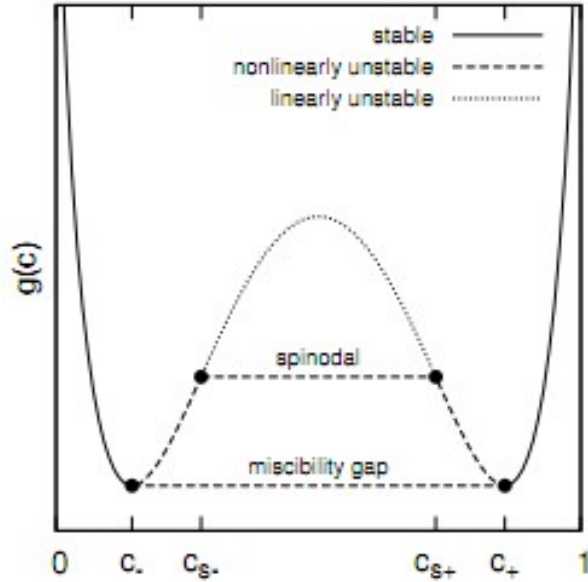


Figure 1. Free energy model for a normal case [1].

Assume the system studying is homogenous. From the above figure 1 we can see that the system has two metastable state  $c_1$  &  $c_+$ . The region between the two metastable points is unstable. A very tiny perturbation will lead to the phase separation. A more detailed explanation is shown in figure 2. It is clear that the energy curve falls below the string of the two points. The phase separation to two metastable points will lead to the lower of the total energy and finally make the system stable.

For figure 3, it shows the spinodal decomposition maps. The inflection point is defined at  $\frac{\partial^2 \Delta G}{\partial X^2} = 0$  in the energy curve. Region outside the inflection points with  $\frac{\partial^2 \Delta G}{\partial X^2} < 0$  will automatically decompose to two states in order to lower the free energy.

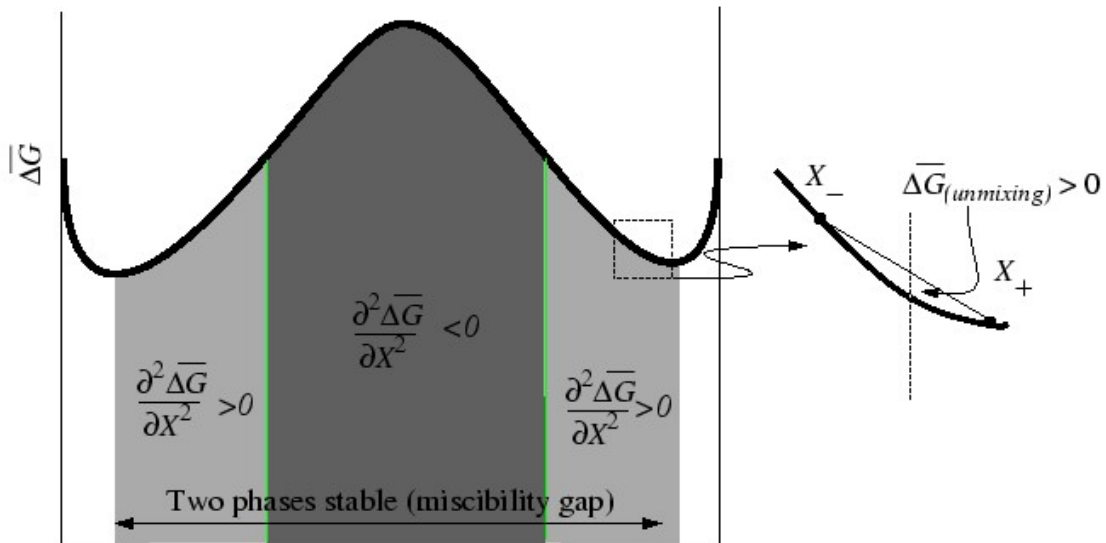


Figure 2. Free energy divided by its second-order derivative [2].

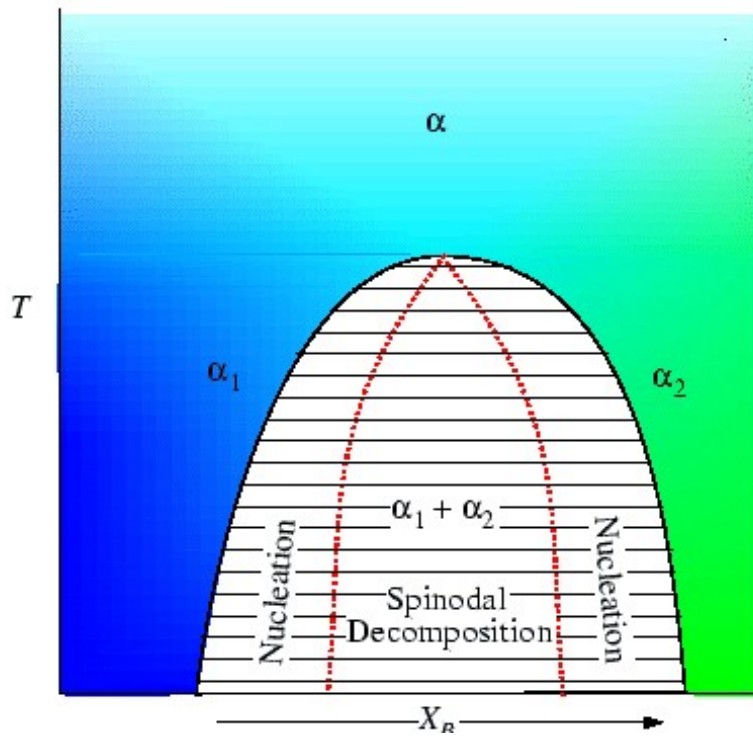


Figure 3. A phase diagram with a spinodal miscibility gap [2].

The above sections and the figures illustrate the basic idea of phase separation. Actually, it shows a binary system which means two components in physical meaning.

For our case, we need to separate asphalt binder into many components. In this report, we consider it as a ternary system consisting of three species: asphaltene, resin, oil. Because wax is dissolved in oil, the distribution of oil reflects the content of wax.

Set the order parameter  $\phi_i(r, t)$  represent the concentration  $i=1, 2, 3$ , which is standing for asphaltene, resin and oil, respectively.

Easily we have

$$\phi_1 + \phi_2 + \phi_3 = 1 \quad (1)$$

Like the phase field model of the binary system, the free energy of a ternary system also has a specific double well form. A free energy of the system as proposed by Boyer and Lapuerta (2006) is defined by [3]

$$F = \sigma_{12}\phi_1^2\phi_2^2 + (\phi_1 + b)(\phi_2 - d)^2 + (e - \phi_1 - \phi_2)(\phi_2 - f)^2 \quad (2)$$

Where  $a, b, d, e$  and  $f$  are given values.

### 1.1.2 Coupled Navier-Stokes-Cahn-Hilliard System

As we have said in the summary part, in order to reflect the rheological property of asphalt, it is considered as a fluid and the classic fluid mechanical equation Navier-Stokes equation is employed later for analysis.

First, based on Cahn and Hilliard's contributions on the phase field theory, we have the flux as

$$j_i = M_i \nabla \mu_i \quad (3)$$

where  $M_i$  is the mobility parameter.

Yue *et al* (2010) gives the Cahn-Hilliard equation as [4]

$$\frac{\partial \phi_i}{\partial t} + u \cdot \nabla \phi_i = \nabla \cdot (M_i \nabla \mu_i) \quad (4)$$

where  $u$  is the velocity and  $M_i$  is the mobility parameter.

In the classic SHRP's report, it considers the asphalt binder as a viscoelastic fluid. In this report, it is considered as a three-component fluid flow that is viscous and incompressible. What should be mentioned here is we use a binary case to study the ternary system since it's easier to calculate the binary system.

According to the Navier – Stokes equation, by coupling with the phase field, we have

$$\rho \left( \frac{\partial u}{\partial t} + u \cdot \nabla u \right) = -\nabla p + \nabla \cdot \eta (\nabla u + (\nabla u)^T) + (\mu_1 \nabla \phi_1 + \mu_2 \nabla \phi_2) \quad (5)$$

where  $u$  is the velocity,  $p$  is the pressure,  $T$  represents the transposed vector signal and  $\eta$  is the viscosity [4].

### 1.1.3 Non-dimensional Multi-phase modeling

In this part, our modeling is non-dimensionalized. Further numerical analysis will be carried out to reveal the differences between the nondimensional equations and the original ones.

$$\text{Set } \nabla^* = L \nabla, u^* = \frac{u}{U}, \mu^* = \mu \frac{\xi^2}{\kappa \phi_B}, p^* = \frac{pL}{\eta_1}, c^* = \frac{c}{c_B}, t^* = \frac{tU}{L}, g^* = \frac{g\xi}{\kappa \phi_B^2}, \eta^* = \frac{\eta}{\eta_1},$$

Where  $U$  is the characteristic value and  $L$  is the characteristic length.

Use the above parameter to nondimensionize the governing equations and we have the multi-phase field model as follows

$$Re \cdot \rho \frac{\partial u}{\partial t} = -\nabla p + \eta \nabla^2 u + \frac{\rho_1}{c_a c_h} \cdot \rho \cdot (\mu_1 \nabla \phi_1 + \mu_2 \nabla \phi_2) \quad (6)$$

$$\frac{\partial \phi_1}{\partial t} + u \cdot \nabla(\phi_1) = \frac{1}{Pe} \nabla \cdot (\nabla \mu_1) \quad (7)$$

$$\frac{\partial \phi_2}{\partial t} + u \cdot \nabla(\phi_2) = \frac{1}{Pe} \nabla \cdot (\nabla \mu_2) \quad (8)$$

$$\mu_1 = \frac{\partial F}{\partial \phi_1} - C_h^2 \nabla^2(\phi_1) \quad (9)$$

$$\mu_2 = \frac{\partial F}{\partial \phi_2} - C_h^2 \nabla^2(\phi_2) \quad (10)$$

$$\phi_1 + \phi_2 + \phi_3 = 1 \quad (11)$$

where the Peclet number  $Pe = \frac{UL\xi^2}{D\kappa}$

$$\text{Capillary number } C_a = \frac{\eta_1 U \xi}{\kappa c_B}$$

$$\text{Cahn number } C_h = \frac{\xi}{L}$$

$$\text{Reynolds number } Re = \frac{\rho_1 U^2}{L}$$

Apply the boundary condition at the wall

$$\hat{n} \cdot \nabla \phi_i = 0 \quad (12)$$

$$u = u_w \quad (13)$$

where  $u_w$  is the boundary wall velocity and  $\hat{n}$  is the unit vector to the domain boundary.

## 1.2 Fracture modeling of asphalt binder based on the phase field

During the past quarter, we have analyzed the asphalt binder fracture process based on Phase Field Method. A viscoelastic phase field model is employed based on the current research progress in mechanical engineering.

In conventional fracture mechanics, the fracture process is described by growth of the crack. Here, it is analyzed with a set of field variable  $\phi$ . Generally, we have  $\phi = 1$  for the intact part and  $\phi = 0$  for a crack region.

Based on the Ginzburg-Landau theory, we can develop the microstructure evolution model of the order parameter  $\phi$ . With the specific physical properties and configuration of asphalt binder, we apply this theory to study the fracture process.

### 1.2.1 Crack opening modes

Generally, there are three crack opening modes based on different stress [5]:



- 1) Mode I crack- Opening mode (a tensile stress normal to the plane of the crack)
- 2) Mode II crack- Sliding mode (a shear stress acting parallel to the plane of the crack and perpendicular to the crack front)
- 3) Mode III crack – Tearing mode (a shear stress acting parallel to the plane of the crack and parallel to the crack front)

All the 3 modes are shown in figure 4.

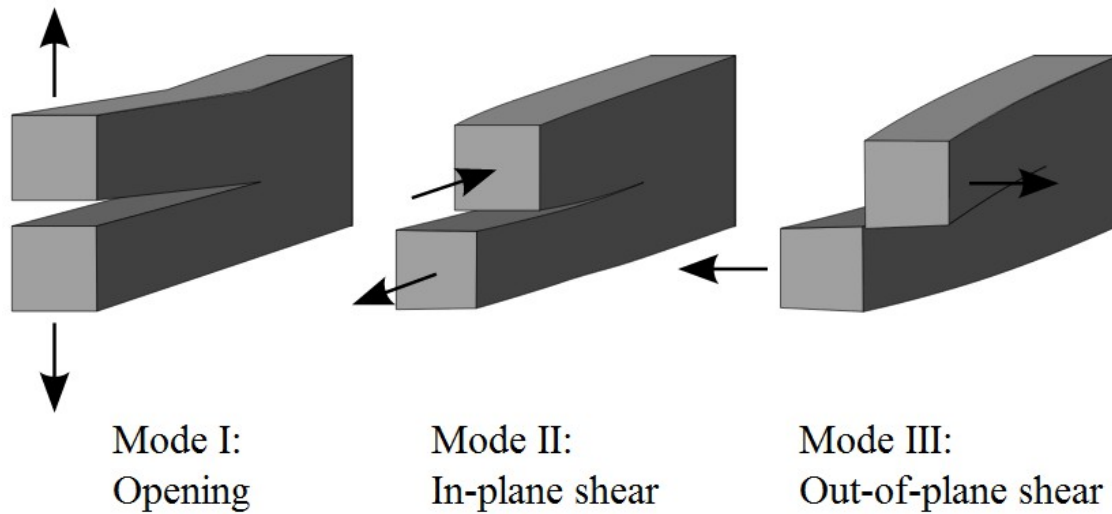


Figure 4. Three modes of crack [5].

In common cases, Mode I and Mode II are the most frequent crack that will happen in asphalt binder. The occurring of Mode III crack means a very bad condition which may lead to the failure of the pavement. In order to simplifying our analysis, we take the Mode I and Mode II crack openings for analysis in this report. The two modes are given in the different initial states of the field variable  $\phi$ .

### 1.2.2 Viscoelastic Stress analysis

In our cases, because the asphalt behaves the viscoelastic property, we consider the crack propagates in the linear viscoelastic material medium.

In the classic mechanical theory, the strain tensor are defined as the symmetrical spatial derivatives of the displacement fields

$$\varepsilon_{ik} = \frac{1}{2} \left( \frac{\partial u_i}{\partial x_k} + \frac{\partial u_k}{\partial x_i} \right) \quad (14)$$

For asphalt, considering it as a viscoelastic material, Diplom-Physiker (2010) gives the corresponding total analysis of the crack propagation by using the phase field method. And the followings show some of his contributions.

The stress field [6] can be divided to two parts as

$$\sigma_{ik}^{total} = \sigma_{ik}^{(el)}(\varepsilon_{ik}) + \sigma_{ik}^{(vis)}(\dot{\varepsilon}_{ik}) \quad (15)$$

where  $\sigma_{ik}^{(el)}$  and  $\sigma_{ik}^{(vis)}$  are the elastic and viscous stresses, respectively.

The elastic stresses can be given by,

$$\sigma_{ik}^{(el)} = \frac{E}{1+\nu}(\varepsilon_{ik} + \frac{1}{1-2\nu}\delta_{ik}\varepsilon_{ll}) \quad (16)$$

where  $E$  is the elastic modulus and  $\nu$  is the Poisson ratio.

And the viscoelastic part [6] is

$$\sigma_{ik}^{(vis)} = \frac{\eta}{1+\zeta}(\dot{\varepsilon}_{ik} + \frac{1}{1-2\zeta}\delta_{ik}\dot{\varepsilon}_{ll}) \quad (17)$$

The coefficient of the viscoelastic part is similar to the elastic part.

### 1.2.3 Phase field modeling

Based on Newton's law of motion, we have

$$\rho\ddot{u}_l = \frac{\partial\sigma_{ik}^{(total)}}{\partial x_k} \quad (18)$$

Robert Spatschek *et al* (2006) presented a free energy form as follows [7],

$$F(\phi) = \int_{\Omega} (f_s + f_{dw} + f_{el})dV \quad (19)$$

Where

$$f_s(\nabla\phi) = 3\gamma\varepsilon(\nabla\phi)^2/2 \quad (20)$$

is the gradient energy density and

$$f_{dw}(\phi) = 6\gamma\phi^2(1-\phi)^2/\varepsilon \quad (21)$$

is the double well potential which reflects the local free energy[6].

And the elastic energy is expressed as

$$f_{el} = \frac{h(\phi)E}{2(1+\nu)} \left( \frac{\nu}{1-2\nu} \varepsilon_{ii}^2 + \varepsilon_{ik}^2 \right) \quad (22)$$

Where  $h(\phi) = \phi^2(3 - 2\phi)$  is an interpolation function [6].

Based on equation (15) and equation (18), the evolution of the elastic fields is determined by

$$\rho \ddot{u}_i = \frac{\partial}{\partial x_i} (\sigma_{ik}^{(el)} + \sigma_{ik}^{(vis)}) \quad (23)$$

where  $\sigma_{ik}^{(el)} = \partial f_{el} / \partial \varepsilon_{ik}$ .

Consider non-conservative situation and employ Allen-Cahn equation. Given the order parameter  $\phi$  as described in the above, employ the equation [7]:

$$\frac{\partial \phi}{\partial t} = - \frac{D}{3\gamma\epsilon} \frac{\delta F}{\delta \phi} \quad (24)$$

where D corresponds to the kinetic coefficient while  $\gamma$  and  $\epsilon$  are relevant to the interface property.

Viscosity is a very important parameter in our analysis. We consider it as constant during the crack propagation. The reason is that viscosity is a bulk value that will not be affected by the phase separation of crack and intact unless the system fails.

Another mathematical treatment we use here is the ignoring of the temperature coupling. As we know, the viscous friction will have an effect in the local temperature field. In order to simplify our model, we consider asphalt binder as a high thermal conductivity material and thus the problem becomes a non-conserved case so that the employing of equation (24) is reasonable. In Diplom-Physiker's thesis paper, he carefully analyze the cracking behavior of the three modes especially the third mode.

For Mode I and Mode II crack propagation, the development is actually the plane crack propagation and thus the analysis is relative simple.

For the third one, since it is a spatial problem, the case is more complex than Mode I & Mode II. The displacement field is express as:  $u_x(x, y)$ ,  $u_y(x, y)$  and  $u_z = (x, y)$ .

Rewrite equation (16) and expand it to the elastic part and viscous part [6]

$$\rho \ddot{u}_i = \frac{\partial \sigma_{ik}^{(el)}}{\partial x_i} + \frac{\partial \sigma_{ik}^{(vis)}}{\partial x_i} \quad (25)$$

Based on equation Considering the Lamé constants  $\mu$  and  $\lambda$ , expand equation (16) to 3 equations [6].

$$\begin{aligned}\rho \frac{\partial^2 u_x(x,y)}{\partial t^2} &= \frac{\partial(\sigma_{xx}^{(el)} + \sigma_{xx}^{(vis)})}{\partial x} + \frac{\partial(\sigma_{xx}^{(el)} + \sigma_{xx}^{(vis)})}{\partial y} \\ &= \frac{\partial}{\partial x} [(\lambda + 2\mu)\varepsilon_{xx} + \lambda\varepsilon_{yy} + \tau_{vis}((\lambda + 2\mu)\varepsilon_{yy})] + 2\frac{\partial}{\partial y} [\mu\varepsilon_{xy} + \tau_{vis}\mu\varepsilon_{xy}]\end{aligned}\quad (26)$$

$$\begin{aligned}\rho \frac{\partial^2 u_y(x,y)}{\partial t^2} &= \frac{\partial(\sigma_{yy}^{(el)} + \sigma_{yy}^{(vis)})}{\partial y} + \frac{\partial(\sigma_{yy}^{(el)} + \sigma_{yy}^{(vis)})}{\partial x} \\ &= \frac{\partial}{\partial z} [\lambda\varepsilon_{xx} + (\lambda + 2\mu)\varepsilon_{yy} + \tau_{vis}(\lambda\varepsilon_{xx} + (\lambda + 2\mu)\varepsilon_{yy})] + 2\frac{\partial}{\partial x} [\mu\varepsilon_{xy} + \tau_{vis}\mu\varepsilon_{xy}]\end{aligned}\quad (27)$$

$$\begin{aligned}\rho \frac{\partial^2 u_z(x,y)}{\partial t^2} &= \frac{\partial(\sigma_{xz}^{(el)} + \sigma_{xz}^{(vis)})}{\partial x} + \frac{\partial(\sigma_{yz}^{(el)} + \sigma_{yz}^{(vis)})}{\partial z} \\ &= 2\frac{\partial}{\partial x} [\mu\varepsilon_{xz} + \tau_{vis}\mu\varepsilon_{xz}] + 2\frac{\partial}{\partial y} [\mu\varepsilon_{yz} + \tau_{vis}\mu\varepsilon_{yz}]\end{aligned}\quad (28)$$

Combining these equations with the phase field equation (24), we can obtain the Mode III crack propagation of asphalt binder. In fact, by simplifying the displacement field model, Mode I and Mode II are easy to figure out.

### 1.3 A Self-healing model based on Phase field modeling

In this part, the very important characteristic physical property of asphalt binder- self- healing- has been analyzed theoretically by using the Phase field method. Currently, the healing mechanism is still under research and many researchers have suggested their theories. However, most of the current research in this area is only focusing on the empirical methods and thus can only suggest some phenomenological formulas that have little physics. During the past quarter, we use Phase Field Method to analyze the problem and successfully unified the process of self- healing and crack propagation in a certain extent.

Actually, the self- healing process is the reverse process of crack propagation. In our analysis, the only difference between them is the development direction, of which the crack propagation tends to develop the crack while the self-healing process tends to shrink the crack. The driving force of both the two process is the free energy.

The way to differentiate the two processes is to find different forms of free energy which have different minimum values. The way to the Minimum Path Free Energy (MPFE) is the development direction. For the healing case, the minimum free energy happens at the state  $\phi = 1$ .

#### 1.3.1 The unifying of healing and cracking

Recall the analysis principle we used in crack analysis. Consider the non-conserved case and give the Allen-Cahn equation

$$\frac{\partial \phi}{\partial t} = -M \frac{\delta F}{\delta \phi} \quad (29)$$

In the crack propagation analysis, we mandatorily regulate that  $\frac{\delta F}{\delta \phi} > 0$  so that  $\frac{\partial \phi}{\partial t} < 0$  which means the crack propagation happens. The free energy  $F$  here only consists of local free energy, surface free energy and elastic energy.

For the healing process, the situation is the contrary.  $\frac{\partial \phi}{\partial t}$  should be larger than zero, which means  $\frac{\delta F}{\delta \phi} < 0$ . In this case, we have to consider the environmental conditions such as temperature. Elastic energy will also play an important role. After obtaining these factors, the healing process can be analyzed.

For the free energy analysis, we use a free energy function suggested by Jou and Lusk (1997) [8]

$$f(\phi) = \frac{1}{4}\eta\phi^2(\phi - 1)^2 + \frac{3\epsilon}{2}\left(\frac{\phi^3}{3} - \frac{\phi^2}{2}\right) \quad (30)$$

where the parameter  $\epsilon$  controls the stability. For  $\epsilon > 0$ , the stable state is at  $\phi = 1$  while for  $\epsilon < 0$ , the stable state is at  $\phi = 0$ . When  $\epsilon$  is equal to zero, both of the  $\phi = 0$  and  $\phi = 1$  are at metastable state.

Given  $\epsilon < 0$  and we can get the following figure

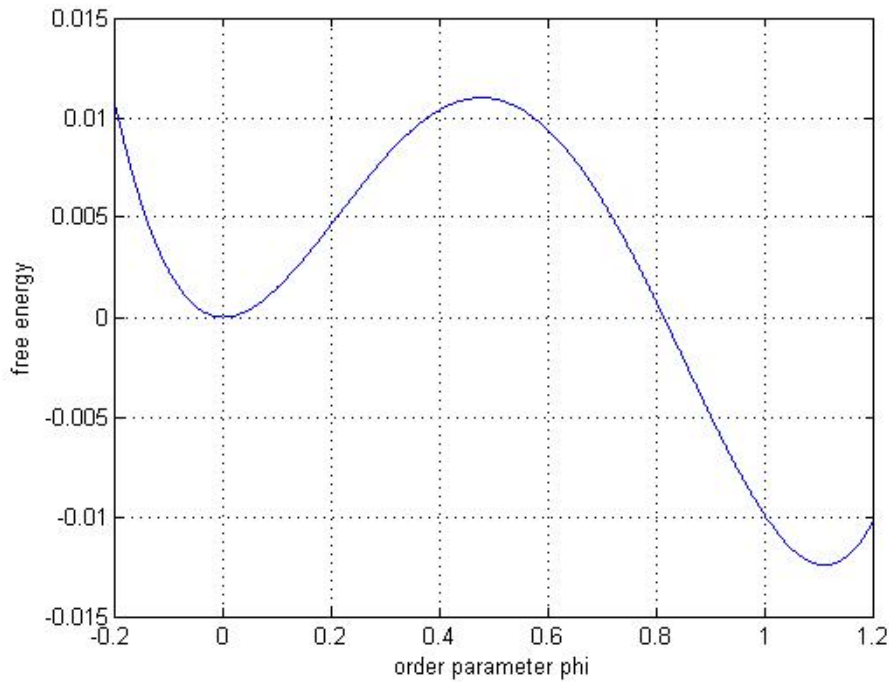


Figure 5. Local free energy give  $\eta = 0.65$  and  $\epsilon = -0.0130$ .

This figure gives us an uneven double well potential which means the system does not have two equal minimum states. One can easily see that the system favors phase  $\phi = 1$ . Recall the concept energy barrier. The minimum free energy happens at  $\phi = 1$  and this state is stable. There exist a fall between  $\phi = 0$  and  $\phi = 1$ . Thus the state at  $\phi = 0$  is metastable. A small perturbation around

the vicinity of  $\phi = 0$  may cause the phase separate to  $\phi = 1$ . That means overcome the energy barrier will lead to self-healing.

The difference of the two states. [8] is expressed as

$$\Delta f = \frac{\epsilon}{4} \quad (31)$$

And the energy barrier [8] is given by

$$f_b = \frac{(\eta-3\epsilon)^3(\epsilon+\eta)}{64\eta^3} \quad (32)$$

With the inflection point is determined by

$$\epsilon = \frac{\eta}{3} \quad (33)$$

For the states around  $\phi = 0$ , only sufficient large perturbation that helps overcome the energy barrier will lead to the minimum stable state  $\phi = 1$ . For the states in the vicinity of  $\phi = 1$ , the system will automatically develop to the minimum state (spinodal decomposition).

The evolution process that the system tends to reach the minimum state  $\phi = 1$  is actually the process of self-healing.

### 1.3.2 Self-Healing modeling

Assume in a standard situation, equation (30) is employed to simulate the free energy.

For the viscoelastic stress part, recall crack propagation analysis.

For the elastic stresses, it can be given by,

$$\sigma_{ik}^{(el)} = \frac{E}{1+\nu} (\epsilon_{ik} + \frac{1}{1-2\nu} \delta_{ik} \epsilon_{ll}) \quad (34)$$

where  $E$  is the elastic modulus and  $\nu$  is the Poisson ration.

For the visco part, we have

$$\sigma_{ik}^{(vis)} = \frac{\eta}{1+\zeta} (\epsilon_{ik} + \frac{1}{1-2\zeta} \delta_{ik} \epsilon_{ll}) \quad (35)$$

The elastic energy is

$$F_{ela} = \int_V \sigma_{ik}^{total} dV \quad (36)$$

Consider the non-conserved situation and employ equation (33), we can have the self-healing process. And in order to make the heal process happens,  $\frac{\delta F}{\delta \phi}$  must be always less than zero.

$$\frac{\partial \phi}{\partial t} = -M \frac{\delta F}{\delta \phi} \quad (37)$$

where  $M$  is the mobility parameter.

### 1.3.3 Modified Model with Relaxation

The abovementioned analysis is for the perfect situation, which means there is no noise term. However, in the actual case, there should exist a noise term and thus become a process involving relaxation dynamics.

Kobayashi introduced fluctuation into the Phase Field Method by adding a term (Xu Hong (2010))  $A\phi(1 - \phi)R$  with a stochastic item [9], which is

$$\langle f(x, t) \rangle = 0 \quad (38)$$

$$\langle f(x, t)f(x', t') \rangle = A^2\phi^2(1 - \phi)^2\delta(x - x')\delta(t - t') \quad (39)$$

And thus the equation can be rewrote as

$$\frac{\partial \phi}{\partial t} = -M \frac{\delta F}{\delta \phi} + ar\phi(1 - \phi) \quad (40)$$

Besides, Tamas Pustai et al [2008] proposed in his paper

$$\frac{\partial \phi}{\partial t} = -M \frac{\delta F}{\delta \phi} + \zeta_\phi \quad (41)$$

The appropriate noise term  $\zeta_\phi$  represents the non-conserved case here. Karma and Rappel (1999) gives this term [10].

$$\frac{\partial \phi}{\partial t} = -\Gamma_\phi \frac{\delta F}{\delta \phi} + \theta(\vec{r}, t) \quad (42)$$

Where  $\theta(\vec{r}, t)$  is the non-conserved white noise while it is Gaussianly distributed with variances. [10]

$$\langle \theta(\vec{r}, t)\theta(\vec{r}', t) \rangle = 2\Gamma_\phi k_B T_M \delta(\vec{r} - \vec{r}')\delta(t - t') \quad (43)$$

While

$$F_u = \frac{2k_B T_M^2 c}{L^2 l^3} \quad (44)$$

where  $F_u$  is the thermal fluctuation amplitude,  $k_B$  is the Boltzmann constant. And thus we have the following. [10]

$$\zeta_\phi = \zeta_{I,\phi} + (\zeta_{I,\phi} - \zeta_{B,\phi})p(\phi) \quad (45)$$

Where  $\zeta_{I,\phi}$  and  $\zeta_{B,\phi}$  are the amplitude of white noise of intact state and broken state.

## II. Research plan for next quarter

The theoretical analysis of asphalt binder is given in the abovementioned analysis. Due to the tight schedule, the numerical analysis has not been carried out and thus our goal for the next quarter is to simulate the above three aspects which include but not limit to the followings:

The computer simulation of multi-phase model needs to be carried out. The detailed results of phase separation process is expected to have;

With the coupling of N-S equation, the multi- phase model should have a different behavior other than (1). The difference should be carefully watched and analyzed;

The simulation of non-dimensional equations for the multi-phase model will be carried out and the comparisons with the dimensional ones will be found;

The simulation of crack propagation will be executed with the introduction of initial Mode I and Mode II crack;

The simulation of self- healing will be carried out to get the results and comparison between healing and cracking will reveal the determination factor in the microevolution process.

The experiment of crack propagation of asphalt binder is expected to carry out. We plan to use a thin-film asphalt binder and heat it to a relatively high temperature. Then the crack propagation during the cooling down process can be watched. The experimental results can be compared with the theoretical numerical part to check the reliability.

## Cited References

1. [http://ocw.mit.edu/courses/chemical-engineering/10-626-electrochemical-energy-systems-spring-2011/lecture-notes/MIT10\\_626S11\\_lec38.pdf](http://ocw.mit.edu/courses/chemical-engineering/10-626-electrochemical-energy-systems-spring-2011/lecture-notes/MIT10_626S11_lec38.pdf). MIT OpenCourseWare.
2. <http://pruffle.mit.edu/3.00/> W. Craig Carter .MIT 3.00 Thermodynamics of Materials
3. Kim J, J. Lowngrub. Phase field modeling and simulation of three-phase flows. *Interface Free Boundaries*, 2005, 7, 435-466.
4. Pengtao Yue, Chunfeng Zhou, James J. Feng. Sharp – interface limit of the Cahn-Hilliard model for moving contact lines. *J. Fluid Mech.* (2010), vol. 645, pp. 279-294.
5. Fracture mechanics. Wikipedia. [http://en.wikipedia.org/wiki/Fracture\\_mechanics](http://en.wikipedia.org/wiki/Fracture_mechanics)
6. Diplom-Physiker. Solid-state transformations and crack propagation: a phase field study. PhD thesis. RWTH. 2010.
7. Robert Spatschek, Miks Hartmann, Efim Brener, Heiner Muller-Krumbhaar. Phase field modeling of fast crack propagation. *Physical review letters*. 96, 015502 (2006).
8. Masao Iwammatsu. Minimum free-energy path of homogeneous nucleation from the phase-field equation. *Journal of Chemical Physics*. **130**, 244507 (2009); doi:10.1063/1.3158471 (7 pages).



9. Xu Hong, Zhang Guowei. The simulation of Phase field method about Fluctuation to the Dendrites growth. 2010 International Conference on Computer Application and System Modeling.
10. Alain Karma and Wouter-Jan Rappel. Quantative phase-field modeling of dendritic growth in two and three dimensionans. Physical Review E. Volume 57, Number 4. April 1998.

***Subtask F3a-3. Obtain temperature-dependent dynamics results for model asphalts that represent asphalts of different crude oil sources (URI)***

Molecular dynamics simulations were continued for new models of SHRP asphalts AAK-1 and AAM-1. The initial simulations are at a high-temperature (473 K) to enable fast relaxations.

***Subtask F3a-4. Simulate changes in asphalt dynamics after inducing representations of chemical and/or physical changes to a model asphalt (URI)***

A manuscript that uses multicomponent Maxwell models to interpret the rheological behavior of asphalts appeared in print (Badami 2011). The idea of this work is to interpret differences in rheological behavior on the basis of differences in relaxation time distribution. The latter related to changes in chemistry in the asphalt.

***Subtask F3a-5. Molecular mechanics simulations of asphalt-aggregate interfaces (VT)***

***Subtask F3a-6. Modeling of fatigue behavior at atomic scale (VT)***

***Subtask F3a-7. Modeling of moisture damage (VT)***

Nothing to report

***Subtask F3a-8. ab initio Calculations of Asphalt Molecular Structures and Correlation to Experimental Physico-Chemical Properties of SHRP Asphalts (WRI-TU Delft)***

Simulating are currently being conducted by TU Delft employing CAPA 3D to model healing properties of asphalt systems.

Work Planned Next Quarter

Computer software will be completed and tested for converting stress fluctuation data from molecular simulations into predictions of complex modulus. Results for different model asphalt systems will be compared with experimental data for SHRP and ARC asphalt binders.

Manuscripts that describe the equilibrium and dynamics properties for the AAA-1 system will be completed and prepared for publication. Molecular simulations will be continued to additional temperatures for the model AAK-1 and AAM-1 bitumen systems.

Data analysis and manuscripts will be completed on a spontaneous wax formation event in a molecular simulation. This work was delayed from the prior quarter in order to focus efforts on conducting and analyzing the AAA-1 molecular simulations.

### Presentations and Publications

Now-completed graduate student Derek D. Li received the Best Transportation Thesis/Dissertation of 2011 Award from the Rhode Island Transportation Research Center.

An overview of the research simulating asphalts on the molecular level was presented by Prof Michael Greenfield at the Northeast Asphalt User Producer Group Meeting in Providence, RI. Many attendees were state DOT professionals who were not aware of the project and its role within the overall ARC effort. The composition and dynamics results for new model AAA-1 asphalt were presented at the American Institute of Chemical Engineers meeting. This kept the chemical engineering community aware of progress being made in simulating asphalts on the molecular level. The audience included petroleum engineers who focus more commonly on asphaltene precipitation and its effects on flow within pipelines. Similar results were presented at the Rhode Island Transportation Forum held at URI.

Greenfield, M. L. 2011, Modeling Asphalt on the Molecular Level (invited), Northeast Asphalt User Producer Group (NEAUPG) Meeting, Providence, RI, October 6, 2011.

Li, Derek D. and M. L. Greenfield, 2011, Chemical and Mechanical Relaxations in Multicomponent Model Bitumens, American Institute of Chemical Engineers (AIChE) Annual Meeting, Minneapolis, MN, October 20, 2011.

Greenfield, M. L. 2011, Progress on Molecular Simulation of Asphalt Chemo-mechanics (invited), Rhode Island Transportation Forum, Kingston, RI, October 28, 2011.

#### *Peer-reviewed publication:*

Badami, Joseph V., and M. L. Greenfield, 2011, Maxwell Model Analysis of Bitumen Rheological Data. *J. Mater. Civil Eng.*, 23: 1387-1395.

This manuscript describes fits of Maxwell constitutive models to rheology data and interprets the corresponding distributions of relaxation times.

### References

Daivis, P. J. and D. J. Evans, 1994, Comparison of Constant Pressure and Constant Volume Nonequilibrium Simulations of Sheared Model Decane. *J. Chem. Phys.*, 100: 541-547.

Ferry, J. D., 1980, *Viscoelastic Properties of Polymers*, 3<sup>rd</sup> ed., New York: Wiley.

Zhang, Liqun and M. L. Greenfield, 2007, Relaxation Time, Diffusion, and Viscosity Analysis of Model Asphalt Systems using Molecular Simulation. *J. Chem. Phys.*, 127: 194502

Zhang, Liqun and M. L. Greenfield, 2010, Rotational Relaxation Times of Individual Compounds within Simulations of Molecular Asphalt Models. *J. Chem. Phys.*, 132: 184502.

### **Work Element F3b: Micromechanics Model**

#### ***Subtask F3b-1: Model Development (TAMU, NCSU, UNL)***

##### Work Done This Quarter

In the last quarter, we have worked on the final report. A draft final report completed was submitted to the Texas A&M University for review.

##### Significant Problems, Issues and Potential Impact on Progress

None.

##### Work Planned Next Quarter

In the next quarter we will update the final report based on feedback/comments from the Texas A&M University.

#### ***Lattice Micromechanical Model (NCSU)***

##### Work Done in This Quarter

###### *Lattice Micromechanical Model*

Based on extensive study of the shape characteristics of air voids, a new algorithm has been proposed for virtually generating air voids in real asphalt microstructure during the previous quarter. The robustness of the algorithm is evident by visual comparison. In addition mechanical characteristics of the specimen are close to what that has been observed from real specimens.

However the developed algorithm can generate realistic air void shapes only in real microstructures which are expensive to obtain. The multi-scale lattice framework is equipped with a virtual microstructure fabrication algorithm which eliminates the need to real specimen. The performance of such virtually generated aggregate structure has been shown before in the absence of air voids. The combination of the recent air void fabrication technique and the virtual aggregate structure generation can be quite useful. However the new air void fabrication algorithm does not generate realistic shapes in virtual microstructure. It has been found that structure of the air voids is dependent on the surrounding microstructure. Therefore further improvement in shape of virtually fabricated air voids is tied to further improvement in virtually fabricated aggregate structure. Improving the virtual aggregate structure is the focus of the current quarter.

In the current virtual microstructure algorithm, aggregates are approximated with randomly shaped octagons. The size distribution and orientation of the octagons follow the general distribution that has been captured from real microstructure. However there are more details about the microstructure of each aggregate that can become important for generating air voids. Aggregate Image Measurement System (AIMS) is designed for characterizing various aggregate shape parameters. This equipment captures 2D images from each aggregate and extracts shape parameters (i.e. angularity, texture and sphericity) from the captured images.

The outputs of AIMS can be used either directly (the captured images) or through the measured parameters to further improve the shape of the virtually generated aggregates. A database has been generated for different sources of aggregates from different parts of the country using AIMS. As an alternative approach, images captured by AIMS have been used as aggregates inside the virtual generation algorithm. These shapes replace the octagons inside each patch. Figure F3b-1.1 compares two specimens using random octagons and actual aggregate shapes captured by AIMS. The new virtual fabrication algorithm generates more realistic shapes visually. The initial stiffness of the new specimen has been measured as a physical parameter and compared with the octagon-shaped aggregates in F3b-1.2. Comparison does not show a drastic change in stiffness while visual comparison does show an improvement. However preliminary studies indicated that this improvement may not be enough for capturing realistic air void shapes.

More studies are underway to further improve the virtual microstructure in order for capturing realistic air void shapes.

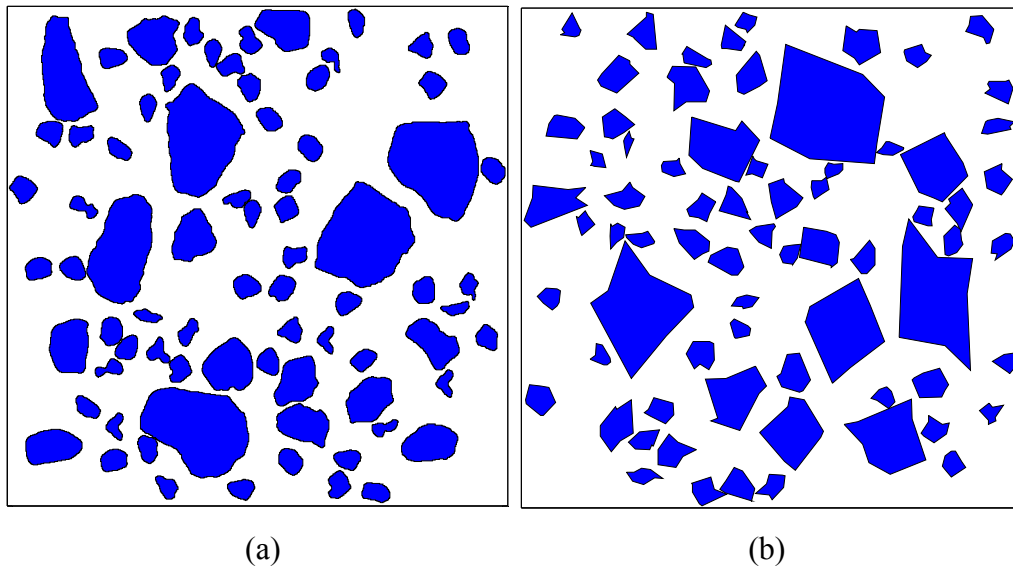


Figure F3b-1.1. Virtually generated microstructure: (a) using real silhouettes, (b) using random octagons.

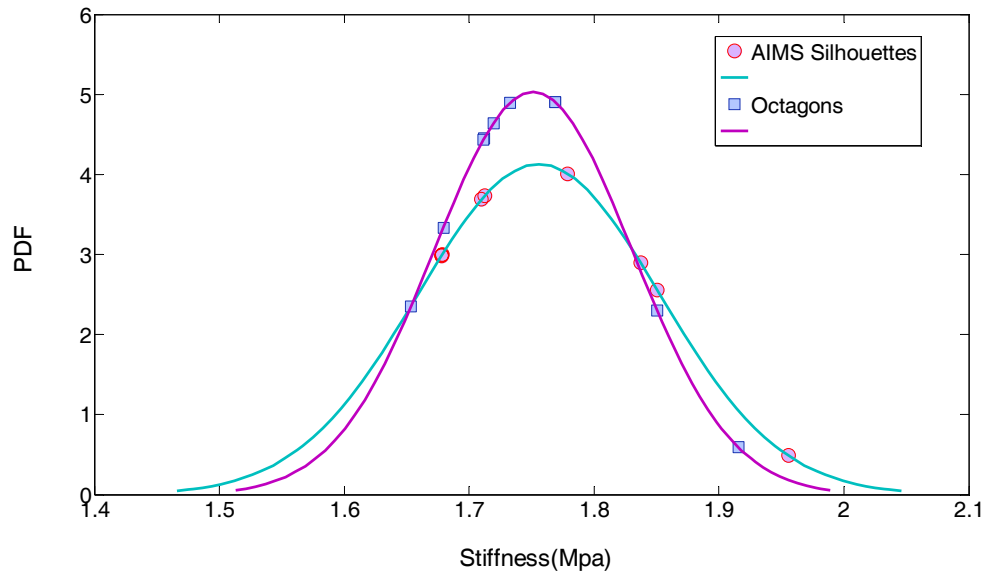


Figure F3b-1.2. Virtually generated air voids (air void content = 4%).

### *Continuum Damage to Fracture*

#### Work Done This Quarter

From previous analyses, it was concluded that the drop of phase angle in middle-failure specimens was related to the large distortion in stress shapes due to fracture. It was also observed that the phase angle could usually drop to zero for middle failure. In this quarter, the drop of phase angle for end-failure specimens is investigated. For end-failure tests, the strain gauge measures the region outside of localization and fracture region. After fracture, the material outside localization region is experiencing relaxation in the control-crosshead tests. Since the on-specimen strain is diminishing, the material is actually coming back to the linear viscoelastic state. In this case, the time dependency (phase angle) is returning to the initial value, not zero (figure F3b-1.3). This is also confirmed by using the linear viscoelastic property and convolution integral to predict strain response given stress history. The conclusion is that, not surprisingly, linear viscoelasticity applies to the whole material for the entire history, except for the region where localization happens. With this confirmation, the focus has been shifted to analyze the localization region in an appropriate way to shed some light on phase angle drop. Since the constitutive behavior of the region away from localization is well known, the displacement associated with the localization region is calculated from the LVDT measurements of middle-failure specimens. This deformation can in turn be used develop appropriate models for the localization region – this is currently under investigation.

In parallel, the development of comprehensive failure criterion is being explored with the help of a larger database.

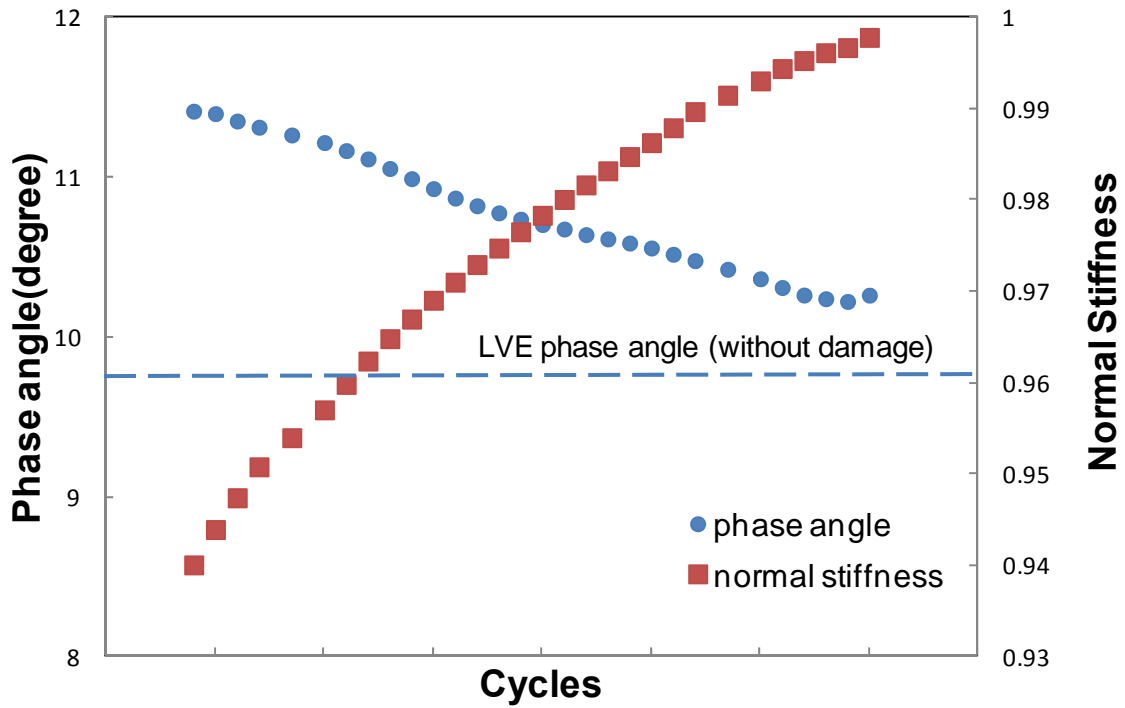


Figure F3b-1.3. Post-localization performance of end failure specimen.

Significant Results

*Lattice Micromechanical Model*

None

*Continuum Damage to Fracture*

None

Significant Problems, Issues and Potential Impact on Progress

None

Work Planned Next Quarter

*Lattice Micromechanical Model*

- Calibration of the air void fabrication algorithm on virtually generated microstructure.
- Evaluating the fatigue performance of the specimen with virtually fabricated air voids and comparing with experimental results.

## *Continuum Damage to Fracture*

- Further understand post-localization deformation
- Continue the exploration of fracture criterion of asphalt concrete

### **Work Element F3c: Development of Unified Continuum Model (TAMU)**

#### Work Done This Quarter

See M4c for details on the progress in the development of the continuum-based moisture-induced damage mode. Also see F1d-8 on the development of the continuum-based micro-damage healing model. We have completed the calibration and validation of the nonlinear viscoelastic and viscoplastic constitutive models in PANDA using the ALF laboratory data based on compression and tension data under different temperatures. However, most of the emphasis in this quarter and previous quarter was placed on the development of a three-dimensional multi-axial thermo-viscoplastic hardening/softening model based on a new novel concept which is the “memory viscoplastic softening surface” (Darabi et al. 2011; Huang et al. 2011).

Work has been continued on applying realistic loading conditions from single- and dual-tires such that normal and shear contact pressures are taken into consideration. This is crucial for the accurate prediction of rutting and fatigue damage in asphalt pavements. Dr. Imad Al-Qadi from University of Illinois-Urbana is helping in this task through predicting the contact pressures from different types of tires at different temperatures. Those predictions will be used as inputs into the realistic rutting and fatigue damage simulations using PANDA. Finally, a parametric study is being conducted to see the effect of viscoplastic hardening/softening model on the rutting predictions under different tire loading conditions. Wheel realistic loading conditions due to normal and shear contact pressure are taken into consideration and their effect is investigated thoroughly.

#### Significant Results

We have developed a model to account for the softening behavior of asphalt mixtures under repeated loading. This model was proven to be essential for predicting accumulation of permanent deformation. Moreover, it is found that the longitudinal and transverse contact shear pressures are as important as the normal contact pressures and should be considered in the rutting and fatigue damage simulations.

#### Significant Problems, Issues and Potential Impact on Progress

None

#### Work Planned Next Quarter

We will work on the simulations of the structural response of the ALF pavements.

## Cited References

Darabi, M.K., R.K. Abu Al-Rub, E.A. Masad, C.W. Huang, and D.N. Little, “A viscoplastic-softening memory surface that enhances the prediction of permanent deformation of asphaltic materials under cyclic loading,” *International Journal of Plasticity*, 2011 (under review).

Huang, C.W., M.K. Darabi, E.A. Masad, R.K. Abu Al-Rub, and D.N. Little, “Development, Characterization and Validation of the Nonlinear Viscoelastic-Viscoplastic and Softening Model of Asphalt Mixtures,” 2011 (in preparation).

## **Continuum-based Model for Aging**

### Work Done This Quarter

The data that has been obtained from the ARC testing using the dynamic modulus test at various aging times (0, 3, and 6 months) has been analyzed in order to calibrate the developed aging evolution law.

### Significant Results

There are no significant results for this quarter.

### Significant Problems, Issues and Potential Impact on Progress

None

### Work Planned Next Quarter

The aging model as part of PANDA will be validated against the available experimental data from the ARC testing.



**TABLE OF DECISION POINTS AND DELIVERABLES FOR FATIGUE**

| <b>Name of Deliverable</b>   | <b>Type of Deliverable</b>                              | <b>Description of Deliverable</b>  | <b>Original Delivery Date</b>  | <b>Revised Delivery Date</b> | <b>Reason for changes in delivery date</b>  |
|--|---|--|--------------------------------|------------------------------|---|
| F1a: Cohesive and Adhesive Properties (TAMU)                       | Draft Report  | Draft Report on Cohesive and Adhesive Properties, 508 compliant  | 11/11                          | N/A                          | N/A   |
|  | Final Report  |  | 6/30/12                        |                              |   |
| F1b-1: Nonlinear viscoelastic response under cyclic loading (TAMU) | Models and Algorithm                                    | A constitutive model that accounts for the nonlinearity and three - dimensional stress state of the material including a method to obtain model constants for asphalt binders. | 3/31/09<br>6/30/10<br>12/31/11 | 3/31/13                      | It is more efficient and informative if the three different final reports, models and algorithms are consolidated into a single final report. The work at UT Austin that will make up the final report is 60% complete. |
|  | Draft report  |  | 12/31/08<br>12/31/11           |                              |   |
|  | Final report  |  | 6/30/08<br>3/31/12             | 6/30/13                      |   |
| F1b-2: Viscoelastic properties under monotonic loading (TAMU)      | Draft Report  | Documentation of PANDA Models and Validation Including the Method for Analysis of Viscoelastic Properties  | 11/11                          | 12/31/12                     | N/A   |
|  | Final Report (M5, M4c, F1b-1, F1c, F1d-8, F3c, and V3c) |  | 3/12                           | 3/31/13                      | N/A   |
| F1c: Aging (Unified Continuum Model for Aging) (TAMU)              | Draft Report  | Draft Report on the aging modeling   | 03/12                          | 12/31/12                     | N/A   |
|  | Final Report (M5, M4c, F1b-1, F1c, F1d-8, F3c, and V3c) |  | 3/31/12                        | 3/31/13                      | Validation of the aging model based on the ARC testing.   |
| F1c-2. Experimental Design (TAMU)                                  | Report  | Experimental Design Report   | 1/09                           | Complete                     | N/A   |

| Name of Deliverable  | Type of Deliverable                                     | Description of Deliverable  | Original Delivery Date           | Revised Delivery Date | Reason for changes in delivery date   |
|--|---|---|----------------------------------|-----------------------|---|
| F1d – 1,2,3,4,5a,5b,8: Healing (TAMU)  | Models and Algorithm                                    | A mathematical model for self-healing at the micron scale, partial validation of this model, measurement of properties related to this model, measurement of overall healing as a function of damage and rest period, and micro to nano scale evaluation of properties that influence fracture and self-healing | 06/30/11                         | 3/31/13               | It is more efficient and informative if the different final reports, models and algorithms are consolidated into a single final report. The final report is based on two theses: the thesis from Texas A&M University is complete and work for the thesis from UT Austin is 70% complete. |
|  | Draft report  |   | 06/30/10<br>06/30/11<br>12/31/11 |                       |   |
| F1d-6: Evaluate relationship between healing and endurance limit of asphalt binders (UWM)          | Draft Report  | Report summarizing major findings for evaluation of healing of binders by means of cyclic testing with rest periods   | 12/11                            | Complete              | First draft submitted to FHWA for review. (report "M")  |
|  | Final Report  | Final report in 508 format on healing characterization of binders and its relation to fatigue performance   | 1/12                             | 4/12                  | The reports for F1d-6, F2e and F2a-5 are combined. (report "M")   |
| F1d-8: Coordinate Form of Healing Parameter with Micromechanics and Continuum Damage Models (TAMU) | Draft Report (M5, M4c, F1b-1, F1c, F1d-8, F3c, and V3c) | Draft Report on the self-healing modeling   | 12/11                            | 12/31/12              | Validation based on ARC testing.  |
|  | Final Report (M5, M4c, F1b-1, F1c, F1d-8, F3c, and V3c) | Report on the self-healing modeling   | 3/12                             | 3/31/13               | Validation based on ARC testing.  |

| <b>Name of Deliverable</b>   | <b>Type of Deliverable</b>                               | <b>Description of Deliverable</b>  | <b>Original Delivery Date</b> | <b>Revised Delivery Date</b> | <b>Reason for changes in delivery date</b>   |
|--|--|--|-------------------------------|------------------------------|--|
| F2a-5: Analyze data and propose mechanisms (UWM)   | Draft Report   | Report summarizing major findings for the effect of modification on asphalt binder performance at high and intermediate temperatures.              | 10/11                         | Complete                     | First draft submitted to FHWA for review. (report "M")   |
|  | Final Report   | Report in 508 format summarizing major findings for the effect of modification on asphalt binder performance at high and intermediate temperatures | 1/12                          | 4/12                         |  |
| F2d: Structural Characterization of Micromechanical Properties in Bitumen using Atomic Force Microscopy (TAMU) | Protocol for Measuring Viscoelastic Properties Using AFM | Protocol for preparing samples and taking measurements in AASHTO format – Protocol development complete, AASHTO format planned for 5/30/11         | 7/31/10                       | Complete                     | The test protocol was successfully used to measure the micro rheology of aged and unaged asphalt binders. The findings and method are current being reviewed as a journal article. |
|  | Evaluation of Impact of Aging and Moisture Conditioning  | Complete   | 12/15/10                      | Complete                     | N/A  |
|  | Final Research Report                                    |  | 2/28/12                       | N/A                          | N/A  |
| F2e-2: Selection of Testing Protocols (UWM)  | Draft Report   | Report on the development and implementation of the Binder Yield Energy (BYET) test and the Linear Amplitude Sweep Test (LAS)                      | 4/09                          | Complete                     | First draft submitted to FHWA for review. (report "M")   |
|  | Final Report   |  | 7/09                          |                              |  |
|  | Draft Report   |  | 4/10                          |                              |  |
|  | Final Report   |  | 7/10                          |                              |  |
| F2e-4: Verification of Surrogate Fatigue Test (UWM)  | Draft Report   | Correspond to reports in F2e-2   | 10/10                         | Complete                     |  |
|  | Final Report   |  | 1/11                          |                              |  |

| Name of Deliverable   | Type of Deliverable                      | Description of Deliverable   | Original Delivery Date | Revised Delivery Date | Reason for changes in delivery date                                     |
|---|--|--|------------------------|-----------------------|---|
| F2e-6:<br>Recommendations for Use in Unified Fatigue Damage Model (UWM) | Draft Report                             | Report summarizing major findings for each subtask. The report includes: evaluation of correlations between binder and mixture fatigue performance, comparison between binder fatigue testing procedures, verification/validation of LAS test  | 11/11                  | 10/11                 | First draft submitted to FHWA for review. (report "M")                  |
|   | Final Report                             | Final report in 508 format on the development and implementation of the Linear Amplitude Sweep (LAS) Test. It includes the latest AASHTO standard.   | 1/12                   | 4/12                  |   |
| F3b-1:<br>Micromechanics Model Development (Fatigue) (UNL)              | Models and Algorithm                     | Cohesive zone fracture modeling of asphalt mixtures considering inelasticity, nonlinearity, rate-dependent fracture, and mixture microstructure: modeling methodology, constitutive theory, testing protocols, test data, model simulation/calibration/validation, user element (UEL) codes in ABAQUS, and user-friendly manuals.<br><br>Multiscale modeling of asphaltic mixtures and pavements: modeling methodology, constitutive theory, and parametric analyses of the model. | 3/31/11                | Complete              | Model to be included in final report.                                   |
|   | Draft report                             |  | 06/30/11               | 12/31/11              | This subtask needs more time for model validation and the final report. |
|   | Final report                             |  | 12/31/11               | 8/14/12               |   |
| F3c: Development of Unified Continuum Model (TAMU)                      | PANDA Workshop                           | Workshop on PANDA Models and Validation Results  | 8/11                   | 4/13                  | Waiting for complete validation of PANDA models.                        |
|   | Draft Report                             | Documentation of PANDA Models and Validation   | 11/11                  | 12/31/12              |   |
|   | Final Report                             |  | 3/12                   | 3/31/13               |   |
|   | UMAT Material                            | PANDA Implemented in Abaqus  | 3/12                   | 3/31/13               |   |
|   | PANDA standalone finite element software | Standalone two-dimensional and three-dimensional finite element software for PANDA   | 3/31/12                | 3/31/13               | Creating the user friendly interface for PANDA                          |

| Fatigue Year 5             |   | Year 5 (4/11-3/12) |   |   |   |   |   |    |       |       |   |       | Team |      |
|----------------------------|---|--------------------|---|---|---|---|---|----|-------|-------|---|-------|------|------|
|                            |   | 4                  | 5 | 6 | 7 | 8 | 9 | 10 | 11    | 12    | 1 | 2     |      | 3    |
| <b>Material Properties</b> |   |                    |   |   |   |   |   |    |       |       |   |       |      |      |
| <b>F1a</b>                 | <b>Cohesive and Adhesive Properties</b>   |                    |   |   |   |   |   |    |       |       |   |       |      |      |
| F1a-1                      | Critical review of literature   |                    |   |   |   |   |   |    |       |       |   |       |      | TAMU |
| F1a-2                      | Develop experiment design   |                    |   |   |   |   |   |    |       |       |   |       |      |      |
| F1a-3                      | Thermodynamic work of adhesion and cohesion   |                    |   |   |   |   |   |    |       |       |   |       |      |      |
| F1a-4                      | Mechanical work of adhesion and cohesion  |                    |   |   |   |   |   |    |       |       |   |       |      |      |
| F1a-5                      | Evaluate acid-base scale for surface energy calculations                                      |                    |   |   |   |   |   | JP |       |       |   |       |      |      |
| <b>F1b</b>                 | <b>Viscoelastic Properties</b>  |                    |   |   |   |   |   |    |       |       |   |       |      |      |
| F1b-1                      | Separation of nonlinear viscoelastic deformation from fracture energy under cyclic loading    |                    |   |   |   |   |   |    |       | JP    | D | M&A,F |      | TAMU |
| F1b-2                      | Separation of nonlinear viscoelastic deformation from fracture energy under monotonic loading |                    |   |   |   |   |   | JP | M&A,D |       |   | F     |      |      |
| <b>F1c</b>                 | <b>Aging</b>  |                    |   |   |   |   |   |    |       |       |   |       |      |      |
| F1c-1                      | Critical review of binder oxidative aging and its impact on mixtures                          |                    |   |   |   |   |   |    |       |       |   |       |      | TAMU |
| F1c-2                      | Develop experiment design   |                    |   |   |   |   |   |    |       |       |   |       |      |      |
| F1c-3                      | Develop transport model for binder oxidation in pavements                                     |                    |   |   |   |   |   | JP |       |       | D | M&A   | F    |      |
| F1c-4                      | Effect of binder aging on properties and performance  |                    |   |   |   |   |   | JP |       |       | D |       | F    |      |
| F1c-5                      | Polymer modified asphalt materials  |                    |   |   |   |   |   |    |       |       | D |       | F    |      |
| <b>F1d</b>                 | <b>Healing</b>  |                    |   |   |   |   |   |    |       |       |   |       |      |      |
| F1d-1                      | Critical review of literature   |                    |   |   |   |   |   |    |       |       |   |       |      | TAMU |
| F1d-2                      | Select materials with targeted properties   |                    |   |   |   |   |   |    |       |       |   |       |      | TAMU |
| F1d-3                      | Develop experiment design   |                    |   |   |   |   |   | JP |       | JP    | D | M&A   | F    | TAMU |
| F1d-4                      | Test methods to determine properties relevant to healing                                      |                    |   |   |   |   |   |    |       |       |   |       |      | TAMU |
| F1d-5                      | Testing of materials  |                    |   |   |   |   |   |    |       |       |   |       |      | TAMU |
| F1d-6                      | Evaluate relationship between healing and endurance limit of asphalt binders                  |                    |   |   |   |   |   | JP |       |       | D | F     |      | UWM  |
| F1d-7                      | Coordinate with AFM analysis  |                    |   |   |   |   |   |    |       |       |   |       | F    | WRI  |
| F1d-8                      | Coordinate form of healing parameter with micromechanics and continuum damage models          |                    |   |   |   |   |   |    |       | JP    | D |       | F    | TAMU |
| <b>Test Methods</b>        |   |                    |   |   |   |   |   |    |       |       |   |       |      |      |
| <b>F2a</b>                 | <b>Binder tests and effect of composition</b>   |                    |   |   |   |   |   |    |       |       |   |       |      |      |
| F2a-1                      | Analyze Existing Fatigue Data on PMA  |                    |   |   |   |   |   |    |       |       |   |       |      | UWM  |
| F2a-2                      | Select Virgin Binders and Modifiers and Prepare Modified Binder                               |                    |   |   |   |   |   |    |       |       |   |       |      |      |
| F2a-3                      | Laboratory Aging Procedures   |                    |   |   |   |   |   |    |       |       |   |       |      |      |
| F2a-4                      | Collect Fatigue Test Data   |                    |   |   |   |   |   |    |       |       |   |       |      |      |
| F2a-5                      | Analyze data and propose mechanisms   |                    |   |   |   |   |   | P  |       |       | D |       | F    |      |
| <b>F2b</b>                 | <b>Mastic testing protocol</b>  |                    |   |   |   |   |   |    |       |       |   |       |      |      |
| F2b-1                      | Develop specimen preparation procedures   |                    |   |   |   |   |   |    |       |       |   |       |      | TAMU |
| F2b-2                      | Document test and analysis procedures in AASHTO format  |                    |   |   |   |   |   |    |       |       |   |       |      |      |
| <b>F2c</b>                 | <b>Mixture testing protocol</b>   |                    |   |   |   |   |   |    |       |       |   |       |      |      |
| F2c-1                      | Evaluate Mixture Fatigue Data   |                    |   |   |   |   |   | P  | P     | P(2)  |   | P(2)  |      |      |
| <b>F2d</b>                 | <b>Tomography and microstructural characterization</b>  |                    |   |   |   |   |   |    |       |       |   |       |      |      |
| F2d-1                      | Micro scale physicochemical and morphological changes in asphalt binders                      |                    |   |   |   |   |   |    |       |       |   |       |      | TAMU |
| <b>F2e</b>                 | <b>Verify relationship between DSR binder fatigue tests and mixture fatigue performance</b>   |                    |   |   |   |   |   |    |       |       |   |       |      |      |
| F2e-1                      | Evaluate Binder Fatigue Correlation to Mixture Fatigue Data                                   |                    |   |   |   |   |   |    |       |       |   |       |      | UWM  |
| F2e-2                      | Selection of Testing Protocols  |                    |   |   |   |   |   |    |       |       |   |       |      |      |
| F2e-3                      | Binder and Mixture Fatigue Testing  |                    |   |   |   |   |   |    |       |       |   |       |      |      |
| F2e-4                      | Verification of Surrogate Fatigue Test  |                    |   |   |   |   |   |    |       |       |   |       |      |      |
| F2e-5                      | Interpretation and Modeling of Data   |                    |   |   |   |   |   |    |       |       |   |       |      |      |
| F2e-6                      | Recommendations for Use in Unified Fatigue Damage Model                                       |                    |   |   |   |   |   |    |       |       | D |       | F    |      |
| <b>Models</b>              |   |                    |   |   |   |   |   |    |       |       |   |       |      |      |
| <b>F3a</b>                 | <b>Asphalt microstructural model</b>  |                    |   |   |   |   |   |    |       |       |   | M&A   |      | F    |
| <b>F3b</b>                 | <b>Micromechanics model</b>   |                    |   |   |   |   |   |    |       |       |   |       |      |      |
| F3b-1                      | Model development   |                    |   |   |   |   |   | D  | JP    | DP    |   | F, SW |      | P    |
| F3b-2                      | Account for material microstructure and fundamental material properties                       |                    |   |   |   |   |   |    |       |       |   |       |      |      |
| <b>F3c</b>                 | <b>Develop unified continuum model</b>  |                    |   |   |   |   |   |    |       |       |   |       |      |      |
| F3c-1                      | Analytical fatigue model for mixture design   |                    |   |   |   |   |   |    |       | M&A,D |   |       |      | F    |
| F3c-2                      | Unified continuum model   |                    |   |   |   |   |   | D  |       | DP    |   | F, SW |      |      |
| F3c-3                      | Multi-scale modeling  |                    |   |   |   |   |   | D  |       |       |   | F     |      |      |
|                            | Lattice Model   |                    |   |   |   |   |   |    |       | JP    |   | JP    |      | F    |
|                            | Continuum Damage to Fracture  |                    |   |   |   |   |   |    |       | JP    |   | JP    |      |      |

**LEGEND**

**Deliverable codes**

- D: Draft Report
- F: Final Report
- M&A: Model and algorithm
- SW: Software
- JP: Journal paper
- P: Presentation
- DP: Decision Point
- [x]

- Work planned
- Work completed
- Parallel topic

**Deliverable Description**

- Report delivered to FHWA for 3 week review period.
- Final report delivered in compliance with FHWA publication standards
- Mathematical model and sample code
- Executable software, code and user manual
- Paper submitted to conference or journal
- Presentation for symposium, conference or other
- Time to make a decision on two parallel paths as to which is most promising to follow through
- Indicates completion of deliverable x

| Fatigue Year 2 - 5         |   | Year 2 (4/08-3/09) |      |      |      | Year 3 (4/09-3/10) |    |    |      | Year 4 (04/10-03/11) |      |      |       | Year 5 (04/11-03/12) |        |       |       | Team  |      |
|----------------------------|---|--------------------|------|------|------|--------------------|----|----|------|----------------------|------|------|-------|----------------------|--------|-------|-------|-------|------|
|                            |   | Q1                 | Q2   | Q3   | Q4   | Q1                 | Q2 | Q3 | Q4   | Q1                   | Q2   | Q3   | Q4    | Q1                   | Q2     | Q3    | Q4    |       |      |
| <b>Material Properties</b> |   |                    |      |      |      |                    |    |    |      |                      |      |      |       |                      |        |       |       |       |      |
| <b>F1a</b>                 | <b>Cohesive and Adhesive Properties</b>   |                    |      |      |      |                    |    |    |      |                      |      |      |       |                      |        |       |       |       |      |
| F1a-1                      | Critical review of literature   |                    |      | JP   |      |                    |    |    |      |                      |      |      |       |                      |        |       | TAMU  |       |      |
| F1a-2                      | Develop experiment design   |                    |      |      |      |                    |    |    |      |                      |      |      |       |                      |        |       |       |       |      |
| F1a-3                      | Thermodynamic work of adhesion and cohesion   |                    |      |      |      |                    |    |    |      |                      |      |      |       |                      |        |       |       |       |      |
| F1a-4                      | Mechanical work of adhesion and cohesion  |                    |      |      |      |                    | JP |    |      | D                    | F    |      |       |                      |        |       |       |       |      |
| F1a-5                      | Evaluate acid-base scale for surface energy calculations                                      |                    |      |      |      |                    |    |    |      |                      |      |      |       | JP                   |        |       |       |       |      |
| <b>F1b</b>                 | <b>Viscoelastic Properties</b>  |                    |      |      |      |                    |    |    |      |                      |      |      |       |                      |        |       |       |       |      |
| F1b-1                      | Separation of nonlinear viscoelastic deformation from fracture energy under cyclic loading    |                    |      | D,JP | M&A  |                    |    |    | JP   | M&A,F,J              | JP   |      | P     |                      |        | JP,D  | F,M&A | TAMU  |      |
| F1b-2                      | Separation of nonlinear viscoelastic deformation from fracture energy under monotonic loading |                    |      | JP   | M&A  |                    |    |    | JP   |                      |      |      | JP    |                      | JP,M&A | D     | F     |       |      |
| <b>F1c</b>                 | <b>Aging</b>  |                    |      |      |      |                    |    |    |      |                      |      |      |       |                      |        |       |       |       |      |
| F1c-1                      | Critical review of binder oxidative aging and its impact on mixtures                          |                    |      |      |      |                    |    |    |      |                      |      |      |       |                      |        |       |       | TAMU  |      |
| F1c-2                      | Develop experiment design   |                    |      | D    |      | F                  |    |    |      |                      |      |      |       |                      |        |       |       |       |      |
| F1c-3                      | Develop transport model for binder oxidation in pavements                                     |                    | P    |      | P,JP |                    | P  |    | P,JP |                      | P,JP | JP   | JP    |                      | JP     | D,M&A | F     |       |      |
| F1c-4                      | Effect of binder aging on properties and performance  |                    |      |      | JP,P |                    | JP | D  | F    |                      |      |      |       |                      | JP     | D     | F     |       |      |
| F1c-5                      | Polymer modified asphalt materials  |                    |      |      |      |                    | P  |    |      |                      |      |      |       |                      |        | D     | F     |       |      |
| <b>F1d</b>                 | <b>Healing</b>  |                    |      |      |      |                    |    |    |      |                      |      |      |       |                      |        |       |       |       |      |
| F1d-1                      | Critical review of literature   |                    |      |      |      |                    |    |    |      |                      |      |      |       |                      |        |       |       | TAMU  |      |
| F1d-2                      | Select materials with targeted properties   |                    |      |      |      |                    |    |    |      |                      |      |      |       |                      |        |       |       | TAMU  |      |
| F1d-3                      | Develop experiment design   |                    |      |      |      |                    |    |    |      |                      |      |      |       |                      |        | JP    | JP,D  | F,M&A | TAMU |
| F1d-4                      | Test methods to determine properties relevant to healing                                      |                    |      |      | JP   |                    |    |    | JP   | D                    | F    |      |       |                      |        |       |       | TAMU  |      |
| F1d-5                      | Testing of materials  |                    |      |      |      |                    | JP |    |      |                      | JP   |      |       |                      |        |       |       | TAMU  |      |
| F1d-6                      | Evaluate relationship between healing and endurance limit of asphalt binders                  | DP                 |      |      |      |                    | DP | JP | DP   |                      |      |      | JP,P  |                      | JP     | D     | F     | UWM   |      |
| F1d-7                      | Coordinate with AFM analysis  |                    |      |      |      |                    |    |    |      | JP                   |      |      |       |                      |        |       |       | WRI   |      |
| F1d-8                      | Coordinate form of healing parameter with micromechanics and continuum damage models          |                    |      |      |      |                    |    |    |      |                      |      |      |       |                      |        | JP,D  | F     | TAMU  |      |
| <b>Test Methods</b>        |   |                    |      |      |      |                    |    |    |      |                      |      |      |       |                      |        |       |       |       |      |
| <b>F2a</b>                 | <b>Binder tests and effect of composition</b>   |                    |      |      |      |                    |    |    |      |                      |      |      |       |                      |        |       |       |       |      |
| F2a-1                      | Analyze Existing Fatigue Data on PMA  |                    |      | DP   |      |                    |    |    |      |                      |      |      |       |                      |        |       |       | UWM   |      |
| F2a-2                      | Select Virgin Binders and Modifiers and Prepare Modified Binder                               |                    |      | DP   |      |                    |    |    |      |                      |      |      |       |                      |        |       |       |       |      |
| F2a-3                      | Laboratory Aging Procedures   |                    |      |      |      |                    |    |    |      |                      |      |      |       |                      |        |       |       |       |      |
| F2a-4                      | Collect Fatigue Test Data   |                    | P    |      | JP   |                    | P  |    | P    |                      |      |      |       | P,DP,JP              |        |       |       |       |      |
| F2a-5                      | Analyze data and propose mechanisms   |                    |      |      | P    |                    | P  |    |      |                      | P    |      |       |                      | P      | D     | F     |       |      |
| <b>F2b</b>                 | <b>Mastic testing protocol</b>  |                    |      |      |      |                    |    |    |      |                      |      |      |       |                      |        |       |       |       |      |
| F2b-1                      | Develop specimen preparation procedures   |                    | D    |      |      |                    |    |    |      |                      | F    |      |       |                      |        |       |       | TAMU  |      |
| F2b-2                      | Document test and analysis procedures in AASHTO format  |                    | D    |      |      |                    |    |    |      |                      | F    |      |       |                      |        |       |       |       |      |
| <b>F2c</b>                 | <b>Mixture testing protocol</b>   |                    | D,JP | F    | P,JP | JP                 | P  | P  | JP   | P                    | P    | JP   | P     | P                    | P(2)   | P(4)  |       |       |      |
| <b>F2d</b>                 | <b>Tomography and microstructural characterization</b>  |                    |      |      |      |                    |    |    |      |                      |      |      |       |                      |        |       |       |       |      |
| F2d-1                      | Micro scale physicochemical and morphological changes in asphalt binders                      |                    |      |      |      |                    | JP |    |      |                      |      |      | JP    |                      |        |       |       | TAMU  |      |
| <b>F2e</b>                 | <b>Verify relationship between DSR binder fatigue tests and mixture fatigue performance</b>   |                    |      |      |      |                    |    |    |      |                      |      |      |       |                      |        |       |       |       |      |
| F2e-1                      | Evaluate Binder Fatigue Correlation to Mixture Fatigue Data                                   |                    |      |      |      |                    |    |    |      |                      |      |      |       |                      |        |       |       | UWM   |      |
| F2e-2                      | Selection of Testing Protocols  |                    |      |      |      | DP,D               | F  |    |      | D                    | F    |      |       |                      |        |       |       |       |      |
| F2e-3                      | Binder and Mixture Fatigue Testing  |                    |      |      |      |                    |    |    |      |                      |      |      |       |                      |        |       |       |       |      |
| F2e-4                      | Verification of Surrogate Fatigue Test  |                    |      |      |      |                    |    |    |      |                      |      |      | D     | F,DP                 |        |       |       |       |      |
| F2e-5                      | Interpretation and Modeling of Data   |                    | JP   |      | P    |                    | JP |    | P    |                      | JP   |      | M&A   |                      |        |       |       |       |      |
| F2e-6                      | Recommendations for Use in Unified Fatigue Damage Model                                       |                    |      |      |      |                    |    |    |      |                      |      |      | P     |                      |        | D     | F     |       |      |
| <b>Models</b>              |   |                    |      |      |      |                    |    |    |      |                      |      |      |       |                      |        |       |       |       |      |
| <b>F3a</b>                 | <b>Asphalt microstructural model</b>  |                    |      |      |      |                    |    | JP |      |                      |      |      |       |                      |        |       | M&A   | WRI   |      |
| <b>F3b</b>                 | <b>Micromechanics model</b>   |                    |      |      |      |                    |    |    |      |                      |      |      |       |                      |        |       |       |       |      |
| F3b-1                      | Model development   |                    |      |      | JP   |                    |    |    | JP   |                      |      | P,JP | P,M&A | D                    | JP,DP  | F,SW  | P     | TAMU  |      |
| F3b-2                      | Account for material microstructure and fundamental material properties                       |                    |      |      |      |                    |    |    |      |                      |      |      |       |                      |        |       |       |       |      |
| <b>F3c</b>                 | <b>Develop unified continuum model</b>  |                    |      |      |      |                    |    |    |      |                      |      |      |       |                      |        |       |       |       |      |
| F3c-1                      | Analytical fatigue model for mixture design   |                    |      |      |      |                    |    |    |      |                      |      |      |       |                      |        | M&A,D |       | F     | TAMU |
| F3c-2                      | Unified continuum model   |                    |      | JP   |      |                    |    | JP |      |                      |      | JP   | M&A   | D                    | DP     | F,SW  |       |       |      |
| F3c-3                      | Multi-scale modeling  |                    |      |      |      |                    |    |    |      |                      |      | JP   | M&A   | D                    |        | F     |       |       |      |
|                            | Lattice Model   |                    |      |      |      |                    |    |    |      |                      |      |      |       |                      | JP     | JP    | F     | NCSU  |      |
|                            | Continuum Damage to Fracture  |                    |      |      |      |                    |    |    |      |                      |      |      |       |                      | JP     | JP    |       |       |      |

**LEGEND**

**Deliverable codes**

- D: Draft Report
- F: Final Report
- M&A: Model and algorithm
- SW: Software
- JP: Journal paper
- P: Presentation
- DP: Decision Point
- [x]

- Work planned
- Work completed
- Parallel topic

**Deliverable Description**

- Report delivered to FHWA for 3 week review period.
- Final report delivered in compliance with FHWA publication standards
- Mathematical model and sample code
- Executable software, code and user manual
- Paper submitted to conference or journal
- Presentation for symposium, conference or other
- Time to make a decision on two parallel paths as to which is most promising to follow through
- Indicates completion of deliverable x



## PROGRAM AREA: ENGINEERED MATERIALS

### CATEGORY E1: MODELING

#### Work element E1a: Analytical and Micro-mechanics Models for Mechanical Behavior of Mixtures (TAMU)

##### Work Done This Quarter

Progress has been made on the healing properties of lab-mixed-lab-compacted (LMLC) asphalt mixtures, fracture and healing properties of filed cores and fine aggregate mixture testing.

##### **1. Healing Properties of LMLC Asphalt Mixtures**

The development work on characterization of healing properties of asphalt mixtures continues in this quarter. The healing properties have been proposed to be studied using the creep and step-loading recovery test. In the last quarter, the crack growth in the creep phase of the creep and step-loading recovery test was modeled through damage density based on the dissipated pseudo strain energy (DPSE) balance equation. The damage density at the end of the creep phase serves as the initial damage density in the healing process. The change between the initial damage density and the damage density at any time during the recovery phase represents the extent of healing that occurs during this period. Therefore, the next step of quantifying healing is to determine the damage density at any time during the recovery phase, which is studied in this quarter.

The damage density during the recovery phase is determined based on the internal stress and the energy balance equations. The measurement of internal stress and the theoretical background for the energy balance equations have been presented in previous quarterly reports. The procedure of using the internal stress and energy balance equations includes: 1) determination of the recovery modulus in the recovery phase using the internal stress; 2) calculation of pseudo strain in the recovery phase in order to calculate the recoverable pseudo strain energy (RPSE); 3) determination of true strain, true internal stress, and true pseudo strain using mathematical models; and 4) solving the average crack size from the RPSE balance equation in the recovery phase. Then the average crack size in the recovery phase is used to calculate the damage density. Step 1 has been introduced in a previous quarterly report; Steps 2 to 4 are discussed in sequence in the following of this report.

##### *Step 2*

In order to calculate the pseudo strain in the recovery phase, the strain in the creep and step-loading recovery test has to be accurately simulated first. A schematic plot of the strain in this test is shown in figure E1a.1. It suggests that the strain consists of three components: a) the strain in the creep phase; b) the strain in the unloading phase; and c) the strain in the recovery phase. Each of these three components is simulated using one mathematical function, respectively, as shown in equation E1a.1:



$$\varepsilon = \begin{cases} \varepsilon_c = \varepsilon_{0,c} + \varepsilon_{1,c} \left( 1 - e^{-\frac{t}{\gamma_c}} \right) & t \in [0, t_0] \\ \varepsilon_u = mt + n & t \in [t_0, t_0 + 1] \\ \varepsilon_r = \varepsilon_{0,r} + \varepsilon_{1,r} e^{-\frac{t}{\gamma_r}} & t \in [t_0 + 1, \infty] \end{cases} \quad (\text{E1a.1})$$

where  $\varepsilon$  is the strain at any time in the creep and step-loading recovery test;  $t$  is time;  $t_0$  is the beginning of the unloading period for the creep load;  $\varepsilon_c$  is the strain component in the creep phase;  $\varepsilon_{0,c}$ ,  $\varepsilon_{1,c}$ , and  $\gamma_c$  are simulation parameters for  $\varepsilon_c$ ;  $\varepsilon_u$  is the strain component in the unloading phase;  $m$  and  $n$  are simulation parameters for  $\varepsilon_u$ ;  $\varepsilon_r$  is the strain component in the recovery phase;  $\varepsilon_{0,r}$ ,  $\varepsilon_{1,r}$ , and  $\gamma_r$  are simulation parameters for  $\varepsilon_r$ .

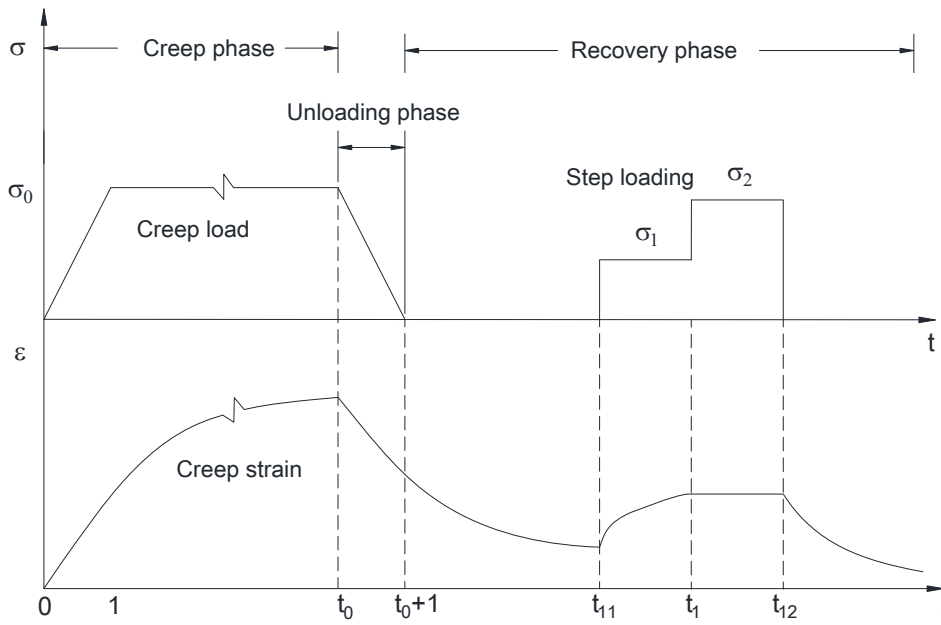


Figure E1a.1. Stress and strain versus time in creep and step-loading recovery test.

Based on the determined strain, the pseudo strain in the recovery phase is calculated as follows:

$$\begin{aligned}\varepsilon_R &= \frac{\sigma_{VE}(t)}{E_R} \\ &= \frac{\varepsilon_c(0)E(t) + \int_0^{t_0} E(t-\xi) \frac{d\varepsilon_c(\xi)}{d\xi} d\xi + \int_{t_0}^{t_0+1} E(t-\xi) \frac{d\varepsilon_u(\xi)}{d\xi} d\xi + \int_{t_0+1}^t E(t-\xi) \frac{d\varepsilon_r(\xi)}{d\xi} d\xi}{E_R}\end{aligned}\quad (\text{E1a.2})$$

where  $\varepsilon_R$  is the pseudo strain;  $\sigma_{VE}(t)$  is the viscoelastic stress of the undamaged asphalt mixture;  $E_R$  is the reference modulus and used to achieve dimensionless variables;  $\xi$  is any arbitrary time between 0 and  $t$ ; and  $E(t-\xi)$  is the relaxation modulus of the undamaged asphalt mixture.

### Step 3

Equation E1a.1 defines the strain measured from the creep and step-loading recovery test. The true strain can use the same formulation but different simulation parameters, which is shown in equation E1a.3:

$$\varepsilon^T = \begin{cases} \varepsilon_c^T = \varepsilon_{0,c}^T + \varepsilon_{1,c}^T \left(1 - e^{-\frac{t}{\gamma_c^T}}\right) & t \in [0, t_0] \\ \varepsilon_u^T = mt + n^T & t \in [t_0, t_0 + 1] \\ \varepsilon_r^T = \varepsilon_{0,r}^T + \varepsilon_{1,r}^T e^{-\frac{t}{\gamma_r^T}} & t \in [t_0 + 1, \infty] \end{cases} \quad (\text{E1a.3})$$

in which the superscript ‘‘T’’ indicate ‘‘true’’. As a result, the true internal stress is calculated using the true strain component in the recovery phase and the recovery modulus as follows:

$$\sigma_i^T(t) = \varepsilon_r^T(t) \cdot R(t) \quad (\text{E1a.4})$$

where  $\sigma_i^T(t)$  is the true internal stress in the recovery phase; and  $R(t)$  is the recovery modulus that is determined in Step 1. The true pseudo strain is determined using the same formulation as shown in equation E1a.2, but based on the true strain calculated in equation E1a.3.

### Step 4

After determining the true strain, true internal stress, and true pseudo strain, they are used to calculate the true RPSE, which is used in the RPSE balance equation to solve for the average crack size. The true RPSE is calculated by integrating the true internal stress and the true pseudo strain as:

$$\text{RPSE}^T = \int_{t_0+1}^t \sigma_i^T(t) d\varepsilon_R^T \quad (\text{E1a.5})$$

where  $RPSE^T$  is the true RPSE; and  $\varepsilon_R^T$  is the true pseudo strain in the recovery phase. Then  $RPSE^T$  is used in the RPSE balance equation as follows:

$$RPSE^A V_m = RPSE^T V_m + RPSE^T \left( \frac{2M_b \pi^2 c_b^3}{3} - \frac{2M_a \pi^2 c_a^3}{3} \right) - \gamma (2M_b \pi c_b^2 - 2M_a \pi c_a^2) \quad (E1a.6)$$

where  $RPSE^A$  is the apparent RPSE;  $V_m$  is the volume of one layer of asphalt mastic;  $M_b$  and  $M_a$  are the numbers of cracks before healing (crack closure) and after healing (crack closure), respectively;  $c_b$  and  $c_a$  are the average crack size before healing (crack closure) and after healing (crack closure), respectively; and  $\gamma$  is the surface energy density (energy per unit area). After solving equation E1a.6, the change of the average crack size with time can be obtained, which is then used to calculate the damage density in the recovery phase.

After completing these four steps, the change of the damage density with time in the recovery phase can be obtained, which is shown in figure E1a.2. The legends AAD and AAM are for two different asphalt mixtures with asphalt binders AAD and AAM, respectively. The result evidently suggests the difference in the healing capacity between these two types of asphalt mixture. Other measures of healing such as the recovery of the damaged modulus depend upon this more basic definition of healing (recovery of damage density) and are empirical inferences.

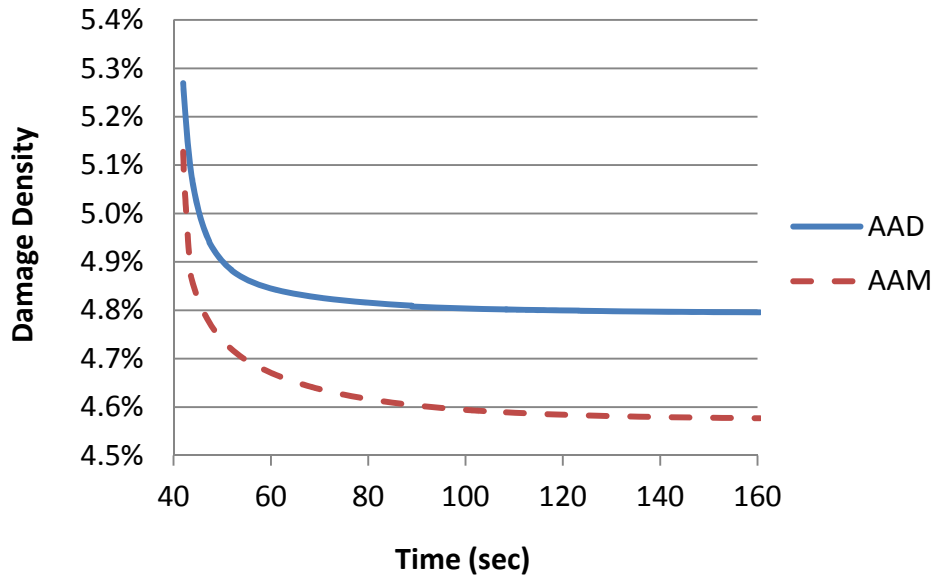


Figure E1a.2. Damage density in the recovery phase of creep and step-loading recovery test.

## **2. Fracture and Healing Properties of Field Cores**

In the previous quarterly report, the analytical procedure to find the actual mean crack width in any loading cycle and the procedure to calculate the healing and fracture properties of the asphalt mixes were provided.

In order to illustrate the methodology with actual test results, a Texas type D mix with a PG 67-22 grade binder was analyzed with the testing analysis method. The binder content of the mix was 5.2%. The specimens were molded at two different air void contents, 4 and 7 percent to compare the effect of air void content on the crack growth, fracture, and healing properties of the mixes. Three replicates of each air void category were used to evaluate the consistency of the model. The laboratory compacted cores were cut to the standard specimen geometry and the specimens were glued on the aluminum plates.

The test outputs were analyzed to obtain both damaged and undamaged properties. Tables E1a.1 and E1a.2 show the results for the undamaged, fracture and healing properties and the results of the statistical analysis. The test results show that the proposed method can accurately determine the undamaged and damaged properties of the asphalt mixes.

The numbers of cycles for the crack to grow a length of 25 mm is counted for two reasons: (a) to reduce the length of time required for the test, and (b) because counting cycles after the crack enters the low strain zone in the top 6 mm low strain in thin samples produces inconsistent results. It should be noted that that in thicker sample the top zone is in compression according to FE analysis results. The coefficient of variance (COV) for the number of cycles corresponding to the crack length of 25 mm is calculated to demonstrate the consistency of the methodology compared to previous methods. The COV values for the number of load cycles of mixes A and B are 19 and 16 percent, respectively.

In addition, the undamaged properties are very consistent. The COV values for the undamaged relaxation moduli of mixes A and B are 2.2 and 6.1 percent, respectively. The fracture and healing parameters' COV are below the 30% level which was a characteristic of the previous method of using the overlay tester. Previous methods of analyzing OT test data by counting the number of load cycles for the crack to reach the top of the sample have shown coefficient of variation of much greater than 30 percent especially for coarse-graded mixes (Walubita, et al., 2009).

The average number of cycles corresponding to 25 mm crack growth is higher in mix A compared with mix B. This happens because of the lower air voids of mix A relative to mix B. As mentioned previously a large amount of healing occurs during each load cycle. The fact that the healing exponent,  $m$ , is larger than the fracture exponent,  $n$ , in both mixes also confirms this observation.

Table E1a.1. Damaged and undamaged properties of the mix A using OT test.

| Mix Properties |                 |                    | Undamaged Properties |      | Damaged Properties |       |       | Healing Properties |       |
|----------------|-----------------|--------------------|----------------------|------|--------------------|-------|-------|--------------------|-------|
| ID             | Percent Air (%) | Binder Content (%) | $E_1$ (MPa)          | m    | N                  | A     | n     | B                  | m     |
| A-1            | 4.2             | 5.2                | 253.8                | 0.42 | 56                 | 0.046 | 1.72  | 0.019              | 3.43  |
| A-2            | 4.4             | 5.2                | 257.4                | 0.41 | 44                 | 0.035 | 1.19  | 0.021              | 2.32  |
| A-3            | 4.2             | 5.2                | 246.4                | 0.4  | 65                 | 0.038 | 1.37  | 0.023              | 2.46  |
| $\mu$          | 4.23            | 5.2                | 252.5                | 0.41 | 55                 | 0.04  | 1.428 | 0.021              | 2.73  |
| $\sigma$       | 0.12            | 0                  | 5.6                  | 0.01 | 10.5               | 0.006 | 0.269 | 0.002              | 0.6   |
| COV            | 2.7             | 0                  | 2.2                  | 2.43 | 19.2               | 14.3  | 18.8  | 9.52               | 22.07 |

Table E1a.2. Damaged and undamaged properties of the mix B using OT test.

| Mix Properties |                 |                    | Undamaged Properties |      | Damaged Properties |       |      | Healing Properties |      |
|----------------|-----------------|--------------------|----------------------|------|--------------------|-------|------|--------------------|------|
| ID             | Percent Air (%) | Binder Content (%) | $E_1$ (MPa)          | m    | N                  | A     | n    | B                  | m    |
| B-1            | 6.9             | 5.2                | 172.4                | 0.53 | 44                 | 0.03  | 1.75 | 0.016              | 3.04 |
| B-2            | 7.4             | 5.2                | 189.4                | 0.48 | 36                 | 0.049 | 1.47 | 0.05               | 2.58 |
| B-3            | 7.4             | 5.2                | 193.8                | 0.54 | 50                 | 0.024 | 1.64 | 0.01               | 2.82 |
| $\mu$          | 7.2             | 0                  | 185.2                | 0.52 | 43.3               | 0.034 | 1.62 | 0.03               | 2.81 |
| $\sigma$       | 0.3             | 0                  | 11.3                 | 0.03 | 7.02               | 0.013 | 0.14 | 0.02               | 0.23 |
| COV            | 4               | 0                  | 6.1                  | 6.8  | 16.2               | 38    | 8.7  | 83.8               | 8.2  |

Figure E1a.3 depicts the actual crack growth estimated using the analytical model. As shown in figure E1a.3, the crack grows very quickly during first few load cycles and the rate of crack growth decreases substantially after that.

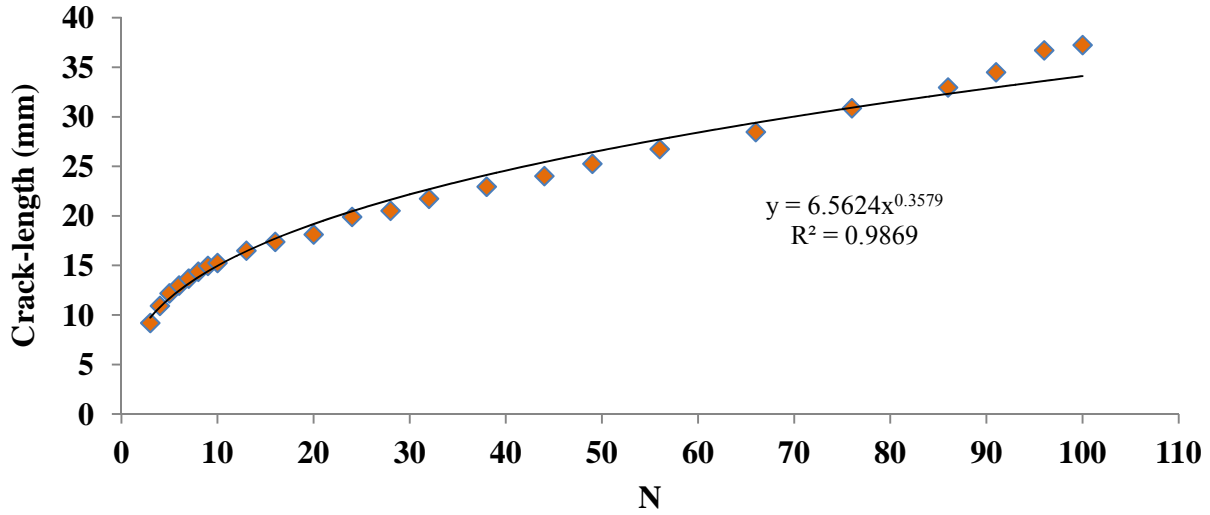


Figure E1a.3. Actual crack growth for a lab mix with 4% air void.

### 3. Fine Aggregate Mixture Testing

In this quarter, the coefficient of water vapor transfer was modeled using equation E1a.7. In order to measure this water vapor diffusion coefficient, the DMA specimens were exposed to a relative humidity of 100% at a constant room temperature of 23°C for a period of 4 months. During the experiment, the overall mass increase of the specimens is measured with a micro balance scale with accuracy of 0.001 gram. The model used to measure the water vapor diffusion coefficient can be expressed as:

$$M_{abs}(t) = M_{max}(1 - e^{-\alpha t}) \quad (E1a.7)$$

Where  $M_{abs}$  = the mass increase of specimens with the increase of time;  $M_{max}$  = the maximum mass that the specimen can gain;  $\alpha$  = the exponential rate of water vapor diffusion;

This model can be modified to satisfy the typical diffusion equation, and an approximation is given in equation E1a.8.

$$M_{abs}(t) = M_{max} \left( 1 - e^{-\frac{3Dt}{(d/2)^2}} \right) \quad (E1a.8)$$

Where D= the diffusivity of fine aggregate mix ( $m^2 / s$ );  $d$  = the diameter of the specimen (m);

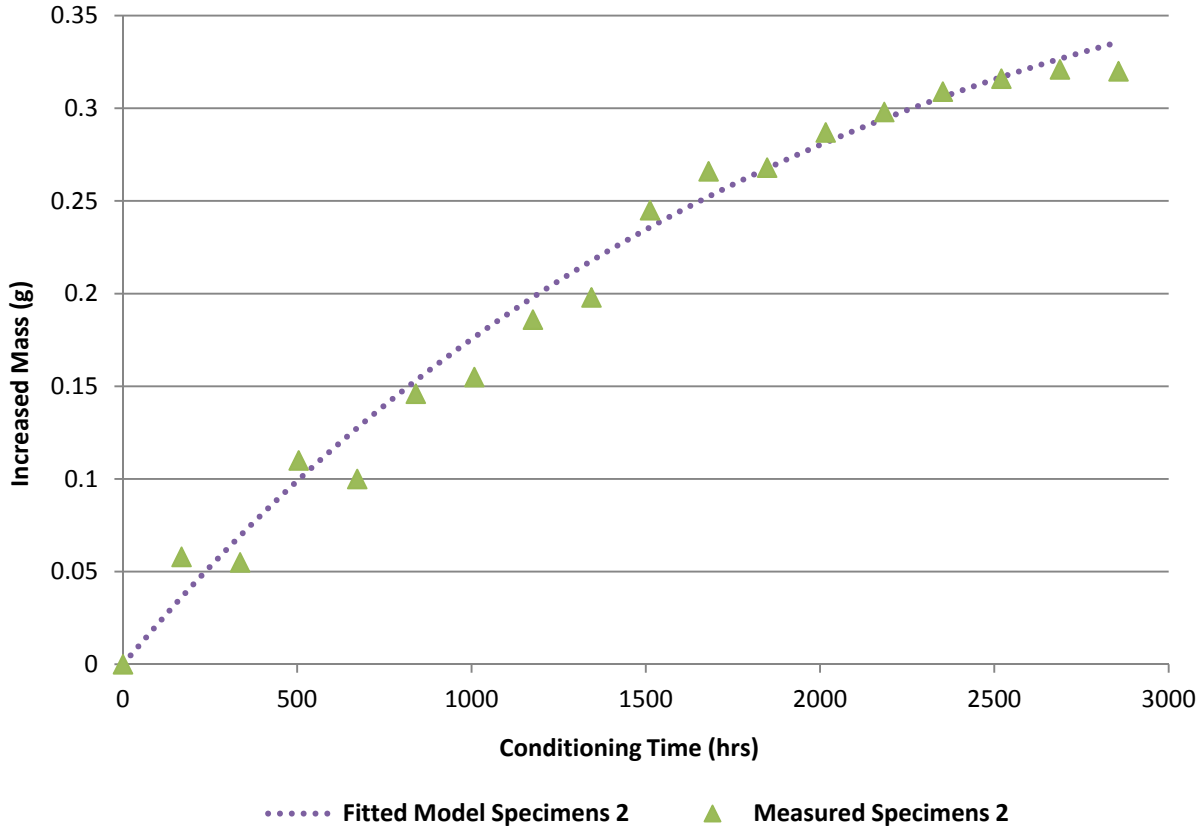


Figure E1a.4. Moisture uptake vs. time.

From the measured data as shown in figure E1a.4, the water vapor diffusivity in the FAM specimen can be obtained as  $D=2.12E^{-11} \text{ m}^2/\text{s}$ , which is comparable to the published data in the literature.

Another task that was accomplished in this quarter is that the wind effect on water vapor diffusion in pavements was established. The flux boundary condition including wind speed can be modeled as follows:

$$\frac{\partial u}{\partial z} = f(u) * (PF_a - PF_s) \tag{E1a.9}$$

where  $PF_a$  = the suction in the air;  $PF_s$  = the suction at the subgrade of the pavement;  $f(u)$  = a function which depends on the mixing characteristics of the air above the surface of pavement;  $f(u)$  can be expressed as follows:

$$f(u) = h * (1 + \alpha_m) \tag{E1a.10}$$

where  $h$  = the water vapor diffusivity at the boundary surface;  $\alpha_m$  = the mass exchange coefficient of water vapor due to the wind at the asphalt mix layer surface;

$$\alpha_m = K \sqrt{V/L} \quad (\text{E1a.11})$$

where  $V$  = the wind speed (miles/hr);  $L$  = width of the highway;

$$K = 0.662 \lambda_m (P_{rm})^{1/3} \left(\frac{1}{\nu}\right)^{1/2} \quad (\text{E1a.12})$$

where  $P_{rm}$  = Prandtl number for air;  $\nu$  = the kinematic viscosity of air ( $m^2 / \text{sec}$ );  $\lambda_m$  considered as constant at an air temperature of 20 °C.

After substituting equations E1a.10, E1a.11 and E1a.12 into the equation E1a.9, the  $f(u)$  can be calculated and then incorporated in the suction model to illustrate how the wind will affect the vapor diffusion in the pavement. As shown in the figure E1a.5, the solid line is the relative humidity in the pavement without wind and the dashed line is the relative humidity in the pavement as the wind blows across the pavement transversely at a speed of 8 miles per hour, which is a commonly observed wind speed in Texas. It is clearly observed that the water vapor diffusion is accelerated due to the wind blowing across the pavement in all of the locations modeled here.



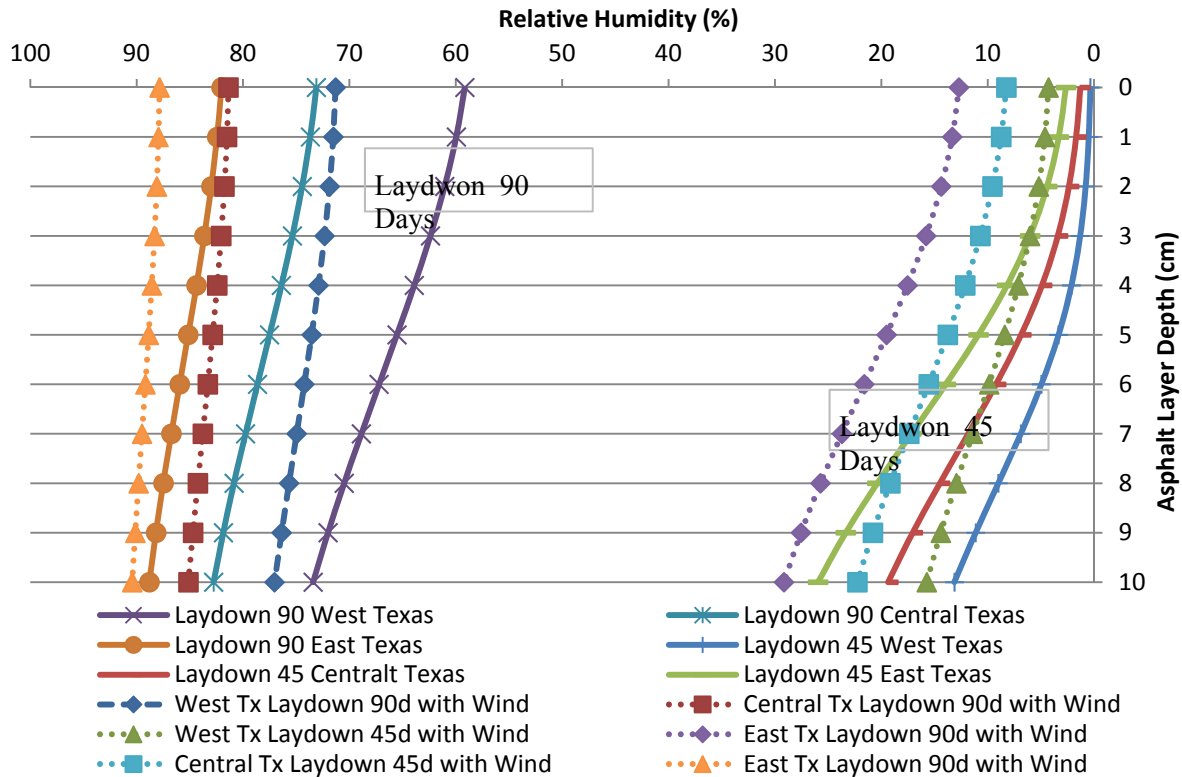


Figure E1a.5. Water vapor diffusion with the incorporation of wind.

### Significant Results

The damage density at any time during the recovery phase is essential to quantify healing of a damaged asphalt mixture. If the change of the damage density with time can be determined for the recovery phase, with determined initial damage density, the extent of healing at any time can be obtained. However, it is impossible to measure the damage density during the recovery phase. Instead, the energy-based approach presented here provides a way to calculate the damage density. It is based on simple mechanistic principles, requires simple measurement of stress/strain/internal stress, and involves the simulation of material responses by simple mathematical models. This approach quickly, efficiently, and accurately characterizes the healing properties of a damaged asphalt mixture.

The OT test method was shown is able to predict the actual crack growth and find both healing and fracture properties of the aged and unaged asphalt mixes with high accuracy and repeatability.

### Significant Problems, Issues and Potential Impact on Progress

The procedure of determining the change of the damage density in the recovery phase as discussed above involves complex calculations and analysis techniques, especially in Step 2 for calculating the pseudo strain and Step 4 for solving equation E1a.6. To ensure accurate results,

all calculations should be carried out very carefully. Equation E1a.6 has to be solved for the entire recovery phase from 40 sec to 160 sec. The data is acquired in increments of 0.1 sec, which indicates that equation E1a.6 has to be solved 1200 times. It seems that this task is redundant, but it can be conducted automatically using Excel. The expression of each variable is carefully typed in the Excel, and all algorithms are embedded in the Excel as a formula or a macro program that solves the problem automatically.

There are some problems to get the time to use the OT machine.

The lab is going through a renovation and the DMA machine is not available for November and December.

### Work Planned Next Quarter

After determining the healing properties of asphalt mixtures, the next step is to examine the application of this energy-based approach. As a result, the work planned for the next quarter is to test different types of asphalt mixtures using the testing protocol developed in previous quarters. Then this energy-based approach will be employed to evaluate the effect of air void content, type of asphalt binder, and aging on the performance of asphalt mixtures. The planned design parameters for asphalt mixtures include: a) two air void contents (4% and 7%); b) four types of asphalt binder (AAD and AAM from Strategic Highway Research Program (SHRP) Materials Reference Library (MRL) (Jones 1993); NuStar binder supplied by NuStar Energy, Paulsboro, NJ; and Valero binder supplied by Valero Refining, Benicia, CA); and c) three aging periods (0, 3, and 6 months).

The same approach will be applied to the field cores with the different stiffness gradients. The stiffness gradient can be plugged into an FE program to find the strain profiles above the crack on aged mixes. This method will allow us to determine the fracture and healing properties of both lab-compacted samples as well as cores taken from aged asphalt layers in the field.

Tests will be conducted on both unaged and unaged specimens made Nustar PG67-22 binder and samples made with the Valero PG64-16 binder.

### Cited References

Afanas'ev, A. M., and B. N. Siplivyi, 2007, Boundary Mass-Exchange Conditions In the Form of the Newton and Dalton Laws. *Journal of Engineering Physics and Thermophysics*, 80 (1).

Jones, D. R., 1993, SHRP Materials Reference Library: Asphalt Cements: A Concise Data Compilation. *Strategic Highway Research Program Rep. No. SHRP-A-645*, National Research Council, Washington, D.C.

Walubita, L. F., V. Umashankar, X. Hu, B. Jamison, F. Zhou, T. Scullion, A. E. Martin, and S. Dessouky, 2009, "New Generation Mix-Designs: Laboratory Testing and Construction of the APT Test Sections." Texas Transportation Institute, Texas A&M University System, College Station, Texas.

## Work element E1b: Binder Damage Resistance Characterization (DRC) (UWM)

### *Subtask E1b-1: Rutting of Asphalt Binders*

#### Work Done This Quarter

Study of the modification of the Multiple Stress Creep and Recovery (MSCR) test procedure continued this quarter. Further analysis was conducted by including in the MSCR procedure 30 cycles of creep and recovery at three stress levels of 100, 3200, and 10,000 Pa. This modified MSCR test procedure is called test method B in this report to be distinguished clearly from the standard procedure in AASHTO TP70. The purpose of this analysis was to explore the effect of number of cycles and stress levels on the binder rutting resistance. Non-recoverable creep compliance (i.e.,  $J_{nr}$ ) of binders and mixtures were measured to identify the relationship between binder and mixture rutting performance. Mixture results from Flow Number (FN) testing were reported at two stress levels, 345 and 1034 kPa and at a single temperature of 46°C.

In addition, the research group continued the microstructure characterization of mixtures using 2D imaging by means of the recently developed iPas<sup>2</sup>. This effort is conducted to understand the role of aggregates in mixture rutting resistance and compare to the significance of binder  $J_{nr}$  values. It is shown that the performance of mixtures can be better characterized by the combination of internal aggregate structure indices such as number of aggregate to aggregate contact zones, length of contact, contact orientation, etc. The interlocking between aggregates can be defined more accurately using the combination of contact length and contact orientation for all the contacts, referred to as the Internal Structure Index (ISI), which is defined as follows:

$$FN \propto ISI = \sum_{i=1}^N \text{Resistant component in the direction of the load} \quad (\text{E1b-1.1})$$

$$ISI = \sum_{i=1}^N \text{Contact length}_i * \text{Sin} (AA_{C_i}) \quad (\text{E1b-1.2})$$

where  $N$  is the number of contact zones in the skeleton, and contact length  $_i$  and  $AA_{C_i}$  are the contact length and orientation for the  $i^{\text{th}}$  contact, respectively. The FN values are plotted in figure E1b-1.1 versus the ISI values calculated for several mixtures. ISI is used to explore the effect of the aggregate structure on the rutting response of asphalt mixtures.

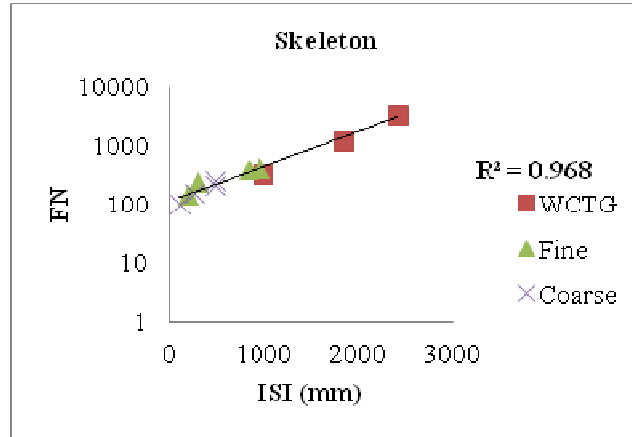


Figure E1b-1.1. Graph. ISI vs. FN in the aggregate skeleton.

### Significant Results

Comparing Jnr of mixtures with Jnr of the binder from the MSCR test method B showed that this modified test method correlates better to mixture results at the same temperature. Average of Jnr in secondary zone of mixtures was used for the calculation of the correlations. For standard MSCR, average Jnr of the 10 cycles were calculated at each stress level. However, in MSCR method B, average of the last 10 cycles was used for the calculation of correlations. Table E1b-1.1 shows the summary of these comparisons.

Table E1b-1.1. Correlation ( $R^2$ ) between Jnr of Mixture and Binder for two MSCR procedures.

| Binder Test Condition |               | Mixture Flow Number @ 46°C |                |
|-----------------------|---------------|----------------------------|----------------|
|                       |               | Fine 344 kPa               | Coarse 344 kPa |
| 46°C- 0.1 kPa         | Standard MSCR | 0.76                       | 0.76           |
|                       | MSCR B        | 0.76                       | 0.83           |
| 46°C- 3.2 kPa         | Standard MSCR | 0.63                       | 0.67           |
|                       | MSCR B        | 0.68                       | 0.73           |

The results showed that the average Jnr of the last 10 cycles has a slightly better correlation to mixture performance in comparison with average Jnr of whole cycles for MSCR method B and standard MSCR results. Analyses of the effect of different stress levels on the Jnr and percent recovery (i.e., R%) were also performed as indicated in figure E1b-1.2.

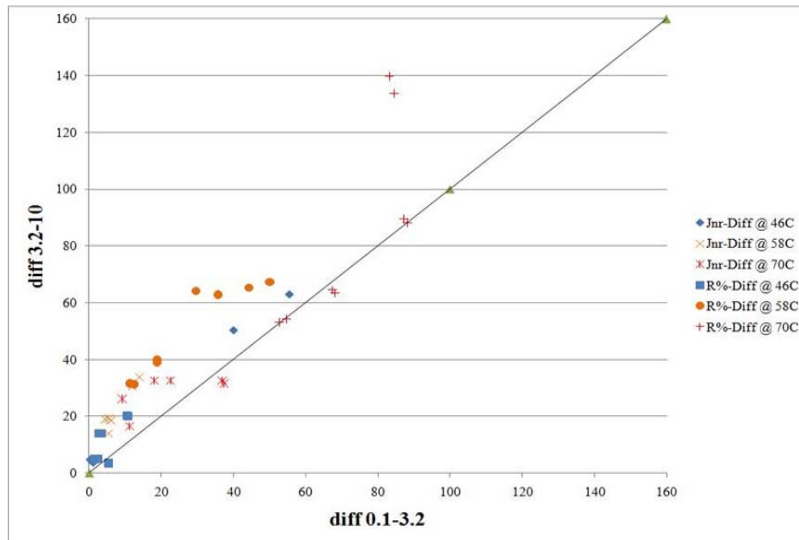


Figure E1b-1.2. Graph. Comparison of binder stress sensitivity.

Figure E1b-1.2 shows that the  $J_{nr\_diff}$  and  $\%R_{diff}$  values between stress levels of 10 kPa and 3.2 kPa are higher than those of 3.2 kPa and 0.1 kPa.  $J_{nr\_diff}$  and  $\%R_{diff}$  were calculated using AASHTO TP 70 standard. The plots show that the majority of the evaluated binders exhibit more pronounced stress sensitivity at higher stress levels than at the lower stress levels currently used in the standard. It is therefore concluded that adding a 10 kPa stress level can result in better evaluation of asphalt binder stress sensitivity. By using higher stress levels in the MSCR test, the response of the asphalt binder captures not only the stiffening effect of polymers, but also the delayed elastic effects. At high stress levels, the binder resistance to deformation starts to decrease as indicated by a sharp increase in  $J_{nr}$ . This rapid changing in non-recoverable creep compliance can be used as an indicator of nonlinear behavior. Based on these analyses, it is recommended that the current MSCR procedure be modified by testing the creep and recovery for 30 cycles at the stress levels of 3.2 and 10 kPa.

$J_{nr}$  of the mixtures were also compared to the proposed internal structural index calculated from digital imaging analysis (figure E1b-1.4). As it is shown, there is a fair correlation between ISI and  $J_{nr}$  of the mixes for 1034 kPa stress level in the primary zone. However, this correlation is more significant in the secondary zone. In the primary zone, the main mechanism is densification of the material by loss of air voids. This process consequently increases the aggregate interlock for the secondary zone. However, the main mechanism taking place in the secondary zone is related to the increase of stress level at contact zones of aggregates. Thus, the behavior in the secondary zone is mainly related to the aggregate structure (i.e., ISI).

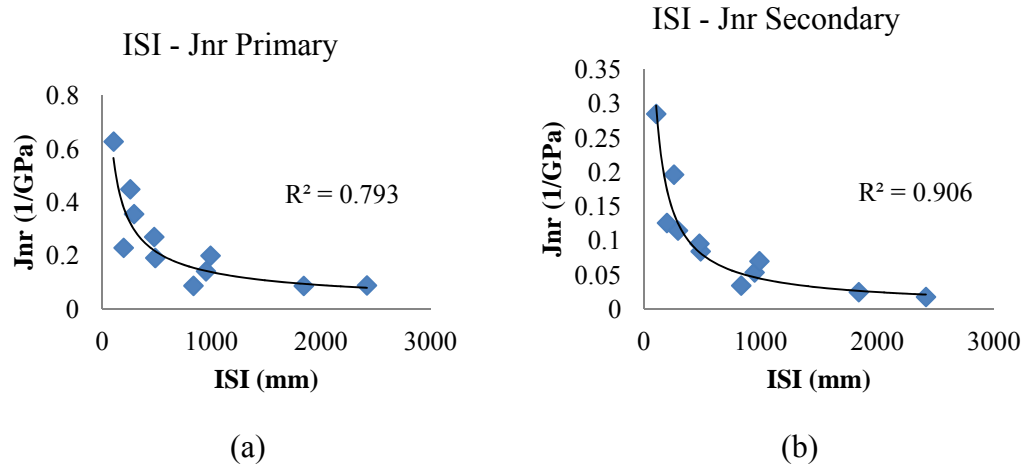


Figure E1b-1.4. Graph. Non-recoverable creep compliance (Jnr) vs. ISI.

#### Work Planned Next Quarter

Work for next quarter will focus on investigating the relationship between binder elasticity and mixture results in terms of rutting performance. Furthermore, an analogical model to predict binder behavior in the MSCR test will be developed to include a nonlinear spring and dashpot.

#### ***Subtask E1b-2: Feasibility of Determining Rheological and Fracture Properties of Asphalt Binders and Mastics using Simple Indentation Tests***

#### Work Done This Quarter

The research team worked on developing and implementing a method to obtain correction factors for sample size on indentation testing. The proposed method is based on work by Walters (1965) for elastic materials and several Finite Element (FE) simulations of the indentation test for visco-elastic materials.

Walters (1965) showed that the deviation from the infinite size behavior for rubber is constant when the  $a/t$  ratio is constant. The parameter “ $a$ ” denotes the radius of the contact and “ $t$ ” denotes the thickness of sample. By means of Finite Element simulations it was found that this observation also applies for visco-elastic materials and therefore a simplified method for calculating correction factors can be implemented.

Let  $d_t$  denote the displacement obtained for the sample thickness  $t$  and  $d_\infty$  denote the displacement obtained for the infinite size sample. Thus the correction factor is the ratio of  $d_t$  and  $d_\infty$ , which is a dimensionless quantity denoted by  $\chi$ :

$$\frac{d_t}{d_\infty} = \chi \left( \frac{t}{a} \right) \tag{E1b-2.1}$$

The radius of contact  $a$  and the depth of indentation  $d_t$  is given by the following equations:

$$a = \frac{K_2 R^{0.5} d_t^{0.5}}{K_1^{0.5}} \quad (\text{E1b-2.2})$$

$$d_t = \frac{K_1 P^{2/3}}{R^{1/3} E^{2/3}} \quad (\text{E1b-2.3})$$

Where  $K_1 = (81/256)^{1/3}$  and  $K_2 = (9/16)^{1/3}$ .

### Significant Results

Five asphalt binders with different creep compliances were considered in the development of the equation to correct for size effects. The binders considered vary from soft to stiff, representing the typical range of asphalt behavior. The creep compliance of the materials considered in FE simulations are shown in figure E1b-2.1.

The magnitude of loading was restricted to ensure that the depth of penetration did not exceed the radius of the indenter and also to increase the span of the  $t/a$  ratio considered.

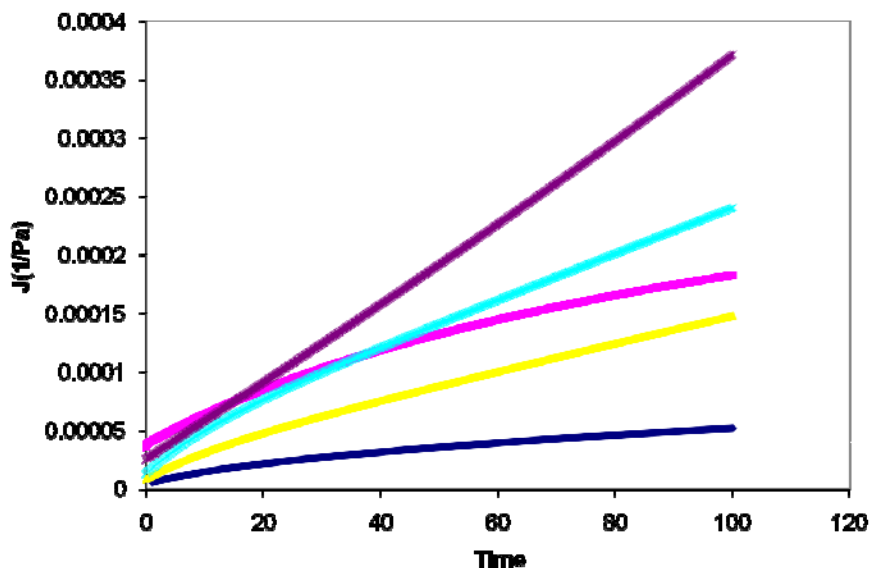


Figure E1b-2.1. Graph. Creep compliance of different asphalt binders considered.

The correction factors for the highly different visco-elastic materials considered fall on the same curve as shown in figure E1b-2.2. These results indicate that a single equation may be proposed to account for size effects in the indentation tests of asphalt binders.

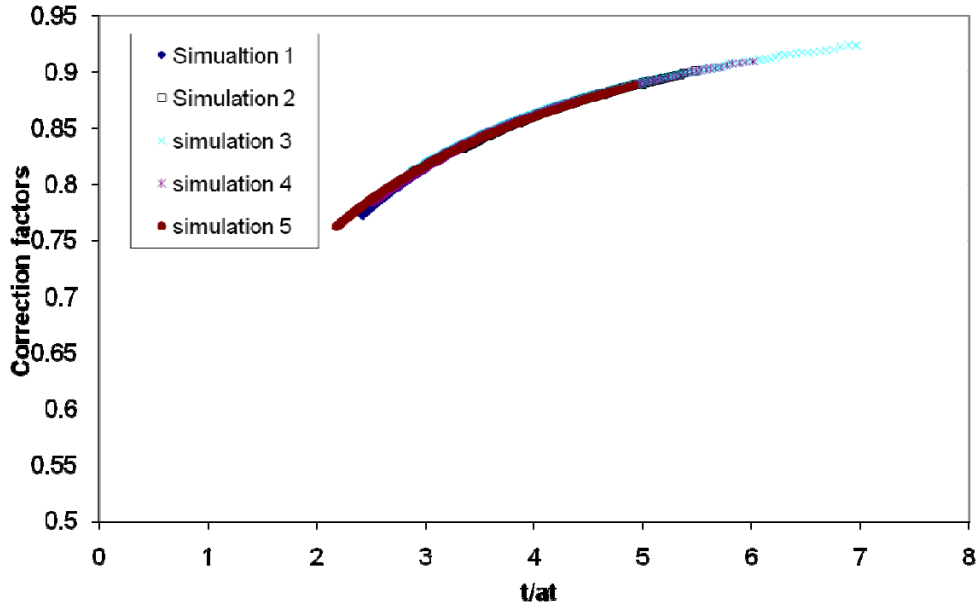


Figure E1b-2.2. Graph. Correction factors obtained using FEM

The equation used to fit the observed correction factors for finite sample size is as follows:

$$\chi\left(\frac{t}{a}\right) = 1 - 0.457e^{-0.297\frac{t}{a}} \quad (\text{E1b-2.4})$$

Note that the constant term in this equation is equal to 1 because the correction factor has to approach unity as the thickness of the sample increases.

#### Significant Problems, Issues and Potential Impact on Progress

The draft report for work element E1b-2 has been consolidated into report O as indicated in the work plan for the 21 month extension. Therefore, the deliverable date for the draft report of this work element has been moved to 3/13. The updated Gantt chart reflects this change.

#### Work Planned Next Quarter

Work next quarter will focus on finalizing the draft report for E1b-2, improving the indentation test setup to allow for temperature control, and on validating the correction factors for size effect developed in previous quarters.

#### References

Meruva, B. V. A., “Modification of the Penetration Test to Measure Rheological Properties of Bitumen”, Master’s Thesis, 2010.



Walters, N. E., 1965, The indentation of thin rubber sheets by spherical indentation. *British Journal of Applied Physics*, 16: 557-563.

## **Work Element E1c: Warm and Cold Mixes**

### ***Subtask E1c-1: Warm Mixes (UWM)***

#### Work Done This Quarter

Work continued in investigating the impacts of WMA additives on binder and mixture workability. In terms of binder workability, development of the asphalt binder lubricity test procedure continued with work focused on investigating the sensitivity of the coefficient of friction parameter to testing conditions, binder modification (SBS), and the presence of WMA additives. Viscosity measurements on all binders used were completed previously, allowing for application of conventional methods for evaluating lubricating fluids and for comparison to mixture data to determine the contribution of asphalt binder properties to overall workability.

For mixtures, efforts remain focused on the impacts of WMA additives on mixture workability and compactability. These terms are adapted from the NCHRP 9-43 mix design guidelines, with workability defined as the ability of the mix to achieve density at the intended compaction temperature. Compactability is defined as the change in density due to a 30°C reduction in compaction temperature and is representative of the temperature sensitivity of the mix. In this quarter, data collection was focused on the effect of WMA additive type and concentration on compaction. Based on the data collected, a modification to the compactability criteria provided in the NCHRP 9-43 guidance was proposed as a means to more clearly define minimum production temperatures.

Analysis of data collected in the previous quarter using a thin film aging procedure revealed that the potential impacts of use of WMA on asphalt binder performance properties are potentially due to both the presence of WMA additives and the reduction in production temperatures. Results demonstrated that for short term aging, the presence of WMA additives impacted both the aging index of binders, given as the ratio of the  $G^*/\sin\delta$  parameter measured after aging at 163°C to the  $G^*/\sin\delta$  of the original binder, and the rate of increase in high temperature shear properties due to increasing aging temperature. Both the conventional Superpave testing protocols and the MSCR test were used in this investigation. Work continues to extend this analysis to evaluation of the effect of WMA additives and short term aging temperature on asphalt binder intermediate and low temperature properties after PAV aging. In parallel, work began on evaluating the effects of WMA additives and reduced production temperatures on mixture performance through use of the Thermal Stress Restrained Specimen Test (TSRST). Mixture testing also includes evaluation of the effect of aging time.

Collaboration with UNR continued on evaluating the impact of WMA production temperatures and entrapped aggregate moisture on moisture damage susceptibility using the Bitumen Bond Strength (BBS) test and dynamic modulus ratio. In this quarter, the research team addressed TRB review comments and re-submitted the paper for consideration for publication. The research

team will present findings at the TRB meeting and re-visit the work plan based on feedback received.

The research team has been unable to obtain WMA field projects with WisDOT, however efforts for coordination continue. WisDOT has recently implemented a new Special Provision to allow for use of WMA on projects, it is expected that this will provide more opportunities for field projects. UNR continues to test the materials collected on PTH14 in Manitoba.

Work continued in compiling Chapters 1-4 of the draft final report. These chapters cover the problem statement/introduction, literature review, experimental design, and results/analysis. The report will be focused on evaluating the impacts of WMA additives on binder workability and the effects of WMA additives and reduced temperatures on performance. Based on results, mixture testing will commence to verify results. Work will continue to summarize research results and submit the report next quarter.

### Significant Results

The Asphalt Binder Lubricity test procedure has been finalized and sensitivity to testing parameters, binder modification, and presence of WMA additives established. Based on the testing results, it is recommended that tests be conducted at a normal force of 10 N due to the better repeatability observed relative to the testing conducted at 20 N. In both cases, the device was able to control normal force throughout the test; however torque readings were considerably more consistent for tests conducted at 10 N. Using two binders, three temperatures, three speeds, and two WMA additives, the pooled standard deviation of the coefficient of friction parameter was approximately 0.01. Based on the values of coefficient of friction observed, this standard deviation results in a coefficient of variation ranging from 10% - 15%. The procedure will be implemented to further investigate the effects of WMA additive type and concentration.

Preliminary results indicate that the aggregate coating criterion proposed in the NCHRP 9-43 mix design procedure is not the controlling factor in determining appropriate production temperatures. For the mixture tested this quarter, the limiting factor in temperature selection was mixture compactability. The research team has proposed, and continues to investigate, a new method to evaluate compactability that fits a function to the relationship between gyrations to 92% Gmm (N92) and compaction temperature. The motivation for this change is to define the minimum compaction temperature that relates to the N92 threshold. The use of this method will be compared with the N92 ratio proposed by NCHRP 9-43 in future work. Preliminary data collected and literature review revealed the concept that the relationship between density and compaction temperature reaches a minimum value. It is hypothesized that the temperature at which this minimum is achieved is dependent on WMA additive type and concentration, and binder modification.

In relation to the impacts of WMA additives and reduced temperatures on potential for moisture damage, both BBS testing and  $E^*$  mixture data revealed the effect of production temperature to be significant. In the BBS test this was simulated through using different aggregate application temperatures. Results indicate that a 30°C decrease in aggregate application temperature significantly reduces the wet bond strength observed for samples conditions at 40°C for 96 hrs in

a moisture bath. Based on these results it appears that the ability of the asphalt to bond to the aggregate is influenced by the application temperature. BBS and E\* results also revealed that the potential negative impacts of reduced production temperature on moisture damage can be offset through selection of proper WMA additives.

### Significant Problems, Issues and Potential Impact on Progress

Mixture workability and performance work has been delayed for two reasons:

- Availability of asphalt binder: An order for additional binder was accepted by the manufacturer, however due to time constraints and staff availability the shipment was delayed approximately 2 months.
- Performance Testing: The mixture axial performance testing machine is under repair and has been unavailable for the last two months. The research team is currently in contact with the manufacturer to address remaining issues. In the meantime, work has progressed on evaluation of potential for thermal cracking via the TSRST test. Sample preparation and TSRST testing will continue until the axial testing machine is repaired.

Submission of the draft final report was delayed three months. It is anticipated that the report will be completed in 2012Q1.

### Work Planned Next Quarter

#### *Development of Mixing and Compaction Guidelines for WMA*

The research team will continue to apply the NCHRP 9-43 WMA mix design procedure to fine and coarse aggregate gradations and a variety of WMA additives. A second aggregate source that demonstrates high water absorption (~2.5%) will be included in the study to assess the impacts of using absorptive aggregates on the mix design procedure. Work will continue on lubricity tests to evaluate the effects of additive type and concentration. Lubricity and viscosity data collected will be compared to mixture workability results to validate the use of coefficient of friction as a measure of binder workability and to define the contribution of asphalt binder workability to mixture densification.

#### *Impacts of Reduced Aging on Mixture Performance*

Thermal Stress restrained Specimen Test (TSRST) will continue next quarter to evaluate the effect of aging temperatures and times on low temperature performance of WMA mixtures. Single Edged Notched Beam (SENB) testing will commence on binders short term aged at two temperatures then PAV aged and compared to TSRST results. Impacts on high and medium temperature performance will be addressed using the Flow Number (FN) test and Indirect Tension Test (IDT) for the samples prepared at different reduced aging temperatures. Evaluation of the BBS test for use in WMA will continue with an emphasis on the effects of application temperature and methods to separate cohesive and adhesive bond strength.

#### *Final Report*

The final report focused on the impacts of WMA on workability and asphalt binder performance will be submitted.

## ***Subtask E1c-2: Improvement of Emulsions' Characterization and Mixture Design for Cold Bitumen Applications (UWM)***

### Work Done This Quarter

Collaboration continued this quarter between the research team and Heritage Research Group (HRG), a private sector company with extensive field experience in cold mix applications. In this quarter the team took steps to finalize the coating procedure in order to identify the protocols needed to determine an optimum mixing time, design emulsion content and aggregate moisture content for the aggregate and emulsion source provided by HRG. Several trials were conducted to develop the proper sample size and analysis procedure. Laboratory compacted CMA mixtures were also prepared using a modified SGC mold that allows water drainage to analyze volumetric properties.

The research team previously provided a general outline of the coating procedure and introduced imaging analysis as a way to objectively quantify coating. During this quarter, revisions to the preparation and analysis steps were implemented to make the procedure more efficient. An office scanner with a fixed-area frame has been employed to standardize the sample area for analysis and picture quality. Calibration of the scanned images using actual moist test aggregates was used to reduce the error in the scanned images. Once calibrated, the effect of sample size and mixing time on the percent aggregate coating was isolated to determine the optimum laboratory mixing time in accordance with the maximum coating that we could reasonably achieve, and to simulate field conditions. Based on HRG team experience 2-3 minutes of initial mixing was assumed to be a good estimate to simulate field conditions (compared to 1.5 minutes specified for HMA).

A follow-up study on the effect of curing on the densities and volumetrics of the CMA mixtures was also completed this quarter. In the absence of a standard protocol for cold mix compaction, mixtures were prepared using the Superpave guidelines for mixtures of pavement with low traffic volume. The mixtures produced were cured for 24 and 72 hours after compaction and the densities were calculated in order investigate the change in volumetric properties of the mixtures during the curing process.

### Significant Findings

To improve the imaging procedure, a “threshold” value for pixel intensity needed to be specified such that the coating determination would be a true representation of the coating percentages. The threshold value is the pixel intensity value at which the software identifies a particle as white or black (coated or uncoated). The research team ‘calibrated’ the software to the aggregate sample by finding the threshold value at which the software just marked the bare aggregate particles as uncoated. Moist aggregates were used for calibrating since this was the condition at which the particles would be ‘darkest’, but not coated with emulsion during actual mixing. Several threshold values were applied, and the black and white (coated and uncoated) pictures were visually inspected. The threshold value at which the software just marked the bare aggregate particles as uncoated (the complete image was approximately white) was chosen for further analysis. There appeared to be some error due to shadows and voids in the scanned

image, which can be used as a ‘calibration factor’ if the most accurate estimate of coating is desired. It is assumed that the error in the analysis will not remain constant for all aggregate types and gradations; the threshold should therefore be calibrated for each specific aggregate type and gradation that will be mixed.

Using the calibrated imaging procedure, the optimum mixing time for the specified aggregate – emulsion combination coating was evaluated. The test matrix is displayed in table E1c-2. The gradation, aggregate moisture, and emulsion content of the mixes were held constant.

Table E1c-2.1. Coating Mixing Time Matrix

| Factors            | Possible Levels | Description  |
|--------------------|-----------------|--------------|
| Mixing Time (min)  | 4               | 1.5          |
|                    |                 | 2.5          |
|                    |                 | 5            |
|                    |                 | 10           |
| Sample Weight (gr) | 2               | 1500         |
|                    |                 | 3000         |
| Mix Schedule       | 2               | Non-agitated |
|                    |                 | Agitated     |

Coating analysis results for the non-agitated, 3000 gram mixture at each of the four mixing times is shown in figure E1c-1.1.

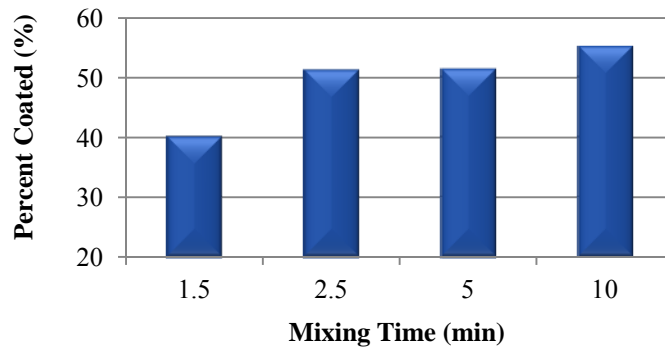


Figure E1c-2.1. Graph. Effect of mixing time on coating.

Three replicates at each mixing time were analyzed. Based on statistical analysis, results confirmed that for mixing times higher than 2.5 minutes, no significant increase in coating percentage could be achieved. However, there was a statistically significant increase in percent coating between the 1.5 minute and the 2.5 minute mixing times. Therefore the 2.5 minute mixing time was selected as optimum for the analyzed aggregate – emulsion combination. It should be noted that this mixing time is in agreement with field observations for aggregate coating.

Observations made during this experiment indicated that there is a certain amount of mixture that gets stuck to the sides of pans and spoons used in mixing, regardless of the sample size (1500 or 3000 grams). It is therefore clear that the lost material would be a smaller percent of the 3000 gram sample. Therefore the 3000 gram sample is the more appropriate size to represent the actual coating that can be achieved during mixing. Using the 3000 g sample, the effect of re-agitation after 24 hours was evaluated. As expected, these mixtures generally exhibited better coating when compared to non-agitated mixes, independent of mixing time.

Another important finding made last quarter is related to density changes during curing. It was noted that significant mass loss occurs over time as a result of moisture evaporation/dissipation for compacted CMA samples, resulting in a significant change in volumetric properties. It was hypothesized that samples exhibited significantly different bulk volumetric properties ( $G_{mb}$ ) when fully cured (72 hours) as compared to 24 hours after compaction due to a reduction in sample volume. The reduction in volume produces a net increase in  $G_{mb}$ , which in turn results in a decrease in mixture air voids. It was demonstrated this quarter that if no free water exists in the mixture (in other words, if the amount of total water in the mixture is less than the aggregate absorption), volumetric shrinkage can occur over time as a result of moisture evaporation. It is hypothesized that for mixtures with the theoretical possibility of free water, the compaction pressure will likely force the majority of this water out of the sample prior to curing. It is then expected that the sample will experience a reduction in volume with curing, albeit most likely to a lesser extent. Work will continue to further investigate this newly observed ‘drying shrinkage’ in CMA mixtures.

#### Significant Problems, Issues and Potential Impact on Progress

None

#### Work Planned Next Quarter

The following work is planned for next quarter:

- *Finalizing Coating Procedure:* Coating experience will be finalized in the future quarter by finishing the coating matrix proposed to include the effect of aggregate gradation, aggregate type, emulsion type, residual asphalt content and aggregate moisture content.
- *Volumetric Analysis:* The research team will investigate and attempt to quantify the phenomenon described above as ‘drying shrinkage’ with additional mixes with varying moisture contents.
- *Mechanical Performance Testing:* An outline for mix design procedure of CMA mixtures using both volumetric studies and mechanical testing will be proposed. The research team will evaluate the mechanical properties of laboratory compacted samples and field cores of constructed CMA pavements. This can be used in order to isolate the appropriate compaction effort in SGC that is the best representative of what is practically done in the field.

## CATEGORY E2: DESIGN GUIDANCE

### Work element E2a: Comparison of Modification Techniques (UWM)

#### Work Done This Quarter

In this quarter the research team focused on developing a guideline for selecting optimum modification based on a performance-based comparative cost analysis. The guidelines were used to estimate the performance-based cost associated with the use of two polymer modifiers.

#### Significant Results

In the calculation of the cost associated with modification the following cost items were taken into consideration:

- Raw materials
- Labor for adding the polymer
- Fuel for heating and storage
- Compaction costs

The raw material cost is calculated based on the asphalt binder price, the amount and approximate price of the modifier and the amount and price of the anti-stripping agents. The labor cost was calculated based on the time required to complete one batch of polymer-modified binder (i.e., time for blending). Note that each modifier requires different blending and digesting temperatures. Therefore, if lower blending temperatures can be achieved, important energy and cost savings can be obtained. Further, different polymers/modifiers can cause a reduction in the viscosity and thus reduce compaction costs by reducing the number of roller passes during construction required to achieve the desired density.

An example of the construction costs for two modifiers taking into account the above factors are shown in Table E2a.1. Since the asphalts used in this study came from different contractors, and only the PG grade was reported, the amount of polymer (i.e., concentration by weight) was estimated from work by Clopotel (2010).

Table E2a.1. Estimating cost per pound for different modifications.

| Price (\$/lb) PMA    | Modifier 1   |              |              | Modifier 2   |              |                |
|----------------------|--------------|--------------|--------------|--------------|--------------|----------------|
|                      | PG (0%)      | PG+6 (~2%)*  | PG+12 (~4%)* | PG (0%)      | PG+6 (~2%)*  | PG+12 (~3.5%)* |
| Raw Materials        | 0.263        | 0.300        | 0.340        | 0.263        | 0.290        | 0.300          |
| Labor                | -            | 0.108        | 0.108        | -            | 0.036        | 0.036          |
| Fuel                 | -            | 0.050        | 0.050        | -            | 0.043        | 0.043          |
| Anti-stripping       | 0.010        | 0.010        | 0.010        | 0.010        | 0.000        | 0.000          |
| Rolling Cost         | 0.009        | 0.014        | 0.014        | 0.009        | 0.009        | 0.009          |
| <b>Total (\$/Lb)</b> | <b>0.282</b> | <b>0.481</b> | <b>0.521</b> | <b>0.282</b> | <b>0.378</b> | <b>0.388</b>   |

\*concentration by weight and estimated from Clopotel (2010)

The ratio between the change in price per pound and the amount of polymer/modifier (i.e., concentration by weight) for two modifiers is shown in table Ea2.2.

Table E2a.2. Ratio between the change in price per pound ( $\Delta (\$/lb)$ ) and concentration by weight of the polymer (% of modifier).

| Modifier | $\frac{\Delta (\$/lb)}{\% \text{ of Modifier}}$ |
|----------|---|
| 1        | 0.068   |
| 2        | 0.035   |

The change in percent recovery (i.e.,  $\Delta\%R$ ) at 3.2 kPa versus the amount of polymer for different asphalts is shown in figure E2a.1, while the change in the non-recoverable creep compliance ( $\Delta J_{nr}$ ) versus the amount of polymer is shown in figure E2a.2.

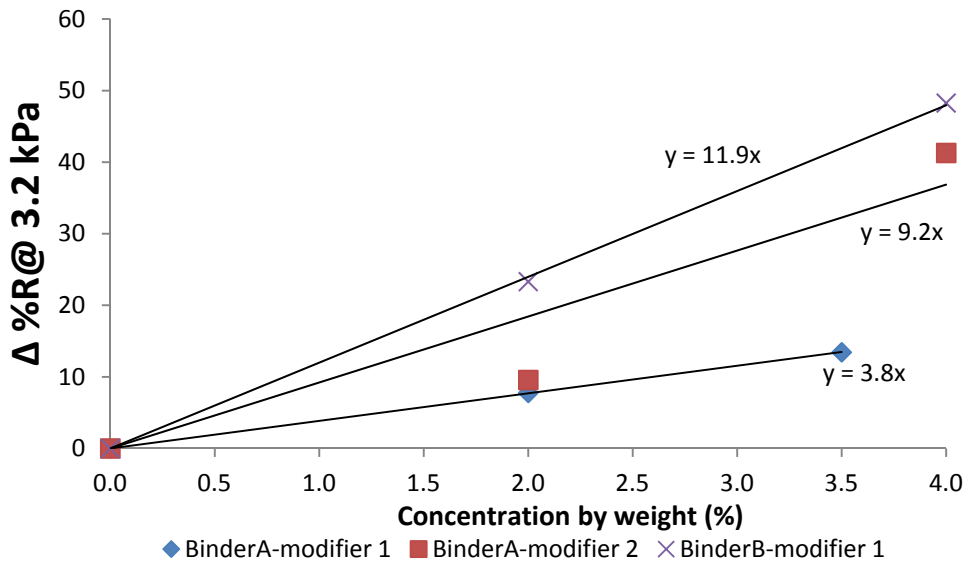


Figure E2a.1. Graph. Change in %R at 3.2 kPa vs. concentration of modifier.



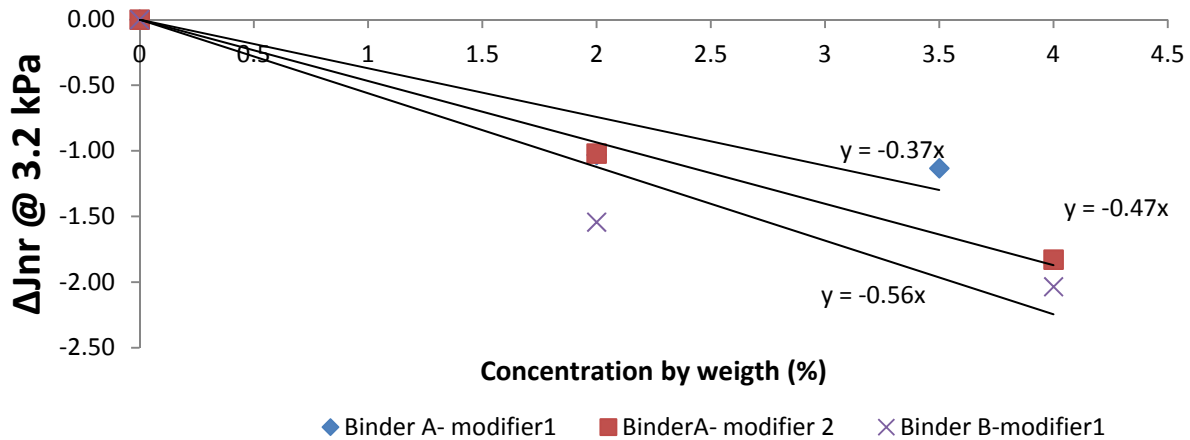


Figure E2a.2. Graph. Change in Jnr at 3.2 kPa vs. concentration of modifier.

The procedure used for calculating the performance-based cost associated with different modifications is depicted in figure E2a.3.

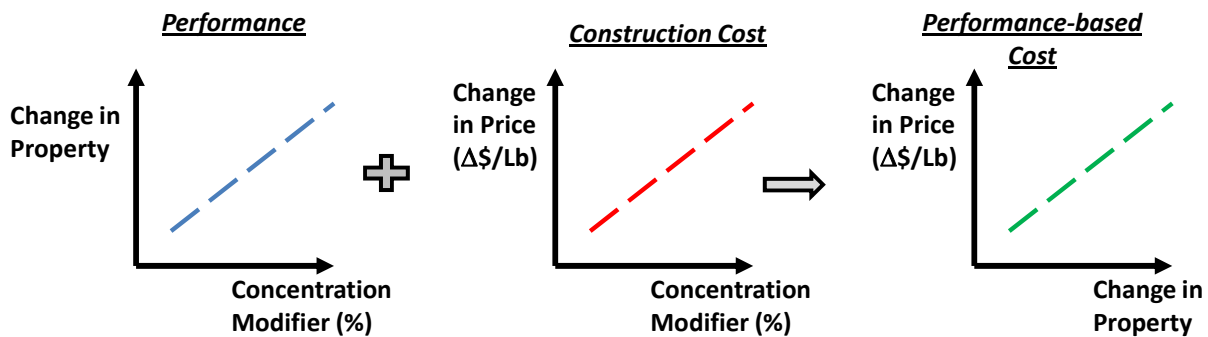


Figure E2a.3. Illustration. Proposed method for calculating performance-based cost associated with modification.

Using the slopes from table E2a.2 and figures E2a.1 and E2a.2 one can calculate the cost associated with the increase in a specific property (e.g., %R and  $J_{nr}$ ). For example, figure E2a.1 shows that for binder *A* with Modifier 1 the elasticity increases by 3.8% for 1% increase in the concentration of polymer. On the other hand, the price increases by 0.068 \$/lb for 1% increase in polymer content. From these two slopes, a ratio between the change in cost with respect to the change of %R is calculated as  $0.017 \frac{\$}{lb \cdot \%R}$ .

To further illustrate this performance-based cost concept, assume that the unmodified binder *A* has a %R of 50%. However, design considerations require a binder with a percent recovery equal to 75%. If Modifier 1 is selected as modification to meet the performance requirements, then the performance-based cost is equal to  $0.017 \cdot (75-50) = 0.425$  \$/lb.

### Work Planned Next Quarter

Work for next quarter will focus on improving the estimation of construction costs for different modifiers. Also, the cost-analysis framework will be improved to include non-linear trends between change in mechanical properties and concentration of the modifier.

### Cited work

Clopotel, C. S., 2010, “Modification of the Elastic Recovery Test of Binders and Its Relationship to Performance Properties of Asphalt Binders,” University of Wisconsin-Madison Master Thesis.

## **Work element E2b: Design System for HMA Containing a High Percentage of RAP Materials (UNR)**

### Work Done This Quarter

This work element is a joint project between University of Nevada, Reno and University of Wisconsin–Madison. This quarter the research team focused on the development of a procedure to estimate the effect of blending time and temperature on the performance indicators ( $G^*$ ) of the blended binder using DSR measurements. The amount and the effect of the blending between RAP binder and virgin binder that occurs in a field mixture are dependent on the mixing and conditioning time at a given temperature. Incomplete blending due to insufficiently low mixing temperatures may not allow for optimum utilization of the recycled material. Mortar samples were conditioned at elevated temperatures and tested at various intervals to determine the changes in  $G^*$  due to blending conditions variations.

An ‘artificial’ RAP source was created by blending heavily aged binder with aggregate material at binder content similar to what is typically observed on field RAP sources. A neat fresh binder was selected and the estimated mixing temperature for the given binder was determined using the ‘equi-viscous’ technique in the Rotational Viscometer (RV). The artificial RAP material and fresh binder were blended at the estimated mixing temperature of 150°C to create a RAP mortar. Similarly, the fresh binder was tested at the estimated mixing temperature to isolate the effect of binder aging due to conditioning at relatively high temperatures. Samples of the RAP mortar and fresh binder were tested immediately after the initial blending. The RAP mortar and the fresh binder were placed in an oven to condition at a temperature of 125°C. Samples of each mortar material were taken after regular intervals of conditioning and tested.

Initial results showed that the mortar approach can clearly demonstrate the effect of blending conditions, after normalizing the blending curves to the effect of fresh binder aging. Analysis of results indicates that at the temperatures tested, the majority of the blending between the RAP binder and the fresh binder occurred during the initial mixing at 150°C. Work continues on a better approach to quantify the rate of blending that occurs in this initial stage.

The subtask E2d-3, “Develop a Mix Design Procedure,” was completed. The data analysis was conducted for the mixing temperature records, grades of the recovered binders, volumetric

properties and mechanical properties using the dynamic modulus. The primary objective of this study is to develop a mixing procedure for the laboratory that best simulates the plant-produced samples after their mixing and production process. Three distinct methods for incorporating the RAP material into the mixing process were examined and compared to the plant-produced samples provided by Granite Construction. The general descriptions of the three methods are as follows:

- Method A: The virgin aggregate, the virgin asphalt binder and the RAP material will all be heated to the appropriate mixing temperature as dictated by the virgin asphalt binder grade.
- Method B: The virgin aggregate will be superheated in accordance with NAPA's recommendations from Information Series 123. The virgin asphalt binder will be heated to the appropriate temperature dictated by the performance grade. The RAP material will be dried and added at the ambient temperature.
- Method C: The virgin aggregate is superheated in accordance with NAPA's recommendations from Information Series 123. The virgin asphalt binder will be heated to the appropriate temperature dictated by the performance grade. The RAP material will be moisturized to the appropriate moisture content and added at the ambient temperature.

To be able to determine which method of incorporating the RAP material into the laboratory mixing process will produce the mixture that most closely simulates the plant-produced mixture several characteristics were analyzed. The mixing temperatures over the duration of the mixing process for each method were examined to provide insight into how effectively the virgin aggregate is transferring heat to the RAP material.

Additionally a short-term oven aging analysis was conducted to determine the appropriate aging time in the laboratory to replicate the aging experienced by the plant-produced mixtures. To assess the different aging levels, the asphalt binder were extracted from the plant-produced and laboratory-produced mixtures and graded according to the Superpave performance grading system. Lastly, compacted samples were created for each mixing method as well as for the plant-produced laboratory-compacted mixtures and an analysis of the volumetric properties and dynamic modulus was conducted.

The paper entitled: "Recommendations for the Characterization of RAP Aggregate Properties Using Traditional Testing and Mixture Volumetrics" has been accepted for presentation at the 2012 Association of Asphalt Paving Technologists (AAPT) meeting in Austin, TX. The paper summarized the findings for the investigation of the influence of extraction methods on aggregate properties. In the paper, recommendations were made for the most appropriate method to estimate the RAP aggregate specific gravities based on acceptable levels of error in voids in mineral aggregates (VMA) for mixtures with varying levels of RAP

### Significant Results

The artificial RAP used in this experiment was created by blending two-cycle PAV aged PG 58-28 fresh binder with #100 natural sand aggregates at a binder content of 12% by weight. The artificial RAP material and the same fresh asphalt binder were brought up to 150°C and blended

for 90 seconds manually. The RAP mortar was blended at 25% binder replacement as a relatively large representative sample of ‘RAP binder’ was desired in the mortar material. Immediately after the initial mixing, the RAP mortar and fresh binder were moved to condition in an oven held at a temperature of 125°C. Samples of the RAP mortar and fresh binder were taken at intervals of 0.5, 1, 2, 4, and 6 hours conditioning time for subsequent testing.

Samples were tested at 64°C in the DSR using the 25 mm parallel plate geometry. A 2 mm testing gap was used for the mortar material. The sample complex shear modulus  $G^*$  was recorded for two replicates at each conditioning time and an index was created by dividing the complex modulus at conditioning time,  $G_t^*$ , by the initial complex modulus immediately after mixing,  $G_o^*$ . This allows the complex modulus (now unit-less) of the RAP mortar to be plotted on the same scale as the fresh binder. Complex shear modulus indices are plotted against the conditioning time in figure E2b.1.

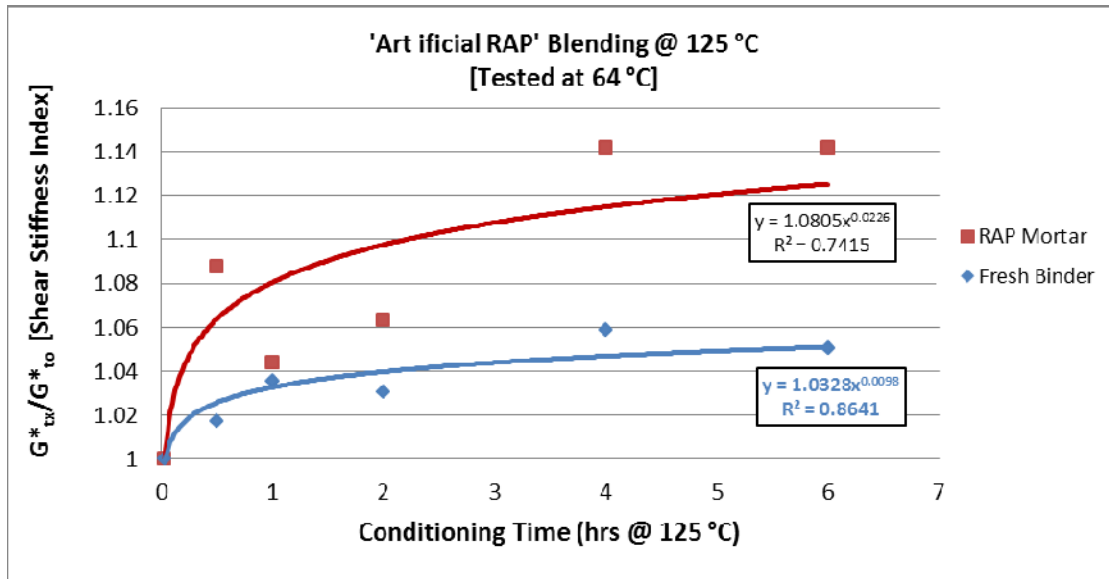


Figure E2b.1. Graph. Effect of conditioning time on RAP binder blending.

Several observations can be made from figure E2b.1. First, it appears that the relative increase in binder modulus, after accounting for the aging in the fresh binder, is less than 10% for six hours of conditioning. This suggests that for this mixing/conditioning temperature combination, the majority of the blending that occurs in the mortar occurs in the initial mixing phase. Lower mixing and conditioning temperatures are suggested in attempt to capture this behavior. Most importantly, however, the mortar test procedure appears to show the effect of blending between the RAP binder and the fresh binder, and may be useful for predicting the extent of blending that occurs in field mixing. It is noted that the mortar analysis procedure does not provide any information regarding the actual diffusion (blending) rate between the RAP and fresh binders since we do not control the diffusion surfaces of either material.

An alternative approach to better isolate the diffusion/blending that occurs between RAP and fresh binders using mastics was also investigated. RAP mastics are prepared in a similar fashion to RAP mortars, with the exception of using passing #200 filler instead of the passing #100 used in mortars. Fresh mastic samples are also created with the same AC% and fine aggregate proportions as the RAP mastic. Mastic samples of 1 mm thickness are placed on each other in the DSR (Shown in figure E2b.2). The temperature then increased for a predetermined amount of conditioning time. After conditioning, samples are trimmed and the DSR test for complex modulus is conducted in 64°C.

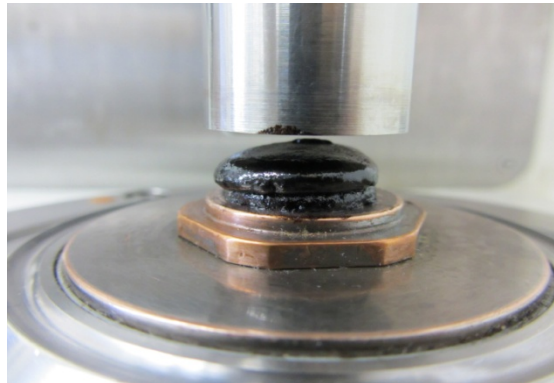


Figure E2b.2. Photograph. Proposed sample geometry to measure blending.

Initial testing using this procedure resulted in excessive sample bleeding during the temperature conditioning. Therefore to reduce this problem, it was proposed that external sample conditioning be conducted. Samples are placed in a special mold and conditioned for the specified duration. Currently this procedure is under development to obtain the required geometry and thickness for samples. The proper shear frequency and strain need to be justified as well.

#### Significant Problems, Issues and Potential Impact on Progress

None

#### Work Planned Next Quarter

The following work is planned for next quarter:

- The alternative blending analysis approach using mastics will be further refined and results will be presented. The sensitivity of the proposed procedure to several conditioning temperatures will also be explored.
- The RAP binder workability procedure presented last quarter will be refined to include the sensitivity of the mortar materials to shear rate. A literature review on the subject suggests that lower shear rates will better replicate field conditions.

## Subtask E2b-2: Compatibility of RAP and Virgin Binders

### Work Done this Quarter

Automated Flocculation Titrimetry (AFT) was completed on extracted binder samples from a FHWA Plant-Mix RAP study conducted by Becky McDaniel and Gerry Huber. (Note: these samples were previously referred to as from the NCHRP 9-12 project but that was in error). In the Plant-Mix study, some of the IDT mix test results showed that some of the mixes had a lower stiffness when RAP was added or when RAP was increased. The Plant-Mix study used four contractors with each contractor producing six mixes. The six mixes were Mix A - PG 64-22 no RAP; Mix B - PG 64-22 with 15% RAP; Mix C - PG 64-22 with 25% RAP; Mix D - PG 64-22 with 40% RAP; Mix E - PG 58-28 with 25% RAP; and Mix F - PG 58-28 with 40% RAP. It is unknown if the PG 64-22 and PG 58-28 virgin asphalts were from the same source and whether or not the different contractors used the same sources. Although not verified, it is probable that the four contractors did not use the same RAP source.

It was of interest to see if AFT could show differences in compatibility of the extracted binders that would correlate with the mix testing. The hypothesis behind this is that if only some components of the RAP asphalt blend with the new virgin asphalt, then a change in the compatibility is possible which may lead to unexpected mix properties (i.e. stiffness).

In almost every case, the change in the AFT P value was inversely related to the change in IDT mix stiffness. Although there is not direct correlation between the absolute value of the AFT P value and mix stiffness, it is a reasonable result that as a binder becomes more compatible, it becomes less stiff and thus the mix stiffness is reduced. An example of one series of mixes from “Contractor #2” is shown in figure E2b-2.1.

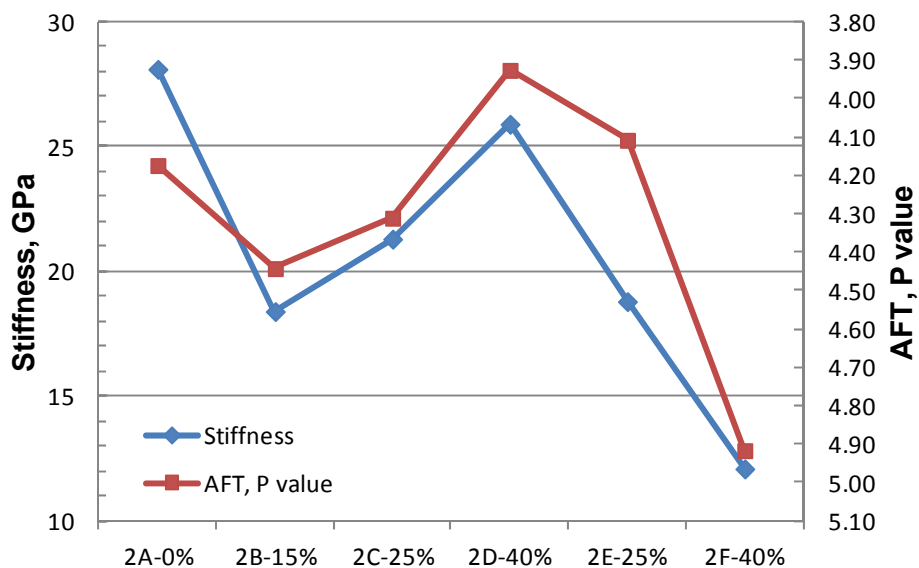


Figure E2b-2.1. Comparison of IDT mix stiffness and AFT P values for Contractor 2 in the FHWA Plant-Mix study.

## Significant Results

None.

## Significant Problems, Issues and Potential Impact on Progress

None.

## Work Planned Next Quarter

In the next quarter, it is planned to continue the BISOM method testing of the laboratory RAP blended samples.

## **Work element E2c: Critically Designed HMA Mixtures (UNR)**

### Work Done This Quarter

Work continued to evaluate the applicability of the recommended deviator and confining stresses for the flow number test. The mix design verifications for all sources have been completed. In addition, the dynamic modulus and the flow number (FN) testing for all mixtures has also been completed. Figure E2c.1 shows the dynamic modulus at 20°C and 7% air-void level for a loading frequency of 10 Hz.

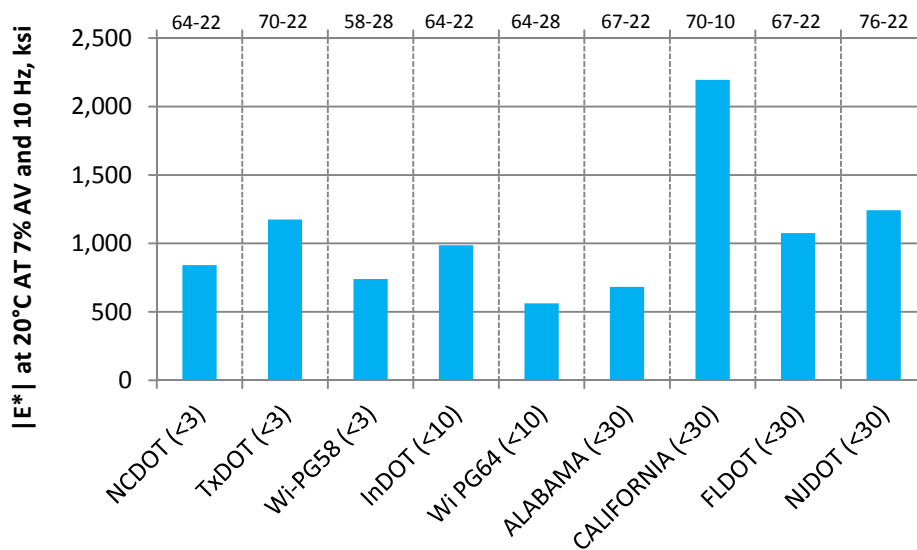


Figure E2c.1 Dynamic modulus at 20°C.

2D-Imaging analyses have been conducted for all mixtures to determine the number of aggregate contact points, aggregate orientation, and mixture segregation. Figure E2c.2 shows an example for the 2D-Image of the California mixture.

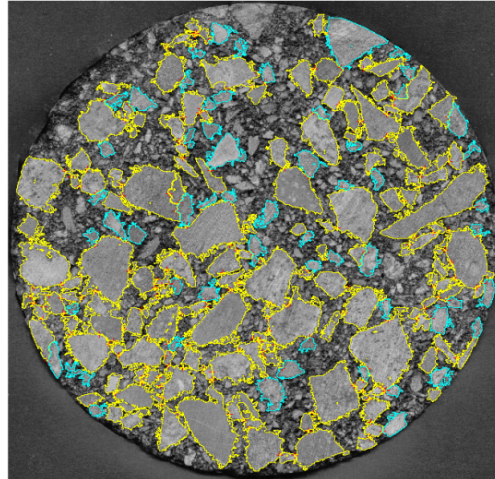


Figure E2c.2 2D-Imaging of California mixture.

### Significant Results

Table E2c.1 and figure E2c.3 show the effective temperatures and the determined critical temperature ranges for the various evaluated mixtures. The critical temperature ( $T_{\text{critical}}$ ) is defined as the temperature at which the mixture exhibits a plastic flow for a defined stress state and loading rate. The data show different critical temperature ranges for the various evaluated mixtures.

Table E2c.1. Effective temperatures critical temperature ranges.

| Mixture Descriptions |         |                   |       | 50% Reliability Temp<br>(50% reliability high pavement temperature from LTPPBind at depth of 20 mm for surface courses) | NCHRP 9-33A<br>(Effective Pavement Temperature Prediction Equation) | NCHRP 9-30A<br>(Effective Pavement Temperature based on rutting prediction in MEPDG) | $T_{\text{critical}}$ Range |
|----------------------|---------|-------------------|-------|---|---|--|-----------------------------|
| Mix No.              | Traffic | Binder Grade (PG) | State |   |   |  |                             |
| 1                    | <3      | 58-28             | WI    | 49.1°C  | 35.8°C  | 29.9°C   | 29.8 - 35.8°C               |
| 2                    | <3      | 64-22             | NC    | 58.6°C  | 34.1°C  | 35.5°C   | 34.1 - 40.1°C               |
| 3                    | <3      | 70-22             | TX    | 62.7°C  | 42.2°C  | 36.0°C   | 36.2 - 42.2°C               |
| 4                    | <10     | 64-28             | WI    | 46.7°C  | 32.3°C  | 29.0°C   | 26.3 - 32.3°C               |
| 5                    | <10     | 64-22             | IN    | 52.1°C  | 35.2°C  | 33.0°C   | 35.2 - 41.2°C               |
| 6                    | <30     | 67-22             | FL    | 63.0°C  | 41.6°C  | 34.3°C   | 41.6 - 47.6°C               |
| 7                    | <30     | 76-22             | NJ    | 50.2°C  | 32.7°C  | 32.0°C   | 50.2 - 56.7°C               |
| 8                    | <30     | 67-22             | AL    | 59.5°C  | 41.3°C  | 35.5°C   | 29.3 - 35.3°C               |
| 9                    | <30     | 70-10             | CA    | 62.5°C  | 29.3°C  | 35.5°C   | 47.2 - 53.2°C               |



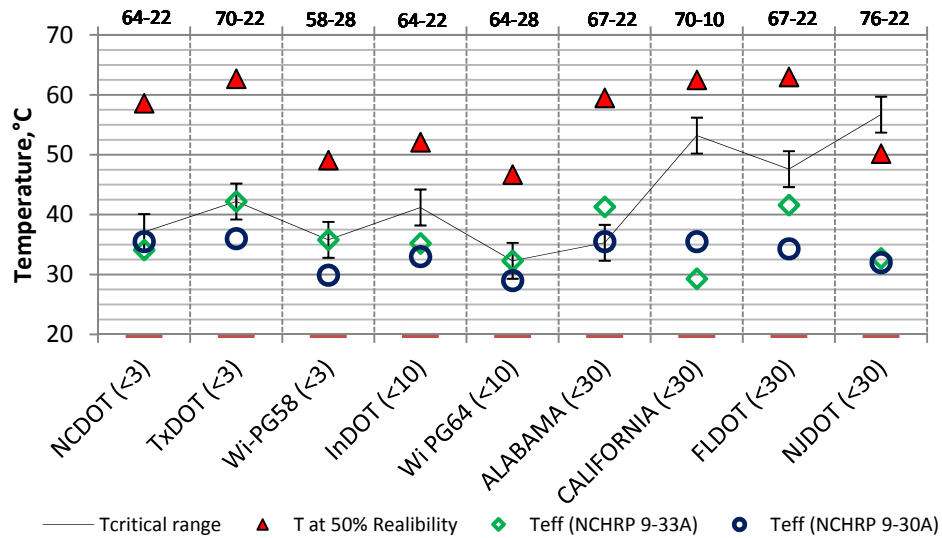


Figure E2c.3 Effective temperatures critical temperature ranges.

### Significant Problems, Issues and Potential Impact on Progress

The large number of mixtures and testing conditions delayed the progress of this effort. The research team will work on summarizing all the test results and findings by end of next quarter.

### Work Planned for Next Quarter

Summarize and present the findings of the Flow Number Task Force experimental plan. Recommend a standard testing procedure for the flow number.

### **Work element E2d: Thermal Cracking Resistant Mixes for Intermountain States (UNR & UWM)**

#### Work Done This Quarter

This work element is a joint project between University of Nevada Reno and University of Wisconsin–Madison. In this quarter, all of the E\*-compression testing and extraction and recovery testing has been completed. Following that process, 93% of the Carbonyl Area (CA) measurements have been completed. Progress continues on the low shear viscosity (LSV) and binder master curve measurements, with nearly 65% of that testing having been completed from this subtask. Further refinement of the Thermal Stressed Restrained Specimen Test (TSRST) testing procedure is nearly finalized. Modifications to the plate geometry and gluing procedures have let to more reliable test results.

Efforts have continued on potential field validation sites for the developing thermal cracking modeling efforts. Two locations in Nevada and four more from Minnesota are included thus far.

All necessary extraction and recovery procedures have been completed and each of the binders are undergoing the necessary aging in the kinetics ovens. Although each of the locations are at different stages of testing the kinetics portion of the field validation efforts are roughly 50% complete.

The order for the second DSR at UNR has been placed, but is still awaiting delivery. Once this additional DSR begins production testing, a significant increase in the rate by which the LSV and binder master curves are being produced is expected.

Effort this quarter also focused on developing software that allows for the prediction of pavement temperature profile as a function of pavement depth following C. Glover proposed model from Texas A&M (refer to previous quarterly reports for more details). The pavement temperature profile is a critical input for the calculation of thermal strains and stresses in the pavement. The inputs for the software consist of layer thicknesses, thermal diffusivities, heat capacities and densities of layers. Additionally, climatic parameters are needed such as hourly air temperature, hourly wind speed, hourly solar radiation, emissivity, absorption and radiation (albedo) coefficients of the pavement surface at the location of interest. Finite difference method of numerical calculation is used to obtain pavement temperature profile. Currently the software is able to calculate annual pavement temperature profile up to the depth of 3.0 m below the surface. Figure E2d.1 is a snapshot of the input window of the software. The calculated temperature profiles versus air temperature for a pavement structure at a given location in Nevada are shown in figure E2d.2. The pavement temperature profiles are obtained at the surface and at the depth of 0.2 meters. Currently, about 60% of the software development has been completed. The software will be used as a subroutine of the overall low temperature crack analyzer package.

The screenshot shows a software interface titled 'Form1' with several input sections:

- Layers specification:** A table with columns for Layer No, Layer Type, Thickness (cm), and Heat Diffusivity (m<sup>2</sup>/sec).
 

| Layer No | Layer Type    | Thickness (cm) | Heat Diffusivity (m <sup>2</sup> /sec) |
|----------|---------------|----------------|--|
| 1        | Asphalt       | 40             | 0.005e-4                               |
| 2        | Granular Base | 60             | 0.005e-4                               |
| 3        | Subgrade      | 200            | 0.0035e-4                              |
- groupBox2:** Material properties including Density of Asphalt Mixture (2376 kg/m<sup>3</sup>), Heat capacity (96e3 Jol/(kg.K)), Stefan-Boltzman constant (0.0000000568 W.m<sup>-2</sup>.K<sup>-4</sup>), The power of wind speed (0.5), Constant factor (e) (1.4), Depth Incremental Step (1 Cm), and Time Incremental Step (30 Sec).
- groupBox1:** Parameters for Winter and Summer.
 

| Parameters | Winter | Summer |
|------------|--------|--------|
| α          | 0.2    | 0.2    |
| ε          | 0.85   | 0.85   |
| εa         | 0.7    | 0.7    |
- groupBox3:** Load Climatic Data table with columns for Year, Month, Day, hour, Air Temp (d-F), Wind Speed (m/sec), Solar radiation (Wh/m<sup>2</sup>), and F8. Data is shown for July 1-13, 1996.
- groupBox4:** Initial and End time of Analysis. Initial time is set to January 2000 and End time to January 2001.

Figure E2d.1. Graph. Input window for temperature profile software.

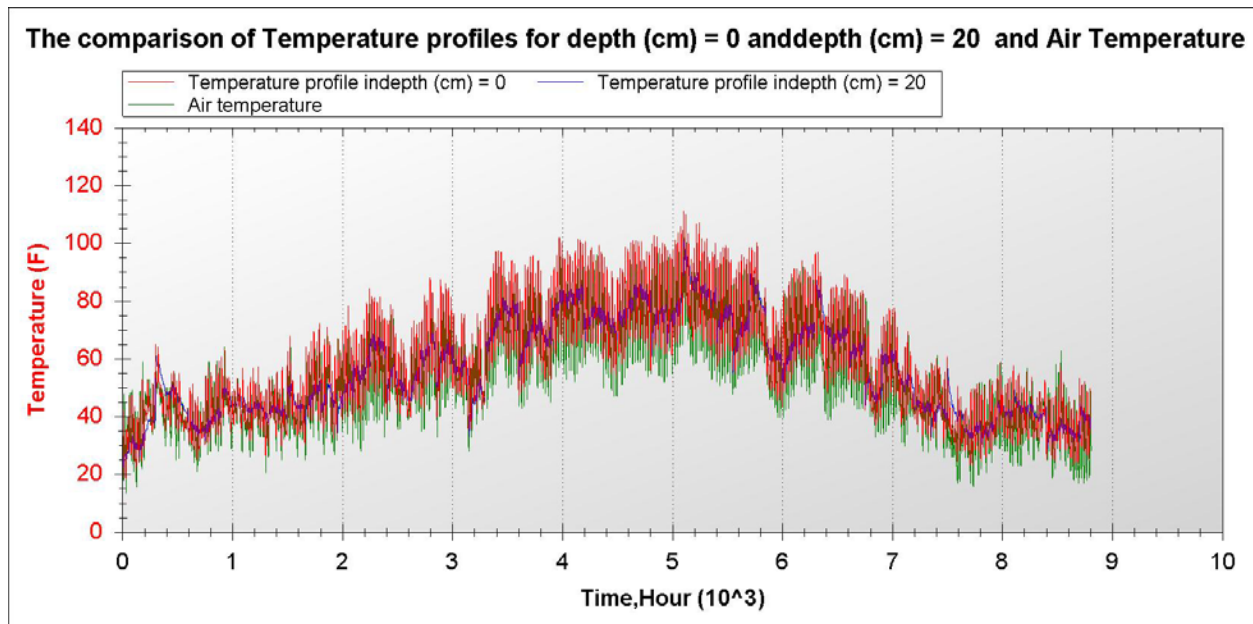


Figure E2d.2. Graph. Air temperature and pavement temperature profiles for year 2000 at the surface and 0.2 meter below the surface.

The UW research team focused on developing a Finite Element (FE) model to simulate the glass transition of various asphalt mixtures. The study focus was on understanding how the glass transition and coefficients of thermal expansion/contraction of the matrix (i.e., asphalt binder + filler) compares to total mixture glass transition, which includes the large aggregate particles.

Dilatometric testing was used to obtain the glass transition behavior of the mastic. The internal structure of the mixture (i.e., number of contact zones, contact length, normal to contact orientation, etc) was characterized by means of digital imaging processing using the iPas<sup>2</sup> software, which is currently under development by the UW research team for rutting characterization. A MATLAB code was used to map resultant pixels from the binary image obtained in iPas<sup>2</sup> into a 4-node bilinear plane stress quadrilateral and reduced integration element (CPS4R) for the FE modeling in ABAQUS software. The model developed considers the mixture as a two-phase heterogeneous material (e.g., asphalt mastic and aggregate).

The simulations were used to assess the effect of volumetric fraction and micro-structural properties of asphalt mixture (e.g., aggregate to aggregate contact length and number of contact points) on the glass transition of the mixture.

In this Quarter, two conference calls were organized between the research groups at the University of Nevada-Reno, the University of Wisconsin-Madison and Texas Transportation Institute to discuss the various components of the overall thermal cracking analysis software. During the first conference call on Oct. 3<sup>rd</sup>, 2011, the University of Nevada-Reno and the University of Wisconsin-Madison presented their research approach and progress. During the second conference call on Dec. 12<sup>th</sup>, 2011, the research group at TTI presented the background

and capabilities of the 2D finite element software, VE2D, for calculating low temperature stresses in asphalt pavements. Possible ways for improving and incorporating UNR and UWM findings into the VE2D software were also discussed. Collaboration between all three groups is progressing toward the combined thermal cracking software package, which is expected to incorporate critical aspects determined in this subtask.

### Significant Results

As the first step in developing an FE simulation for the mixture glass transition it was decided to perform an initial investigation of the effect of microstructure using an idealized mixture beam consisting of uniform round aggregates. The idealized geometry was used to eliminate any unwanted effects of the complex binary mixture model from the results.

Three simple mixtures with circular aggregate particles and the same volumetric fraction (i.e., 10 percent aggregate) but different aggregate structures were considered as shown in figure E2d.3.

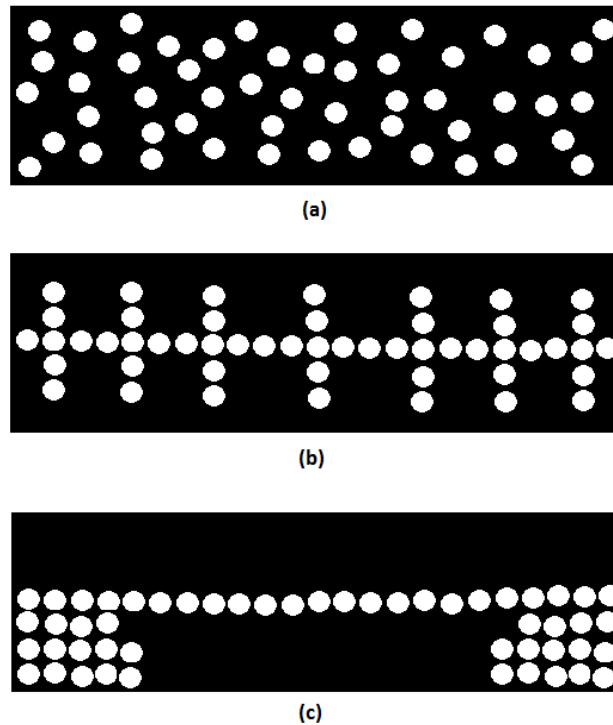


Figure E2d.3. Illustration. (a) Random structure (b) First structure (c) Second structure.

These artificial mixes were subjected to temperature loading and analyzed in ABAQUS. In figure E2d.4, the thermal contraction coefficients of the mixtures are plotted versus temperature. As it can be seen, the thermal contraction/expansion coefficient (CTE) of the mixture decreased as the connectivity of the aggregates increased. This is thought to be due to the increase in aggregate connectivity interfering with the mastic-matrix contraction, causing a reduction in the overall thermal strain rate.

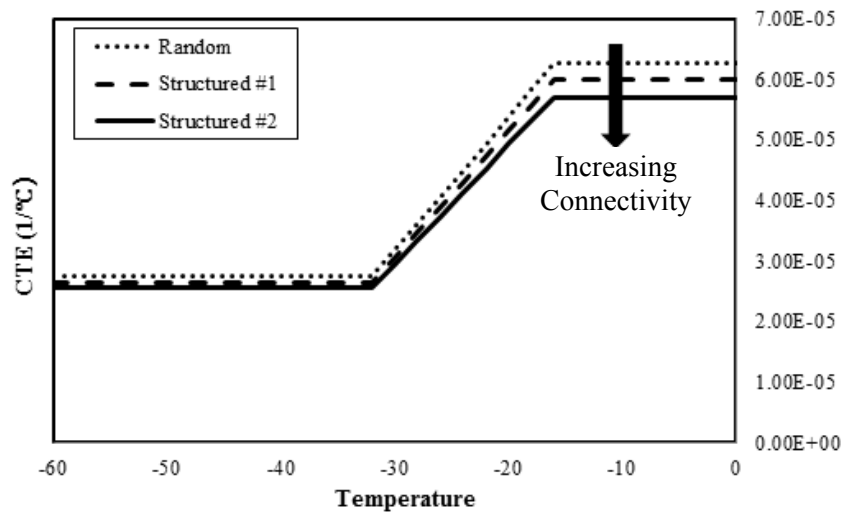


Figure E2d.4. Graph. CTE versus temperature.

### Significant Problems, Issues and Potential Impact on Progress

Progress on the E\*-tension testing has been delayed due to some of the samples delaminating from the test plates during testing. Production testing of those samples has been postponed to allow for further evaluation of the current testing system.

### Work Planned Next Quarter

The carbonyl testing is expected to be completed for the laboratory portion of the study and will continue for the field validation efforts. With the additional DSR installed the low shear viscosity and binder master curves are to be completed for the laboratory phase during this quarter. The E\*-tension testing is expected to resume following some minor adjustments in the protocol. Testing on the TSRST samples are also expected to get underway as the exact testing conditions are nearly determined. Efforts will continue to perform the necessary measures for the selected field validation sections.

The improvement and validation of the pavement temperature profile software will continue in the next quarter. Also the work on the diffusion and transport models software will continue.

The simple model discussed in the previous section highlighted how the internal aggregate structure can be an important factor in determination of the thermo-volumetric properties of the mixture. The research team will use the number of aggregate to aggregate contact zones, and the overall length of the aggregate to aggregate contact to study the effect of microstructure on the thermo-volumetric properties of asphalt mixtures. These internal structure parameters are calculated using the iPas<sup>2</sup> 2-D image analysis software. Preliminary analysis shows that aggregate connectivity have a clear effect on the mixture thermo-volumetric response. The UW research team will continue investigating this relationship to better understand the process of thermal contraction in asphalt mixtures in the next quarter.

The research team has also made considerable progress in writing the first draft of the E2d final report. These efforts will continue in the next quarter.

## **Work element E2e: Design Guidance for Fatigue and Rut Resistance Mixtures (AAT)**

### Work Done This Quarter

#### *Hirsch Model Refinements*

Laboratory work continued this quarter on the experiments to refine the Hirsch model. Three experiments were planned to improve the Hirsch model: (1) curing time experiment, (2) limiting modulus experiment, (3) stress dependency experiment. Each of these experiments addresses a specific aspect of the Hirsch model and dynamic modulus testing. The curing time experiment addresses whether specimen aging significantly affects measured dynamic modulus values. The limiting modulus experiment address whether the limiting minimum modulus is a HMA is significantly affected by the modulus of the aggregate used in the mixture. Finally, the stress dependency experiment address the effect of stress level on the limiting minimum modulus of HMA. Initial data analysis was completed this quarter based on approximately 75 percent of the data. Work on the Hirsch model refinements is approximately 80 percent complete.

#### *Resistivity Model Refinements*

The objective of this work is to refine the rutting model developed in NCHRP Projects 9-25 and 9-31 to better address modified binders by using data from the multiple stress creep recovery tests to characterize the binders. A final experimental design for the resistivity model refinements was developed based on the aggregates selected for the Hirsch model refinement. It includes nine binders with high temperature grade ranging from PG 58 to PG 82. Five of the binders are polymer modified, one is air blown, and three are neat. Eighteen mixtures will be tested. A total of 34 binder/mixture/temperature combinations will be used in the testing. Approximately 50 percent of the specimens for this study were fabricated this quarter.

#### *Fatigue Model Refinements*

The two paper submitted to the Association of Asphalt Paving Technologists (AAPT) were combined into a single paper based on comments received from the reviewers. The revised paper titled, Analysis of FHWA ALF Fatigue Data Using a Continuum Damage Approach, will be presented at the AAPT annual meeting and published in the AAPT Journal.

The research team decided to pursue the continuum damage fatigue testing using AAT's general purpose servo-hydraulic load frame after Interlaken's software engineer left for another job opportunity. NCHRP's Interlaken Asphalt Mixture Performance Tester does not provide the capability for the user defined programming needed to conduct the geometric stress progression and rest period testing planned for this experiment. Programming of AAT's general purpose load frame and specimen fabrication for this experiment was initiated.

### Work Planned Next Quarter

Laboratory work will continue for the Hirsch model, resistivity model, and continuum damage fatigue model experiments. The Hirsch model and resistivity model experiments will be completed next quarter. Most of the testing for the continuum damage fatigue model experiments will also be completed.

### Significant Problems, Issues and Potential Impact on Progress

The laboratory experiments in this Work Element are behind schedule. Materials have been procured and laboratory work proceeding. These experiments will be completed in the first quarter of 2012.

**TABLE OF DECISION POINTS AND DELIVERABLES FOR ENGINEERED MATERIALS**

| <b>Name of Deliverable</b>   | <b>Type of Deliverable</b> | <b>Description of Deliverable</b>  | <b>Original Delivery Date</b> | <b>Revised Delivery Date</b> | <b>Reason for changes in delivery date</b>  |
|--|----------------------------|--|-------------------------------|------------------------------|---|
| E1a- Model and Algorithm (TAMU)  | Model and Algorithm        | The model and algorithm for testing and analysis of damaged asphalt mixtures in tension  | 9/1/11                        | 08/31/12                     | Late arrival of aggregates for fabrication specimens.   |
| E1a- Continuum Damage Permanent Deformation Analysis for Asphalt Mixtures (TAMU) | Final Report               | Ph.D. dissertation at TAMU that describes the viscoplastic mechanism for permanent deformation of the asphalt mixtures and provides the testing protocols and analysis methods to acquire the input parameters of the PANDA program. | 12/31/2010                    | 8/31/12                      | Late arrival of aggregates  |
| E1a- Develop a RDT DMA Testing Protocol (TAMU)                                   | Technology Transfer        | This new testing protocol is stress controlled repeated tension testing method and will be used to replace the previous torsional DMA testing method   | 08/15/2010                    | Complete                     | Presented as Technology Development #14   |
| E1a- Standardize Testing Procedure for Specifications (TAMU)                     | AASHTO Specification       | Develop a Standard Specification to use as a comparative test to evaluate fracture properties, healing and moisture damage of FAM  | 4/30/11                       | Submitted                    | Expanded scope  |
| E1a- Develop a New DMA Testing Protocol for Compression (TAMU)                   | AASHTO Specification       | Develop a Standardized testing method to use as a comparative test to evaluate compressive properties of FAM   | 9/15/11                       | 3/15/12                      | More time need due to the machine data acquisition deficiency (machine built-in LVDT cannot meet needed strain precision) will fabricate special grip to incorporate the external magnetic sensor |
| E1b1-5: Standard Testing Procedure and Recommendation for Specifications (UWM)   | Draft Report               | Report on final conclusions and proposed procedures and specifications   | 7/11                          | 3/13                         | Additional work planned in project extension. The reports for E1b-2 and E1b1-5 are combined. (report "O")   |
|  | Final Report               |  | 1/12                          | 10/13                        |   |



| <b>Name of Deliverable</b>   | <b>Type of Deliverable</b> | <b>Description of Deliverable</b>   | <b>Original Delivery Date</b> | <b>Revised Delivery Date</b> | <b>Reason for changes in delivery date</b>  |
|--|----------------------------|---|-------------------------------|------------------------------|---|
| E1b-2i. Literature review (UWM)  | Draft Report               | Review of previous work on indentation and closed formed solution to the indentation problem.   | 7/09                          | 3/13                         | Additional work planned in project extension. The reports for E1b-2 and E1b1-5 are combined. (report "O") |
| E1b-2iii. Preliminary testing and correlation of results (UWM)   | Draft Report               | The use of indentation test for characterization of asphalt binders.  | 1/10                          | 10/13                        |   |
| E1b-2iv. Feasibility of using indentation tests for fracture and rheological properties (UWM)            | Draft Report               | Report on Finite element simulations of the indentation test and correlations with DSR results.   | 1/11                          | 3/13                         |   |
|  | Final Report               |   | 4/11                          | 10/13                        |   |
| E1c-1ii. Effects of Warm Mix Additives on Mixture Workability and Stability (UWM)                        | Draft Report               | Report of reviewed relevant literature and studies (to be combined with final report)   | 10/08                         | Complete                     | Additional work planned in the project extension. (Integrated with report "P")                            |
|  | Final Report               |   | 1/09                          |                              |   |
|  | Draft Report               | Impacts of WMA Additives on Asphalt Binder Performance and Mixture Workability  | 4/11                          | 3/13                         |   |
|  | Final Report               |   | 1/12                          | 10/13                        |   |
| E1c-1v. Field Evaluation of Mix Design Procedures and Performance Recommendations (UWM)                  | Draft Report               | Report on WMA Field Evaluation of Mix Design Procedures and Performance   | 10/11                         | 3/13                         |   |
|  | Final Report               |   | 1/12                          | 10/13                        |   |
| E1c-2: Improvement of Emulsions' Characterization and Mixture Design for Cold Bitumen Applications (UWM) | Practice                   | Mix design method for cold-in-place recycling (CIR) that is consistent with the Superpave technology and that can be used to define the optimum combination of moisture content and emulsion content. | 12/11                         | 3/13                         | Additional work planned in project extension. (Integrated with report "Q")                                |
|  | Practice                   | Mix design method for cold mix asphalt (CMA) that is consistent with the Superpave technology and that can be used to define the optimum combination of moisture content and emulsion content.        | 03/12                         | 10/13                        |   |
| E1c-2i: Review of Literature and Standards (UWM)   | Draft Report               | Review of Literature and Standards that will be combined with the final draft reports (to be combined with E1c-2vii and E1c-2ix final reports)  | 7/08                          | Complete                     | Additional work planned in project extension. (Integrated with report "Q")                                |
|  | Final Report               |   | 10/08                         |                              |   |
|  | Draft Report               |   | 4/09                          |                              |   |
|  | Draft Report               |   | 7/09                          |                              |   |
|  | Draft Report               |   | 1/10                          |                              |   |
| E1c-2iii: Identify Tests and Develop Experimental Plan (UWM)   | Draft Report               | Reports outlining the required tests and experimental plan for the study (to be combined with E1c-2vii and E1c-2ix final reports)   | 4/09                          | Complete                     |   |
|  | Draft Report               |   | 10/09                         |                              |   |
| E1c-2v. Conduct Testing Plan (UWM)   | Draft Report               | Report on the results and analysis of tests run in accordance to test plan (to be combined with E1c-2vii and E1c-2ix final reports)   | 10/09                         | Complete                     |   |

| <b>Name of Deliverable</b>   | <b>Type of Deliverable</b> | <b>Description of Deliverable</b>  | <b>Original Delivery Date</b> | <b>Revised Delivery Date</b> | <b>Reason for changes in delivery date</b>   |
|--|----------------------------|--|-------------------------------|------------------------------|--|
| E1c-2vii. Validate Guidelines (UWM)  | Draft Report               | Draft report of the performance and Rheological and Bond Properties of Emulsions (to be combined with E1c-2vii final report)   | 7/09                          | 3/13                         | Additional work planned in the project extension. (Integrated with report "Q")               |
|  | Final Report               | Final report of the performance and Rheological and Bond Properties of Emulsions   | 4/11                          | 10/13                        |  |
| E1c-2ix. Develop CMA Performance Guidelines (UWM)  | Draft Report               | Draft and final report of the performance guidelines of Cold Mix asphalt pavements   | 10/11                         | 3/13                         |  |
|  | Final Report               |  | 1/12                          | 10/13                        |  |
| E2a-4: Write asphalt modification guideline/report on modifier impact over binder properties (UWM) | Draft Report               | Report summarizing effect of modification on low, intermediate, and high temperature performance of asphalt binders. It includes guidelines for modification and cost index for different modification types | 10/11                         | 3/13                         | Delay caused by difficulty in obtaining economic information for use of different modifiers. |
|  | Final Report               | Report in 508 format that addresses comments/concerns from Draft Report  | 1/12                          | 10/13                        | Additional work planned in the project extension. (Report "N")                               |
| E2b-1: Develop a System to Evaluate the Properties of RAP Materials (UNR with UWM input)           | Draft Report               | Report on Test Method to Quantify the Effect of RAP and RAS on Blended Binder Properties without Binder Extraction (To be combined with E2b1-b draft and final reports) (UWM input)                          | 4/09                          | 6/30/2013                    | Additional work planned in the project extension. (All reports integrated into report "G")   |
|  | Final Report               |  | 4/09                          | 12/31/2013                   |  |
|  | Practice                   | Recommend the most effective methods for extracting RAP aggregates based on their impact on the various properties of the RAP aggregates and the volumetric calculations for the Superpave mix design.       | 12/10                         | 6/30/2013                    |  |

| Name of Deliverable   | Type of Deliverable | Description of Deliverable   | Original Delivery Date | Revised Delivery Date | Reason for changes in delivery date  |
|---|---------------------|--|------------------------|-----------------------|--|
| E2b-1.b: Develop a System to Evaluate the Properties of the RAP Binder (UWM)            | Draft Report        | Report on the developed testing and analysis procedure system to estimate the RAP binder properties from binder and mortar testing including fracture results. | 10/11                  | 6/30/2013             | Additional work planned in project extension. (All reports integrated into report "G")     |
|   | Final Report        |  | 1/12                   | 12/30/2013            |  |
| E2b-3: Develop a Mix Design Procedure (UNR)   | Draft report        | Report summarizing the laboratory mixing experiment.   | 02/12                  | 6/30/2013             | Additional work planned in project extension. (All reports integrated into report "G")     |
|   | Final report        |  | 08/12                  | 12/31/2013            |  |
| E2b-4: Impact of RAP Materials on Performance of Mixtures And E2b-5: Field Trials (UNR) | Draft report        | Report summarizing the laboratory and field performance of field mixtures.   | 02/12                  | 6/30/2013             | Additional work planned in project extension. (All reports integrated into report "G")     |
|   | Final report        |  | 08/12                  | 12/31/2013            |  |
| E2c-2: Conduct Mixtures Evaluations (UNR)   | Draft report        | Approach to identify critical conditions of HMA mixtures   | 09/11                  | Complete              | N/A  |
|   | Final report        |  | 03/12                  | N/A                   | N/A  |
| E2c-3: Develop a Simple Test (UNR)  | Draft report        | Report summarizing the evaluation of mixtures from the Flow Number Task Force group.   | 11/11                  | 04/12                 | The large number of mixtures and testing conditions delayed the progress of this effort.   |
|   | Final report        |  | 05/12                  | N/A                   | N/A  |
| E2c-4: Develop Standard Test Procedure (UNR)  | Practice            | Recommended practice to identify the critical condition of an HMA mix at the mix design stage to avoid accelerated rutting failures of HMA pavements.          | 12/11                  | 04/12                 | The large number of mixtures and testing conditions delayed the progress of this effort.   |
| E2c-5: Evaluate the Impact of Mix Characteristics (UNR)                                 | Draft report        | Report summarizing the impact of mixture characteristics on the critical condition of the HMA mixes  | 02/12                  | N/A                   | N/A  |
|   | Final report        |  | 08/12                  | N/A                   | N/A  |
| E2d-2: Identify the Causes of the Thermal Cracking (UNR)                                | Draft report        | Report summarizes the testing and findings for materials from LTPP sections.   | 12/11                  | 4/30/2013             | Additional work planned in the project extension. (All reports integrated into report "I") |
|   | Final report        |  | 06/12                  | 10/31/2013            |  |

| <b>Name of Deliverable</b>  | <b>Type of Deliverable</b> | <b>Description of Deliverable</b>   | <b>Original Delivery Date</b> | <b>Revised Delivery Date</b> | <b>Reason for changes in delivery date</b>  |
|---|----------------------------|---|-------------------------------|------------------------------|---|
| E2d-3: Identify an Evaluation and Testing System (UNR with UWM input)       | Draft report               | Low Temperature Cracking Characterization of Asphalt Binders by Means of the Single-Edge Notch Bending (SENB) Test (UWM input)  | 04/11                         | 4/30/2013                    | Additional work planned in the project extension. (All reports integrated into report "I")  |
|   | Final report               |   | 10/11                         | 10/31/2013                   |   |
| E2d-4: Modeling and validation of the Developed System (UNR with UWM input) | Draft report               | Thermal cracking characterization of mixtures by means of the unified Tg-TSRST device. (UWM input)  | 10/11                         | 4/30/2013                    |   |
|   | Final report               |   | 04/12                         | 10/31/2013                   |   |
|   | Model                      | Model that can effectively simulate the long-term properties of HMA mixtures in the intermountain region and assess the impact of such properties on the resistance of HMA mixtures to thermal cracking.  | 03/12                         | 4/30/2013                    |   |
| E2d-5: Develop a Standard (UNR with UWM input)                              | Draft standard             | Draft standards for the use of the SENB, binder Tg and the ATCA device (Mixture Tg). (UWM input)  | 10/11                         | 4/30/2013                    |   |
| E2d-5: Develop a Standard (UNR with UWM input)                              | Final standard             |   | 01/12                         | 10/31/2013                   |   |
| E2d-5: Develop a Standard (UNR with UWM input)                              | Draft standard             | Draft standard for the use of the TSRST with cylindrical specimens compacted using the SGC.   | 03/11                         | 4/30/2013                    | Delayed due to issues with specimens breaking at the edge. Working on refining sample preparation. Added the capability of measuring the strain change during testing. (Report "I") |
|   | Final standard             |   | 01/12                         | 10/31/2013                   |   |
| E2e: Improved Models  | Models                     | Improved composition to engineering property models. <ul style="list-style-type: none"> <li>• Hirsch Model for dynamic modulus</li> <li>• Resistivity Model for rutting resistance</li> <li>• Continuum Damage Fatigue Model</li> <li>• Permeability</li> </ul> | 1/1/2012                      | 6/30/12                      | Testing delays  |
| E2e: New Model  | Model                      | Damage tolerance as a function of mix fracture properties   | 12/31/2012                    | N/A                          | New work  |

| <b>Name of Deliverable</b>               | <b>Type of Deliverable</b> | <b>Description of Deliverable</b>  | <b>Original Delivery Date</b> | <b>Revised Delivery Date</b> | <b>Reason for changes in delivery date</b>  |
|--|----------------------------|--|-------------------------------|------------------------------|---|
| E2e: Report documenting Work Element E2e | Draft Report               | Draft Report for Design Guidance for Fatigue and Rut Resistance Mixtures | 1/1/2012                      | 3/31/2012                    | Testing delays and addition of damage tolerance as a function of mix fracture properties. |
|  | Final Report               |  | 3/31/2012                     | 12/31/2012                   |   |

| Engineered Materials Year 5  | Year 5 (4/2011-3/2012) |   |      |    |    |    |      |       |      |     |         |   | Team    |
|--|------------------------|---|------|----|----|----|------|-------|------|-----|---------|---|---------|
|  | 4                      | 5 | 6    | 7  | 8  | 9  | 10   | 11    | 12   | 1   | 2       | 3 |         |
| <b>(1) High Performance Asphalt Materials</b>  |                        |   |      |    |    |    |      |       |      |     |         |   |         |
| E1a: Analytical and Micro-mechanics Models for Mechanical behavior of mixtures   |                        |   |      |    |    |    |      |       |      |     |         |   | TAMU    |
| E1a-1: Analytical Micromechanical Models of Binder Properties  |                        |   |      |    |    |    |      |       | D,JP |     |         | F |         |
| E1a-2: Analytical Micromechanical Models of Modified Mastic Systems  |                        |   |      |    |    |    |      |       | D    |     | SW, M&A | F |         |
| E1a-3: Analytical Models of Mechanical Properties of Asphalt Mixtures  |                        |   | P(2) |    |    |    | P(2) |       | D,JP |     | SW, M&A | F |         |
| E1a-4: Analytical Model of Asphalt Mixture Response and Damage   |                        |   |      |    |    |    | P(2) |       | D    |     | SW, M&A | F |         |
| E1b: Binder Damage Resistance Characterization   |                        |   |      |    |    |    |      |       |      |     |         |   | UWM     |
| E1b-1: Rutting of Asphalt Binders  |                        |   |      |    |    |    |      |       |      |     |         |   |         |
| E1b-1-i: Literature review   |                        |   |      |    |    |    |      |       |      |     |         |   |         |
| E1b1-2: Select Materials & Develop Work Plan   |                        |   |      |    |    |    |      |       |      |     |         |   |         |
| E1b1-3: Conduct Testing  |                        |   |      |    |    |    |      |       |      |     |         |   |         |
| E1b1-4: Analysis & Interpretation  |                        |   | JP   |    |    |    |      |       |      |     |         |   |         |
| E1b1-5: Standard Testing Procedure and Recommendation for Specifications   | P                      |   |      | D  |    |    | JP   |       |      |     |         |   |         |
| E1b-2: Feasibility of determining rheological and fracture properties of asphalt binders and mastics using simple indentation tests (modified title) |                        |   |      |    |    |    |      |       |      |     |         |   | UWM     |
| E1b-2i: Literature Review  |                        |   |      |    |    |    |      |       |      |     |         |   |         |
| E1b-2ii: Proposed SuperPave testing modifications  |                        |   |      |    |    |    |      |       |      |     |         |   |         |
| E1b-2iii: Preliminary testing and correlation of results   | JP                     |   |      |    |    |    |      |       |      |     |         |   |         |
| E1b-2iv: Feasibility of using indentation tests for fracture and rheological properties  |                        |   |      |    |    |    |      | D     |      |     | F       |   |         |
| E2a: Comparison of Modification Techniques   |                        |   |      |    |    |    |      |       |      |     |         |   | UWM     |
| E2a-1: Identify modification targets and material suppliers  |                        |   |      |    |    |    |      |       |      |     |         |   |         |
| E2a-2: Test material properties  |                        |   |      |    |    |    |      |       |      |     |         |   |         |
| E2a-3: Develop model to estimate level of modification needed and cost index   |                        |   |      |    |    |    |      |       |      |     |         |   |         |
| E2a-4: Write asphalt modification guideline/report on modifier impact over binder properties   |                        |   |      |    |    |    |      |       |      |     | F       |   |         |
| E2c: Critically Designed HMA Mixtures  |                        |   |      |    |    |    |      |       |      |     |         |   | UNR     |
| E2c-1: Identify the Critical Conditions  |                        |   |      |    |    |    |      |       | D,F  |     |         |   |         |
| E2c-2: Conduct Mixtures Evaluations  |                        |   |      |    |    |    |      |       |      |     |         |   |         |
| E2c-3: Develop a Simple Test   |                        |   |      |    | JP |    |      | D     |      | F   |         |   |         |
| E2c-4: Develop Standard Test Procedure   |                        |   |      |    |    |    |      |       |      | D,F |         |   |         |
| E2c-5: Evaluate the Impact of Mix Characteristics  |                        |   |      |    |    |    |      |       |      |     |         | D | F       |
| E2d: Thermal Cracking Resistant Mixes for Intermountain States   |                        |   |      |    |    |    |      |       |      |     |         |   | UNR/UWM |
| E2d-1: Identify Field Sections   |                        |   |      |    |    |    |      |       |      |     |         |   |         |
| E2d-2: Identify the Causes of the Thermal Cracking   |                        |   |      |    |    |    |      |       |      | D   | P       |   | F       |
| E2d-3: Identify an Evaluation and Testing System   | D                      |   |      | JP |    |    |      | F     |      |     | P       |   |         |
| E2d-4: Modeling and Validation of the Developed System   |                        |   |      | JP |    |    |      | D     |      |     | F, P    |   |         |
| E2d-5: Develop a Standard  |                        |   |      | JP |    |    |      | D     |      |     | F, P    |   |         |
| E2e: Design Guidance for Fatigue and Rut Resistance Mixtures   |                        |   |      |    |    |    |      |       |      |     |         |   | AAT     |
| E2e-1: Identify Model Improvements   |                        |   |      |    |    |    |      |       |      |     |         |   |         |
| E2e-2: Design and Execute Laboratory Testing Program   |                        |   |      |    |    |    |      |       |      |     |         |   |         |
| E2e-3: Perform Engineering and Statistical Analysis to Refine Models   |                        |   |      |    |    |    |      |       |      |     |         |   |         |
| E2e-4: Validate Refined Models   |                        |   |      |    |    |    |      |       |      |     |         |   |         |
| E2e-5: Prepare Design Guidance   |                        |   |      |    |    |    |      |       | D    |     |         | F |         |
| <b>(2) Green Asphalt Materials</b>   |                        |   |      |    |    |    |      |       |      |     |         |   |         |
| E2b: Design System for HMA Containing a High Percentage of RAP Material  |                        |   |      |    |    |    |      |       |      |     |         |   | UNR     |
| E2b-1: Develop a System to Evaluate the Properties of RAP Materials  |                        |   |      | JP |    |    |      | D, P  |      |     | F       |   |         |
| E2b-2: Compatibility of RAP and Virgin Binders   |                        | P |      |    |    |    |      |       |      |     |         |   | WRI     |
| E2b-3: Develop a Mix Design Procedure  |                        |   |      |    |    |    |      | JP, P |      |     | D       | F |         |
| E2b-4: Impact of RAP Materials on Performance of Mixtures  |                        |   |      |    |    |    |      |       |      |     | D       | F |         |
| E2b-5: Field Trials  |                        |   |      |    |    |    |      |       |      |     | D       | F |         |
| E1c: Warm and Cold Mixes   |                        |   |      |    |    |    |      |       |      |     |         |   | UWM     |
| E1c-1: Warm Mixes  |                        |   |      |    |    |    |      |       |      |     |         |   |         |
| E1c-1i: Effects of Warm Mix Additives on Rheological Properties of Binders   |                        |   |      |    |    |    |      |       |      |     | D       |   |         |
| E1c-1ii: Effects of Warm Mix Additives on Mixture Workability and Stability  |                        |   |      |    |    |    |      |       |      |     |         |   |         |
| E1c-1iii: Mixture Performance Testing  |                        |   |      |    |    |    |      |       |      |     |         |   |         |
| E1c-1iv: Develop Revised Mix Design Procedures   |                        |   |      |    |    |    |      |       |      |     |         |   |         |
| E1c-1v: Field Evaluation of Mix Design Procedures and Performance Recommendations  |                        |   |      |    |    |    |      |       |      |     | D       |   |         |
| E1c-2: Improvement of Emulsions' Characterization and Mixture Design for Cold Bitumen Applications   |                        |   |      |    |    |    |      |       |      |     |         |   | UWM/UNR |
| E1c-2i: Review of Literature and Standards   |                        |   |      |    |    |    |      |       |      |     |         |   |         |
| E1c-2ii: Creation of Advisory Group  |                        |   |      |    |    |    |      |       |      |     |         |   |         |
| E1c-2iii: Identify Tests and Develop Experimental Plan   |                        |   |      |    |    |    |      |       |      |     |         |   |         |
| E1c-2iv: Develop Material Library and Collect Materials  |                        |   |      |    |    |    |      |       |      |     |         |   |         |
| E1c-2v: Conduct Testing Plan   |                        |   |      |    |    | JP |      |       |      |     |         |   |         |
| E1c-2vi: Develop Performance Selection Guidelines  |                        |   |      |    |    | JP |      |       |      |     |         | F |         |
| E1c-2vii: Validate Performance Guidelines  |                        |   |      |    |    |    |      |       |      |     |         |   |         |
| E1c-2viii: Develop CMA Mix Design Guidelines   |                        |   |      |    |    |    |      |       |      |     |         |   | P       |
| E1c-2ix: Develop CMA Performance Guidelines  |                        |   |      |    |    |    |      |       |      |     |         |   | P       |

**Deliverable codes**  
D: Draft Report  
F: Final Report  
M&A: Model and algorithm  
SW: Software  
JP: Journal paper  
P: Presentation  
DP: Decision Point

**Deliverable Description**  
Report delivered to FHWA for 3 week review period.  
Final report delivered in compliance with FHWA publication standards  
Mathematical model and sample code  
Executable software, code and user manual  
Paper submitted to conference or journal  
Presentation for symposium, conference or other  
Time to make a decision on two parallel paths as to which is most promising to follow through

Work planned  
Work completed  
Parallel topic

| Engineered Materials Year 2 - 5  | Year 2 (4/08-3/09) |          |      |       | Year 3 (4/09-3/10) |      |       |       | Year 4 (04/10-03/11) |          |        |        | Year 5 (04/11-03/12) |       |       |            | Team    |     |
|--|--------------------|----------|------|-------|--------------------|------|-------|-------|----------------------|----------|--------|--------|----------------------|-------|-------|------------|---------|-----|
|  | Q1                 | Q2       | Q3   | Q4    | Q1                 | Q2   | Q3    | Q4    | Q1                   | Q2       | Q3     | Q4     | Q1                   | Q2    | Q3    | Q4         |         |     |
| <b>(1) High Performance Asphalt Materials</b>  |                    |          |      |       |                    |      |       |       |                      |          |        |        |                      |       |       |            |         |     |
| E1a: Analytical and Micro-mechanics Models for Mechanical behavior of mixtures   |                    |          |      |       |                    |      |       |       |                      |          |        |        |                      |       |       |            |         |     |
| E1a-1: Analytical Micromechanical Models of Binder Properties  |                    |          |      | P, JP | JP                 | P    | P     | JP    |                      | P        |        | P      |                      |       | D, JP | F          | TAMU    |     |
| E1a-2: Analytical Micromechanical Models of Modified Mastic Systems  |                    |          |      | P, JP | JP                 | P    | P     |       |                      | P        |        | P      |                      |       | D     | F, SW, M&A |         |     |
| E1a-3: Analytical Models of Mechanical Properties of Asphalt Mixtures  | P                  | P, JP    |      | P, JP | JP                 | P    | P     | M&A   |                      | P, JP(3) | JP (2) | P, M&A | JP(2)                | P(2)  | D, JP | F, SW, M&A |         |     |
| E1a-4: Analytical Model of Asphalt Mixture Response and Damage   |                    |          |      | P, JP | JP                 | P    | P     |       |                      |          |        | P      |                      | P(2)  | D     | F, SW, M&A |         |     |
| E1b: Binder Damage Resistance Characterization   |                    |          |      |       |                    |      |       |       |                      |          |        |        |                      |       |       |            |         |     |
| E1b-1: Rutting of Asphalt Binders  |                    |          |      |       |                    |      |       |       |                      |          |        |        |                      |       |       |            |         |     |
| E1b-1-i: Literature review   |                    |          |      |       |                    |      |       |       |                      |          |        |        |                      |       |       |            |         |     |
| E1b-1-ii: Select Materials & Develop Work Plan   | DP, P              |          | P    |       |                    |      |       |       |                      |          |        |        |                      |       |       |            |         |     |
| E1b-1-iii: Conduct Testing   |                    |          |      |       |                    | JP   |       | P     | DP                   |          |        |        |                      |       |       |            |         |     |
| E1b-1-iv: Analysis & Interpretation  |                    |          |      | JP    | P                  | JP   |       |       |                      |          |        |        | JP                   |       |       |            |         |     |
| E1b-1-v: Standard Testing Procedure and Recommendation for Specifications  |                    |          |      |       |                    |      |       |       |                      | P        |        | DP     | P                    | D, JP |       | F          |         |     |
| E1b-2: Feasibility of Determining rheological and fracture properties of asphalt binders and mastics using simple indentation tests (modified title) |                    |          |      |       |                    |      |       |       |                      |          |        |        |                      |       |       |            |         |     |
| E1b-2i: Literature Review  |                    |          |      |       |                    | D    |       |       |                      |          |        |        |                      |       |       |            |         |     |
| E1b-2ii: Proposed SuperPave testing modifications or new testing devices   |                    |          |      |       |                    | P    |       |       |                      |          |        |        |                      |       |       |            |         |     |
| E1b-2iii: Preliminary testing and correlation of results   |                    |          |      |       |                    |      |       | D     |                      | JP       |        |        | JP                   |       |       |            |         |     |
| E1b-2iv: Feasibility of using indentation tests for fracture and rheological properties  |                    |          |      |       |                    | JP   |       | P     |                      |          |        | P, D   |                      |       | D     | F          |         |     |
| E2a: Comparison of Modification Techniques   |                    |          |      |       |                    |      |       |       |                      |          |        |        |                      |       |       |            |         |     |
| E2a-1: Identify modification targets and material suppliers  |                    |          |      | DP    |                    | DP   |       |       |                      |          |        |        |                      |       |       |            |         |     |
| E2a-2: Test material properties  |                    |          |      |       |                    |      |       | P     |                      | P        |        |        |                      |       |       |            |         |     |
| E2a-3: Develop model to estimate level of modification needed and cost index   |                    |          |      |       |                    |      |       |       |                      |          |        |        |                      |       |       |            |         |     |
| E2a-4: Write asphalt modification guideline/report on modifier impact over binder properties   |                    |          |      |       |                    |      |       |       |                      |          |        | JP     |                      |       |       | F          |         |     |
| E2c: Critically Designed HMA Mixtures  |                    |          |      |       |                    |      |       |       |                      |          |        |        |                      |       |       |            |         |     |
| E2c-1: Identify the Critical Conditions  |                    | JP       |      | D, F  |                    | JP   | D     | F     |                      |          |        |        |                      |       |       |            |         |     |
| E2c-2: Conduct Mixtures Evaluations  |                    |          |      |       |                    |      |       | D     |                      |          |        | JP     |                      | D, F  |       |            |         |     |
| E2c-3: Develop a Simple Test   |                    |          |      |       |                    |      |       |       |                      |          |        |        |                      | JP    | D, F  |            |         |     |
| E2c-4: Develop Standard Test Procedure   |                    |          |      |       |                    |      |       |       |                      |          |        |        |                      |       | D, F  |            |         |     |
| E2c-5: Evaluate the Impact of Mix Characteristics  |                    |          |      |       |                    |      |       |       |                      |          |        |        |                      |       | D, F  |            |         |     |
| E2d: Thermal Cracking Resistant Mixes for Intermountain States   |                    |          |      |       |                    |      |       |       |                      |          |        |        |                      |       |       |            |         |     |
| E2d-1: Identify Field Sections   |                    | D, F     | D, F | D     | F                  |      |       |       |                      |          |        |        |                      |       |       |            |         |     |
| E2d-2: Identify the Causes of the Thermal Cracking   |                    |          |      |       |                    |      |       |       |                      |          |        |        |                      |       | D     | F, P       |         |     |
| E2d-3: Identify an Evaluation and Testing System   |                    |          |      |       | DP                 | JP   | DP, D |       |                      | JP       |        | JP, P  | D                    | JP    | F     | P          |         |     |
| E2d-4: Modeling and Validation of the Developed System   |                    |          |      |       |                    |      |       |       |                      | JP       |        | P      |                      | JP    | D     | F, P       |         |     |
| E2d-5: Develop a Standard  |                    |          |      |       |                    |      |       |       |                      |          |        |        |                      | JP    | D     | F, P       |         |     |
| E2e: Design Guidance for Fatigue and Rut Resistance Mixtures   |                    |          |      |       |                    |      |       |       |                      |          |        |        |                      |       |       |            |         |     |
| E2e-1: Identify Model Improvements   |                    |          |      |       |                    |      |       |       |                      |          |        |        |                      |       |       |            |         |     |
| E2e-2: Design and Execute Laboratory Testing Program   |                    |          |      |       |                    |      |       |       |                      |          |        |        |                      |       |       |            |         |     |
| E2e-3: Perform Engineering and Statistical Analysis to Refine Models   |                    |          |      |       |                    |      |       |       |                      |          |        |        |                      | JP    |       |            |         |     |
| E2e-4: Validate Refined Models   |                    |          |      |       |                    |      |       |       |                      |          |        |        |                      |       |       |            |         |     |
| E2e-5: Prepare Design Guidance   |                    |          |      |       |                    |      |       |       |                      |          |        |        |                      |       | D     | F          |         |     |
| <b>(2) Green Asphalt Materials</b>   |                    |          |      |       |                    |      |       |       |                      |          |        |        |                      |       |       |            |         |     |
| E2b: Design System for HMA Containing a High Percentage of RAP Material  |                    |          |      |       |                    |      |       |       |                      |          |        |        |                      |       |       |            |         |     |
| E2b-1: Develop a System to Evaluate the Properties of RAP Materials  |                    | JP       |      | P     | D                  | D, F | D     |       | P, JP                | JP       | P      |        |                      | P     | JP    | D, P       | F       | UNR |
| E2b-2: Compatibility of RAP and Virgin Binders   |                    |          |      |       |                    |      |       |       |                      |          |        |        |                      |       |       |            |         |     |
| E2b-3: Develop a Mix Design Procedure  |                    |          |      |       |                    |      |       | D     |                      |          |        | D      |                      |       | JP, P | D, F       |         |     |
| E2b-4: Impact of RAP Materials on Performance of Mixtures  |                    |          |      |       |                    |      |       |       |                      |          |        |        |                      |       |       | D, F       |         |     |
| E2b-5: Field Trials  |                    |          |      |       |                    |      |       |       | JP                   |          |        |        |                      |       |       | D, F       |         |     |
| E1c: Warm and Cold Mixes   |                    |          |      |       |                    |      |       |       |                      |          |        |        |                      |       |       |            |         |     |
| E1c-1: Warm Mixes  |                    |          |      |       |                    |      |       |       |                      |          |        |        |                      |       |       |            |         |     |
| E1c-1-i: Effects of Warm Mix Additives on Rheological Properties of Binders  |                    |          |      |       |                    |      |       |       |                      |          |        |        |                      |       |       |            |         |     |
| E1c-1-ii: Effects of Warm Mix Additives on Mixture Workability and Stability   |                    |          |      |       |                    |      |       |       |                      |          |        | JP     |                      |       |       |            |         |     |
| E1c-1-iii: Mixture Performance Testing   |                    | P        | D    | F, DP |                    |      |       |       |                      |          |        |        |                      |       |       | D          | UWM     |     |
| E1c-1-iv: Develop Revised Mix Design Procedures  |                    |          |      |       |                    | JP   |       | P, DP | DP, P                |          |        |        |                      |       |       |            | UWM/UNR |     |
| E1c-1-v: Field Evaluation of Mix Design Procedures and Performance Recommendations   |                    |          |      |       |                    |      |       |       |                      |          |        |        |                      |       |       | D          | UWM/UNR |     |
| E1c-2: Improvement of Emulsions' Characterization and Mixture Design for Cold Bitumen Applications   |                    |          |      |       |                    |      |       |       |                      |          |        |        |                      |       |       |            |         |     |
| E1c-2-i: Review of Literature and Standards  |                    | JP, P, D | F    |       | D1                 | D2   |       | D3    |                      |          |        |        |                      |       |       |            |         |     |
| E1c-2-ii: Creation of Advisory Groups  |                    |          |      |       |                    |      |       |       |                      |          |        |        |                      |       |       |            |         |     |
| E1c-2-iii: Identify Tests and Develop Experimental Plan  |                    |          |      | P, DP | D1                 |      | D4    |       |                      |          |        |        |                      |       |       |            |         |     |
| E1c-2-iv: Develop Material Library and Collect Materials   |                    |          |      |       |                    |      |       |       |                      |          |        |        |                      |       |       |            |         |     |
| E1c-2-v: Conduct Testing Plan  |                    |          |      |       |                    | JP   | D5    | P     |                      | JP       |        | P      |                      | JP    |       |            |         |     |
| E1c-2-vi: Develop Performance Selection Guidelines   |                    |          |      |       |                    |      |       |       | JP                   |          | P      |        |                      | JP    |       | F          |         |     |
| E1c-2-vii: Validate Guidelines   |                    |          |      |       |                    | D2   |       |       |                      |          |        |        |                      |       |       |            |         |     |
| E1c-2-viii: Develop CMA Mix Design Procedure   |                    |          |      |       |                    |      |       |       |                      |          |        |        |                      |       |       | P          |         |     |
| E1c-2-ix: Develop CMA Performance Guidelines   |                    |          |      |       |                    |      |       |       |                      |          |        |        |                      |       |       | P          |         |     |

**Deliverable codes**  
D: Draft Report  
F: Final Report  
M&A: Model and algorithm  
SW: Software  
JP: Journal paper  
P: Presentation  
DP: Decision Point

**Deliverable Description**  
Report delivered to FHWA for 3 week review period.  
Final report delivered in compliance with FHWA publication standards  
Mathematical model and sample code  
Executable software, code and user manual  
Paper submitted to conference or journal  
Presentation for symposium, conference or other  
Time to make a decision on two parallel paths as to which is most promising to follow through

Work planned  
Work completed  
Parallel topic  
Delayed

## **PROGRAM AREA: VEHICLE-PAVEMENT INTERACTION**

### **CATEGORY VP1: WORKSHOP**

#### **Work element VP1a: Workshop on Super-Single Tires (UNR)**

This work element is complete.

### **CATEGORY VP2: DESIGN GUIDANCE**

#### **Work element VP2a: Mixture Design to Enhance Safety and Reduce Noise of HMA (UWM)**

##### Work Done This Quarter

Research efforts this quarter focused on completing the draft final report. The report presents a literature review on prominent friction and noise measurement devices, materials and methods used in the study, results and analysis, and recommendations for future work. The main emphasis of the report is on friction, though noise absorption and generation are also treated to a lesser degree. The draft final report represents the culmination of this work element.

In closing out this work element, researchers concluded field and laboratory research during the quarter. To evaluate if pavement friction characteristics can be estimated from lab tests using Superpave Gyratory Compactor (SGC) samples, researchers compared laser profiles taken from seven field sections to SGC samples compacted using loose mix samples obtained from these field sites.

Researchers also initiated a polishing study to determine if a procedure could be developed in the laboratory to simulate aggregate polishing observed in the field. It is well known that frictional characteristics of roadways change over time as pavement surfaces are subjected to weathering and tire abrasion. To reduce the need for expensive and complicated test equipment, the procedure outlined relies on use of a standard drill press and polishing pad to abrade laboratory-prepared hot mix asphalt (HMA) samples. Researchers devised a preliminary experiment to simulate surface polishing using the factors and levels outlined below in table VP2a.1. Researchers considered three polishing times: 0 seconds (no polishing), 30 seconds, and 60 seconds. A foam pad abraded the surfaces of dense and porous HMA samples with a given air void percentage. Researchers selected the lowest rotational speed of 540 rpm given the equipment used in the experiment. During the experiment, a fixed displacement of 4-5 mm is applied to the polishing pad to force contact between the abrasion pad and HMA sample surface.



Table VP2a.1. Experimental design for the polishing experiment.

| Factor                  | Levels        |
|-------------------------|---------------|
| Polishing Time (second) | 0, 30, 60     |
| Pad Type                | Foam          |
| Sample Type             | Dense, Porous |
| Air Voids (%)           | 2, 8          |
| Rotational Speed (rpm)  | 540           |

### Significant Results

Statistical analysis results for the comparison are shown in table VP2a.2. The results indicate that there is not a statistically significant difference between the surface texture of constructed field sections and SGC samples compacted to densities of 98 percent ( $N_{max}$ ) and 92 percent ( $N_{ini}$ ) of the  $G_{mm}$  in terms of the  $L_{TX, 0.5-32}$  texture parameter. This is supported by the high p-values for the Field vs.  $N_{max}$  and Field vs.  $N_{ini}$  comparisons. Compaction to 2% air voids yields a much higher p-value of 0.888 compared to that of 0.348 for 8% air voids. This finding suggests that laboratory samples can be prepared to capture field conditions in terms of surface texture by compacting mixtures to 2% air voids. The analysis also demonstrates a statistically insignificant difference between laboratory compaction levels.

Table VP2a.2. ANOVA for compaction comparison.

| Compaction Comparison                          | Source           | DF | SS    | MS   | F    | P     |
|--|------------------|----|-------|------|------|-------|
| Field vs. $N_{max}$<br>(2% Air Voids)          | Compaction Level | 1  | 0.8   | 0.8  | 0.02 | 0.888 |
|  | Error            | 26 | 983.5 | 37.8 |      |       |
|  | Total            | 27 | 984.2 |      |      |       |
| Field vs. $N_{ini}$<br>(8% Air Voids)          | Compaction Level | 1  | 4.9   | 4.9  | 0.93 | 0.348 |
|  | Error            | 18 | 94.1  | 5.2  |      |       |
|  | Total            | 19 | 99.0  |      |      |       |
| $N_{max}$ vs. $N_{ini}$<br>(2% & 8% Air Voids) | Compaction Level | 1  | 13.3  | 13.3 | 3.92 | 0.063 |
|  | Error            | 18 | 61.1  | 3.4  |      |       |
|  | Total            | 19 | 74.4  |      |      |       |

Results from the polishing study indicate that the test method described here shows reductions in texture level with increasing polishing time. This is particularly evident at smaller wavelengths, which demonstrates the degradation of micro-texture and smaller macro-texture wavelengths. Figure VP2a.1 demonstrates the degradation of surface texture for three profiles taken from the same SGC sample. Micro-texture diminishes significantly with increased polishing time. Macro-texture also decreases, which may be due either to the abrasion of aggregates or the filling of surface voids with abraded particles. It is recognized that relatively large amounts of aggregate abrasion, which would result in a decrease in macro-texture characteristics, is undesirable as this

behavior is not expected in the field. It is hypothesized that load controlled testing, as opposed to the displacement controlled testing used in this study, would better simulate field conditions and may reduce the measured loss of macro-texture observed in this study.

Researchers compared the selected texture parameter for three samples types at three polishing times. Results are presented in figure VP2a.2. Over the friction spectrum  $L_{TX, 0.5-32}$ , different samples exhibit different types of behavior. For the porous sample, minimal change in texture is observed over three polishing intervals. For the dense samples compacted to 8% air voids, an initial drop in surface texture is observed, which then diminishes very little at later polishing intervals. The dense sample compacted to 2% air voids shows the greatest change in texture, with more significant drops in texture observed at 30 second and 60 second polishing intervals.

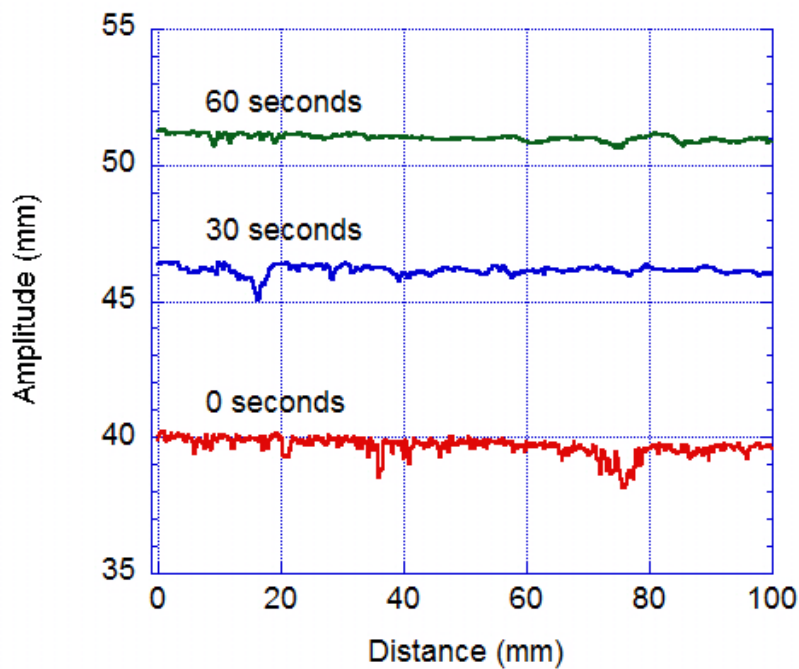


Figure VP2a.1. Graph. Surface profiles at different polishing times show that polishing reduces texture.

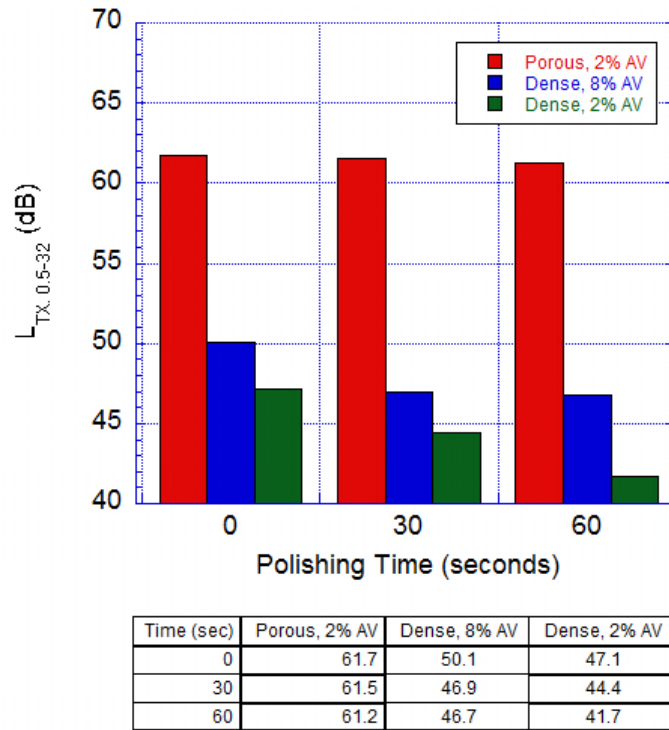


Figure VP2a.2. Graph. Comparison of texture levels for three different samples at three polishing times.

#### Significant Problems, Issues and Potential Impact on Progress

None.

#### Work Planned Next Quarter

This work element has been completed, thus no work is planned for the next quarter.

#### Presentations and Publications

A paper was submitted to TRB for presentation and publication. Paper was accepted and was revised and re-submitted for publication.

## CATEGORY VP3: MODELING

### Work element VP3a: Pavement Response Model to Dynamic Loads (UNR)

#### Work Done This Quarter

The activities on three fronts were undertaken during this quarter relative to our work on 3D-Move Analysis software. They are: (1) Modifications to Option C: User Selected Tire Configuration and Contact Distribution from Database; (2) Continued development of the Pavement Performance Module (PPM); and (3) Development of User Guide. Brief descriptions on selected significant components are presented below. These activities will be integrated into 3D-Move version 2.0 software, which has been under further internal evaluation for bugs and errors.

In 3D-Move, non-uniform contact pressure distribution can be defined by selecting the - Option C from Axle Configuration/Contact Pressure Distribution. Measured non-uniform contact stress distributions from various sources (UCB and NATC) are available under this option. In the earlier versions of 3D-Move, contact pressure distributions for 7 different tire types were able to be accessed. In the version being developed, seventeen additional contact pressure distributions that are available for two Michelin tire types are integrated. Table VP3a.1 shows the new data relative to tire pressure, tire loading for the Michelin tires. Figure VP3a.1 shows the modified menu under Option C. The new additions relative to Michelin tires appear at the bottom of the drop-down box on the top left.

Table VP3a.1. Non-uniform contact pressure distribution.

| Tire Type            | Configuration              | Instrument | Database | Pressure, kPa | Load, kN | Speed   |
|----------------------|----------------------------|------------|----------|---------------|----------|---|
| Michelin 495/45R22.5 | (Super Single)<br>(1 test) | Kistler    | NATC     | 482           | 62       | 2 mph   |
| Michelin 275/80R22.5 | (Dual)<br>(16 Tests)       | Kistler    | NATC     | 420           | 35       | All tests were performed at the speeds of 2, 20, 30, and 40 mph |
|                      |                            |            |          | 517           | 35       |   |
|                      |                            |            |          | 690           | 35       |   |
|                      |                            |            |          | 827           | 35       |   |

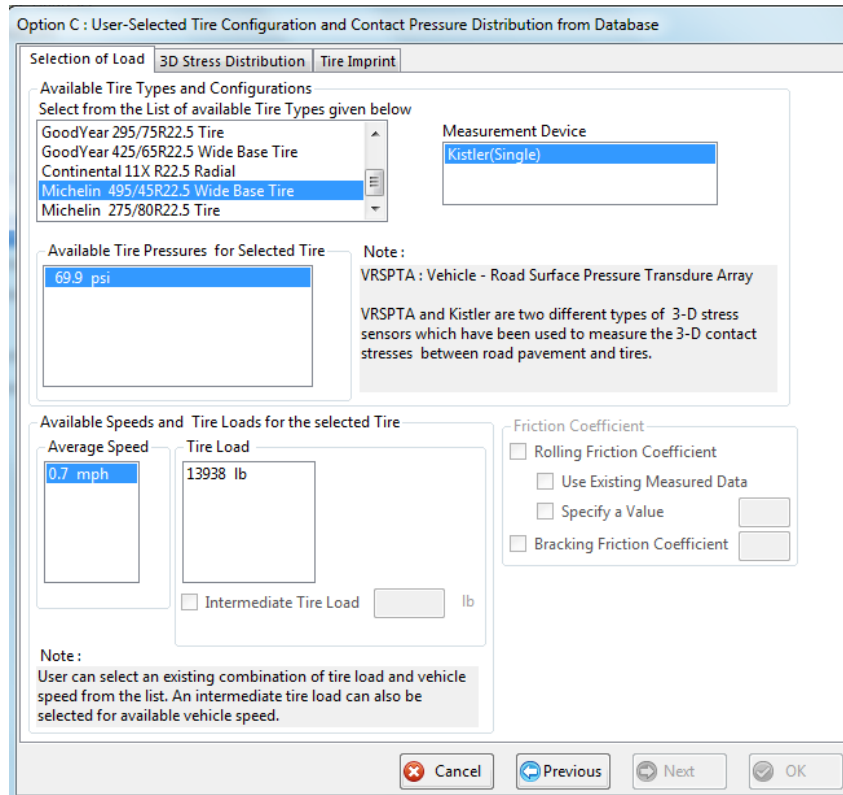


Figure VP3a.1. Option C for Michelin 495/45R22.5 Wide Base Tire.

The work on Pavement Performance Model (PPM) continued to present many unexpected problems. Many of such issues can be directly traced to the difference in US vs. SI units as many of the Pavement Performance Models are unit sensitive. In addition, some performance models require certain specific inputs that are unique to those models and they have to be evaluated to use such models. It should be noted that the PPM work is based mainly on NCHRP 1-37A and VESYS models. The NCHRP 1-37A performance model comprises of six failure modes: AC Top down cracking, AC Bottom up cracking, AC rutting, Base rutting, Subbase rutting and Subgrade rutting, whereas VESYS performance model contains the following four failure modes: Fatigue cracking, Layer rutting, System rutting, and Roughness. These failure modes are associated with the corresponding different layers in the pavement structure. User can uncheck the failure modes depending on the intended analysis. NCHRP 1-37A failure modes are associated with limiting values and reliability levels whereas VESYS failure modes are available with only limiting values. Each failure mode appears with some default values and it can be over written by user. There is an Info link button has been pinned next to each of the models. It links to additional information on these PPMs.

This quarter was also spent on assisting users with issues ranging from usage questions, concepts clarifications, and bugs. The 3D-Move Analysis software developing team worked on fixing the reported bugs.

### Significant Results

As pointed out earlier the integration of PPM had become unexpectedly involved. The issues that need to be resolved included the need to consider traffic loading from non-uniform contact stress distributions, the handling of unit-sensitive PPMs. When non-uniform contact stress conditions are considered, the location of maximum response is not readily predictable. The maximum response locations need to be evaluated internally by the software.

The new version of 3D-Move (version 2) has been internally alpha-tested and the beta-testing is continuing. It is anticipated that this version will be released this quarter.

### Significant Problems, Issues and Potential Impact on Progress

The release of version 2.0 of the software was delayed because of extensive verification of the Pavement Performance Module (PPM).

The 3D-Move Analysis verification plan was postponed until the release of the version 2.0 of the software that will have the various new features and address the various bugs.

The draft report has not been finalized yet since new information is being added to the new version of 3D-Move.

### Work Planned Next Quarter

Continue working on the 3D-Move model to make it a menu-driven software. Complete the beta-testing of version 2.0 of the software. Continue to solve any issues and bugs that users may encounter. Continue to maintain the 3D-Move Forum.

**TABLE OF DECISION POINTS AND DELIVERABLES FOR VEHICLE-PAVEMENT INTERACTION**

| <b>Name of Deliverable</b>   | <b>Type of Deliverable</b> | <b>Description of Deliverable</b>   | <b>Original Delivery Date</b> | <b>Revised Delivery Date</b> | <b>Reason for Changes in Delivery Date</b>  |
|--|----------------------------|---|-------------------------------|------------------------------|---|
| VP2a-4: Run parametric studies on tire-pavement noise and skid response (UWM)                                | Draft Report               | Draft report on proposed design guideline for noise reduction, durability, safety and costs | 1/10                          | 12/11                        | Reports have been integrated into report "R". The final draft   |
| VP2a-7: Proposed optimal guideline for design to include noise reduction, durability, safety and costs (UWM) | Final Report               | Final report on proposed design guideline for noise reduction, durability, safety and costs | 1/12                          | 9/12                         | has been prepared. Final editing and formatting is underway for submission by late Jan, or early Feb 12.            |
| VP3a-4: Overall Model (UNR)  | Software                   | Release of version 2.0 of the 3D-Move pavement response model                               | 06/11                         | 03/12                        | Extensive verification of the Pavement Performance Module (PPM) delayed the release of version 2.0 of the software. |
|  | Draft report               | Summarizing <i>3D-Move Analysis</i> software  | 12/11                         | 03/12                        | The release of version 2.0 delayed this effort.   |
|  | Final report               |   | 06/12                         | N/A                          | N/A   |
|  | Software                   | Release of final version of the 3D-Move pavement response model                             | 03/12                         | N/A                          | N/A   |

**Vehicle-Pavement Interaction Year 5**

|  | Year 5 (4/2011-3/2012) |   |    |   |    |   |    |    |    |   |   |   | Team  |     |
|--|------------------------|---|----|---|----|---|----|----|----|---|---|---|-------|-----|
|  | 4                      | 5 | 6  | 7 | 8  | 9 | 10 | 11 | 12 | 1 | 2 | 3 |       |     |
| <b>(1) Workshop</b>  |                        |   |    |   |    |   |    |    |    |   |   |   |       |     |
| VP1a: Workshop on Super-Single Tires   |                        |   |    |   |    |   |    |    |    |   |   |   |       | UNR |
| <b>(2) Design Guidance</b>   |                        |   |    |   |    |   |    |    |    |   |   |   |       |     |
| VP2a: Mixture Design to Enhance Safety and Reduce Noise of HMA   |                        |   |    |   |    |   |    |    |    |   |   |   |       | UWM |
| VP2a-1: Evaluate common physical and mechanical properties of asphalt mixtures with enhanced frictional skid characteristics   |                        |   |    |   |    |   |    |    |    |   |   |   |       |     |
| VP2a-2: Evaluate pavement macro- and micro-textures and their relation to tire and pavement noise-generation mechanisms  |                        |   |    |   |    |   |    |    |    |   |   |   |       |     |
| VP2a-3: Develop a laboratory testing protocol for the rapid evaluation of the macro and micro-texture of pavements   |                        |   |    | P |    |   |    |    |    |   |   |   |       |     |
| VP2a-4: Run parametric studies on tire-pavement noise and skid response  |                        |   |    |   |    |   |    |    |    |   |   |   |       |     |
| VP2a-5: Establish collaboration with established national laboratories specialized in transportation noise measurements. Gather expertise on measurements and analysis |                        |   |    |   |    |   |    |    |    |   |   |   |       |     |
| VP2a-6: Model and correlate acoustic response of tested tire-pavement systems  |                        |   |    |   | JP | P |    |    |    |   |   |   |       |     |
| VP2a-7: Proposed optimal guideline for design to include noise reduction, durability, safety and costs   |                        |   |    |   |    | P |    |    |    | D |   |   |       |     |
| <b>(3) Pavement Response Model Based on Dynamic Analyses</b>   |                        |   |    |   |    |   |    |    |    |   |   |   |       |     |
| VP3a: Pavement Response Model to Dynamic Loads   |                        |   |    |   |    |   |    |    |    |   |   |   |       | UNR |
| VP3a-1: Dynamic Loads  |                        |   |    |   |    |   |    |    |    |   |   |   |       |     |
| VP3a-2: Stress Distribution at the Tire-Pavement Interface   |                        |   |    |   |    |   |    |    |    |   |   |   |       |     |
| VP3a-3: Pavement Response Model  |                        |   |    |   |    |   |    |    |    |   |   |   |       |     |
| VP3a-4: Overall Model  |                        |   | SW |   |    |   |    |    |    | D |   |   | F, SW |     |

**Deliverable codes**

- D: Draft Report
- F: Final Report
- M&A: Model and algorithm
- SW: Software
- JP: Journal paper
- P: Presentation
- DP: Decision Point

**Deliverable Description**

- Report delivered to FHWA for 3 week review period.
- Final report delivered in compliance with FHWA publication standards
- Mathematical model and sample code
- Executable software, code and user manual
- Paper submitted to conference or journal
- Presentation for symposium, conference or other
- Time to make a decision on two parallel paths as to which is most promising to follow through

|  |                |
|--|----------------|
|  | Work planned   |
|  | Work completed |
|  | Parallel topic |



**Vehicle-Pavement Interaction Years 2 - 5**

|  | Year 2 (4/08-3/09) |     |    |    | Year 3 (4/09-3/10) |          |    |    | Year 4 (04/10-03/11) |    |    |    | Year 5 (04/11-03/12) |       |    |       | Team |
|--|--------------------|-----|----|----|--------------------|----------|----|----|----------------------|----|----|----|----------------------|-------|----|-------|------|
|  | Q1                 | Q2  | Q3 | Q4 | Q1                 | Q2       | Q3 | Q4 | Q1                   | Q2 | Q3 | Q4 | Q1                   | Q2    | Q3 | Q4    |      |
| <b>(1) Workshop</b>  |                    |     |    |    |                    |          |    |    |                      |    |    |    |                      |       |    |       |      |
| VP1a: Workshop on Super-Single Tires   |                    |     |    |    |                    |          |    |    |                      |    |    |    |                      |       |    |       | UNR  |
| <b>(2) Design Guidance</b>   |                    |     |    |    |                    |          |    |    |                      |    |    |    |                      |       |    |       |      |
| VP2a: Mixture Design to Enhance Safety and Reduce Noise of HMA   |                    |     |    |    |                    |          |    |    |                      |    |    |    |                      |       |    |       | UWM  |
| VP2a-1: Evaluate common physical and mechanical properties of asphalt mixtures with enhanced frictional skid characteristics   |                    |     |    | DP |                    |          |    |    |                      |    |    |    |                      |       |    |       |      |
| VP2a-2: Evaluate pavement macro- and micro-textures and their relation to tire and pavement noise-generation mechanisms  |                    |     |    | DP |                    |          |    |    |                      |    |    |    |                      |       |    |       |      |
| VP2a-3: Develop a laboratory testing protocol for the rapid evaluation of the macro and micro-texture of pavements   |                    | M&A |    |    |                    |          |    |    |                      |    |    |    |                      | P     |    |       |      |
| VP2a-4: Run parametric studies on tire-pavement noise and skid response  |                    |     |    |    |                    | JP       |    | D  | JP                   |    |    |    |                      |       |    |       |      |
| VP2a-5: Establish collaboration with established national laboratories specialized in transportation noise measurements. Gather expertise on measurements and analysis |                    |     |    |    |                    |          |    |    |                      |    |    |    |                      |       |    |       |      |
| VP2a-6: Model and correlate acoustic response of tested tire-pavement systems  |                    |     |    |    |                    |          |    |    | JP, P                |    |    |    |                      | JP, P |    |       |      |
| VP2a-7: Proposed optimal guideline for design to include noise reduction, durability, safety and costs   |                    |     |    |    |                    |          |    |    |                      |    | P  |    | P                    | D     |    |       |      |
| <b>(3) Pavement Response Model Based on Dynamic Analyses</b>   |                    |     |    |    |                    |          |    |    |                      |    |    |    |                      |       |    |       |      |
| VP3a: Pavement Response Model to Dynamic Loads   |                    |     |    |    |                    |          |    |    |                      |    |    |    |                      |       |    |       | UNR  |
| VP3a-1: Dynamic Loads  |                    |     | JP |    |                    |          |    |    |                      |    |    |    |                      |       |    |       |      |
| VP3a-2: Stress Distribution at the Tire-Pavement Interface   |                    |     |    |    |                    |          |    |    |                      |    |    |    |                      |       |    |       |      |
| VP3a-3: Pavement Response Model  |                    |     |    |    |                    | SW, v. β |    |    |                      |    | JP |    |                      |       |    |       |      |
| VP3a-4: Overall Model  |                    |     |    |    |                    |          |    |    |                      | SW |    | SW |                      | D     |    | F, SW |      |

**Deliverable codes**

- D: Draft Report
- F: Final Report
- M&A: Model and algorithm
- SW: Software
- JP: Journal paper
- P: Presentation
- DP: Decision Point

**Deliverable Description**

- Report delivered to FHWA for 3 week review period.
- Final report delivered in compliance with FHWA publication standards
- Mathematical model and sample code
- Executable software, code and user manual
- Paper submitted to conference or journal
- Presentation for symposium, conference or other
- Time to make a decision on two parallel paths as to which is most promising to follow through

- Work planned
- Work completed
- Parallel topic

## **PROGRAM AREA: VALIDATION**

### **CATEGORY V1: FIELD VALIDATION**

#### **Work element V1a: Use and Monitoring of Warm Mix Asphalt Sections (WRI)**

##### Work Done This Quarter

No WMA monitoring was planned for this quarter. Work will continue on the core samples from the Manitoba and Yellowstone sites.

##### Significant Results

None.

##### Significant Problems, Issues and Potential Impact on Progress

None.

##### Work Planned Next Quarter

No WMA monitoring is planned for the next quarter.

#### **Work element V1b: Construction and Monitoring of Additional Comparative Pavement Validation Sites (WRI)**

##### Work Done This Quarter

The annual monitoring of the Minnesota CR 112 sections was conducted in October 2011. Milestone Materials (a Mathy company) personnel provided the traffic control, coring equipment, and personnel for the core samples. Core samples were obtained for both WRI and for Gerald Reinke at MTE Services (Mathy) testing. After the 2010 annual monitoring, WRI recommended to Mike Sheehan, Olmstead County Engineer, that crack sealing should be conducted. Crack sealing has occurred at the site. Differential distress is continuing at the site but at a reduced rate.

The Arizona comparative pavement performance site was monitored in December 2012. Differential distress is continuing at this site also. Since annual core samples have been taken over the last several years, it was decided to not take core samples this year.

##### Significant Results

None.

Significant Problems, Issues and Potential Impact on Progress

None.

Work Planned Next Quarter

No site monitoring activity is planned in the next quarter. A list of possible new performance sites of interest to the ARC will be prepared for the LTPP regional support contractors. The list is for the LTPP contractors to present to the states where older LTPP sections are planned for rehabilitation or reconstruction. This may enable the ARC to take advantage of the wealth of data already collected at these sites by finding new experiments for continuing the LTPP sections.

**CATEGORY V2: ACCELERATED PAVEMENT TESTING**

**Work element V2a: Accelerated Pavement Testing including Scale Model Load Simulation on Small Test Track**

Work Done This Quarter

No activity this quarter. This work element was included in order to accommodate any accelerated testing that may occur during the project.

Significant Results

None.

Significant Problems, Issues and Potential Impact on Progress

None.

Work Planned Next Quarter

No accelerated (field) testing is planned.

**Work element V2b: Construction of Validation Sections at the Pecos Research & Testing Center**

This work element is included to indicate that this may be a possibility for accelerated pavement testing for ARC research because it is a facility in the TAMU system.

## **CATEGORY V3: R&D VALIDATION**

### **Work element V3a: Continual Assessment of Specifications (UWM)**

#### Work Done This Quarter

Research efforts focused on continuing asphalt binder testing as part of the Western Cooperative Test Group (WCTG) round-robin study. Researchers conducted performance-grade (PG) and performance-grade-plus (PG+) tests to continue investigation of method efficacy and repeatability. Binder testing also served as a check to ensure that laboratory test machines remain properly calibrated for all other work elements.

Also in this quarter, the research team focused on solidifying ongoing participation from WCTG and the Rocky Mountain Asphalt User/Producer Group (RMAUPG) following the eventual termination of this work element. In coordination with RMAUPG and WCTG leaders, research personnel outlined key objectives and deliverables at the RMAUPG annual meeting after recognizing the importance and significance of this work element. Project stakeholders are discussing possible paths forward to extend the progress made with this work element.

Reporting for this element has been integrated into the final reports of other work elements (E1b-1 and E2d) as indicated in the 21 month extension work plan. Therefore, there will be no final report for this specific work element.

#### Significant Results

Results from WCTG binder testing reveal issues with several laboratory test devices. Within the past quarter, the Rolling Thin-Film Oven (RTFO), Dynamic Shear Rheometer (DSR), and Rotational Viscometer (RV) have all come under scrutiny because binder test results repeatability have fallen beyond acceptable limits imposed by a 95 percent confidence interval. Research personnel and lab technicians have taken the necessary steps to re-calibrate problematic test equipment to ensure proper operation of these devices moving forward.

#### Problems and Implications for Work

Mixture testing remains on hold while mechanical testing equipment is repaired. It is expected that this equipment will be online within the next quarter. Binder testing equipment has been recently calibrated as well.

#### Work Planned Next Quarter

Work in the next quarter will focus on the following tasks:

- Participating in WCTG binder testing.
- Transitioning data collection and analysis templates to WCTG leadership.
- Fixing mixture testing equipment and continuing related tests.

**Work element V3b: Validation of the MEPDG Asphalt Materials Models Using New MEPDG Sites and Selected LTPP Sites (UNR, UWM)**

***Subtask V3b-1: Design and Build Sections (Start Year 1, Year 2, and Year 3)***

***Subtask V3b-2: Additional Testing (Start Year 2, Year 3, and Year 4)***

Work Done This Quarter

None

Significant Results

None

Significant Problems, Issues and Potential Impact on Progress

Only two agencies have committed to the construction of MEPDG sites: the Washoe RTC in northern Nevada in 2008, The South Dakota DOT in 2009/2010. The researchers are facing significant hesitation from the DOTs to use the MEPDG to design and construct HMA pavements. The level of this work element has been reduced.

Work Planned Next Quarter

None

***Subtask V3b-3: Select LTPP Sections (Start Year 1 thru Year 5)***

Work Done This Quarter

In this quarter the efforts were directed towards determining a strong link between the LTPP thermal cracking data and the test result parameters (i.e. fracture energy,  $G_f$ ) obtained from SENB tests performed on binders corresponding to LTPP sections.

Previously, the number of thermal cracks in each section was normalized by the sections' Freeze Indexes. Recognizable trends were observed between the SENB fracture parameters and the number of recorded thermal cracks. In order to better investigate the SENB's predictive capabilities for thermal cracking in the field, it was recognized that data deficiencies in the LTPP database must be addressed for the analyzed sections. The most notable deficiencies are undocumented surface treatments and repairs performed between consequent data collections, and no clear indication of the actual cracking temperature in the pavement, as it is probable that many of the observed thermal cracks could have occurred before the pavement reached the minimum recorded temperature.

In the first step, data from sections for which surface repairs had been performed over the period of data gathering were identified and eliminated from the scope of analysis. Furthermore, in order to identify a narrower range in which the actual cracking occurs, the minimum experienced

temperature in which no cracking occurred was identified from the section climatic history. This temperature is the upper bound of the range of possible critical cracking temperatures. The lower bound of the range is the minimum temperature occurring in the period of observed thermal cracking for the section. An example is shown in table V3b-3.1.

Table V3b-3.1. Example of thermal cracking data for section ID370960.

| <b>SHRP ID</b> | <b>Survey date</b> | <b>Minimum Period Temperature [°C]</b> | <b>No. of thermal cracks</b> |
|----------------|--------------------|--|------------------------------|
| 370960         | 5/21/2002          | -10.1                                  | 0                            |
|                | 4/12/2005          | -12.6                                  | 15                           |

In table V3b-3.1 it can be seen that in 2002 the temperature reached -10.1°C, without resulting in thermal cracking. The survey in 2005 showed that 15 thermal cracks occurred in the section in the period of 5/21/2002 to 4/12/2005. In this period the minimum temperature was -12.6. Thus for this section the critical cracking temperature can be inferred to be within the window of -10.1 to -12.6°C. In such a case a critical temperature of -12°C would be used for comparison of LTPP performance with SENB results.

### Significant Results

Field cracking data was compared to SENB fracture energy parameter for the corresponding binders. SENB tests for each section were carried out at temperature in the critical cracking temperature range identified as discussed above. The results are also shown in table V3b-3.2, in which a trend of decreased number of thermal cracks with increasing  $G_f$  is visible. In this table the LTPP thermal cracking performance grouped in terms of number of observed cracks (high, moderate and low cracking). Similar groupings were also performed in terms of SENB fracture energy. The grouping criteria are solely for the purpose of comparison of the present data set and are not intended as formal SENB specification limits. Table V3b-3.2 shows that in most cases the SENB and LTPP grouping agree. These results indicate that SENB fracture energy seems to be able to represent and rank asphalt pavements in terms of amount of thermal cracking susceptibility.

Table V3b-3.2. Comparison between LTPP thermal cracking performance and SENB results (ranking).

| Section ID | No. of Cracks | Performance Grouping | $G_f$ (J/m <sup>2</sup> ) | SENB Grouping | SENB-LTPP Agreement |
|------------|---------------|----------------------|---------------------------|---------------|---------------------|
| 350902     | 0             | 1                    | 34                        | 1             | Yes                 |
| 350902     | 0             | 1                    | 27.5                      | 1             | Yes                 |
| 340901     | 2             | 1                    | 24.5                      | 1             | Yes                 |
| 370964     | 0             | 1                    | 25                        | 1             | Yes                 |
| 370963     | 0             | 1                    | 27                        | 1             | Yes                 |
| 340902     | 0             | 1                    | 17.5                      | 1             | Yes                 |
| 370962     | 0             | 1                    | 14.5                      | 2             | No                  |
| 340961     | 11            | 2                    | 15.5                      | 2             | Yes                 |
| 370960     | 15            | 3                    | 8.5                       | 3             | Yes                 |
| 370901     | 29            | 3                    | 9.7                       | 3             | Yes                 |

<sup>1</sup>LTPP performance grouping: Group 1: 0-2 cracks, Group 2: 3-14 cracks, Group 3: More than 15 cracks

<sup>2</sup>SENB  $G_f$  grouping (J/m<sup>2</sup>): Group 1:  $G_f$  above 15, Group 2:  $G_f$  from 10 to 15, Group 3,  $G_f$  less than 10.

### Work Planned Next Quarter

In the next quarter the research team will focus on finalizing conclusions for the LTPP validation of the SENB test. Furthermore, efforts will begin for the validation of the modified MSCR test (method B) using the LTPP binders.

Based on the Year 6 extension work plan, subtask V3b will not have an independent final report. Relevant sections were included in report “M” (fatigue), and will be included in report “I” (thermal cracking) and report “O” (rutting).

### **Work Element V3c: Validation of PANDA (TAMU)**

#### Work Done this Quarter

Please refer to the details presented in work elements M4c, F1d-8, and F3c. These work elements outline what has already been accomplished in validating the constitutive models that are implemented in PANDA as well as the validation work that will be carried out in the coming quarter.

In this quarter, emphasis has been placed on the development of a systematic procedure for calibrating the viscodamage evolution law as part of PANDA based on the ALF tension data for different mixtures.

Also, we have started to carry out the ARC testing plan in compression. The aging data based on the dynamic modulus test are available and currently used for calibration and validation of the oxidation aging model. The list of planned tests has been presented in the previous quarterly report. Dr. Richard Kim from North Carolina State University has finished the un-aged and un-

moisture-conditioned tension testing for one mixture. Those data will be used in calibrating and validating the PANDA viscodamage evolution law.

### Significant Results

See the significant results sections in work elements M4c, F1d-8, and F3c.

### Significant Problems, Issues and Potential Impact on Progress

See the significant results sections in work elements M4c, F1d-8, and F3c.

### Work Planned Next Quarter

Focus will be placed on validation of PANDA using the ARC testing plan. The compression testing is currently conducted at Texas A&M University whereas the tensile testing is conducted at North Carolina State University (NCSU). Data from NCSU will be available by March of 2012 for one mixture, and by the end of 2012 for the other two mixtures. See the previous quarterly report for the list of planned tensile and compressive tests that will be conducted (tables V3c.3-8).

## **PANDA Software**

### Work Done This Quarter

In this quarter, work has been continued on the development of the main engine and solver of the standalone finite element code PANDA. Figure V3c.1 shows the list of two-dimensional (2D) and three-dimensional (3D) finite elements that are currently implemented in PANDA. Particularly, in this quarter, the 3D twenty-node finite element has been implemented into PANDA. Notice that the 2D elements can be used to solve plane stress, plane strain, or axisymmetric problems. Moreover, work is in progress of writing the installation and user manual of PANDA. Work is in progress in writing two chapters; the first on “Using PANDA” and the second on “Keywords” for writing the input file for PANDA.

Finally, a Fortran subroutine is coded that includes an extensive library of tensor operations that are useful in the implementation of complex material constitutive models. This tensor library is essential for the numerical implementation of the ARC developed constitutive models into the developed stand-alone software.



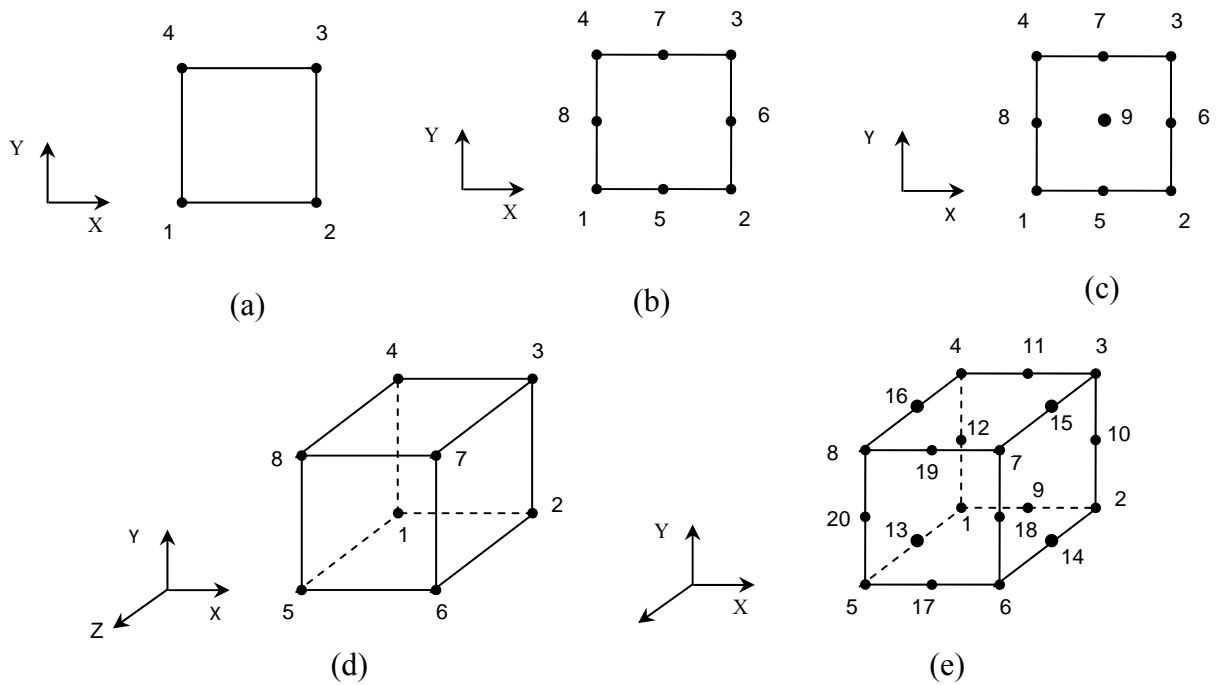


Figure V3c.1. The implemented 2D and 3D finite elements: (a) 2D four-node finite element, (b) 2D eight-node finite element, (c) 2D nine-node finite element, (d) 3D eight-node brick finite element, and (e) 3D twenty-node brick finite element.

Significant Results

None

Significant Problems, Issues and Potential Impact on Progress

None

Work Planned Next Quarter

In next quarter, work will be started on transferring the developed constitutive models that have been developed as part of the UMAT subroutine in Abaqus to the standalone PANDA finite element software. It is expected that all the constitutive models (linear-nonlinear viscoelasticity, viscoplasticity, viscodamage, moisture damage, healing, and aging models) will be transferred to PANDA. The results from PANDA and UMAT-Abaqus will be compared to make sure that the transfer has been done correctly.

**Work Element V3d: Engineered Properties Testing Plan (TAMU)**

Work Done this Quarter

The work completed this quarter relates to work described in Work Elements F2c and E1a.

Work Planned Next Quarter

Please refer to Work Elements F2c and E1a.

**TABLE OF DECISION POINTS AND DELIVERABLES FOR VALIDATION**

| <b>Name of Deliverable</b>  | <b>Type of Deliverable</b> | <b>Description of Deliverable</b>   | <b>Original Delivery Date</b> | <b>Revised Delivery Date</b> | <b>Reason for changes in delivery date</b>   |
|---|----------------------------|---|-------------------------------|------------------------------|--|
| V3a-1: Evaluation of the PG-Plus practices and the motivations for selecting the “plus” tests. (UWM)  | Draft Report               | Detailed analysis of PG and PG+ tests   | 10/08                         | 6/12                         | Additional work planned in project extension. V3a and V3b will not have independent reports. Results will be included as chapters in reports G, I, L, M, O, P and Q. |
|   | Final Report               | Report on 508 format on benefits of PG+ and new ARC tests in comparison to PG tests. Repeatability of PG+ and newly developed ARC procedures          | 12/08                         | 3/13                         |  |
| V3a-2: Detailed analysis of all PG-Plus tests being proposed or in use today, documentation of benefits and costs of these tests, and comparison with new tests (UWM) | Draft Report               | Refer to Draft Report for V3a-1   | 4/09                          | 6/12                         |  |
| V3a-4: Development of specification criteria for new tests based on field evaluation of construction and performance (UWM)  | Draft Report               | Refer to Draft Report for V3a-1   | 7/09                          | 6/12                         | Refer to Draft Report for V3a-1  |
| V3a-5: Interviews and surveys for soliciting feedback on binder tests and specifications (UWM)  | Draft Report               | Report summarizing collaboration between Western Cooperative Test Group (WCTG), the Rocky Mountain Asphalt User-Produce Group (RMAUPG) and UW-Madison | 12/11                         | 6/12                         | Refer to Draft Report for V3a-1  |
|   | Final Report               | Report in 508 format on Development and maintenance of database for evaluation of PG, PG+, and new ARC tests.   | 1/12                          | 3/13                         |  |

| <b>Name of Deliverable</b>   | <b>Type of Deliverable</b>                              | <b>Description of Deliverable</b>  | <b>Original Delivery Date</b> | <b>Revised Delivery Date</b> | <b>Reason for changes in delivery date</b>   |
|--|---|--|-------------------------------|------------------------------|--|
| V3b-3: Select LTPP Sites to Validate New Binder Testing Procedures (UWM) | Draft Report  | Report summarizing characterization of LTPP binders by means of the Linear Amplitude Sweep (LAS), Single Edge-Notch Beam (SENB) and Bitumen Bond Strength (BBS) tests. | 12/11                         | 6/12                         | Additional work planned in project extension. V3a and V3b will not have independent reports. Results will be included as chapters in reports G, I, L, M, O, P and Q. |
|  | Final Report  | Final report in 508 format on validation/verification of fatigue, thermal cracking, and moisture damage procedures using LTPP binders.                                 | 1/12                          | 3/13                         |  |
| V3c: Validation of PANDA (TAMU)  | PANDA Workshop  | Workshop on PANDA Models and Validation Results  | 8/11                          | 4/13                         | Waiting for full calibration and validation of PANDA   |
|  | Draft Report  | Documentation of PANDA Models and Validation   | 11/11                         | 12/31/12                     | Validation against ARC testing   |
|  | Final Report (M5, M4c, F1b-1, F1c, F1d-8, F3c, and V3c) | Documentation of PANDA Models and Validation   | 3/12                          | 3/31/13                      | N/A  |
|  | UMAT Material   | PANDA Implemented in Abaqus  | 3/12                          | 3/31/13                      | N/A  |
|  | Software  | Standalone Software to support the use of and future utility and flexibility of PANDA  | 3/12                          | 3/13                         | Creating user friendly interface for PANDA   |

**Validation Year 5**

|  | Year 5 (4/2011-3/2012) |   |    |      |    |   |    |    |    |   |   |   | Team |                 |
|--|------------------------|---|----|------|----|---|----|----|----|---|---|---|------|-----------------|
|  | 4                      | 5 | 6  | 7    | 8  | 9 | 10 | 11 | 12 | 1 | 2 | 3 |      |                 |
| <b>(1) Field Validation</b>  |                        |   |    |      |    |   |    |    |    |   |   |   |      |                 |
| V1a: Use and Monitoring of Warm Mix Asphalt Sections   |                        |   |    |      |    |   |    |    |    |   |   |   |      | WRI             |
| V1b: Construction and Monitoring of additional Comparative Pavement Validation sites   |                        |   |    |      |    |   |    |    |    |   |   |   |      | WRI             |
| <b>(2) Accelerated Pavement Testing</b>  |                        |   |    |      |    |   |    |    |    |   |   |   |      |                 |
| V2a: Accelerated Pavement Testing including Scale Model Load Simulation on small test track<br>(This work element will include all accelerated pavement testing) |                        |   |    |      |    |   |    |    |    |   |   |   |      | WRI             |
| V2b: Construction of validation sections at the Pecos Research & Testing Center  |                        |   |    |      |    |   |    |    |    |   |   |   |      | WRI             |
| <b>(3) R&amp;D Validation</b>  |                        |   |    |      |    |   |    |    |    |   |   |   |      |                 |
| V3a: Continual Assessment of Specification   |                        |   |    |      |    |   |    |    |    |   |   |   |      | UWM             |
| V3a-1: Evaluation of the PG-Plus practices and the motivations for selecting the "plus" tests.   |                        |   |    |      |    |   | D  |    |    |   |   |   |      |                 |
| V3a-2: Detailed analysis of all PG-Plus tests being proposed or in use today, documentation of benefits and costs of these tests, and comparison with new tests  |                        |   |    |      |    |   |    |    |    |   |   |   |      |                 |
| V3a-3: Development of protocols for new binder tests and database for properties measured  |                        |   |    |      |    |   |    |    |    |   |   |   |      |                 |
| V3a-4: Development of specification criteria for new tests based on field evaluation of construction and performance   |                        |   | P  |      |    |   |    |    |    |   |   |   |      |                 |
| V3a-5: Interviews and surveys for soliciting feedback on binder tests and specifications   |                        | P |    |      |    |   |    |    |    |   |   |   |      |                 |
| V3b: Validation of the MEPDG Asphalt Materials Models and Early Verification of Technologies Developed by ARC using new MEPDG Sites and Selected LTPP sites      |                        |   |    |      |    |   |    |    |    |   |   |   |      | UNR/UWM/<br>WRI |
| V3b-1: Design and Build Sections   |                        |   |    |      |    |   |    |    |    |   |   |   |      | UNR             |
| V3b-2: Additional Testing (if needed)  |                        |   |    |      |    |   |    |    |    |   |   |   |      | UWM             |
| V3b-3: Select LTPP Sites to Validate New Binder Testing Procedures   |                        |   |    |      | JP |   |    |    | D  | F |   |   |      |                 |
| V3b-4: Testing of Extracted Binders from LTPP Sections   |                        |   |    |      |    |   |    |    |    |   |   |   |      |                 |
| V3b-5: Review and Revisions of Materials Models  |                        |   |    |      |    |   |    |    |    |   |   |   |      |                 |
| V3b-6: Evaluate the Impact of Moisture and Aging   |                        |   |    |      |    |   |    |    |    |   |   |   |      |                 |
| V3c: Validation of PANDA   |                        |   |    |      |    |   |    |    |    |   |   |   |      | TAMU            |
| V3d: Engineered Properties Testing Plan  | JP                     |   | JP | P(4) |    |   |    |    |    |   |   |   |      |                 |

**Deliverable codes**

- D: Draft Report
- F: Final Report
- M&A: Model and algorithm
- SW: Software
- JP: Journal paper
- P: Presentation
- DP: Decision Point

**Deliverable Description**

- Report delivered to FHWA for 3 week review period.
- Final report delivered in compliance with FHWA publication standards
- Mathematical model and sample code
- Executable software, code and user manual
- Paper submitted to conference or journal
- Presentation for symposium, conference or other
- Time to make a decision on two parallel paths as to which is most promising to follow through

|  |                |
|--|----------------|
|  | Work planned   |
|  | Work completed |
|  | Parallel topic |

**Validation Years 2 - 5**

|   | Year 2 (4/08-3/09) |    |     |    | Year 3 (4/09-3/10) |    |    |    | Year 4 (04/10-03/11) |        |    |          | Year 5 (04/11-03/12) |    |    |    | Team    |
|---|--------------------|----|-----|----|--------------------|----|----|----|----------------------|--------|----|----------|----------------------|----|----|----|---------|
|   | Q1                 | Q2 | Q3  | Q4 | Q1                 | Q2 | Q3 | Q4 | Q1                   | Q2     | Q3 | Q4       | Q1                   | Q2 | Q3 | Q4 |         |
| <b>(1) Field Validation</b>   |                    |    |     |    |                    |    |    |    |                      |        |    |          |                      |    |    |    |         |
| V1a: Use and Monitoring of Warm Mix Asphalt Sections  |                    |    |     |    |                    |    |    |    |                      |        |    |          |                      |    |    |    | WRI     |
| V1b: Construction and Monitoring of additional Comparative Pavement Validation sites  |                    |    |     |    |                    |    |    |    |                      |        |    |          |                      |    |    |    | WRI     |
| <b>(2) Accelerated Pavement Testing</b>   |                    |    |     |    |                    |    |    |    |                      |        |    |          |                      |    |    |    |         |
| V2a: Accelerated Pavement Testing including Scale Model Load Simulation on small test track   |                    |    |     |    |                    |    |    |    |                      |        |    |          |                      |    |    |    | WRI     |
| V2b: Construction of validation sections at the Pecos Research & Testing Center   |                    |    |     |    |                    |    |    |    |                      |        |    |          |                      |    |    |    | WRI     |
| <b>(3) R&amp;D Validation</b>   |                    |    |     |    |                    |    |    |    |                      |        |    |          |                      |    |    |    |         |
| V3a: Continual Assessment of Specification  |                    |    |     |    |                    |    |    |    |                      |        |    |          |                      |    |    |    | UWM     |
| V3a-1: Evaluation of the PG-Plus practices and the motivations for selecting the "plus" tests.  |                    | P  | D,F |    |                    |    |    |    |                      |        |    |          |                      | D  |    |    |         |
| V3a-2: Detailed analysis of all PG-Plus tests being proposed or in use today, documentation of benefits and costs of these tests, and comparison with new tests |                    |    |     | P  | D                  |    |    |    |                      |        |    |          |                      |    |    |    |         |
| V3a-3: Development of protocols for new binder tests and database for properties measured   |                    |    |     |    |                    | JP |    |    |                      | P      |    |          |                      |    |    |    |         |
| V3a-4: Development of specification criteria for new tests based on field evaluation of construction and performance  |                    |    |     |    |                    | D  |    | P  | P                    |        |    | JP       | P                    |    |    |    |         |
| V3a-5: Interviews and surveys for soliciting feedback on binder tests and specifications  |                    |    |     |    |                    |    |    |    | P                    |        | JP |          | P                    |    |    |    |         |
| V3b: Validation of the MEPDG Asphalt Materials Models and Early Verification of Technologies Developed by ARC using new MEPDG Sites and Selected LTPP sites     |                    |    |     |    |                    |    |    |    |                      |        |    |          |                      |    |    |    | UNR/UWM |
| V3b-1: Design and Build Sections  |                    |    |     |    |                    |    |    |    |                      |        |    |          |                      |    |    |    |         |
| V3b-2: Additional Testing (if needed)   |                    |    |     |    |                    |    |    |    |                      |        |    |          |                      |    |    |    |         |
| V3b-3: Select LTPP Sites to Validate New Binder Testing Procedures  |                    |    |     |    | DP                 |    |    | P  |                      | JP, DP |    | P        |                      | JP | D  | F  |         |
| V3b-4: Testing of Extracted Binders from LTPP Sections  |                    |    |     |    |                    |    |    |    |                      |        |    |          |                      |    |    |    |         |
| V3b-5: Review and Revisions of Materials Models   |                    |    |     |    |                    |    |    |    |                      |        |    |          |                      |    |    |    |         |
| V3b-6: Evaluate the Impact of Moisture and Aging  |                    |    |     |    |                    |    |    |    |                      |        |    |          |                      |    |    |    |         |
| V3c: Validation of PANDA  |                    |    |     |    |                    |    |    |    |                      |        |    |          |                      |    |    |    | TAMU    |
| V3d: Engineered Properties Testing Plan   |                    |    |     |    |                    |    |    |    |                      | P(2)   | JP | P(3), JP |                      |    |    |    |         |

**Deliverable codes**

- D: Draft Report
- F: Final Report
- M&A: Model and algorithm
- SW: Software
- JP: Journal paper
- P: Presentation
- DP: Decision Point

**Deliverable Description**

- Report delivered to FHWA for 3 week review period.
- Final report delivered in compliance with FHWA publication standards
- Mathematical model and sample code
- Executable software, code and user manual
- Paper submitted to conference or journal
- Presentation for symposium, conference or other
- Time to make a decision on two parallel paths as to which is most promising to follow through

- Work planned
- Work completed
- Parallel topic



## PROGRAM AREA: TECHNOLOGY DEVELOPMENT

### Work element TD1: Prioritize and Select Products for Early Development (Year 1) (AAT, WRI)

This work element has been completed. Six early development products were identified.

### Work element TD2: Develop Early Products (Year 3) (AAT, WRI)

#### Work Done This Quarter

Table TD2.1 summarizes the progress on the Products for Early Development. The test method for Automated Flocculation Titrimetric Analysis has been published as an ASTM standard method of test, ASTM D6703 – 07. Draft AASHTO Standards have been completed for other 5 products; however, the Draft AASHTO Standard for simplified continuum damage fatigue analysis for the Asphalt Mixture Performance Tester, is being revised significantly based on the findings of the analyses being conducted in the continuum damage fatigue model refinement in Work Element E2e. The Draft AASHTO Standard for Determination of Polymer in Modified Asphalt is available on the outreach portion of the ARC website at:

<http://www.arc.unr.edu/Outreach.html#TechDevelopmentProducts>.

Table TD2.1. Summary of progress on early development products.

| No. | Product   | ARC Research Program | Format      | Estimated Completion Data | ARC Partner | Draft AASHTO Standard? |
|-----|---|----------------------|-------------|---------------------------|-------------|------------------------|
| 1   | Simplified Continuum Damage Fatigue Analysis for the Asphalt Mixture Performance Tester | Prior                | Test Method | 3/31/2012                 | AAT         | Yes                    |
| 2   | Wilhelmy Plate Test   | Prior                | Test Method | Completed                 | TTI         | Yes                    |
| 3   | Universal Sorption Device   | Prior                | Test Method | Completed                 | TTI         | Yes                    |
| 4   | Dynamic Mechanical Analysis   | Prior                | Test Method | Completed                 | TTI         | Yes                    |
| 5   | Automated Flocculation Titrimetric Analysis   | Prior                | Test Method | Completed                 | WRI         | No (ASTM)              |
| 6   | Determination of Polymer in Asphalt   | Prior                | Test Method | Completed                 | WRI         | Yes                    |



Significant Problems, Issues and Potential Impact on Progress

None.

Work Planned Next Quarter

AAT will continue revising the Draft AASHTO Standard for simplified continuum damage fatigue analysis for the Asphalt Mixture Performance Tester based on the findings from the continuum damage fatigue model refinement in Work Element E2e. Based on the ratings from the ETGs, support will be provided for advancing the selected products through AASHTO for publication as Provisional AASHTO Standards.

**Work element TD3: Identify Products for Mid-Term and Long-Term Development (Years 2, 3, and 4) (AAT, TTI, UNR, UW-M, WRI)**

This work element has been completed. A total of 38 mid- and long-term products were identified. Table TD3.1 summarizes these products.

Table TD3.1. Summary of mid- and long-term technology development products.

| No. | Product   | ARC Work Element | Format                       | Estimated Completion Date | ARC Partner            |
|-----|---|------------------|------------------------------|---------------------------|------------------------|
| 7   | A Method for the Preparation of Specimens of Fine Aggregate Matrix of Asphalt Mixtures  | M1c              | Test Method                  | 12/31/2010                | TTI                    |
| 8   | Measuring intrinsic healing characteristics of asphalt binders  | F1d              | Test Method                  | 12/31/2012                | TTI / UT Austin        |
| 9   | Lattice Micromechanical Model for Virtual Testing of Asphalt Concrete in Tension  | F3b              | Analysis Program             | 2/28/2012                 | NCSU                   |
| 10  | Cohesive Zone Modeling as an Efficient and Powerful Tool to Predict and Characterize Fracture Damage of Asphalt Mixtures Considering Mixture Microstructure, Material Inelasticity, and Moisture Damage | F3b              | Performance Predicting Model | 12/31/2010                | University of Nebraska |
| 11  | Pavement Analysis Using Nonlinear Damage Approach (PANDA)   | F3c              | Test Method                  | 12/31/2012                | TTI                    |

Table TD3.1 continued. Summary of mid- and long-term technology development products.

|    |  |            |  |            |     |
|----|--|------------|--|------------|-----|
| 12 | Test Methods for Determining the Parameters of Material Models in PANDA (Pavement Analysis Using Nonlinear Damage Approach)    | F3c<br>E1a | Test Method                              | 12/31/2011 | TTI |
| 13 | Continuum Damage Permanent Deformation Analysis for Asphalt Mixtures   | E1a        | Test Method                              | 9/30/2011  | TTI |
| 14 | Characterization of Fatigue and Healing Properties of Asphalt Mixtures Using Repeated Direct Tension Test                      | E1a        | Test Method & Data Analysis Program      | 9/30/2011  | TTI |
| 15 | Nondestructive Characterization of Tensile Viscoelastic Properties of Undamaged Asphalt Mixtures                               | E1a        | Test Method & Data Analysis Program      | Completed  | TTI |
| 16 | Nondestructive Characterization of Field Cores of Asphalt Pavements  | E1a        | Test Method & Data Analysis Program      | 9/30/2011  | TTI |
| 17 | Self-Consistent Micromechanics Models of Asphalt Mixtures  | E1a        | Analytical Model & Data Analysis Program | 6/30/2011  | TTI |
| 18 | Nondestructive Characterization of Anisotropic Viscoelastic Properties of Undamaged Asphalt Mixtures under Compressive Loading | E1a        | Test Method                              | Completed  | TTI |
| 19 | Mix Design for Cold-In-Place Recycling (CIR)   | E1c        | Practice                                 | 12/31/2011 | UNR |
| 20 | Mix Design for Cold Mix Asphalt  | E1c        | Practice                                 | 3/31/2012  | UNR |
| 21 | Evaluation of RAP Aggregates   | E2b        | Practice                                 | 4/30/2011  | UNR |
| 22 | Identification of Critical Conditions for HMA mixtures   | E2c        | Practice                                 | 12/31/2011 | UNR |
| 23 | Thermal Stress Restrained Specimen Test (TSRST)  | E2d        | Test Method                              | 9/30/2011  | UNR |
| 24 | HMA Thermal Stresses in the Intermountain Region   | E2d        | Model                                    | 3/31/2012  | UNR |

Table TD3.1 continued. Summary of mid- and long-term technology development products.

|    |  |      |                          |            |      |
|----|--|------|--------------------------|------------|------|
| 25 | Dynamic Model for Flexible Pavements 3D-Move   | VP3a | Software                 | 3/31/2011  | UNR  |
| 26 | Bitumen Bond Strength Test (BBS)   | M1a  | Test Method              | Completed  | UWM  |
| 27 | Elastic Recovery – DSR   | F2a  | Test Method              | 12/31/2010 | UWM  |
| 28 | Linear Amplitude Sweep (DSR)   | F2e  | Test Method              | Completed  | UWM  |
| 29 | Binder Yield Energy Test ( BYET)   | F2e  | Test Method              | Completed  | UWM  |
| 30 | Rigden Voids for fillers   | F2e  | Test Method              | 9/30/2011  | UWM  |
| 31 | Binder Lubricity Test – DSR  | E1c  | Test Method              | 12/31/2010 | UWM  |
| 32 | RAP Binder PG True Grade Determination   | E2b  | Test Method / Software   | 3/31/2011  | UWM  |
| 33 | Single Edge Notch Bending  | E2d  | Test Method              | 5/31/2011  | UWM  |
| 34 | Binder Glass Transition Test   | E2d  | Test Method              | 5/31/2011  | UWM  |
| 35 | Asphalt Mixture Glass Transition Test  | E2d  | Test Method              | 5/31/2011  | UWM  |
| 36 | Planar imaging/ Aggregate Structure  | E1b  | Test Method/ Software    | 3/31/2011  | UWM  |
| 37 | Gyratory Pressure Distribution Analyzer (GPDA)   | E1c  | Test Method              | Completed  | UWM  |
| 38 | Improved Oxygen and Thermal Transport Model of Binder Oxidation in Pavements   | F1c  | Methodology, Publication | 3/31/2011  | TAMU |
| 39 | Field Validation of an Improved Oxygen and Thermal Transport Model of Binder Oxidation in Pavements  | F1c  | Methodology, Publication | 3/31/2011  | TAMU |
| 40 | Validation of an improved Pavement Temperature Transport Model for use in an Oxygen and Thermal Transport Model of Binder Oxidation in Pavements | F1c  | Methodology, Publication | 3/31/2011  | TAMU |
| 41 | Pavement Air Voids Size Distribution Model for use in an Oxygen and Thermal Transport Model of Binder Oxidation in Pavements                     | F1c  | Methodology, Publication | 3/31/2011  | TAMU |

Table TD3.1 continued. Summary of mid- and long-term technology development products.

|    |  |     |                          |           |      |
|----|--|-----|--------------------------|-----------|------|
| 42 | Improved Understanding of Fast-Rate, Constant-Rate Binder Oxidation Kinetics Mechanism through the Effects of Inhibitors | F1c | Publication              | 3/31/2011 | TAMU |
| 43 | Improved Understanding of Fatigue Resistance Decline with Binder Oxidation   | F1c | Publication              | 3/31/2011 | TAMU |
| 44 | Micromechanical Properties of Various Structural Components in Asphalt using Atomic Force Microscopy (AFM)               | F2d | Test and Analysis Method | 3/31/2011 | TAMU |

**Work Element TD4: Develop Mid-Term and Long-Term Products (Years 3, 4, and 5)  
(AAT, TTI, UNR, UW-M, WRI)**

Work Done This Quarter

Work continued on the development of the mid-term and long-term products. Responses to the product rating request issued to the ETGs by the FHWA were compiled by the research team and included in the June 2011 progress report. These responses are being considered by the research team in selecting the effort that will be expended on each of the mid- and long-term products.

Work Planned Next Quarter

The research team will continue with the development of the mid- and long-term technology development products.

Significant Problems, Issues and Potential Impact on Progress

None.



## **PROGRAM AREA: TECHNOLOGY TRANSFER**

### **CATEGORY TT1: OUTREACH AND DATABASES**

#### **Work element TT1a: Development and Maintenance of Consortium Website (Duration: Year 1 through Year 5) (UNR)**

##### Work Done This Quarter

The ARC website was maintained and updated. The ARC quarterly technical progress report, July 1- September 30, 2011, was uploaded to the ARC website. The ARC newsletter (Vol. 5, Issue 3) was uploaded to the website. The following references and files were updated:

- List of Publications and Conference Proceedings under the “Publications” webpage.
- List of Presentations and Posters under the “Outreach” webpage.

The 3D-Move Discussion Group Forum and the ARC Database Forum were also maintained.

##### Significant Results

None

##### Significant Problems, Issues and Potential Impact on Progress

None

##### Work Planned Next Quarter

Continue maintaining and updating the ARC website. Update the list of Publications and Conference Proceedings. Update the list of Presentations and Posters and the list of Theses and White Papers. Post information and new releases for 3D-Move. Maintain the 3D-Move Discussion Group Forum and the ARC Database Forum.

#### **Work element TT1b: Communications (Duration: Year 1 through Year 5) (UNR)**

##### Work Done This Quarter

Published the ARC Newsletter Vol. 5, Issue 3: “Researchers Investigating Fatigue Cracking in Mixtures Have Identified Material Properties Related to Healing.”

##### Significant Results

None

## Significant Problems, Issues and Potential Impact on Progress

None

## Work Planned Next Quarter

Prepare and publish the eleventh ARC Newsletter.

## **Work element TT1c: Prepare Presentations and Publications (All)**

### Presentations

Bahia, H., N. Tabatabaee, C. Clopotel, and A. Golalipour, "Evaluation of the MSCR Test for Modified Binders' Specification." Presentation at the 56th Annual Conference of Canadian Technical Asphalt Association, November 2011.

Banadaki, A.D., M.N. Guddati, and Y.R. Kim, "An Algorithm for Virtually Fabricating Air Voids in Asphalt Concrete," To be presented at the 2012 TRB Annual Meeting, Washington, DC, 2012.

Greenfield, M. L. 2011, Modeling Asphalt on the Molecular Level (invited), Northeast Asphalt User Producer Group (NEAUPG) Meeting, Providence, RI, October 6, 2011.

Greenfield, M. L. 2011, Progress on Molecular Simulation of Asphalt Chemo-mechanics (invited), Rhode Island Transportation Forum, Kingston, RI, October 28, 2011.

Hajj, E. Y. PCCAS-Paving Asphalt Committee, "Update on Asphalt Research Consortium," Oct. 25, 2011.

Li, Derek D., and M. L. Greenfield, 2011, Chemical and Mechanical Relaxations in Multicomponent Model Bitumens, American Institute of Chemical Engineers (AIChE) Annual Meeting, Minneapolis, MN, October 20, 2011.

Swiertz, D., and H. Bahia, "Test Method to Quantify the Effect of RAP and RAS on Blended Binder Properties without Binder Extraction." Presented at the Canadian Technical Asphalt Association annual conference. In Canadian Technical Asphalt Association (CTAA) Proceedings, Vol. LVI, Quebec City, Quebec, 2011, pp. 43-60.

Velasquez, R., T. Miller, and H. Bahia, "On going and Proposed MARC Research for RMAUPG." Presentation at the Rocky Mountain Asphalt User/Producer Group Annual Meeting, Billings, MT, October 19, 2011.

### Publications

Alavi, M., E. Hajj, A. Hanz, and H.U. Bahia, "Evaluating Adhesion Properties and Moisture Damage Susceptibility of Warm Mix Asphalts Using Bitumen Bond Strength (BBS) and

Dynamic Modulus Ratio (ESR) Tests.” Submitted to the 91st Annual Meeting of the Transportation Research Board. Transportation Research Board of the National Academies, Washington D.C., 2012. *Revised and Submitted for Re-Review*.

Aragão, F. T. S., and Y. Kim, 2012, Mode I Fracture Characterization of Bituminous Paving Mixtures at Intermediate Service Temperatures, *Experimental Mechanics*, in print.

Badami, Joseph V., and M. L. Greenfield, 2011, Maxwell Model Analysis of Bitumen Rheological Data. *J. Mater. Civil Eng.*, 23: 1387-1395.

Ban, H., and Y. Kim, 2012, Computational Microstructure Modeling to Estimate Progressive Moisture Damage Behavior of Asphaltic Paving Mixtures. *International Journal for Numerical and Analytical Methods in Geomechanics*, under review.

Ban, H., and Y. Kim, 2012, Integrated Experimental-Numerical Approach to Model Progressive Moisture Damage Behavior of Bituminous Paving Mixtures, *Canadian Journal of Civil Engineering*, in print.

Banadaki, A.D., M.N. Guddati, and Y.R. Kim, “Multiscale Micromechanical Lattice Modeling of Cracking in Asphalt Concrete,” Accepted for publication in the Proceedings of the 7<sup>th</sup> RILEM International Conference on Cracking in Asphalt Pavements, 2012.

Feng, Z., P. Zhang, M.N. Guddati, and Y.R. Kim, The Development and Evaluation of a Virtual Testing Procedure for the Prediction of the Cracking Performance of Hot Mix Asphalt. In *Pavements and Materials: Testing and Modeling in Multiple Length Scales*, Trends in Engineering Mechanics Special Publication No. 1, ASCE Engineering Mechanics Institute, 2010, pp. 142-158.

Han, R., Jin, X., and Glover, C.J., Oxygen Diffusivity in Asphalts and Mastics. *Petroleum Sci. and Technol.*, in press.

Han, Rongbin, Xin Jin, and C.J. Glover, Modeling Pavement Temperature for Use in Binder Oxidation Models and Pavement Performance Prediction. *Journal of Materials in Civil Engineering*, 23(4), 351-359 (2011).

Hintz, C., R. Velasquez, Z. Li, and H. Bahia, 2011, Effect of Oxidative Aging on Binder Fatigue Performance. *Journal of the Association of Asphalt Paving Technologists*, 80, 527-545.

Kim, Y., and F. T. S. Aragão, 2012, Microstructure Modeling of Rate-dependent Fracture Behavior in Bituminous Paving Mixtures. *Fatigue and Fracture of Engineering Materials and Structures*, under review.

Koohi, Y., R. Luo, R. L. Lytton, and T. Scullion, 2012, “New Methodology to Find the Healing and Fracture Properties of Asphalt Mixes Using Overlay Tester.” Submitted for review, *Journal of Materials in Civil Engineering*, American Society of Civil Engineers (ASCE).



Loria, L., E. Y. Hajj, P. E. Sebaaly, M. Barton, S. Kass, and T. Liske, "Performance Evaluation of Asphalt Mixtures with High Recycled Asphalt Pavement Content." *Transportation Research Record: Journal of the Transportation Research Board*, No. 2208, Vol. 2, Transportation Research Board of the National Academies, Washington, D.C., 2011, pp. 72–81.

Luo, X., R. Luo, and R.L. Lytton, 2012, Characterization of Fatigue Damage in Asphalt Mixtures Using Pseudo Strain Energy. Submitted for review, *Journal of Materials in Civil Engineering*, American Society of Civil Engineers (ASCE).

Moraes, R., R. Velasquez, and H. Bahia, "The Effect of Bitumen Stiffness on the Adhesive Strength Measured by the Bitumen Bond Strength Test." Full paper submitted to 5th Eurasphalt and Eurobitume Congress, Istanbul, Turkey, June 13-15, 2012.

Moraes, R., A. Hanz, G. Andreoni, and H. Bahia, "Verification of Warm Mix Asphalt (WMA) Moisture Susceptibility Using the Bitumen Bond Strength Test (BBS)." Abstract submitted and accepted to ISAP 2nd International Symposium on Asphalt Pavements & Environment, Fortaleza, Brazil, October 1-3, 2012.

Morian, N., E. Y. Hajj, C. J. Glover, and P. E. Sebaaly, "Oxidative Aging of Asphalt Binders in Hot-Mix Asphalt Mixtures." *Transportation Research Record: Journal of the Transportation Research Board*, No. 2207, Vol. 1, Transportation Research Board of the National Academies, Washington, D.C., 2011, pp. 107–116.

Roohi Sefidmazgi, N., L. Tashman, and H. U. Bahia, 2011, Internal Structure Characterization of Asphalt Mixtures for Rutting Performance Using Imaging Analysis. *Journal of the Association of Asphalt Pavement Technologies*.

Tabatabaee, H.A., R. Velasquez, and H. U. Bahia, "Predicting Low Temperature Physical Hardening in Asphalt Binders." Submitted for publication to *the Journal of Construction and Building Materials*, Elsevier, 2012.

Tabatabaee, H., R. Velasquez, and H. Bahia, "Modeling Thermal Stress in Asphalt Mixtures Undergoing Glass Transition and Physical Hardening." Accepted for publication and presentation at the 91st Annual Transportation Research Board Meeting, January 22-26, 2012, Washington DC.

Velasquez, R., H. Tabatabaee, and H. Bahia, "Low Temperature Cracking Characterization of Asphalt Binders by Means of the Single-Edge Notch Bending (SENB) Test." *Journal of the Association of Asphalt Paving Technologists*, pp. 583-604, Vol. 80, 2011.

## Work element TT1d: Development of Materials Database (Duration: Year 2 through Year 5) (UNR)

### Work Done This Quarter

The following list describes the work items completed or in progress this quarter:

- File Management System (File Upload form)
- File Management System – Download Files and Reports form
- Addition of Material Characteristics
- Implementation of n-dimensional properties
- Implementation of Data Import from UWM and Others
- Enhancement of Public User approval form
- Other Improvements

### Significant Results

#### *File Management System (File Upload form)*

Optimizing the File Transfer form to refresh only on demand and optimize scrolling was in this quarter's work plan. The default attribute subsystem required enhancement so that default metadata could be reapplied to previously uploaded files. This task was completed this quarter with significantly more enhancements than were planned. Many of these enhancements were suggested during the ARC monthly technical meetings.

As work had progressed, numerous features were added to the File Transfer form. This form allowed consortium users to upload files to the ARC database, to apply metadata to those uploaded files, and to reapply metadata to files that had already been uploaded. While feature rich, the form was becoming confusing, cumbersome, and susceptible to performance degradation. As a result, The File Transfer form was factored into two forms (Upload Files, and Reapply File Metadata) having the following characteristics:

**Upload Files:** The Upload Files form is now only used to upload support files to the ARC database. The user interface has been reorganized into a three step process.

- In step 1, the user selects the target folder where files will be uploaded. Note that this feature has been encapsulated into a user control. Authorized users can also create and delete folders as before.
- In step 2, the user selects the metadata that will be applied. Note that the user interface has been modified to make keyword selection more intuitive. In addition, it's possible to apply default values only for selected fields. Default data can be applied to multiple materials and multiple work elements. Buttons have been added to apply or clear all of the default settings.
- In step 3, the files themselves are selected and uploaded. *Note that user warning messages appear unless steps 1 and 2 have been completed.* As mentioned in previous quarterly reports, files are uploaded in fixed-size chunks. The development team has

tuned the chunk size so as to improve upload performance while not imposing undue load on the Web server.

Note that the help files have been updated according to reflect the changes in this form. Figure TT1d.1 shows the revised and simplified File Upload form.

The image shows a web form for file uploads, divided into two main sections: 'STEP 2: Define default metadata' and 'STEP 3: Select and upload files'.

**STEP 2: Define default metadata** includes the following fields and options:

- Date Added:** 12/31/2011 2:37:07 P  Apply Default
- Date Approved:** 12/31/2011 2:37:07 P  Apply Default
- Description:**   Apply Default
- Primary Keyword:** Accelerated Testing
- Secondary Keyword:** ALF
- Selected Keywords:**   Apply Default
- Approved for Public Use:**   Apply Default
- Property Group:** [NONE]  Apply Default
- File Metadata:** [NONE]  Apply Default
- Material:** ABI 0001 TTI -- Brownwood Limestone+SHRP AAB-1  
ABI 0002 TTI -- Brownwood Limestone+SHRP AAD-1  
ABI 0003 TTI -- Brownwood Limestone+SHRP ABD  
ABI 0004 TTI -- Nevada Andesite+SHRP AAB-1  
ABI 0005 TTI -- Nevada Andesite+SHRP AAD-1  Apply Default  Overwrite (checked)

Below the fields, there is a checkbox for 'CHECK TO ASSOCIATE SUBTASKS WITH THESE FILES' (unchecked) and a checked checkbox for 'Overwrite (checked)'. A note states: 'Note that you must explicitly Save Defaults before uploading files for the default values to be applied to the uploaded files.' A 'Save Defaults' button is located at the bottom of this section.

**STEP 3: Select and upload files** includes the following elements:

- Selected Files (Version 1.3):** An empty list box.
- Buttons:** 'Select Files', 'Upload Files', and 'Clear Files'.
- Upload Status:** An empty area for displaying upload progress.
- Files Uploaded:** A status bar showing 'Files Uploaded = 0'.

Figure TT1d.1 File Upload form

As shown in figure TT1d1, improvements have been made to the user interface.

- The user interface has been more clearly organized into sequential steps.
- The process of keyword selection was simplified.
- It is easier to apply selected defaults or all default values.

**Reapply Default Metadata.** This form is now used to reapply metadata to files that have already been uploaded. Again, the form is configured as a multi-step process as follows:

- In step 1, the user selects the metadata to be applied to one or more existing files. This step works identically to step 1 on the Upload Files form. It is now possible to either append or replace material assignments or subtask assignments.
- In step 2, the user can apply filters used to select files. Features in this step have been expanded significantly as follows:
  - Selected files can be filtered by user (the user who uploaded the file), by date range, by property group or file extension. These filters can be applied individually or be applied using logical AND conditions.
  - The user interface to select keywords has been enhanced.
  - Multiple materials can be selected.
  - It is possible to reapply only selected default values to previously uploaded files.
  - The Program Area / Task Selector was enhanced to allow multiple subtasks or work elements to be applied or selected concurrently.
  - The user can now delete files that have been previously uploaded.

|                 |   |  |
|-----------------|---|--|
| Added by User:  | Michael Ekedahl                                       | <input type="checkbox"/> Select Filter |
| Date Range:     | Start: <input type="text"/> End: <input type="text"/> | <input type="checkbox"/> Select Filter |
| Property Group: | AGG_DESIGN_SIEVE                                      | <input type="checkbox"/> Select Filter |
| File Metadata:  | None (*)  | <input type="checkbox"/> Select Filter |

**No records available.**  
[Upload New File](#)

Figure TT1d.2. Reapply File Metadata form.

As shown in the above figure, the user can now select files based on various filters which can be applied independently.

#### File Management System – Download Files and Reports form

Several changes were implemented in the filter section of the form as planned. There are now options available to filter the selected files by the date the files were uploaded, specific materials and property groups that are associated to files, and the uploading user and organization of files. Currently, these filters are applied to the set of all files in the database in a mutually exclusive

manner. Enhancements continue to be made in order to allow these filters to be applied in an overlapping fashion. That is, these proposed changes will allow for logical AND, and logical OR operations to be applied to filters. Figure TT1d.3 shows part of the revised Download Files and Reports form:

### Download Files and Reports

MESSAGES

▲ ▼

[Help](#)

SEARCH FILES

Filter By Subtask     
  Filter By Folder     
  Filter By Keyword     
  Filter By Material  
 Filter By Date     
  Filter By Property Group     
 Filter By Organization     
 Filter By Uploading User

Select the uploading organization to filter by:

University of Wisconsin-Madison ▼

SELECTED FILES    [Download Selected Files](#)

|                         | ID  | File Name                                       | Description | Date Finalized | Internal URL  | Download                 |
|-------------------------|-----|---|-------------|----------------|---|--------------------------|
| <a href="#">Details</a> | 319 | Hassan_C-20 Pa58-28 LTCII 20_-18C 1_5-19-10.txt |             | 9/28/2011      | /Program Area/Engineered Materials (E)/E2 Design Guidance/E2d Thermal Cracking Resistant Mixes for Intermountain States/E2d-3 Identify an Evaluation and Testing System/Hassan_C-20 Pa58-28 LTCII 20_-18C 1_5-19-10.txt | <input type="checkbox"/> |

Figure TT1d.3. Download Files and Reports form.

The following list describes other selected enhancements:

- When applying filters, such as filtering by organization, only those organizations appear for which there are loaded files. The other filters work similarly.

#### Addition of Material Characteristics

Measures are applied to materials via a test run. This way, multiple tests can be performed for the same material and those tests compared over time. Similar to quantitative and qualitative properties, quantitative and qualitative material characteristics needed to be created for test runs. In addition, to the notion of material characteristics, a need has emerged that multidimensional properties and measures be extended from at most 2 dimensions to 3 or more dimensions. These two topics are discussed separately in this report. The next section talks about the planned implementation of n-dimensional properties.

This new facility has been partially implemented. First a new material characteristics form was created allowing both quantitative and qualitative material characteristics to be define. Figure TT1d.4 shows the editor for Quantitative characteristics.

|   |                                  |
|---|----------------------------------|
| MATERIAL CATEGORY (QUANTITATIVE)          |                                  |
| SELECTED MATERIAL CATEGORY (QUANTITATIVE) |                                  |
| <b>Field</b>                              | <b>Value</b>                     |
| Characteristic ID:                        |                                  |
| Characteristic Name:                      | E# Months Elapsed                |
| Unit ID:                                  | <input type="text" value=""/> ▾  |
| Hard Minimum:                             | <input type="text" value="0"/>   |
| Hard Maximum:                             | <input type="text" value="100"/> |
| Soft Minimum:                             | <input type="text" value="1"/>   |
| Soft Maximum:                             | <input type="text" value="100"/> |
| Comment:                                  | E* measured at Month X           |
| <b>Insert</b> <b>Cancel</b>               |                                  |

Figure TT1d.4. Material Characteristics form (Quantitative).

As shown in the figure, material characteristics are dynamic and can be depicted as quantitative types. Any number of material characteristics can be defined. Users specify valid values for qualitative types via a list box as shown in figure TT1d.5.

|  |   |
|--|---|
| MATERIAL CATEGORY (QUALITATIVE)          |   |
| SELECTED MATERIAL CATEGORY (QUALITATIVE) |   |
| <b>Field</b>                             | <b>Value</b>  |
| Characteristic ID:                       |   |
| Characteristic Name:                     | Moisture  |
| Comment:                                 |   |
|  | <input type="text" value="Wet"/> <input type="button" value="Add"/> <input type="button" value="Delete"/> |
| Qualitative Values:                      | <input type="text" value="Dry"/><br><input type="text" value="Wet"/>                                      |
| <b>Insert</b> <b>Cancel</b>              |   |

Figure TT1d.5. Material Characteristics form (Qualitative).

The form allows the administrator or designee to manage these standard types. In addition to defining Material characteristics, consortium users must be able to associate one or more

qualitative or quantitative type through the test run implementation. The implementation of this part of the sub system is under development.

#### Implementation of n-dimensional properties

Another area of development is in the implementation of a system which will allow for more than two dimensions of multi-dimensional properties to exist in the database. This system is currently in the conceptual planning stage of development. Several possible options exist by which the system can be expanded. The most feasible option to implement is to alter the values that are currently stored in the field [fldDimType] ('primary' or 'secondary') of the table [tblPropDim] to instead store the number of the dimension ('1', '2', '3', etc), and to then change the current implementation of the system that creates and stores multidimensional properties to allow for more than two dimensions. This option requires only localized changes to the current ARC web application. Other options would most likely require more global changes to occur seeing as how most other options would require a change in the physical structure of the underlying ARC database. This option is currently being implemented against a test database to verify its feasibility.

#### Enhancement of Public User approval form

It is now possible to delete requests and view the details of requests for user applications. On the FormView control for the details about the requests now include the following fields: First/Last Name, CreationDate, UserName, Email, PasswordQuestion, PasswordAnswer, Address, City, State, Zip, Country, GeneralUsersCompany, and Notes.

#### Implementation of Data Import from UWM and Others

As planned, work has started on importing the data supplied by the University of Wisconsin, Madison. Presently The ARC development team is communicating with Hassan Tabatabee at UWM and Brian Lippincott of Crystal Computer, Inc. the following questions have been posted and we are awaiting resolution:

- The development team must determine how the files will be received (e-mail attachment) and the folder structure of those files (flat, complex directory architecture). Are the files small enough to send in a zip folder by email or would it be easiest to send them on a DVD by mail?
- Second, the folder structure used to save the imported files must be determined. If the files are going to need to be uploaded into different folders on the ARC database, it would be best if the a column was added to the excel file that you sent attached to the email below which included the directory path to which each file should be uploaded.
- Other questions might arise was the development team continues to work through the file import subsystem.

### Other Improvements

- Eric Weaver reported that the purpose of the MESSAGES section at the top of all forms was unclear. The title has been changed to STATUS / ERROR MESSAGES. In addition, the field containing the message data is no longer editable.
- As more and more data is being entered into the system, selected field sizes and visible field widths have been increased, as necessary.
- As forms get longer, scroll window positioning has become more important. All forms have been modified to scroll to the position seen by the user before a page postback.
- So that we can collect preliminary usage data, the ARC database has been added to Google Analytics allowing us to begin tracking page views.
- It was requested that the Material Tree display those materials having corresponding uploaded files. This feature has been implemented as shown in the following figure.

Select Material To Edit From Tree:

**Filters**

| Material Type | Material Category | Primary Organization | Supplier |
|---------------|-------------------|----------------------|----------|
| [ALL]         | [ALL]             | [ALL]                | [ALL]    |

Work Tasks       Validation Sections       Component Material

Refresh Material List

- ▣ **ABI 0001 TTI -- Brownwood Limestone+SHRP AAB-1**
- ▣ ABI 0002 TTI -- Brownwood Limestone+SHRP AAD-1 (Files Attached)
- ▣ ABI 0003 TTI -- Brownwood Limestone+SHRP ABD (Files Attached)
- ▣ ABI 0004 TTI -- Nevada Andesite+SHRP AAB-1
- ▣ ABI 0005 TTI -- Nevada Andesite+SHRP AAD-1
- ▣ ABI 0006 TTI -- Nevada Andesite+SHRP ABD
- ▣ AGC 0002E CORE (HAC) -- New Braunfels-TX [TTI-BLEND]

Figure TT1d.5. Extended Material Tree.

### Help System

Work continues on the Help system as modifications are made to existing forms and new forms are created. During this quarter, all of the data definition forms were modified to reflect changes to the database structure.

### Significant Problems, Issues and Potential Impact on Progress

None



### Work Planned for Next Quarter

- For convenience, the File Upload system requires that users be able to move files from one folder to another.
- The implementation of the prototype to import existing data and files from UWM will be in place.
- Complete the implementation of the subsystem to apply qualitative and quantitative measures to test runs.
- Finalize the feasibility and implement, if possible, properties having 3 or more dimensions.

In addition, selected ARC members will continue to hold Web meetings roughly every five weeks to monitor status.

### **Work element TT1e: Development of Research Database (Duration: Year 2 through Year 5) (UNR)**

#### Work Done This Quarter

Uploaded the quarterly technical progress report and the ARC newsletter to the ARC website. Updated the “Publications” and “Outreach” web pages.

#### Significant Results

None.

#### Significant Problems, Issues and Potential Impact on Progress

None.

#### Work Planned Next Quarter

Upload the ARC quarterly technical progress report to the ARC website. Publish the ARC newsletter on the ARC website.

### **Work Element TT1f: Workshops and Training (UNR lead)**

#### Work Done This Quarter

None

Significant Results

None

Significant Problems, Issues and Potential Impact on Progress

None

Work Planned Next Quarter

None

## TABLE OF DECISION POINTS AND DELIVERABLES FOR TECHNOLOGY TRANSFER

| Name of Deliverable   | Type of Deliverable | Description of Deliverable  | Original Delivery Date | Revised Delivery Date | Reason for Changes in Delivery Date |
|---|---------------------|---|------------------------|-----------------------|-------------------------------------|
| TT1a: Development and Maintenance of Consortium Website (UNR) | Progress report     | Upload quarterly progress report and newsletter   | 07/11                  | Complete              | N/A                                 |
|   | Newsletter          | Upload newsletter   | 07/11                  | Complete              | N/A                                 |
|   | Progress report     | Upload quarterly progress report and newsletter   | 10/11                  | Complete              | N/A                                 |
|   | Newsletter          | Upload newsletter   | 11/11                  | Complete              | N/A                                 |
|   | Progress report     | Upload quarterly progress report and newsletter   | 01/12                  | N/A                   | N/A                                 |
|   | Newsletter          | Upload newsletter   | 03/12                  | N/A                   | N/A                                 |
|   | Progress report     | Upload quarterly progress report and newsletter   | 04/12                  | N/A                   | N/A                                 |
| TT1b: Communications (UNR)                                    | Newsletter          | Publish newsletter  | 07/11                  | Complete              | N/A                                 |
|   | Newsletter          | Publish newsletter  | 11/11                  | Complete              | N/A                                 |
|   | Newsletter          | Publish newsletter  | 03/12                  | N/A                   | N/A                                 |
| TT1d: Development of Materials Database (UNR and All)         | Workshop            | Training for “super users” and “sub users” on how to use the materials database and validation section and to evaluate the potential errors, bugs and the ease of use of the database system. | 04/11                  | Complete              | N/A                                 |
|   | Database            | Materials database software   | 03/12                  | N/A                   | N/A                                 |
| TT1f: Workshops and Training (UNR and All) (TAMU)             | Workshop            | Training for “super users” and “sub users” on how to use the materials database and validation section and to evaluate the potential errors, bugs and the ease of use of the database system. | 04/11                  | Complete              | N/A                                 |
|   | Workshop            | PANDA software training   | 8/11                   | 4/13                  | N/A                                 |

**Technology Transfer Year 5**




|  | Year 5 (4/2011-3/2012) |   |   |   |   |   |    |    |    |   |   |   | Team |
|--|------------------------|---|---|---|---|---|----|----|----|---|---|---|------|
|  | 4                      | 5 | 6 | 7 | 8 | 9 | 10 | 11 | 12 | 1 | 2 | 3 |      |
| <b>(1) Outreach and Databases</b>                                    |                        |   |   |   |   |   |    |    |    |   |   |   |      |
| TT1a: Development and Maintenance of Consortium Website              |                        |   |   |   |   |   |    |    |    |   |   |   | UNR  |
| TT1b: Communications   |                        |   |   |   |   |   |    |    |    |   |   |   | UNR  |
| TT1c: Prepare presentations and publications                         |                        |   |   |   |   |   |    |    |    |   |   |   | UNR  |
| TT1d: Development of Materials Database                              |                        |   |   |   |   |   |    |    |    |   |   |   | UNR  |
| TT1d-1: Identify the overall Features of the Web Application         |                        |   |   |   |   |   |    |    |    |   |   |   |      |
| TT1d-2: Identify Materials Properties to Include in the Materials    |                        |   |   |   |   |   |    |    |    |   |   |   |      |
| TT1d-3: Define the Structure of the Database                         |                        |   |   |   |   |   |    |    |    |   |   |   |      |
| TT1d-4: Create and Populate the Database                             |                        |   |   |   |   |   |    |    |    |   |   |   |      |
| TT1e: Development of Research Database                               |                        |   |   |   |   |   |    |    |    |   |   |   | UNR  |
| TT1e-1: Identify the Information to Include in the Research Database |                        |   |   |   |   |   |    |    |    |   |   |   |      |
| TT1e-2: Define the Structure of the Database                         |                        |   |   |   |   |   |    |    |    |   |   |   |      |
| TT1e-3: Create and Populate the Database                             |                        |   |   |   |   |   |    |    |    |   |   |   |      |
| TT1f: Workshops and Training   |                        |   |   |   |   |   |    |    |    |   |   |   | UNR  |

**Deliverable codes**

D: Draft Report  
 F: Final Report  
 M&A: Model and algorithm  
 SW: Software  
 JP: Journal paper  
 P: Presentation  
 DP: Decision Point

**Deliverable Description**

Report delivered to FHWA for 3 week review period.  
 Final report delivered in compliance with FHWA publication standards  
 Mathematical model and sample code  
 Executable software, code and user manual  
 Paper submitted to conference or journal  
 Presentation for symposium, conference or other  
 Time to make a decision on two parallel paths as to which is most promising to follow through

|   |                |
|---|----------------|
|  | Work planned   |
|  | Work completed |
|  | Parallel topic |

| Technology Transfer  | Year 2 (4/08-3/09) |    |    |    | Year 3 (4/09-3/10) |    |          |    | Year 4 (04/10-03/11) |    |    |    | Year 5 (04/11-03/12) |    |    |    | Team |
|--|--------------------|----|----|----|--------------------|----|----------|----|----------------------|----|----|----|----------------------|----|----|----|------|
|  | Q1                 | Q2 | Q3 | Q4 | Q1                 | Q2 | Q3       | Q4 | Q1                   | Q2 | Q3 | Q4 | Q1                   | Q2 | Q3 | Q4 |      |
| <b>(1) Outreach and Databases</b>  |                    |    |    |    |                    |    |          |    |                      |    |    |    |                      |    |    |    |      |
| TT1a: Development and Maintenance of Consortium Website                    |                    |    |    |    |                    |    |          |    |                      |    |    |    |                      |    |    |    | UNR  |
| TT1b: Communications   |                    |    |    |    |                    |    |          |    |                      |    |    |    |                      |    |    |    | UNR  |
| TT1c: Prepare presentations and publications                               |                    |    |    |    |                    |    |          |    |                      |    |    |    |                      |    |    |    | ALL  |
| TT1d: Development of Materials Database                                    |                    |    |    |    |                    |    |          |    |                      |    |    |    |                      |    |    |    | UNR  |
| TT1d-1: Identify the overall Features of the Web Application               |                    |    |    |    |                    |    |          |    |                      |    |    |    |                      |    |    |    |      |
| TT1d-2: Identify Materials Properties to Include in the Materials Database |                    |    |    |    |                    |    |          |    |                      |    |    |    |                      |    |    |    |      |
| TT1d-3: Define the Structure of the Database                               |                    |    |    |    |                    |    |          |    |                      |    |    |    |                      |    |    |    |      |
| TT1d-4: Create and Populate the Database                                   |                    |    |    |    |                    |    | SW, v, β | SW |                      |    |    |    |                      |    |    |    |      |
| TT1e: Development of Research Database                                     |                    |    |    |    |                    |    |          |    |                      |    |    |    |                      |    |    |    | UNR  |
| TT1e-1: Identify the Information to Include in the Research Database       |                    |    |    |    |                    |    |          |    |                      |    |    |    |                      |    |    |    |      |
| TT1e-2: Define the Structure of the Database                               |                    |    |    |    |                    |    |          |    |                      |    |    |    |                      |    |    |    |      |
| TT1e-3: Create and Populate the Database                                   |                    |    |    |    |                    |    |          |    |                      |    |    |    |                      |    |    |    |      |
| TT1f: Workshops and Training   |                    |    |    |    |                    |    |          |    |                      |    |    |    |                      |    |    |    | UNR  |

**Deliverable codes**

D: Draft Report  
 F: Final Report  
 M&A: Model and algorithm  
 SW: Software  
 JP: Journal paper  
 P: Presentation  
 DP: Decision Point

**Deliverable Description**

Report delivered to FHWA for 3 week review period.  
 Final report delivered in compliance with FHWA publication standards  
 Mathematical model and sample code  
 Executable software, code and user manual  
 Paper submitted to conference or journal  
 Presentation for symposium, conference or other  
 Time to make a decision on two parallel paths as to which is most promising to follow through

 Work planned  
 Work completed  
 Parallel topic